Sponsored by:
MISSISSIPPI DEPARTMENT OF TRANSPORTATION

Design and Construction Control Guidance for Chemically Stabilized Pavement Base Layers

Final Report

FHWA/MS-DOT-RD-13-206

December 31, 2013

Written and Performed By:

Isaac L. Howard

W. Griffin Sullivan

Brennan K. Anderson

Jay Shannon

Tim Cost

Mississippi State University

"An Industry, Agency & University Partnership"

U.S. Department of Transportation Federal Highway Administration

JAMES WORTH BAGLEY COLLEGE OF ENGINEERING
MISSISSIPPI STATE UNIVERSITY
CIVIL & ENVIRONMENTAL ENGINEERING

Technical Report Documentation Page

1. Report No. FHWA/MS-DOT-RD-13-206	2. Government Accession No.	3. Recipient's Catalog No.
4. Title and Subtitle Design and Construction Control Guidance for Chemically Stabilized Pavement Base Layers		5. Report Date December 31, 2013 6. Performing Organization Code
7. Author(s) *Isaac L. Howard*, Materials and Construction Industries Chair, MSU *W. Griffin Sullivan*, Former Graduate Research Assistant, MSU *Brennan K. Anderson*, Former Graduate Research Assistant, MSU *Jay Shannon*, Graduate Research Assistant, MSU *Tim Cost*, Senior Technical Service Engineer, Holcim (US), Inc.		8. Performing Organization Report No.
9. Performing Organization Name and Address Mississippi State University (MSU) Civil and Environmental Engineering Department 501 Hardy Road: P.O. Box 9546 Mississippi State, MS 39762		10. Work Unit No. (TRAIS) 11. Contract or Grant No. State Study 206
12. Sponsoring Agency Name and Address Mississippi Department of Transportation (MDOT) Research Division P.O. Box 1850 Jackson, MS 39215-1850		13. Type of Report and Period Covered Final Report January 2008 to December 2013 14. Sponsoring Agency Code

Supplementary Notes: Work performed under Mississippi State University research project titled: *Performance Specification for Chemically Stabilized Pavement Layers.* The project was performed under Mississippi Department of Transportation State Study 206 and principal investigator Isaac L. Howard.

16. Abstract

A laboratory and field study was conducted related to chemically stabilized pavement layers, which is also referred to as soil-cement. Soil-cement practices within MDOT related to Class 9C soils used for base layers were evaluated in this report. The overall objective was to provide draft design and quality control guidance that could be incorporated and/or specified to improve performance of soil-cement base layers. A total of 2,101 tests were performed to evaluate a variety of parameters. Testing included strength versus time, strength variability, compaction, elastic modulus, wheel tracking, and thermal profile measurement. One key component of the research was development of economical thermal profile equipment to evaluate compacted soil-cement during the first few hours of hydration. The primary intention of this equipment is a quality control tool. Another key component of the research was development of equipment that allowed soil-cement to be compacted inside a plastic mold that could be used for laboratory mix design, specimen preparation for pavement layer thickness design, and for quality control. Results indicated the plastic mold compaction approach has many advantages and should be implemented into design and quality control operations. At the present time, widespread use of thermal profiles for quality control is not recommended. Additional study, however, could result in effective implementation of thermal profiles into soil-cement construction projects on a more frequent basis.

17. Key Words Soil-Cement, Quality Control, Thermal Profiles, Portland Cement, Slag Cement, Proctor Compaction, Elastic Modulus, Design		18. Distribution Statement No distribution restrictions.	
19. Security Classif. (of this report) Unclassified	20. Security Classif. (of this page) Unclassified	21. No. of Pages 162	22. Price

Form DOT F 1700.7 (8-72) **Reproduction of completed page authorized**

NOTICE

The contents of this report reflect the views of the author, who is responsible for the facts and accuracy of the data presented herein. The contents do not necessarily reflect the views or policies of the Mississippi Department of Transportation or the Federal Highway Administration. This report does not constitute a standard, specification, or regulation.

This document is disseminated under the sponsorship of the Department of Transportation in the interest of information exchange. The United States Government and the State of Mississippi assume no liability for its contents or use thereof.

The United States Government and the State of Mississippi do not endorse products or manufacturers. Trade or manufacturer's names appear herein solely because they are considered essential to the object of this report.

TABLE OF CONTENTS

LIST OF FIGURES

LIST OF TABLES

ACKNOWLEDGEMENTS

Thanks are due to many for the successful completion of this report. The MDOT Research Division is owed special thanks for funding State Study 206. Randy Battey served as State Research Engineer during the project's early stages, and James Watkins served as State Research Engineer during the project's later stages. Bill Barstis (Pavement Research Engineer) served a critical role for MDOT and provided considerable technical support to the authors.

Richard Sheffield help formulate several of the early concepts of the research performed, and was MDOT's Assistant Chief Engineer of Operations during the project's early stages.

The MDOT Materials Division supported the project in a variety of manners including hosting members of the research team at central lab on multiple occasions and assembling the necessary information that allowed the soil-cement database to be assembled. James Williams, Caleb Hammons, and Jeremy Robison (formerly of MDOT and currently with Soil Tech Consultants) provided invaluable support.

Several MDOT employees facilitated acquisition of soil samples and/or field testing: Graham Clarke, Will Davis, Brad Lewis, Nan Mitchell, Brian Ratliff, Albert White, and Alex Zivic.

Alissa Collins (Holcim (US), Inc Theodore Alabama plant) provided technical support and in kind test data, and Holcim (US) provided in kind raw materials. Howard Hornsby, Robert Varner, and Dr. Randy Ahlrich of Burns Cooley Dennis, Inc. provided technical support.

Joe Ivy of Mississippi State University (MSU) provided considerable technical support by way of developing equipment initiated during State Study 206. Several MSU students provided assistance with specimen fabrication, testing, and data reduction. Students deserving special thanks were: Austin Byrd, Derek Cameron, Will Crawley, Web Floyd, Patrick Kuykendall, Drew Sensing, Will Smith, and Tim Woolman.

LIST OF SYMBOLS

A	Mass of Container and Wet Soil
A_s	Area Beneath the Thermal Profile Curve
$A_{\Delta T}$	Area Difference Between Measured Thermal Profile and Reference Specimen
AASHTO	American Association of State Highway and Transportation Officials
ACI	American Concrete Institute
ANOVA	Analysis of Variance
APA	Asphalt Pavement Analyzer
ASTM	American Society for Testing and Materials
B	Mass of Container and Dry Soil
BCD	Burns, Cooley, Dennis, Inc.
C	$1 + C_w/100$
C_A	C_i Value for Pit A
C_B	C_i Value for Pit B
C_C	C_i Value for Pit C
C_F	Constant for Linear Fit Line
C_i	Equation Line Constant for i Line
C_I	Cement Index
C_L	Constant for Lower Boundary Line
C_m	Mass of Container
C_U	Constant for Upper Boundary Line
C_w	Cement Content by Dry Soil Mass (%)
CBR	California Bearing Ratio
CF	Compaction Frame
CI	Confidence Interval
CMRC	Construction Materials Research Center
COV	Coefficient of Variation
D	Oven-dry Density of Soil-Cement (lb/ft^3)
D_{fr}	Final Rut Depth
D_{SM}	Mass of Compacted Specimen and Mold
DOT	Department of Transportation
E	Elastic Modulus
E_a	Apparent Activation Energy (J/mol)
E_{Comp}	Elastic Modulus From Compressometer
E_e	Real Elastic Modulus
E_{fp}	Modulus of Elasticity at a Strength level of *fp*
E_m	Mass of Mold
E_{sc}	Elastic Modulus in Compression
$E_{X\text{-}Head}$	Modulus From Crosshead Displacement
EPS	Expanded Polystyrene
fp	Uniaxial Compressive Strength
F	Mold Factor
FWD	Falling Weight Deflectometer

G	Gradation Modulus
G_s	Specific Gravity
G_{sb}	Bulk Specific Gravity of Plus 12.5 mm Material
GGBFS	Ground Granulated Blast Furnace Slag
GV	Holcim Cement Saint Genevieve, MO
h/d	Height to Depth Ratio
H_o	Null Hypothesis
H_a	Alternative Hypothesis
HC	Honeycomb Insulation
HLWT	Hamburg Loaded Wheel Tester
IC	Isothermal Calorimetry
IQR	Inter Quartile Range
LAC	Linear Asphalt Compactor
LB	Lower Boundary
LF	Linear Fitted Regression Line
LL	Liquid Limit
M	Maturity Index (˚C-hours or ˚C-days)
$M_{r12.5}$	Moisture Adjustment of Material Retained on 12.5 mm Sieve
MDOT	Mississippi Department of Transportation
ME	Margin of Error
MEPDG	Mechanistic-Emperical Pavement Design Guide
ML	Inorganic Silt with Low Plasticity
MSU	Mississippi State University
MT-8	Mississippi Test Method 8
MT-9	Mississippi Test Method 9
MT-9-Mod	Modified Version of Mississippi Test Method 9
MT-25	Mississippi Test Method 25
MT-26	Mississippi Test Method 26
n	Number of Test Replicates
n_{comp}	Number of points used to calculate E_{Comp}
n_o	Number of Outliers
n_{reps}	Number of replicates needed to obtain a desired level of confidence with a prescribed margin of error
N_b	Number of Blows Required to Compact Specimen
N_p	Total Number of Mixing Passes
NC	National Cement (SR9)
NCHRP	National Cooperative Highway Research Program
NP	Non-Plastic
OMC	Optimum Moisture Content
OMC_{adj}	Adjusted Optimum Moisture Content
$OMC_{p12.5}$	Optimum Moisture Content of Material Passing 12.5 mm Sieve
P-Value	Critical Value Used to Determine if Data is Normally Distributed
$P_{p12.5}$	Percent Passing 12.5 mm Sieve
$P_{r12.5}$	Percent Retained on 12.5 mm Sieve
PA	Pit Soil A
PB	Pit Soil B

PC	Pit Soil C
PCA	Portland Cement Association
PD	Pit Soil D
PE	Pit Soil E
PFA	Pulverized Fuel Ash
PI	Plasticity Index
Pit A	Soil Sampled From US Interstate 20 Interchange Near Meridian, MS
Pit B	Soil Sampled From US Highway 45 Near Saltillo, MS
Pit C	Soil Sampled From US Highway 84 Near Prentiss, MS
Pit D	Soil Sampled From State Route 9 Near Tupelo, MS
Pit E	Soil Sampled From State Route 475 in Rankin County, MS
PL	Plastic Limit
PM	Plastic Mold
PM-CF	Plastic Mold in Compaction Frame
PM-P	Plastic Mold Compacted by Modified Proctor Hammer
PRI	Prediction Interval
PW	PURWheel
$P\gamma_d$	Percentage of Target Maximum Dry Density
q_t	Strength After t days of Curing
q_u	Unconfined Compressive Strength
q_{28}	Strength Value at 28 Days After Curing
Q1	1st Quartile
Q3	3rd Quartile
r	Correlation Coefficient
R	Universal Gas Constant (8.314 J/mol-K)
R_{SI}	Insulation R-Value (m^2-K/W)
R^2	Coefficient of Determination
RTO	Linear Regression Through Origin
SAC	Semi-Adiabatic Calorimetry
SC	Soil + Cement
SCB	Soil-Cement Bentonite
SCM	Supplementary Cementitious Material
SGC	Superpave Gyratory Compactor
SL	Soil + Lime
SLC	Soil + Lime + Cement
SR9	State Route 9
SR475	State Route 475
SS	State Study
ST	Strength vs Time
Stdev	Standard Deviation
SV	Design Strength Variability
SVM	Design Strength Variability Using the MDOT Curing Method
t	Elapsed Time (hours or days)
t_c	Time of Start Cement Spread
t_{comp}	Time of End Compaction with Rubber-Tire Roller
t_d	Compaction Delay Time

t_e	Equivalent Age at the Reference Temperature (hours or days)
t_m	Time of First Mixing Pass
t_{max}	Time at Which T_{max} Occurs
t_{vib}	Time at End of Vibratory Compaction
$t_{\sigma max}$	Time at Which σ_{max} Was Tested
T	Average Temperature During Δt (˚C)
T_{BL}	Thermal Measurement Device Temperature
T_i	Initial Material Temperature
T_{max}	Maximum Temperature Recorded
T_r	Temperature of Reference
T_s	Temperature of Specimen
T_0	Datum Temperature (˚C)
TC	Thermocouple
TM	Thermister
TH	Holcim Cement Theodore, AL
TH_{SR475}	Holcim Cement Theodore, AL (SR475 Field Cement)
TTF	Temperature-Time Factor
UB	Upper Boundary
UC	Unconfined Compressive Tests
USACE	United States Army Corps of Engineers
USCS	Unified Soil Classification System
V	Volume
V_{PM}	Volume of Plastic Mold
W	Dry Density
W_{S-C}	Weight of Soil-Cement Material per Lift
$\bar{x}$	Mean of Sample Set
XLPRE	Cross Linked Polyethylene
$Z_{a/2}$	Z-score for a Specified Confidence Interval
Δt	Time Interval (hours or days)
ΔT	Change in Temperature (At highest point, Specimen to Reference)
ΔT_b	Change in Temperature (Air to Empty EPS Block)
ΔT_i	Change in Temperature at Time (i)
α	Level of Significance
γ	Wet Density
γ_d	Maximum Dry Density
$\gamma_{d12.5}$	Maximum Dry Density of Material Passing 12.5 mm Sieve
$\gamma_{d_{adj}}$	Adjusted Maximum Dry Density
γ_w	Unit Weight of Water
σ_{max}	Maximum Compressive Strength
$\sigma_{max\ adj}$	Adjusted Compressive Strength
ω	Moisture Content of Specimen
$\omega_{air\text{-}dried}$	Air-Dried Moisture Content
$\omega_{natural}$	Natural Moisture Content

CHAPTER 1 - INTRODUCTION

1.1 Background

Soil-cement has been a popular chemical stabilization technique for roadways, airport pavements, embankments, and foundations for decades. Soil-cement is defined by ACI (2009) and PCA (2001) as "a mixture of soil and measured amounts of portland cement (and/or other cementitious materials) and water, compacted to a high density to form a hardened material with specific engineering properties." Soil-cement technology has been used since 1915, when a mixture of shells, sand, and portland cement was blended with a plow and compacted (ACI 2009).

Soil-cement mixtures were first studied as an engineering material for roadway base courses in the early 1930s by the South Carolina State Highway Department and the Portland Cement Association (Scullion et al. 2005). Today, portland cement stabilization is one of the most widely used and economical soil stabilization methods for highways (Griffin and Tingle 2009). This is particularly the case for regions containing natural soils and aggregates with marginal engineering properties.

Soil-cement design has evolved over decades. In 1935, the Portland Cement Association (PCA) started developing procedures to produce uniform and durable soil-cement (Scullion et al. 2005). PCA ultimately developed ASTM D558, D559 and D560 to determine optimum moisture content, maximum standard proctor dry density, and minimum design cement content (Scullion et al. 2005). D559 and D560 utilize a method for determining minimum cement content based on material durability. Testing involves 12 cycles of wetting and drying or freezing and thawing, along with a specified procedure of specimen brushing to induce mass loss. The mass lost is compared to standards found from PCA acceptance criteria, and the tests provide a minimum design cement content.

Over time, many agencies have adapted to using only compressive strength criterion for soil-cement design. Correlations between durability and compressive strength were used to move away from the wet-dry test and freeze-thaw test. Agencies preferred design based on compressive strength rather than using D559 and D560. The reasons include the wet-dry and freeze-thaw tests required a longer test time (one month compared to one week), more lab equipment, and more technician involvement (Scullion et al. 2005). Also, the poor repeatability of the wet-dry and freeze-thaw tests because of brushing inconsistencies between laboratories has contributed to the reduced use of these tests in favor of design using compressive strength (Samson 1986; Scullion et al. 2005).

Unlike the uniform criterion from PCA for the wet-dry and freeze-thaw tests, agencies have adopted their own standards for design compressive strength. For example, design of soil cement in Mississippi is governed by Mississippi Test Method 25 (MT-25). The Mississippi Department of Transportation (MDOT) has set a minimum compressive strength of 2070 kPa (300 psi) for design of pavement base layers. Specimens are made at the estimated design cement index (C_I) as well as plus one and minus one percent of the estimated design cement index. One specimen is tested for compressive strength per cement index per curing time (7 or 14 days). The design cement index is the least amount of cement that produces a compressive strength of 2070 kPa or greater in 7 or 14 days.

ACI (2009) describes two general methods for mixing and constructing soil-cement pavement layers. The first method is in-place mixing which utilizes a single-shaft mixer. This method can adequately pulverize and mix practically all types of soil (granular to fine-grained), but this method may also require multiple mixing passes. The second method is central plant mixing which utilizes a rotary drum mixer, a continuous flow pug mill mixer, or a batch-type pug mill mixer. This method works best with granular borrow materials, but the mixed material must be transported (typically within 30 min) to the project site. Once on site, the material is placed using a motor grader, a spreader box, or a paver. Compaction and curing are the same for in-place and central plant mixing methods. Suitable compaction equipment includes sheeps-foot, vibratory, and rubber-tire rollers. Curing methods include continuous water-sprinkling and bituminous membranes.

Overall, design, construction, quality control, and ultimately performance of soil-cement materials has room for enhancements even after decades of use and research. Many factors influence the design and performance of soil-cement pavement layers. This report investigates factors that influence the design and performance of soil-cement pavement layers in Mississippi.

1.2 Objectives

The objectives of this study are focused on addressing issues that have arisen over the past several years associated with MDOT's soil-cement use in pavement layers. For example, density specification of chemically stabilized soils was an issue for MDOT in the years prior to State Study 206 initiation, which prompted the authors to assemble a soil-cement database and conduct proctor compaction testing that used a protocol different than what MDOT currently follows. The goal of activities such as the previous example was to enhance and modify existing design and quality control protocols related to soil-cement.

The overall objective of this report was to provide draft design and quality control guidance that could be incorporated and/or specified to improve performance of soil-cement base layers. This overall objective considered laboratory mix design protocols to select design cement contents, as well as quality control measures to enhance MDOT's ability to obtain the desired properties during construction. Additionally, this report's efforts aimed to provide information that can be used when selecting layer thicknesses during pavement design. MDOT is in the process of adopting Mechanistic-Empirical (M-E) pavement design procedures. Incorporating laboratory mix design, M-E pavement design, and construction quality control procedures together is a formidable task.

1.3 Scope

This was a multi-year project, whose original scope was revised to enhance the overall usefulness of findings. MDOT approved the revised scope of work in November of 2010, which is the scope described in the remainder of this section. The scope of work described was undertaken to meet the project objectives presented in the previous section.

Only pavement base layers constructed with MDOT Class 9C materials were considered. Class 9C soils were taken from north, central, and south Mississippi and tested in conjunction with multiple portland cements. A blend of portland cement and ground granulated blast furnace slag (GGBFS, also called slag cement) was also investigated to a

modest extent. Since cement suppliers can now deliver blended cements in a manner allowing it to be placed in a single spread, its appeal has increased relative to past years where multiple spreads were usually required.

In addition to a traditional literature review, an MDOT practice review was performed where a considerable amount of information was assembled statewide that was complimented by a survey developed and sent to all other state DOT's related to their soil-cement practices. This information was analyzed for overall trends and used as appropriate in remaining State Study 206 activities.

An experimental program was undertaken as the primary component of this study that included laboratory and field components. The experimental program investigated a variety of behaviors including proctor compaction, strength versus time, mix design considering strength variability, elastic modulus, wheel tracking, and thermal profiles. Strength variability and thermal profiles were investigated in the most detail. Strength variability was a key component for making recommended mix design changes, while thermal profile testing was primarily investigated for its usefulness in measuring cement content as part of a quality control program. Elastic modulus and wheel tracking were performed largely for purposes of mechanistic-empirical (M-E) pavement design.

A key part of the experimental program was to develop and evaluate equipment suitable for determining laboratory cement content based on unconfined compressive testing that could also be used for quality control during construction. Additionally, economical thermal profile equipment suitable for quality control construction activities was also investigated in notable detail. The specimen preparation equipment was developed so specimens could be compacted in plastic molds, thus allowing thermal profiles and compressive strength to be measured on the same specimen.

This report made use of two graduate student thesis written during State Study 206 activities. Sullivan (2012) and Anderson (2013) contain some of the same information presented in this report, and in some cases contain drawings, raw data, and survey sheets as appendices that were not incorporated into this report in the interest of brevity. Terminology was maintained between these two documents and this report to allow for the appendices in those documents to benefit this report. Both Sullivan (2012) and Anderson (2013) are publically available, and a link was provided in the references section that allows electronic download of both documents.

CHAPTER 2 - LITERATURE REVIEW

2.1 Overview of Literature Review

A literature review was performed to locate information in the areas of current soil-cement mix design procedures for stabilized base courses, soil-cement quality control, estimation of in-situ strength of constructed soil-cement layers, thermal measurements, strength gain with time, unconfined compressive strength, elastic modulus, and wheel tracking. Overall, few studies were located that incorporated thermal measurement of soil-cement mixtures into analysis or quality control, which reinforces the need for the research performed in this project.

2.2 Cement Stabilized Base Course Design

Current soil-cement design procedures are usually based on durability and/or unconfined compressive strength. Soil-cement mixtures are designed to optimize cement content for satisfactory performance and economy. The following sections contain soil-cement design procedures, criteria, and protocols developed by the Portland Cement Association (PCA), United States Army Corps of Engineers (USACE), and state Departments of Transportation (DOTs).

2.2.1 PCA Design Procedure

PCA developed a design procedure based on strength and durability criteria (PCA 1992). Strength of soil-cement mixtures is determined by unconfined compression tests according to ASTM D1633, and specimens are made according to ASTM D1632. Specimens with height to diameter (h/d) ratio of 2.00 are recommended for a more accurate determination of compressive strength. In most cases, specimens with h/d ratio of 1.15 (101.6 mm diameter and 116.4 mm height) are tested because these specimens make use of common compaction equipment (standard proctor mold and hammer). With all variables constant, specimens with 1.15 h/d ratio are reported to achieve 10 percent greater unconfined compressive strength (σ) than 2.00 h/d ratio specimens.

Durability of soil-cement mixtures is evaluated using wet-dry tests (ASTM D 559) and freeze-thaw tests (ASTM D 560). Table 2.1 contains criteria developed by the PCA for adequate base course performance of soil-cement mixtures which is documented by Terrel et al. (1979) and Scullion et al. (2005). Cement contents with specimen weight loss less than those indicated in Table 2.1 after 12 cycles of wet-dry-brushing or freeze-thaw-brushing are considered adequate to produce a durable mixture (PCA 1992).

PCA (1992) recommends that all laboratory cement contents be expressed as a percentage of dry soil mass. After determining the optimum cement content, the percentage cement by dry soil mass can be converted to a percentage by volume for field construction control. Equation 2.1 shows PCA's calculation to convert cement content by dry soil mass to cement content by volume. The percentage by volume calculation is based on the volume of a 94 pound US bag of cement (PCA 1992).

Table 2.1. PCA Soil-Cement Design Criteria (Terrel et al. 1979; and Scullion et al. 2005)

Soil Classification		Max Weight Loss for 12 Wet-Dry or Freeze-Thaw Cycles (%)	Typical σ (kPa)[1]	
AASHTO	**USCS**		**7-day**	**28-day**
A-1, A-2-4, A-2-5, A-3	GW, GC, GP, GM, SW, SC, SP, SM	14	2069 - 4137	2758 - 6895
A-4, A-5	ML, CL	10	1724 - 3447	2069 - 6205
A-6, A-7	MH, CH	7	1379 - 2758	1724 - 4137

1: Specimens were saturated in water prior to strength testing.

Additional Criteria noted by PCA (1992), Scullion et al. (2005), and Terrel et al. (1979):

- *Max volume change should not exceed 2% of original specimen volume.*
- *Max water content should be less than the quantity required to saturate the specimen.*
- *Compressive strength should always increase with age of specimen.*

$$Percent\ Cement\ by\ Volume = \frac{D - \frac{D}{C}}{94} \times 100 \qquad \text{(Eq 2.1)}$$

Where:
D = Oven-dry density of soil-cement (lb/ft^3)
$C = 1 + (C_w/100)$
C_w = Cement content by dry soil mass (%)
94 = Unit weight of US bag of cement (lb/ft^3)

2.2.2 USACE Design Procedure

USACE (1994) developed design procedures similar to PCA with slightly different criteria for durability and strength. USACE testing procedures are the same as PCA procedures. Table 2.2 shows USACE criteria for soil-cement base course materials.

Table 2.2. Soil-Cement Design Criteria from USACE (1994)

		Minimum σ at 7 days (kPa)	
Type of Soil	**Max Weight Loss for 12 Wet-Dry or Freeze-Thaw Cycles (%)**	**Flexible Pavement**	**Rigid Pavement**
Granular, PI < 10	11	5171	3447
Granular, PI > 10	8		
Silt	8		
Clays	6		

2.2.3 DOT Design Procedures

State departments of transportation (DOTs) have independently developed design procedures and criteria that are loosely based on the PCA and USACE procedures. Several variations of soil-cement design are implemented by state DOTs, but design criteria are predominantly based on unconfined compressive strength. To insure adequate durability, DOTs have developed correlations between strength and durability for the soil type being used in base course construction (Scullion et al. 2005). These correlations are used to specify a minimum compressive strength to meet durability requirements, thus eliminating separate

durability testing. DOTs have adopted compressive strength criteria for soil-cement design largely because of the need for a more expedient testing regime. Wet-Dry and Freeze-Thaw testing usually requires 4 to 6 weeks to conduct whereas compressive strength testing only requires 1 to 4 weeks (Scullion et al. 2005). Table 2.3 contains compressive strength criteria, specimen size, and curing protocols for 13 state DOTs located in the southeastern United States of America.

Table 2.3. State DOTs Soil-Cement Design Criteria

State[1]	Reference	h/d ratio[2]	Req'd σ (kPa)	Curing Protocol
AL	ALDOT (2012)	1.15	1720 to 4140	7-day moist cure, sealed, 5hr soak
AR	AHTD (2003)	1.15 or 1.00	2760	7-day moist cure, sealed, 5hr soak
GA	GDOT (2001)	1.15	2070	7-day moist cure, no soak
LA	LaDOT (2006)	1.15 or 1.00	1034 to 3450	7-day moist cure, no soak
MS	MDOT (2004)	1.15 or 1.00	2070	14-day moist cure, sealed, 5hr soak
NC	NCDOT (2002)	1.15	1380	7-day moist cure, 5hr soak
SC	SCDOT (2007)	1.00 or 0.76	NA	7-day moist cure, overnight soak
TX	TxDOT (2004)	1.33	1210 or 2070	7-day moist cure, no soak
VA[3]	VDOT (2007)	1.15	NA	7 & 28-day moist cure, 4hr soak

Note: Table information was obtained from corresponding state DOT standard specifications as of May 2012.
1: FL (FDOT 2010), KY (KYTC 2012), TN (TDOT 2006), and WV (WVDOT 2002) no longer utilize soil-cement as a base course pavement layer.
2: In some cases, specimen h/d ratio depends on material gradation.
3: Virginia requires durability testing to be performed on soil-cement mixture. Virginia also specifies use of ASTM D 806 to check cement content. All other states only check cement spread rates.

Use of supplementary cementitious materials (SCM's) such as ground granulated blast furnace slag (GGBFS) has become more popular with DOTs as a primary soil stabilizer. As of May 2012, all states, with exception of North Carolina and South Carolina, listed in Table 2.3 allow slag cement blends to be used as a stabilizer in soil-cement base courses. The potential benefits and performance of slag cement blends are documented in multiple sources (Cost and Ahlrich 2005, George 2002, George 2006).

2.3 Soil-Cement Quality Control

The American Concrete Institute (ACI) identifies six soil-cement quality control factors: pulverization, cement content, moisture content, mixing uniformity, compaction, and curing. Checking and monitoring the quality of all six factors is vital to ensure proper construction practices according to appropriate plans and specifications to produce a well performing soil-cement layer (ACI 2009). Only quality control measures relating to in-place mixing are discussed in this literature review.

Pulverization is monitored by sieve analysis with the 4.75 mm sieve as the controlling sieve size. The degree of required pulverization varies, but most specifications require approximately 80 percent of the soil-cement mixture to pass the 4.75 mm sieve and 100 percent pass the 25.0 mm sieve. Pulverization is significantly affected by the amount of moisture present in the soil (ACI 2009, PCA 2001).

Cement is normally placed using bulk cement spreaders. Cement content is monitored with spot checks and overall checks. Spot checks involve: 1) placing a sheet of canvas or metal pan of known weight and area in front of the cement spreader; 2) carefully

picking up and weighing the canvas or pan after cement is spread on top; and 3) if necessary, adjusting the cement spreader until the proper amount of cement is spread per unit area. Overall checks involve closely monitoring the area or distance in which a cement truckload of known tonnage is spread (ACI 2009, PCA 2001).

ASTM D806 and ASTM D5982 are two specifications that can be followed to determine the cement content of soil-cement mixtures. ASTM D806 utilizes a chemical analysis (titration method) of CaO content in hardened soil-cement samples to determine cement content. This method requires soil-cement samples to have a significant degree of cement hydration or hardening and is not applicable to soils containing significant amounts of dissolved calcium oxide. ASTM D5982 uses a thermal measurement approach to estimate cement content of freshly mixed, uncompacted soil-cement. This method measures the peak temperature from an exothermic reaction between the calcium hydroxide in the soil-cement mixture and a sodium acetate-glacial acetic acid solution.

Optimum moisture content (OMC) determined in the lab is used as a guide for field control during construction. On site, moisture content is typically estimated by observation and feel. A mixture at OMC will usually dampen the hands when squeezed into a tight cast, and the cast can be broken into two pieces with little or no crumbling. Actual moisture contents can be checked by nuclear or conventional methods (ACI 2009, PCA 2001).

Mixing uniformity is evaluated by visual inspection throughout the entire mixing depth. Checking mix uniformity is performed by digging trenches or a series of holes at regular intervals for the full depth of treatment. Uniform color and texture signifies adequate mixing, whereas, streaked appearance suggests inadequate mixing of materials (ACI 2009, PCA 2001).

Proper compaction equipment is dictated by the soil type, and generally soil-cement should be compacted between 95 and 100 percent of maximum density as determined by moisture-density tests. Compacted densities are typically checked with a nuclear density gauge immediately after compaction operations are complete (ACI 2009).

Typical curing protocols specify a bituminous membrane to be applied to the finished grade at a rate between 0.82 and 1.63 L/m^2 (USACE 1994). Prior to applying the bituminous membrane, the finished soil-cement surface should remain moist and free of loose material. Most specifications require 3 to 7 days of undisturbed curing before traffic or subsequent paving layers can be placed on the soil-cement layer.

2.4 Traffic Opening and Early Age Properties

Teng and Fulton (1974) evaluated the performance of several soil-cement test sections located on Mississippi state route 395. Two of these sections were constructed to compare the effects of undisturbed curing and artificial trafficked curing of a soil-cement base course. Both sections were constructed with AASHTO A-2 soil (MDOT Class 9C) and were stabilized with Type I portland cement at a dosage of 6.5 percent by volume of raw soil with a target strength of 3540 kPa (no further clarification was given for cement content calculations using volume of raw soil). After 7 days of curing, cracks in the soil-cement layer were mapped, and subsequently the soil-cement layer was covered with asphalt pavement. After 2 years, each section was mapped again for cracks in the asphalt pavement. The pavement mapping was compared to the soil-cement mapping to determine how well each soil-cement curing method prevented reflective cracking. It was concluded both the

undisturbed and artificially trafficked sections yielded numerous fine cracks, and for the most part, cracks did not reflect through the asphalt pavement. Based on these results, the traditional 7 day no-traffic curing period was recommended to be deleted from specification.

Findings of Teng and Fulton (1974) were later supported by George (2006). George (2006) evaluated the performance of several soil-cement test sections (9C material, target strength of 2070 kPa) on Mississippi State Route 302, and two of these sections investigated precracking or preloading of the soil-cement layer after 1 day cure. George (2006) concluded that precracking techniques produced numerous fine cracks which do not reflect through the pavement surface and recommended the implementation of precracking techniques. Benefits of precracking in soil-cement layers are well documented (Adaska and Luhr 2004, George 2002, George 2006, Sebesta 2005).

PCA (2001) and Halsted et al. (2006) suggest soil-cement layers can be opened to low-speed local and construction traffic provided the soil-cement mixture has sufficiently hardened to resist marring or permanent deformation and proper curing protocols are not impaired. Also, subsequent pavement layers can be placed soon after construction given the soil-cement layer has hardened sufficiently to resist marring or permanent deformation. George (2002) recommends that subsequent pavement layers be constructed no sooner than 3 days but no later than 7 days after construction of the soil-cement layer. Early placement of subsequent pavement layers may prevent moisture loss from the soil-cement layer, thus mitigating potential for shrinkage cracking. Early trafficking and early placement of subsequent pavement layers offer several benefits, but it is critical to evaluate the in-situ strength of the soil-cement layer to ensure the layer will not sustain permanent damage.

2.5 Measurement of In-Situ Strength

According to Griffin and Tingle (2009), there is no standard method for determining the strength capacity of cement stabilized soils after construction other than field cores. Two potential non-destructive approaches for monitoring the extent of cement hydration in soil-cement mixtures were identified. The first approach is field measurements using devices such as the dynamic cone penetrometer, Clegg Hammer, soil stiffness gauge, Proceq Type PT test hammer, and portable falling-weight deflectometer. These devices are referred to as Strength Estimating Devices in this report. The second approach is the maturity concept for cementitious materials.

2.5.1 Strength Estimating Devices

Guthrie et al. (2005), Abu-Farsakh et al. (2004), and Okamoto et al. (1991) presented favorable results supporting the use of the dynamic cone penetrometer, Clegg Hammer, soil stiffness gauge, Proceq Type PT test hammer, and portable falling-weight deflectometer as indicators of strength gain in cement treated bases. Griffin and Tingle (2009) conducted a similar study and compared the instrument readings with compressive strengths and modulus values from traditional laboratory tests. The study reported a poor to moderate relationship between instrument measurements, actual strength, and modulus measurements. Griffin and Tingle (2009) concluded that these instruments are better served to monitor strength gain rather than predict actual strength.

2.5.2 Maturity Method

The maturity method is an analysis approach used to account for the combined effect of time and temperature on the development of hydration and strength of cementitious materials (Carino and Lew 2001). Saul (1951) proposed the following principle which is known as the maturity rule: "Concrete of the same mix at the same maturity (reckoned in temperature-time) has approximately the same strength whatever combination of temperature and time go to make up that maturity." There are two predominant maturity functions presented in literature which are derived from the work of Nurse (1949), Saul (1951), and Hansen and Pederson (1977). ASTM C1074 refers to these functions as temperature-time factor and equivalent age, respectively.

Nurse (1949) and Saul (1951) examined the strength development of concrete at different elevated temperature curing methods and proposed that the product of time and temperature could be utilized for the purpose of characterizing strength development. This idea led to the development of Equation 2.2 which is commonly known as the Nurse-Saul maturity function (Carino and Lew 2001, Tikalsky 2003).

$$M = \sum_{0}^{t} (T - T_0)\Delta t \qquad \text{(Eq 2.2)}$$

Where:
M = Maturity index (ºC-hours or ºC-days)
T = Average temperature during Δt (ºC)
T_0 = Datum temperature (ºC)
t = Elapsed time (hours or days)
Δt = Time interval (hours or days)

Equation 2.2 is based on the assumption of a linear relationship between the initial rate of strength gain and temperature. This approximation has been stated by some to be invalid when curing temperatures vary over a wide range. Chanvillard and D'Aloia (1997) noted that the Nurse-Saul equation tends to underestimate the influence of high temperatures on compressive strength development at very early ages and overestimate at later ages. Despite controversy, Equation 2.2 is still a widely used means to characterize maturity of cementitious materials. A similar maturity function was proposed by Hansen and Pederson (1977) and is based on the Arrhenius equation shown in Equation 2.3.

$$t_e = \sum_{0}^{t} \left[e^{\frac{-Ea}{R}\left(\frac{1}{T} - \frac{1}{T_0}\right)} \right] \times \Delta t \qquad \text{(Eq 2.3)}$$

Where:
t_e = Equivalent age at the reference temperature (hours or days)
E_a = Apparent activation energy (J/mol)
R = Universal gas constant (8.314 J/mol-K)
Δt = Time interval (hours or days)

T = Average absolute temperature during interval Δt (Kelvin)
T_0 = Absolute reference temperature usually 296 K (Kelvin)

The Arrhenius equation characterizes the effect of temperature on the rate of a chemical reaction. Equation 2.3 incorporates the Arrhenius equation which allows for a non-linear relationship between the initial rate of strength gain and temperature. The nonlinear maturity function is believed to better represent the effect of temperature on strength development over a wide range of temperatures. However, this maturity function is unreliable to predict the effects of early-age temperature on later-age strength according to several researchers (Carino and Lew 2001, Schindler 2004, Chitambira et al. 2007).

The key parameter in Equation 2.3 is the mixture apparent activation energy (E_a). The apparent activation energy defines the temperature sensitivity of the hydration process and the rate of strength development of a particular cementitious mixture. A higher value indicates a greater sensitivity to changes in temperature while a lower value indicates a lower sensitivity. The activation energy is determined by first evaluating the hydration extent as a function of time. Unconfined Compressive (UC) strength is a commonly measured parameter for cementitious materials and is a function of the degree of hydration; therefore, UC strength can be used to evaluate the hydration process (Chitambira et al. 2005). Chitambira et al. (2007) presents a simple graphical method for determining the apparent activation energy. This approach is similar to methods described in ASTM C1074. Table 2.4 shows a range of apparent activation energies for a variety of cementitious materials.

Table 2.4. Apparent Activation Energy from Literature

Cement Type	Mixture Type	Type of Testing[1]	*E* (J/mol)	Reference
Type I[2]	Concrete	SAC	41,977 to 46,269	Schindler (2004)
Type II	Concrete	SAC	41,788	Schindler (2004)
Type III	Concrete	SAC	49,955	Schindler (2004)
Type IV	Concrete	SAC	39,978	Schindler (2004)
Type V	Concrete	SAC	37,461	Schindler (2004)
Type I, *PFA*[3]	Soil, Sand	SAC	63,220 to 70,990	Chitambira et al. (2007)
Type I, Lime, *SCB*[4]	Soil, Sand	SAC	63,220 to 70,990	Chitambira et al. (2007)
Type I	Cement Paste	IC	39,000	Ma et al. (1994)

1: SAC = Semi-Adiabatic Calorimetry; IC = Isothermal Calorimetry.
2: Sampled from three sources.
3: PFA = pulverized fuel ash.
4: SCB = Soil-Cement Bentonite.

The maturity approach is commonly used in the concrete industry to predict in place concrete strength. Mohsen et al. (2004) documents the widespread use of the maturity concept in concrete highway construction. Other works document the successful application of maturity concepts to chemically stabilized soils (Anday 1963, Circeo et al. 1962, and Chitambira et al. 2005, 2006 and 2007).

Anday (1963) used the maturity concept to compare field cured and laboratory cured specimens of lime stabilized cohesive soils. Lab specimens were cured under accelerated conditions in an oven at 49 °C. Specimens cured under these conditions for two days were found to have the same strength as field specimens at about 3,000 ºC-days using a datum temperature of 0 °C. The actual curing temperature for each lab cured specimen was taken to be the temperature of the oven (49 °C).

Circeo et al. (1962) compiled over 500 sets of data for portland cement treated soils with varying curing times up to five years and was able to develop a relationship between curing time and UC strength. The relationship was observed to be both semi-logarithmic and logarithmic in nature. The study concluded that the relationship was affected by cement content, curing temperature, specimen density, moisture content, chemical additives, soil type, specimen size, and curing protocols.

Studies conducted by Chitambira et al. (2005, 2006, 2007) have shown that the maturity method using the apparent activation energy derived from UC-temperature results can be used to model the hydration of cement stabilized soils. These works demonstrate the applicability of modeling cement hydration using the maturity concept and the Arrhenius equation approach.

2.6 Thermal Measurements Testing

Thermal measurements testing is sometimes referred to as Semi-Adiabatic Calorimetry (SAC) or thermal profile testing. Thermal measurements testing is defined by Cost and Gardiner (2009) as the "process of measuring and recording the changing temperatures of a hydrating cementitious sample, with relatively little influence from ambient temperature changes, as an indication of the hydration heat energy evolved from the sample." The thermal profile of a specimen refers to the graph of changing temperatures over time during the initial hours of hydration. Thermal profile characteristics (e.g. magnitude and timing of peaks, shape, etc.) can be useful in analysis as indicators of mixture performance when compared to other similar mixtures of known performance (Cost and Gardiner 2009). It is important to note that thermal measurement testing cannot provide quantified measurements or corrected approximations of actual hydration heat like in isothermal or adiabatic calorimetry but can serve as a simple and expedient tool for comparison of relative performance of a particular mixture (Morabito 1998).

Thermal measurement devices are relatively simplistic in nature, which is a notable advantage over isothermal or semi-adiabatic calorimetry. Devices usually consist of the following components: insulation provided by a thermos flask or some form of polystyrene or equivalent material; instrumentation in the form of thermistors or thermocouples; and data logging devices to record temperature measurements over time. The amount of insulation and the instrumentation type for a device largely depend on the objectives and goals of a particular study (Cost and Gardiner 2009, Morabito 1998). According to Morabito (1998), most thermos flask devices can only accommodate specimens of 2.5 kg or less. Alternatively, devices utilizing polystyrene material as insulation can be built to accommodate cylindrical or cube specimens of any size. The cement and concrete industries utilize thermal measurements to evaluate setting characteristics, compatibility of different cementitious materials, sulfate balance, and early strength development of concrete, mortar, and paste mixtures. In a limited capacity, this technology has been applied to stabilized soils (Sullivan et al. 2012).

Sullivan et al. (2012) conducted thermal measurement testing on cementitiously stabilized clays at high moisture contents. The study showed that thermal measurement equipment is capable of detecting and recording thermal profiles of cement stabilized soils at low cement dosages (as low as 3% by mass was tested). Also, the magnitudes, shape, and timing of thermal peaks were directly influenced by specimen size, amount of insulation, and

mix proportions (namely cement and water). The study also developed specimen preparation protocols where the thermal profile and UC strength were measured on the same specimen. Sullivan et al. (2012) concluded that thermal measurement testing shows merit as a potential quality control measure in the laboratory and field.

Peethamparan et al. (2008) performed thermal profile and UC tests on kaolinite clays stabilized with cement kiln dust. Separate specimens were prepared for thermal profile testing and UC testing. Temperature profiles and UC strength data clearly demonstrate performance differences in the four cement kiln dusts tested. From a design perspective, thermal measurement and UC strength results gave an indication of the effectiveness of the cementitious material as a soil stabilizer.

Scavuzzo (1991) utilized a thermal measurement approach to determine the cement content of freshly mixed soil-cement by measuring the heat of neutralization. In the study, uncompacted freshly mixed soil-cement was mixed with a sodium acetate-glacial acetic acid buffer solution and the peak temperature rise of the resulting exothermic reaction was recorded using thermal measurement equipment. The amount of heat generated was proportional to the quantity of cement in the sample. The relationship between the heat generated and cement content was linear. A calibration curve was developed in the laboratory which correlated the measured peak temperature and cement content for a particular mixture. The proposed test method would allow for the cement content to be checked in the field in approximately 15 minutes and would be ideal for quality control and quality assurance. For field applications, Scavuzzo (1991) concluded that the cement content of a soil-cement mixture can be predicted within ±1% of actual cement content.

2.7 Strength Gain with Time Literature Review

Strength gain with time was investigated by Felt and Abrams (1957) for four different soil cement materials. In general, strength gain between time periods became smaller as time progressed for the sandy materials. Figure 2.1 plots strength gain versus time of an A-2-4 material at different cement contents.

As curing time increased, there was a less drastic strength increase. Also, the authors noted specimens that were dried at 54˚C for 6 days after a 21 day moist cure before compression testing exhibited approximately twice the compressive strength as those that were completely moist cured. Specimens of different h/d ratios (1.15 and 2.00) were tested and compared to ASTM C42's correction. The correction evaluated was a strength correction factor for conversion between a 2.00 to a 1.15 h/d ratio. The correction factor was to multiply a 2 h/d ratio strength by 1.1 to obtain an equivalent strength of a 1.15 h/d ratio. Results aligned with published corrections in ASTM C42.

George (2006) conducted a field trial study in order to find materials, additives, and procedures that would help solve the problems with crack susceptibility in cement-treated materials. Six test sections were designated for the study, including different material/additive/procedure combinations. The study used the falling weight deflectometer (FWD) for deflection and modulus testing, cored samples for unconfined compression testing, and dynamic cone penetration for subgrade testing.

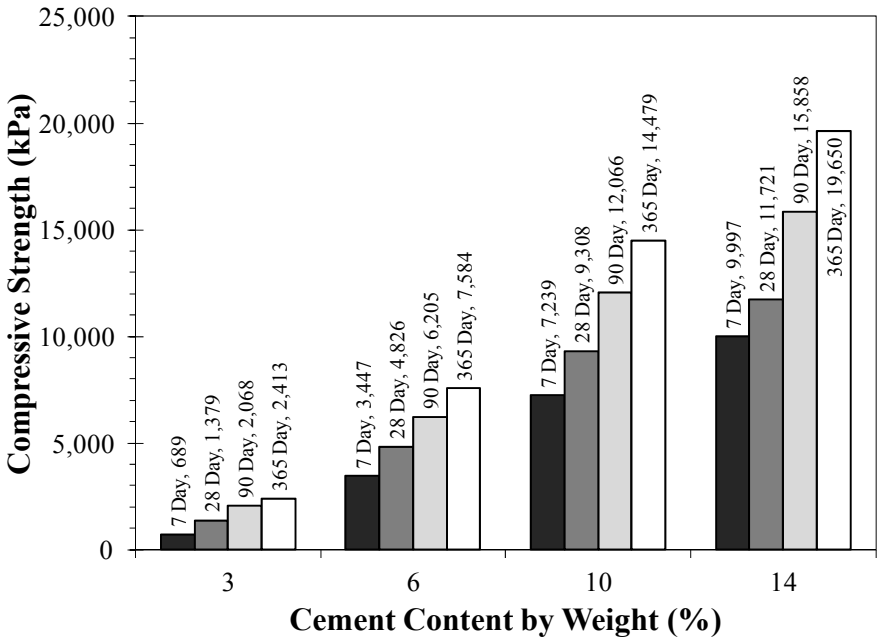

Figure 2.1. Strength vs. Time of A-2-4 Soil from Felt and Abrams (1957)

Cores were cut from the test sections after specified curing times. The first cores were cut after 28 days of curing. Coring was performed with typical pavement coring equipment. Samples were wiped dry before being brought to a laboratory for testing. Two to three cores were taken from each test section. Compressive strengths were found in accordance with ASTM D 1633. Since h/d ratios were different for each core, all strengths were normalized to an h/d ratio of 2:1 and reported. Table 2.5 reports test section description and compressive strengths of sampled cores.

Table 2.5. Field Core Compressive Strengths from George (2006)

			Compressive Strength (kPa)		
Section ID	**Additives/%**	**Procedures**	**28 day**	**440 day**	**1564 day**
1A/3A	Cement/5.5	Control	710	1670	1730
2	Cement/5.5	Precracked	880	2370	3370
1B/3B	Cement/5.5	Precut	1070	1910	2630
4	Cement/3.5 Fly Ash/8	---	910	2470	3270
5	Lime/2 GGBFS/6	---	1390	3720	5730
6	Lime/3 Fly Ash/12	---	240	910	1280

Note: All material stabilized was an MDOT Class 9c material.
Additive/% - Denotes additives used in section/Percent by mass of additives

The author noted that all the compressive strengths increase during both time intervals: 28 to 440 days and 440 to 1564 days. However, the amount of increase between additives and procedures was different. It was seen that the conventional approach to constructing cement treated layers (1A/3A) yielded lower compressive strengths than the

procedures including precutting and precracking. The highest increases in strength occurred with the use of lime and GGBFS.

Okyay and Dias (2010) conducted an experimental study that investigated mechanical properties of cement and lime stabilized soils for pile supported load transfer platforms. A portion of the study included obtaining the behavior with regard to compressive strength of these materials over time. The authors tested compressive strength of specimens at 7, 28, 90, and 350 days.

The material used in the study was classified as inorganic silt with low plasticity, ML, according to the unified soil classification system and an A-4 according to the AASHTO classification system. The liquid limit of the A-4 material was 30 with a plasticity index of 10. Cylindrical specimen dimensions were 100 mm tall by 50 mm diameter. Specimens were compacted to standard proctor dry density and optimum moisture content by means of static compaction pressure (2200 kPa) at a rate of 1 mm/min. Curing took place in plastic bags at 20˚C for the assigned curing duration. Compression tests were conducted at a constant loading rate of 0.1 mm/min. Table 2.6 shows the notation, additive concentrations, and the number of replicates of each for compression strength tests. Figure 2.2 shows the strength gain with time for each of the combinations given in Table 2.6.

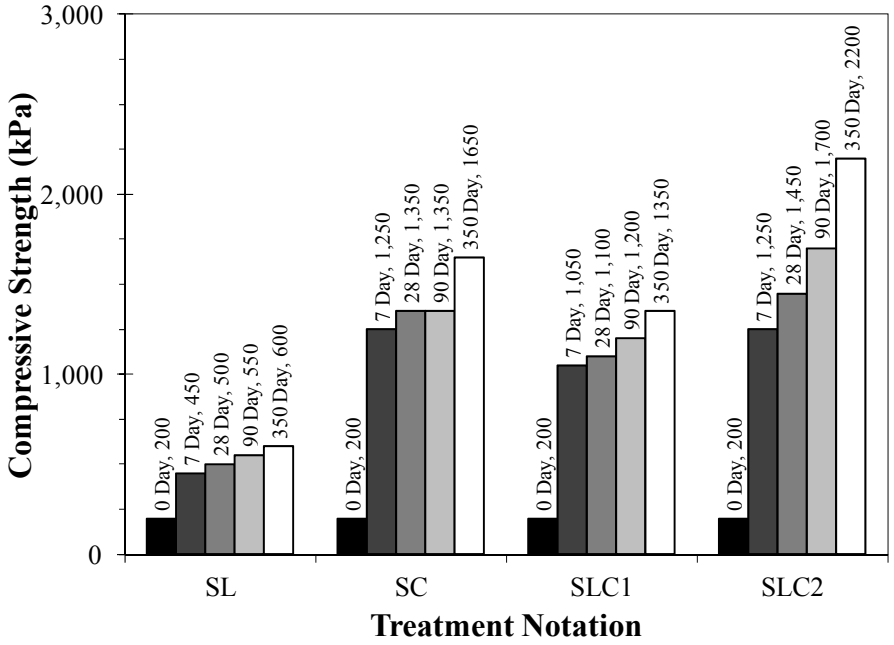

Figure 2.2. Strength Gain with Time from Okyay and Dias (2010)

Table 2.6. Compressive Strength Information from Okyay and Dias (2010)

	Treatment	Additive Concentration by Wt.		
Materials	**Notation**	**Lime (%)**	**Cement (%)**	***n***
Soil + Lime	SL	3	---	12
Soil + Cement	SC	---	6	12
Soil + Lime +Cement	SLC1	2	3	12
	SLC2	2	5	12

Values taken from Figure 6 in Okyay and Dias (2010)

The authors noted that the compressive strength of the specimens increased with time. However at some point, the strengths seemed to plateau. Material treated with only cement achieved more than 80% of 350 day compressive strength in the first 90 days. The authors found that SC, SL, and SLC1 exhibited the same strength behavior over time. Behavior over time of the SC, SL, and SLC1 treatments can be represented by a linear logarithmic function shown in Equation 2.4.

$$q_t / q_{28} = 0.81 + 0.058 \ln(t) \quad \text{(Eq. 2.4)}$$

Where:
q_t = strength after t days of curing
q_{28} = strength value at 28 days after curing
t = curing time in days

2.7.1 Unconfined Compression Strength Variability Literature Review

Felt and Abrams (1957) conducted a variability study on twenty-four 7.1 cm diameter by 14.2 cm tall cylinders, at 6% and 14% cement contents by mass. Material used for this study was an AASHTO classified A-4. Specimens were cured in a moist room for 28 days. Results can be found in Table 2.7. The authors concluded the variability results were good to excellent in the case of compressive strength (σ_{max}) of the soil cement mixture.

Table 2.7. Felt and Abrams (1957) Compressive Strength Variability

Test	C_w (%)	n	Mean	Stdev	COV (%)
σ_{max} (kPa)	6	6	3378	241	7.1
	14	6	6426	172	2.7

Kasama et al. (2007) experimented with the high strengthening of cement treated clay by mechanical dehydration in order to produce material with comparable strength to concrete. The authors conducted a literature review on the compressive strength of cement treated soils. A comparison of cemented material types was created within the findings of the literature review. The compressive strengths literature investigation included proceedings from the 26th to the 34th (in 1999) Japan National Conference on Geotechnical Engineering. The author acknowledged several factors (i.e. cement content, cure time, moisture content, curing environment) influence compressive strength. The statistics gave a general reference for the mean unconfined compressive strength, coefficients of variation, and maximum unconfined compressive strengths for the values found in the proceedings. A wide range of materials was included in the literature findings with mean compressive strengths from 260 to 10,740 kPa. Authors suggested that more variation in compressive strength was found with decreasing grain size.

Varner (2011) conducted a variability study on in place cement treated pavement layers within MDOT highway projects. Design requirements for cement treated pavement layers changed in 2004 and the study was to investigate the variability of the new design standards. The variables that were considered in the study were layer thickness, unit weight, cement content, and unconfined compressive strength. Two highways were included in the study: a section of Highway 84 in Jefferson Davis County and a section of Highway 25 in

Winston County. Twenty cores were taken from each location, along with unstabilized base material from the shoulder of the roadway.

The material from Highway 84 classified as an A-2-6 with a design cement content by weight of 3.8%; the material from Highway 25 classified as an A-2-4 with a design cement content by weight of 3.1%. Unconfined compression strengths were corrected for different h/d ratios because cores were not the same length after coring and trimming. The design requirement for unconfined compression strength was 2068 kPa. Table 2.8 shows the adjusted unconfined compression strength statistics obtained for each tested highway.

Table 2.8. Hwy 84 and 25 Compressive Strength Variability

Highway	n	Mean (kPa)	Stdev (kPa)	COV (%)	% Meeting σ Req'd
84	17	4579	1251	27.3	100
25	19	2437	844	34.7	63

Specimens adjusted based on lab produced correlation to h/d ratio of 1.15:1.

The author noted the higher COV values for the compressive strength of the field cores indicate the presence of poor construction methods and poor quality control methods. The author recommended the following with regard to the study: cement content be prescribed as a percent by mass and that unconfined compression strength should be included in the quality control program for cement-treated pavement layers.

2.8 Modulus Literature Review

Reinhold (1955) investigated the elastic behavior of four blended materials (Table 2.9), made from fine material with Heppenheim clay. Rectangular specimens were made at optimum moisture content and were 7.07 by 7.07 by 23.21 cm. Compression testing was performed with a 500 ton hydraulic testing machine. Strain measurements were taken on the middle 10 cm of each specimen by a mirror apparatus. The cement content was prescribed as a ratio of cement to dry soil. For example, the 1:6 cement to soil ratio denoted one part cement to six parts dry soil by weight. Table 2.9 provides average test results. σ_{MAX} was defined as the maximum compressive stress and E_e was defined as the real elastic modulus up to 0.33 σ_{MAX}.

Reinhold (1955) noted the stress strain diagrams indicated the materials behaved almost perfectly elastically up to approximately 0.33 σ_{MAX}. Thus, E_e in Table 2.9 shows the average elastic modulus of each material and cement content in the region up to 0.33 σ_{MAX}. The author stated the elastic behavior of soil cement is generally a function of its strength. The data suggests that higher cement contents within a mixture produce higher elastic modulus values. The research concluded that (1) compressive strength is the determinant for soil cement elastic behavior, (2) density, cement content, moisture content, and clay content influence elastic behavior of soil cement, (3) and a linear stress-strain relationship can be assumed up to one third of a specimen's compressive strength.

Felt and Abrams (1957) provided a range of strength and elastic properties in soil cement mixtures with different soils, described relationships between these properties, and showed new methods to develop and perform the tests. Also provided was a brief variability study on elastic modulus. The paper was part of a comprehensive study of soil cement mixture physical characteristics. Four different soils from Illinois were tested; in particular

Soil 2, an A-2-4 soil based on the U.S. Bureau of Public Roads classification. Specimens used for determining modulus of rupture, static modulus of elasticity in flexure, dynamic resonance modulus, dynamic Poisson's ratio, and modified cube compressive strength tests were 7.6 by 7.6 by 28.6 cm beams. Specimens used for compressive strength, static elastic modulus in compression, and static Poisson's ratio were 7.1 cm diameter by 14.2 cm tall cylinders. Specimens used only for compressive strength were 5.1 cm diameter by 5.1 cm tall cylinders. Also, 10.2 cm diameter by 11.7 cm tall cylinders were used for compressive strength. Specimens were compacted to ASTM D558-44 (standard proctor) optimum moisture and maximum density.

Table 2.9. Average Elastic Properties, Reinhold (1955)

Soil	Sand (%)	Clay (%)	LL (%)	PI (%)	Cement:Soil Ratio	σ_{MAX} (kPa)	E_e (GPa)
A	100	0	---	NP	1:6	8766	13.6
					1:8	5796	11.0
					1:10	4179	8.9
C	75	25	17	NP	1:6	11769	14.0
					1:8	7854	11.2
					1:10	5649	9.1
D	50	50	25	9	1:6	7119	9.1
					1:8	4914	8.1
					1:10	3972	6.5
F	0	100	39	18	1:6	5250	4.5
					1:8	3825	3.8
					1:10	2943	2.9

The author utilized a compressometer outfitted with an SR-4 clip gage to measure displacements in the middle 7.6 cm of each specimen. Specimens were capped with gypsum plaster before testing. Elastic modulus in compression as well as compressive strength specimens were aged in a moist environment for 7, 28, and 90 days. 365 day tests were also cured for compressive strength tests. The elastic modulus in compression was taken as the secant modulus at approximately 33% of the ultimate load. For the A-2-4 soil, the elastic modulus in compression ranged from 2.1 GPa to 19.3 GPa at cement contents ranging from 3 to 14% by weight. The author compared elastic modulus in compression values with the work of Reinhold (1955), finding similar results for similar materials. This work concluded that modulus of rupture, compressive strength, and modulus of elasticity depend on soil type, cement content, curing time, and curing method. It was also noted that all parameters increased as the cement content and moist curing time increased.

Table 2.10. Felt and Abrams (1957) Elastic Modulus Variability

Test	C_w (%)	n	Mean	Stdev	COV (%)
E_{sc} (GPa)	6	6	3.5	0.26	7.3
	14	6	4.6	0.36	7.8

The authors conducted a variability study on twenty-four 7.1 cm diameter by 14.2 cm tall cylinders, at 6% and 14% cement contents by mass (Table 2.10). Material used for this study was an AASHTO classified A-4. Specimens were cured in a moist room for 28 days.

The authors concluded the variability results were good to excellent in the case of elastic modulus in compression (E_{sc}) of the soil cement mixture.

A study was performed to investigate the shear strength and elastic properties of typical lime and soil mixtures and to determine any relationship between the elastic properties and the unconfined compressive strength of these mixes. Four typical soils in Illinois were classified as an A-7-6 (18), A-6 (6), A-6 (8), and A-4 (8). The lime used was a commercially produced high-calcium hydrated lime. Specimens dimensions were 50.8 mm tall by 101.6 mm diameter compacted in three lifts, with a compaction effort of 20 blows per layer with a 1.8 kg hammer dropped from a height of 305 mm. Specimens were compacted to maximum dry density and optimum moisture content. Curing took place in a sealed container at 49˚C for 0, 1, 2, 4, and 6 days. Compression testing was at a rate of 1.27 mm/min and was conducted with confining pressures from 0 to 241 kPa. Readings of load and total deformation were recorded during testing.

Confining pressure was found to have little effect on the calculated elastic modulus values. Elastic modulus values were noted to be much higher after the addition of lime. These elastic modulus values for the lime-soil mixtures ranged from 0.14 GPa to 1.10 GPa. A linear regression analysis (Equation 2.5) was conducted between the unconfined strength and elastic modulus of the specimens that were tested at a confining pressure of 103 kPa. Analysis found a highly significant regression at an $\alpha = 0.01$.

$$E = 9.98 + 0.124q_u \qquad \text{(Eq. 2.5)}$$

Where:
E = Elastic Modulus (ksi)
q_u = unconfined compression strength (psi)

Kolias and Williams (1984) derived a relationship between a term referred to as gradation modulus (defined in the next paragraph), uniaxial compressive strength, and the modulus of elasticity of typical materials used in cement stabilization. The method proposed gives a rapid approximation of the modulus of elasticity without laboratory testing, which could be used for pavement analysis. The authors used data from a previous study, as well as data from Reinhold (1955). Materials ranged from a flint gravel aggregate to a fine grained silty material. Specimens used for the procedure included prismatic (101.6 by 101.6 by 254 mm) and cylindrical (101.6 mm diameter by 254 mm tall) types compacted to refusal according to British Standard Methods for Stabilized Soils (BS 1924:1967). Reinhold (1955) compacted specimens to maximum standard proctor density. Gradation modulus correlation to elastic modulus was stronger than that of mean aggregate size. Trends were further strengthened through data obtained from other literature, including Williams and Patankar (1968), Fossberg et al. (1972), Felton (1975, unpublished), Felt and Abrams (1957), and Toklu (1976).

Gradation modulus (G) is found by adding the percentages passing the standard ASTM 37.5 mm, 19.0 mm, 9.5 mm, 4.75 mm, 2.36 mm, 1.18 mm, 600 µm, 300 µm, 150 µm, and 75 µm sieves and dividing by 100. Equation 2.6 is used to determine an approximate modulus of elasticity for cement stabilized materials. The authors noted that good agreement was found between data collected for prediction of elastic modulus and data used from other publications as verification of the method.

$$E_{fp} = (15.5\text{-}1.3G)(f_p)^{1/2} \quad \text{(Eq. 2.6)}$$

Where:
E_{fp} = modulus of elasticity at a strength level of f_p (GPa)
f_p = uniaxial compressive strength (MPa)
G = Gradation modulus

James et al. (2009) conducted a study on the effects of compaction and moisture content on the strength of soils that are chemically stabilized and used in Mississippi pavement construction. Seven soils typically found in Mississippi were tested ranging from silty clays to clayey sand. Three of the soils were similar to those evaluated in this report. Specimens were prepared with different standard proctor compaction efforts at OMC and +3% over OMC, using three equal lifts per specimen. Phase one utilized the CBR (ASTM D1883) and UC test (MT-26) to relate behaviors to the presently used pavement structural design procedures used by MDOT. Phase two utilized the resilient modulus test (per NCHRP 1-28A document) for lime stabilized materials and UC tests for cement stabilized and lime/fly ash stabilized materials. The study used Equation 2.7 to calculate elastic modulus. A sample of elastic modulus values from materials similar to ones used in the present study are provided in Table 2.11.

Table 2.11. Cement Stabilized Elastic Modulus (James et al. 2009)

Mat. ID	USCS Mat. Type	C_w (%)	Blows per Lift	% Proctor γ		Elastic Modulus (GPa)			
						@ OMC		@ OMC + 3%	
				OMC	+3% OMC	7 Day	14 Day	7 Day	14 Day
5	SM	5	10	92.1	94.0	0.4	0.6	0.5	0.6
			25	98.2	97.8	0.7	0.9	0.5	0.9
			40	100.8	97.8	0.9	1.2	0.5	0.7
6	SM	5	10	91.4	95.1	1.4	1.7	1.1	1.4
			25	98.6	96.8	2.6	2.5	1.3	1.6
			40	101.3	97.2	2.3	2.9	1.4	1.7
6R	SM	4	10	92.7	94.6	2.1	2.4	1.7	2.0
			25	99.7	96.3	2.9	3.4	1.4	1.7
			40	101.2	96.9	2.9	3.4	1.3	1.5
7	SC	5	10	88.0	92.0	1.1	1.4	1.7	2.0
			25	97.7	96.7	2.4	2.7	1.9	2.5
			40	101.1	97.1	3.0	4.0	2.0	2.5

Note: Materials shown are A-2-4 according to AASHTO classification.
C_w represents portland cement content based on weight of dry soil.
All elastic modulus values calculated from Equation 2.4.
Percent of density calculated from 7 and 14 day average.

$$E = 1200 * q_u \quad \text{(Eq. 2.7)}$$

Where:
E = Elastic Modulus (psi)
q_u = unconfined compression strength (psi)

The study found that, although a smaller density range was observed for cement stabilized materials compared to other stabilizing methods investigated, there was an increase in compressive strength and elastic modulus with an increase in density. In some cases, increasing the amount of blows per layer from ten to forty doubled the elastic modulus, while in other cases only increased it by approximately 50%. Also, it was found OMC +3% generally produced lower elastic modulus compared to specimens made at OMC. Material characterization of soil cement layers for the MEPDG is not well established as acknowledged in the background information of the problem statement for NCHRP 04-36. The MEPDG uses elastic and/or resilient modulus at 28 days as the primary performance parameter.

2.9 Rutting and Wheel Tracking Literature Review

Scullion et al. (2005) evaluated the effectiveness of a wheel tracking durability test. Durability tests were once part of the design process (i.e. AASTHO T135 and T136). The authors used the South African Wheel Tracking Test to evaluate durability.

The South African Wheel Tracking Test is an erosion durability test that measures the rutting of prismatic specimens under a loaded wheel. The prismatic specimens are submerged in water, covered with a rough neoprene membrane, and tracked with a 17.78 kg beveled rim wheel. The depth of erosion is measured at 15 points along the specimen after 5000 passes. Averaging these depths yields the erosion index for the test. Specimens were cured for 21 days.

After testing, the authors concluded the wheel tracking test was helpful in determining how the cemented materials react to the abrasive service conditions. Rutting measurements ranged from 0.2 mm to 4.8 mm. Some material/cement content combinations failed the wheel tracking test (>1 mm of rut) while passing other vital design specifications. However, it was concluded that the South African Wheel Tracking test requires specialized equipment and is not readily found in the U.S. The authors recommend this test only be used for research purposes, special studies, or unusual materials that need further study.

Wu and Yang (2012) conducted a study to compare the MEPDG design software to pavement performance data from the pavement management system in Louisiana on 40 strategically selected asphalt concrete pavements including 16 with soil cement bases. Also, the authors used this study to develop local calibrations for the MEPDG model for use in the state. The study used the traffic, climate, materials, and structural characteristics of the region in the model. Conclusions were that the MEPDG over-predicted the rutting of pavements with asphalt concrete over a soil cement base layer. This over-prediction was most likely from the high rutting in the subgrade. The authors indicated that the MEPDG model for rutting does not take into account rutting from the soil cement layer; there is no rutting model for cemented base layers in the MEPDG.

CHAPTER 3 - PRACTICE REVIEW

3.1 General Overview of Practice Review, Database, and DOT Survey

In Mississippi, use of cement stabilized soil for pavement base course layers was widespread as of the date of this report. As of early 2009, the majority of MDOT chemical stabilization activities incorporated portland cement (around 90% according to informal conversation). This chapter details current laboratory test methods used by MDOT to design soil-cement base courses. This chapter also includes a detailed analysis of the *MDOT* soil-cement database, which includes all soil-cement mixture designs performed from 2005 through 2010 that were made available by the MDOT Materials Division (raw data is provided in Sullivan (2012) Appendix A) Additionally this chapter presents findings of a DOT survey sent to other states that includes soil design procedures, testing approaches, results evaluation, and pending concerns within the practice (a copy of the survey is provided in Anderson (2013) Appendix D).

3.2 Materials Criteria

All of the material used in soil-cement base course construction must meet the criteria outlined in section 700 of MDOT (2004). The soil must classify as Class 9 Group C (9C) material or better (Table 3.1). The soil is allowed to have a maximum Liquid Limit (LL) of 30 and a maximum Plasticity Index (PI) of 10. In most cases, the soil is obtained from a local borrow pit near the construction site, and the size and scale of the borrow pit can range from a commercially owned and operated borrow pit to a hillside on residential property.

Soils are typically stabilized with Type I or Type II portland cement, but occasionally, an alternative cementitious blend with Ground Granulated Blast Furnace Slag (GGBFS) or Class F fly ash replacement is permitted. Type I cement is most frequently used, while Type II and/or alternative blends are usually required when the soil has an elevated soluble sulfate content. Soils with negligible sulfate content (0.00 to 0.09%) are usually stabilized with Type I cement. Soils with moderate sulfate content (0.10 to 0.19%) require either Type II cement or Type I cement with 50% GGBFS or 50% Class F fly ash replacement. Soils with severe sulfate content (>0.20%) require Type II cement with 50% GGBFS replacement or 25% Class F fly ash replacement.

Table 3.1. Soil Gradation Requirements of Class 9 Group C (9C)

Sieve Size (µm)	Sieve Designation Number	Percent Passing (%)
425	40	20 to 100
250	60	15 to 85
75	200	6 to 40

Note: 9C material must have 30 to 100 percent passing the 2 mm sieve (No. 10). Criteria given in Table 3.1 are applied to 9C material passing the 2 mm sieve (e.g. 20 to 100% of the material passing the 2 mm sieve must pass the 425 µm sieve).

3.3 Mississippi Test Methods for Soil-Cement Design

All soil-cement mixture designs are performed by MDOT's central laboratory in Jackson, MS. A soil sample from the borrow pit source is sent to the central laboratory for material approval and to determine mixture proportions for design. Material approval is based on soil properties including hydroscopic moisture content, full gradation, Atterberg Limits, and soluble sulfate content. Test methods used to determine soil properties include AASHTO T87, T265, T27, T11, T88, T85, T89, T90, T92, and Mississippi Test Method 58. Material approval is dependent upon the material meeting the criteria given in Section 3.2. After the material is approved, the design cement content for the soil-cement mixture is determined using Mississippi Test Methods 8, 9, 25 and 26. The following sections discuss each of these methods.

3.3.1 Mississippi Test Method 8

In general, Mississippi Test Method 8 (MT-8) is a modification of AASHTO T99 with a few notable modifications. This test method is applicable to embankment soils, design soils, and untreated subgrade and base materials. Before testing, the soil is air dried and processed according to AASHTO T87. Typically, soil processing is performed by light tamping with hand tools and/or use of a soil mortar and pestle. MT-8 is divided into Case 1 (≈90% of material passes the 4.75 mm sieve) and Case 2 (≈10% of material is retained on the 4.75 mm sieve). Case 1 corresponds to Method A described in T99 and Case 2 loosely corresponds to Method B described in T 99.

MT-8 Case 1 protocols do not deviate from T99 Method A protocols. Approximately 3 kg of processed soil passing the 4.75 mm sieve is mixed with water to about 4 percentage points below the expected optimum moisture content. Normally, all mixing is performed by hand, but MT-8 notes that a suitable mechanical mixing apparatus is desired. Then, the soil is compacted in a 101.6 mm diameter ($V = 943e^{-6}$ m^3) proctor mold in three equal layers to give a total compacted depth to fill the mold but not to exceed 127 mm. Each layer is compacted with 25 equally distributed blows from a 2.5 kg hammer dropping from a height of 305 mm above the top of the soil. Both manual and mechanical compaction hammers are acceptable, but a mechanical compaction hammer with a segmented head is desired and used routinely for laboratory compaction. After compaction, the soil specimen is trimmed even with the top of the mold, weighed, extruded, and sampled for moisture content determination. The remaining portion of the molded specimen is thoroughly broken up by hand and combined with the remaining prepared sample. Additional water is added to the sample to increase the moisture content 1 to 2 percentage points, and the process is repeated until a decrease or no change in the wet mass of the compacted specimen is observed between consecutive trials.

Equation 3.1 and Equation 3.2 are used to calculate the moisture content and dry density for each trial. The optimum moisture content (OMC) and maximum dry density (γ_d) of the soil sample is determined by plotting moisture content versus dry density and drawing a curve through the points. The coordinates corresponding to the apex of the curve are OMC and γ_d.

$$\omega = \frac{A - B}{B - C} \times 100 \quad \text{(Eq 3.1)}$$

Where:
ω = Moisture content of specimen (%)
A = Mass of container and wet soil (g)
B = Mass of container and dry soil (g)
C_m = Mass of container (g)

$$W = \frac{(D - E) \times F}{\omega + 100} \times 100 \quad \text{(Eq 3.2)}$$

Where:

W = Dry density (kg/m^3)
D_{SM} = Mass of compacted specimen and mold (kg)
E_m = Mass of mold (kg)
F = Mold factor; 1059.43 for 101.6 mm mold; 470.74 for 152.4 mm mold (1/m^3)
ω = Moisture content of specimen (%)

MT-8 Case 2 protocols are similar to T99 Method B protocols with a few notable differences. MT-8 Case 2 requires approximately 9 kg of material passing the 12.5 mm sieve whereas T99 requires 7 kg of material passing the 4.75 mm sieve. Overall, Case 2 procedures are the same as Case 1 with the exception of compaction mold size, number of lifts and number of blows. MT-8 Case 2 specifies specimens to be compacted in a 152.4 mm diameter by 116.3 mm tall (V = 2124e^{-6} m^3) mold in 4 equal lifts with 56 blows per lift (T99 Method B specifies 3 lifts with 56 blows per lift). Moisture contents and dry densities are determined in the same manner as Case 1 using Equations 3.1 and 3.2. The procedure for selecting OMC and γ_d is the same as Case 1. After selecting the OMC and γ_d, Equations 3.3 and 3.4 are used to adjust the OMC and γ_d to account for the plus 12.5 mm material.

$$OMC_{adj} = \frac{M_{r12.5}}{100} \times \left(P_{r12.5} + \frac{OMC_{p12.5}}{100} \times P_{p12.5} \right) \quad \text{(Eq 3.3)}$$

Where:
OMC_{adj} = Adjusted optimum moisture content (%)
$M_{r12.5}$ = Moisture content of material retained on 12.5 mm sieve (%)
$P_{r12.5}$ = Percent retained on 12.5 mm sieve (%)
$OMC_{p12.5}$ = Optimum moisture content of material passing 12.5 mm sieve (%)
$P_{p12.5}$ = Percent passing 12.5 mm sieve (%)

$$\gamma_{dadj} = \frac{1}{\left(\frac{1}{\gamma_d} \times P_{p12.5}\right) + \left(\frac{1}{G_{sb} \times \gamma_w} \times P_{r12.5}\right)} \times 100 \quad \text{(Eq 3.4)}$$

Where:
$\gamma_{d_{adj}}$= Adjusted maximum dry density (kg/m^3)
γ_d = Maximum dry density of material passing 12.5 mm sieve (kg/m^3)
γ_w = Unit weight of water (kg/m^3)
G_{sb} = Bulk specific gravity of plus 12.5 mm material

3.3.2 Mississippi Test Method 9

Mississippi Test Method 9 (MT-9) is a modification of AASHTO T134. This test method is applicable to all soil mixtures to be stabilized with cementitious materials. MT-9 Method A is used for design procedures while Method B is utilized during construction. MT-9 Method A is further broken into Case 1 and 2, which have the same criteria and distinction as defined in MT-8. The protocols of MT-9 are the same as MT-8 with the exception of the compaction mold size for Case 2 and cement addition. MT-9 Case 2 specifies a 152.4 mm diameter by 152.4 mm tall (V = 2832e^{-6} m^3) mold, which is different from the mold specified in MT-8. Cement is added and mixed with the dry processed soil prior to water addition and mixing. Mixing operations are the same as MT-8. After mixing the cement, soil, and water, the procedures and calculations to determine the OMC and γ_d are identical to MT-8 (including re-use of material). Unlike MT-8, the top surface of each lift is scarified to eliminate compaction planes between lifts.

Mississippi Test Method 25 (MT-25), which is described in 3.3.3, states that the cement content used to perform MT-9 should be estimated using the untreated γ_d determined by MT-8 and the soil PI; although, MT-25 does not state how these values are to be used to estimate the cement content. To the knowledge of the author, common practice relies on material handling experience to estimate the cement content to be used in MT-9. Typically, the estimated cement content will be between 4 and 8 percent according to MDOT's current cement content definitions.

Cement content is currently expressed as a percentage referencing volume which is similar to PCA (1992) cement content calculations for field control factors during construction (see Section 2.2.1). The cement content calculation is based on the volume of a 94 pound U.S. bag of cement rather than the volume of the soil mixture; this is not necessarily intuitive and may be misleading.

Equations 3.5 through 3.8 are example calculations from MT-9 which show how to calculate the amount of cement needed to perform a treated proctor test given a 4500 gram sample of dry soil, an untreated maximum dry density of 120.6 lb/ft^3 and an estimated cement content of 4 percent by MDOT's current definition.

$$\frac{4\%}{100} \times 94 \frac{lb}{ft^3} = 3.76 \frac{lb}{ft^3} \quad \text{(Eq 3.5)}$$

$$120\frac{lb}{ft^3} + 3.76\frac{lb}{ft^3} = 124.36\frac{lb}{ft^3} = \text{assumed density of soil-cement mixture} \quad \text{(Eq 3.6)}$$

$$\frac{3.76\frac{lb}{ft^3}}{120.6\frac{lb}{ft^3}} \times 100 = 3.12\% = \text{percent cement by dry soil mass} \quad \text{(Eq 3.7)}$$

$$\frac{3.12\%}{100} \times 4500 \text{ grams} = 140.4 \text{ grams of cement} \quad \text{(Eq 3.8)}$$

If the maximum dry density obtained from MT-9 varies from the assumed density of soil-cement mixture (Eq 3.6) by more than 1 lb/ft^3, the test should be repeated using the maximum dry density obtained, and Equations 3.9 through 3.12 are used to re-calculate the amount of cement. For this example, the first test yielded a standard maximum dry density of 122.7 lb/ft^3 and all other factors remain the same.

$$\frac{4\%}{100} \times 94\frac{lb}{ft^3} = 3.76\frac{lb}{ft^3} \quad \text{(Eq 3.9)}$$

$$122.7\frac{lb}{ft^3} - 3.76\frac{lb}{ft^3} = 118.94\frac{lb}{ft^3} \quad \text{(Eq 3.10)}$$

$$\frac{3.76\frac{lb}{ft^3}}{118.94\frac{lb}{ft^3}} \times 100 = 3.16\% = \text{percent cement by dry soil mass} \quad \text{(Eq 3.11)}$$

$$\frac{3.16\%}{100} \times 4500 \text{ grams} = 142.2 \text{ grams of cement} \quad \text{(Eq 3.12)}$$

According to the example, 4 percent cement by volume is equal to 3.16 percent by weight of dry soil mass, and 142.2 grams of cement is required to dose 4500 grams of dry soil. As the example calculations show, the cement content is not a true mixture volume calculation. A cement content by compacted soil volume should be less than the same value reported by mass (portland cement specific gravity is higher than the other materials), not more as seen in the previous example. Therefore, the commonly expressed cement content by volume is referred to as a cement index (C_I) for the remainder of this paper.

3.3.3 Mississippi Test Method 25

Mississippi Test Method 25 (MT-25) specifies the design cement content selection for soil-cement mixtures. The design cement content selection is based solely on compressive strength. The design cement content is the minimum cement content that will produce a minimum 14 day compressive strength of 2070 kPa (300 psi). MT-25 provides the recommended design cement index and the number of curing days (7 or 14) required to achieve a compressive strength of 2070 kPa.

Six specimens are prepared according to MT-9 Method A. Two specimens are prepared at 1 percentage point below the estimated design cement index, two are prepared at the estimated design cement index, and two are prepared at 1 percentage point above the estimated design cement index. Following compaction according to MT-9, specimens are trimmed even with top of the mold, extruded carefully, and placed under a damp cloth for 4 hours. Common practice is to leave specimens under a damp cloth overnight. Then, specimens are placed into plastic bags and set in a moisture room for curing. For each tested cement index level, one specimen is tested for compressive strength at 7 days, and the other specimen is tested for compressive strength at 14 days. At the end of the 7 and 14 day curing periods, specimens are immersed in water for 5 hours and tested according to Mississippi Test Method 26. The soaking period is routinely incorporated into the last 5 hours of the 7 and 14 day cure times.

3.3.4 Mississippi Test Method 26

Mississippi Test Method 26 (MT-26) is the procedure for determining the unconfined compressive strength of 101.6 mm diameter soil-cement cylinders prepared according to Mississippi Test Method 11 ("Preparation of Field Specimens of Soil Cement") or MT-25. MT-26 is also applicable to compressive strength testing of soil-cement field cores. After the appropriate curing time, specimens are immersed in water for 5 hours (48 hours for field cores). Usually, the 5 hour soaking time is included in the total cure time as noted in Section 3.3.3. MT-26 allows specimens to be capped before testing to satisfy smoothness criteria, but specimen capping is rarely needed. A compression load frame equipped with a spherically-seated head loads the specimen at a constant rate of 1.27 mm/min (0.05 in/min) until failure. The max load at failure is recorded to the nearest 40 N (10 lbs), and the compressive strength is calculated by dividing the max load at failure by the original specimen cross-sectional area.

3.4 MDOT Soil-Cement Database

MDOT maintains statewide records of soil-cement mixture designs used for highway construction. The database was obtained and analyzed to investigate current MDOT soil-cement design practices. A total of 176 soil-cement mix designs were acquired which includes all documented cementitiously stabilized subgrade and base course designs performed over the six year period from January 2005 to December 2010.

The MT-25 compressive strength results for the design cement index were used to distinguish between subgrade and base course designs. If the design cement index produced a compressive strength less than 2070 kPa (300 psi), the mix was considered to be a subgrade

design; otherwise, it was considered to be a base course design. Twelve mix designs were missing MT-25 results; therefore, the type of design was identified and sorted using additional descriptions and notes given in the database. Of the 176 mix designs, 55 were found to be subgrade designs, and 121 were base course designs.

The database was further sorted to only include mix designs with soils meeting the Class 9 Group C material criteria defined in Section 3.2. A preliminary investigation was conducted and presented at the 2011 Mississippi Transportation Institute Conference titled "State of Practice in Soil Cement" which used 98 mix designs in analysis, but ultimately the total number of mix designs analyzed was reduced to 94 after closer examination of the database. For the current work, 94 mix designs met the criteria for 9C cement stabilized base courses and were used in analysis. The 94 mix designs include the three designs conducted for the current study. Approximately 2 percent of the database could not be located. Sullivan (2012) Appendix A contains the MDOT soil-cement database obtained for analysis.

3.4.1 Database Trends

First, the soil-cement database was analyzed to observe general trends among the design cement contents and soil properties. Figures 3.1, to 3.3 contain relative frequency histograms showing the distributions of the recommended design cement indexes, tested cement indexes, and soil properties. Each histogram notes the total number of data points (n), mean, standard deviation (Stdev), and coefficient of variation (COV) for the data.

Figure 3.1a shows the recommended design cement index (C_I) was 4, 5, or 6 percent in most cases. The minimum and maximum design cement indexes were 3.5 and 7 percent, respectively, with an average design cement index of about 5 percent. Figure 3.1b shows the same design cement indexes expressed as a percentage of dry soil mass (C_w). The cement content by dry soil mass is always less than the cement index. The average design cement content by dry soil mass was about 4 percent, and the minimum and maximum cement contents were 2.7 and 6.3 percent, respectively. Figure 3.1c shows all of the cement indexes tested in MT-25. Again, the most common indexes tested were 4, 5, or 6 percent. The minimum and maximum cement indexes tested were 3 and 8 percent, respectively, with an approximate average of 5 percent.

Figures 3.1d, 3.1e, 3.1f, 3.2a, and 3.2b contain relative histograms showing the distributions of percent passing each sieve size. Figure 3.1d shows that approximately 82 percent of the mix designs have 90 to 100 percent passing the 4.75 mm sieve. This indicates that about 82 percent of the mix designs should be performed according to Case 1 protocols in MT-8 and MT-9, and approximately 18 percent of the mix designs should be performed according to Case 2 protocols. Figure 3.1e shows that approximately 81 percent of the mix designs have 90 to 100 percent passing the 2 mm sieve, and Figure 3.1f shows that approximately 47 percent of the mix designs have 90 to 100 percent passing the 425 μm sieve. Figures 3.2a and 3.2b show a fairly equal distribution among the histogram bins for the percent finer than 250 μm and 75 μm, respectively.

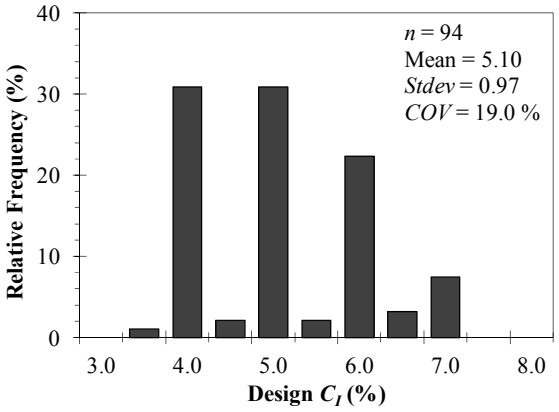

(a) Design Cement Index (C_I)

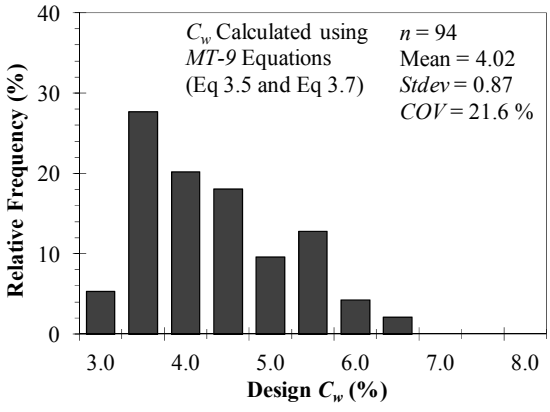

(b) Design C_w (Using Eq 3.5 and 3.7)

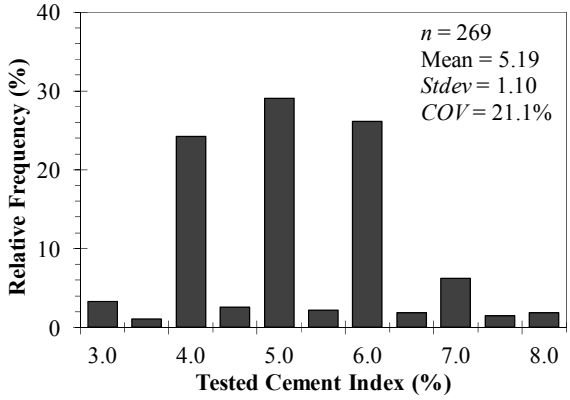

(c) Tested Cement Indexes

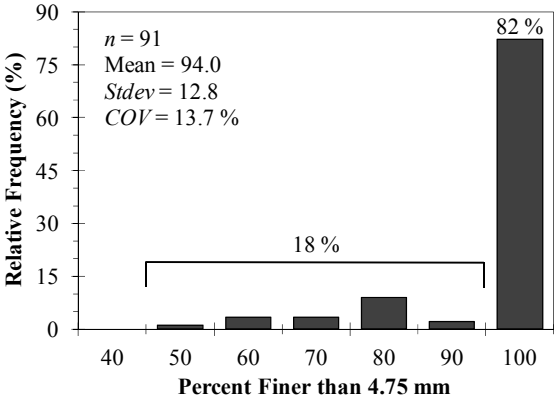

(d) Percent Finer than 4.75 mm Sieve

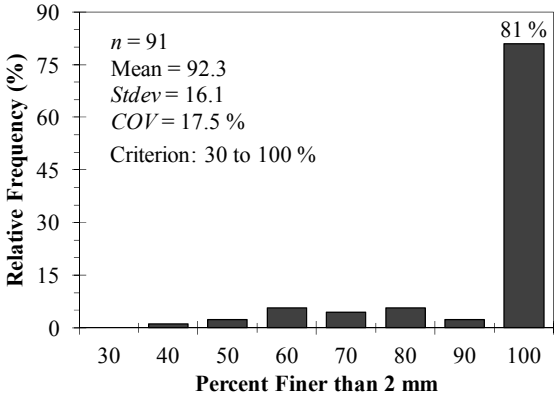

(e) Percent Finer than 2 mm Sieve

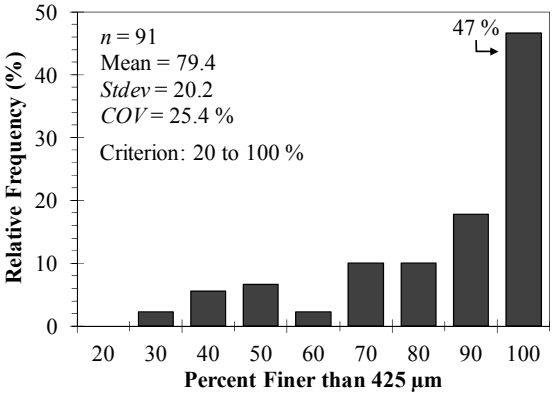

(f) Percent Finer than 425 µm Sieve

Figure 3.1. MDOT Soil-Cement Database Histograms (1 of 3)

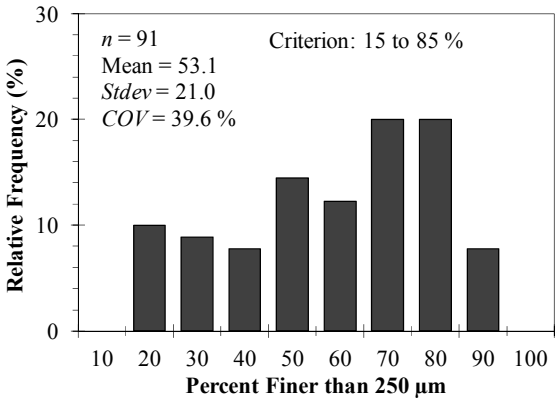

(a) Percent Finer than 250 µm Sieve

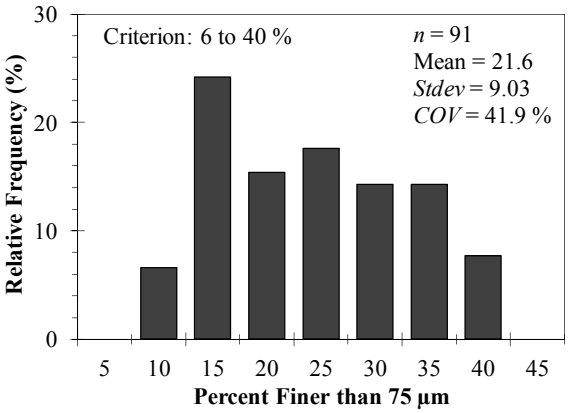

(b) Percent Finer than 75 µm Sieve

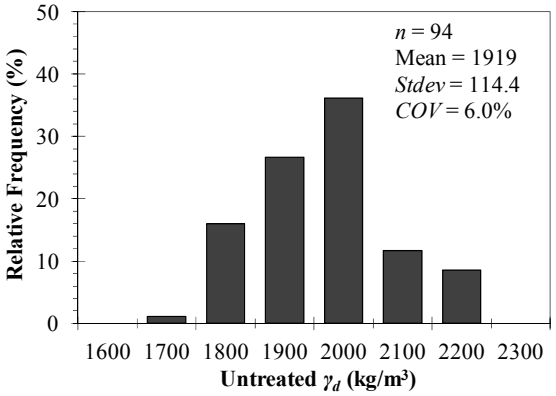

(c) Untreated Maximum γ_d

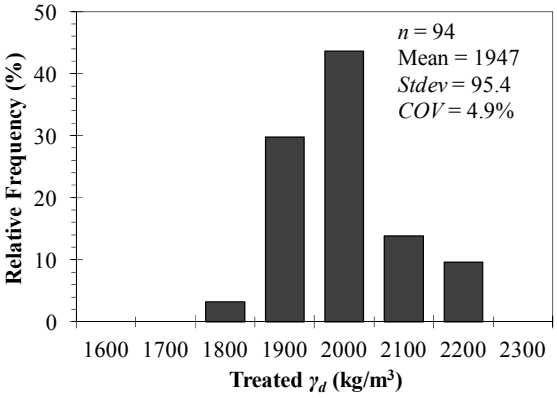

(d) Treated Maximum γ_d

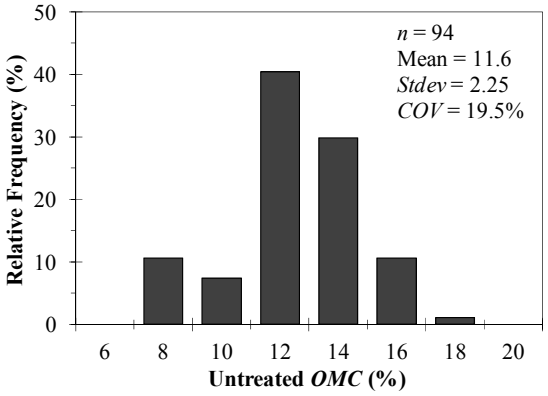

(e) Untreated OMC

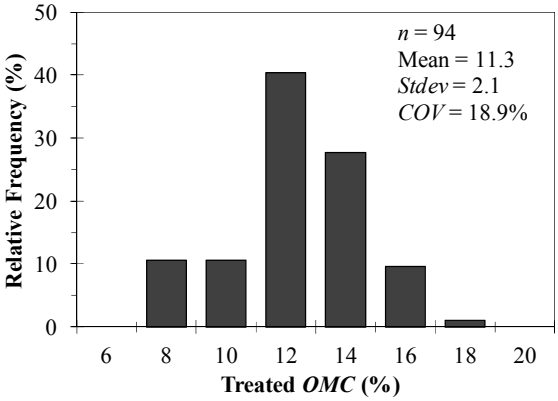

(f) Treated OMC

Figure 3.2. MDOT Soil-Cement Database Histograms (2 of 3)

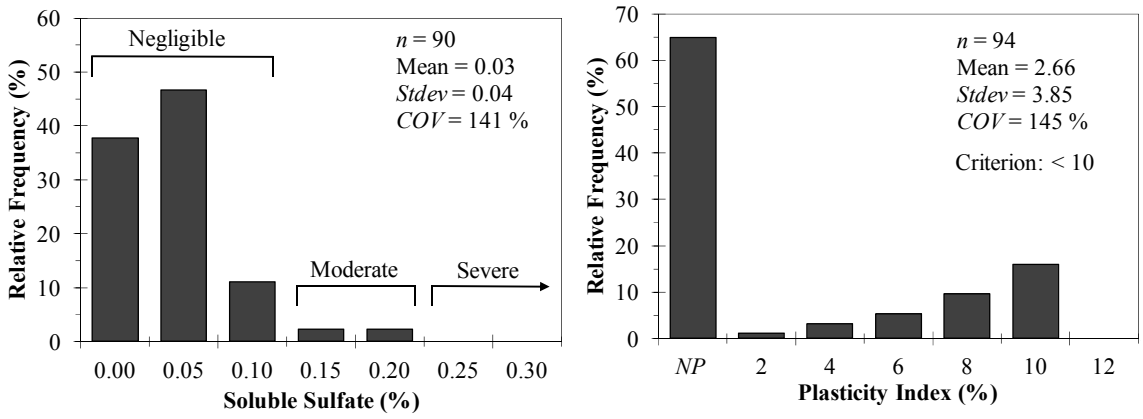

(a) Soluble Sulfate Content (b) Plasticity Index

Figure 3.3. MDOT Soil-Cement Database Histograms (3 of 3)

Figures 3.2c, 3.2d, 3.2e, and 3.2f contain relative histograms of untreated and treated values for maximum dry density (γ_d) and optimum moisture content (OMC) obtained from MT-8 and MT-9. Figure 3.2c shows the distribution of untreated standard maximum dry densities with a mean of 1919 kg/m^3 and standard deviation of 114 kg/m^3. Figure 3.2d shows the distribution of treated standard maximum dry densities with a mean of 1947 kg/m^3 and standard deviation of 95 kg/m^3. Figure 3.2e shows the distribution of untreated optimum moisture contents with a mean of 11.6%. Figure 3.2f shows the distribution of treated optimum moisture contents with a mean of 11.3%. Overall, a slight increase in standard maximum dry density and a slight decrease in optimum moisture content were observed with the addition of cement.

Figure 3.3a shows a relative histogram of the soluble sulfate contents. Approximately 5 percent of the mix designs had a moderate soluble sulfate content, 95 percent of the mix designs had a negligible soluble sulfate content, and no soil-cement designs had severe soluble sulfate content levels. Figure 3.3b contains a relative histogram for soil plasticity index (PI). Approximately 65 percent of the mix designs were non-plastic (NP).

3.4.2 Soil Property Correlations to Design Cement Content

The soil-cement database was analyzed to detect any correlations between measured soil properties and the design cement content. Each soil property was plotted on the x-axis with the corresponding design cement content for the mixture on the y-axis. Soil properties were plotted against both the design cement index and the equivalent design cement content expressed as a percentage of dry soil mass (C_w). Results from this analysis yielded very poor to no correlations between any soil property and the design cement content. Linear, exponential, logarithmic, and power trendlines were considered to develop a correlation between the data, but ultimately, a linear function was deemed appropriate to describe the relationships. Table 3.2 summarizes the results. The strongest observed correlation was the percent passing the 75 μm sieve ($R^2 = 0.24$).

Table 3.2. Summary of Soil Property Correlations to Design Cement Content

Abscissa (x)	Ordinate (y)	*n*	Correlation	R^2
Percent Finer 75 µm	Design C_I	91	y = -0.05x + 6.26	0.23
Percent Finer 250 µm	Design C_I	91	y = -0.01x + 5.69	0.05
Percent Finer 420 µm	Design C_I	91	y = -0.01x + 5.93	0.05
Percent Finer 2 mm	Design C_I	91	y = -0.02x + 6.51	0.06
Percent Finer 4.75 mm	Design C_I	91	y = -0.02x + 6.95	0.07
Dust Ratio[1]	Design C_I	92	y = -0.03x + 5.85	0.07
Plasticity Index	Design C_I	94	y = -0.02x + 5.14	0.00
Soluble Sulfate	Design C_I	90	y = -0.17 + 5.14	0.00
Raw Max γ_d	Design C_I	94	y = -0.03x + 8.81	0.05
Percent Finer 75 µm	Design C_w	91	y = -0.05x + 5.06	0.24
Percent Finer 250 µm	Design C_w	91	y = 0.00x + 4.18	0.00
Percent Finer 420 µm	Design C_w	91	y = 0.00x + 4.00	0.00
Percent Finer 2 mm	Design C_w	90	y = 0.00x + 4.11	0.00
Percent Finer 4.75 mm	Design C_w	91	y = 0.00x + 4.17	0.00
Dust Ratio[1]	Design C_w	92	y = -0.03 + 4.97	0.16
Plasticity Index	Design C_w	94	y = -0.05x + 4.15	0.04
Soluble Sulfate	Design C_w	90	y = 0.55x + 4.04	0.00
Raw Max γ_d	Design C_w	94	y = -0.06x + 11.37	0.23

1: One data point was believed to be erroneous and was omitted from analysis.

3.4.3 Batching Calculations

As of January 2011, MDOT uses a computer program to calculate soil-cement mixture proportions to perform MT-9 and MT-25. Closer examination of the computer program revealed a discrepancy between the program calculation equations and the MT-9 example calculation equations for amount of cement (discussed in Section 3.3.2). Equations 3.13 through 3.16 show the actual program equations used to calculate the amount of cement for MT-9 and MT-25, and equations 3.17 and 3.18 show the calculations for the amount of soil and water. For comparison, the same given values from Section 3.3.2 were used (C_I = 4%, untreated γ_d = 120.6 lb/ft^3, hydroscopic moisture = 0.5%, OMC for soil-cement mixture = 10.3%).

$$\frac{4\%}{100} \times 94 \frac{lb}{ft^3} = 3.76 \frac{lb}{ft^3} \qquad \text{(Eq 3.13)}$$

$$120.6 \frac{lb}{ft^3} - 3.76 \frac{lb}{ft^3} = 116.84 \frac{lb}{ft^3} \qquad \text{(Eq 3.14)}$$

$$\frac{3.76 \frac{lb}{ft^3}}{116.84 \frac{lb}{ft^3}} \times 100 = 3.22\% = \text{percent by dry soil mass} \qquad \text{(Eq 3.15)}$$

$$\frac{3.22\%}{100} \times 4500 \text{ grams} = 144.9 \text{ grams} \quad \text{(Eq 3.16)}$$

$$4500 \times \frac{(0.5 + 100)}{100} = 4522.5 \text{ grams} = \text{(amount of batched soil)} \quad \text{(Eq 3.17)}$$

$$(4500 + 144.9) \times \frac{(10.3\% - 0.5\%)}{100} = 455.2 \text{ grams} = \text{(amount of water)} \quad \text{(Eq 3.18)}$$

According to the MDOT program calculations, the soil-cement mixture should consist of 144.9 grams of cement, 4522.5 grams of air-dried soil with 0.5 % hydroscopic moisture, and 455.2 grams of water for a desired total batch weight after mixing of 5122.6g (4,500g of dry soil). The discrepancy is contained within Equation 3.15. In order to be consistent with MT-9 equations, the treated maximum dry density should be used instead of the untreated maximum dry density. To the knowledge of the author, the calculation equations defined in MT-9 (discussed in Section 3.3.2) are not used, and Equations 3.13 through 3.18 were used herein to calculate mixture quantities for all mixtures found in the soil-cement database. The program calculations produce an increase in cement content within the soil-cement mixture, but the increase is not dramatic. Additionally, common practice is to batch 4500 grams of soil even though the calculations adjust the amount of batched soil to account for the moisture in the soil (4522.5 grams for the example above). Omitting the adjustment for moisture in the batched soil increases the cement content as well as decreases the moisture content.

Figure 3.4a shows the relationship between cement index and cement content by dry soil mass (C_w). The data plotted includes all of the MT-25 tested cement indexes from the database. The cement content by dry soil mass was calculated using equations defined in MT-9 (Equations 3.5 and 3.7). In every case, the cement content by dry soil mass was considerably less than the cement index. Figure 3.4b shows the same relationship as Figure 3.4a, but the program calculations (Equations 3.13 through 3.15) were used to calculate C_w.

The soil-cement database provides MT-25 batch weights for the cement, soil, and water for each mix design. This data was utilized to evaluate the discrepancies associated with the program calculations and batching practices related to MT-25. From the batch weights, the actual cement content by dry soil mass (C_w) was calculated for each specimen tested. To demonstrate the effect of batching discrepancies, the cement index was back-calculated using the program calculations (Equations 3.13 through 3.15) and the actual cement contents by dry soil mass were calculated from the database batch weights. Figure 3.4c shows how the actual back-calculated cement indexes deviate from the targeted cement indexes. It is clear that in some cases the batching discrepancies have a noticeable effect on the cement content of tested specimens, though overall the two approaches have a trendline slope of 1 and have a near zero intercept.

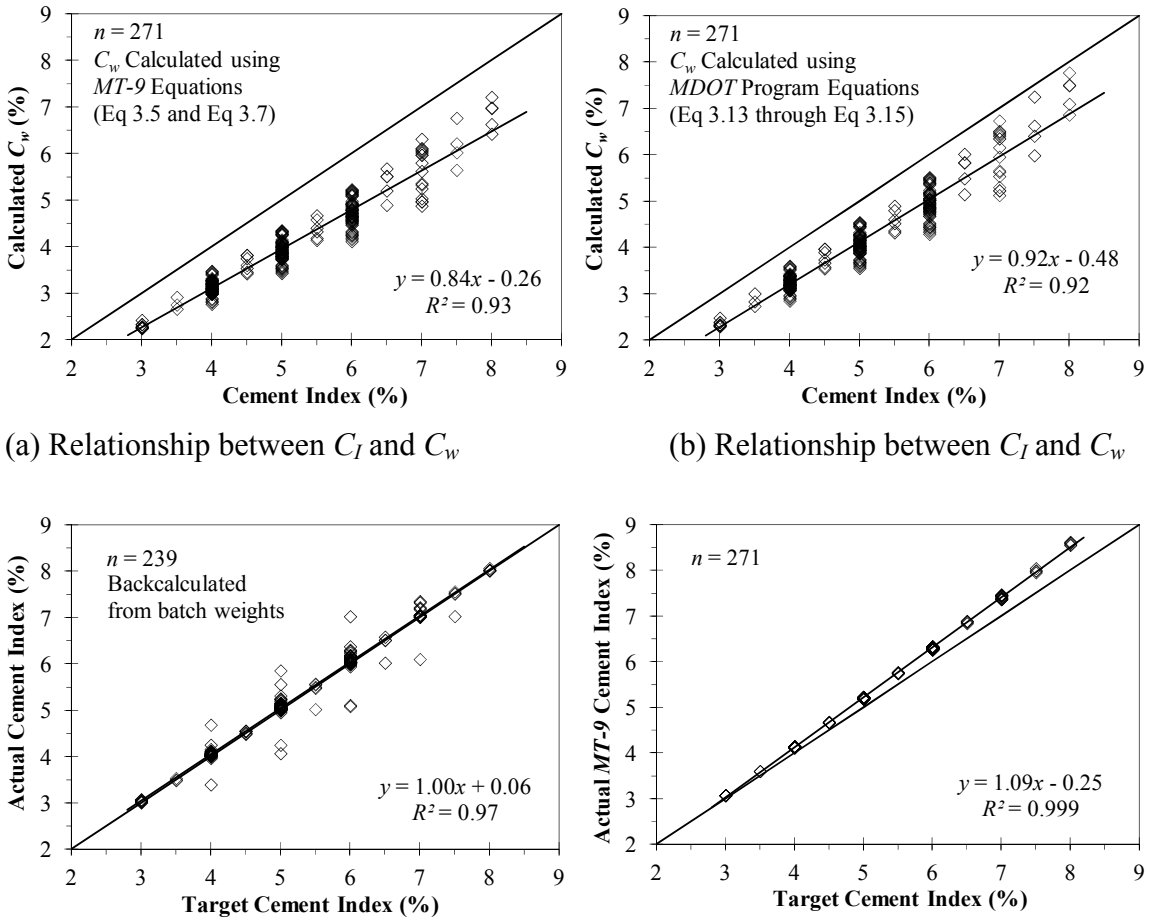

(a) Relationship between C_I and C_w

(b) Relationship between C_I and C_w

(c) Effect of Batching Discrepancies

(d) Index Correction by Calculation

Figure 3.4. Database Cement Contents and Calculations

Figure 3.4d shows the discrepancy solely associated with the program calculations. First, the target cement indexes were converted to cement content by dry soil mass using the batching program calculations (Equations 3.13 through 3.15). Then, the actual MT-9 cement index tested was back-calculated using MT-9 defined equations (Equations 3.5 and 3.7) and the program calculated cement content by dry soil mass. The back-calculated MT-9 cement indexes were then plotted against the target cement indexes to produce a correction equation (R^2 near 1). The correction equation was confirmed by back-calculating the program cement index and the MT-9 cement index from the batch weights given in the database; this equation only differed from Figure 3.4d due to rounding differences. The formula that should be used to adjust the program calculations to MT-25 is given in Equation 3.19.

$$y = 1.09x - 0.25 \qquad \text{(Eq 3.19)}$$

Where:
y = Actual cement index tested
x = Target cement index

3.4.4 Treated Proctor Density

Overall, the database demonstrated a slight increase in maximum dry density with cement addition. Upon closer examination, a considerable portion of the mix designs showed a drop in maximum dry density with cement addition. Figure 3.5a shows a relative histogram of the difference between treated and untreated maximum dry densities, and Figure 3.5b shows an equality plot of the same data.

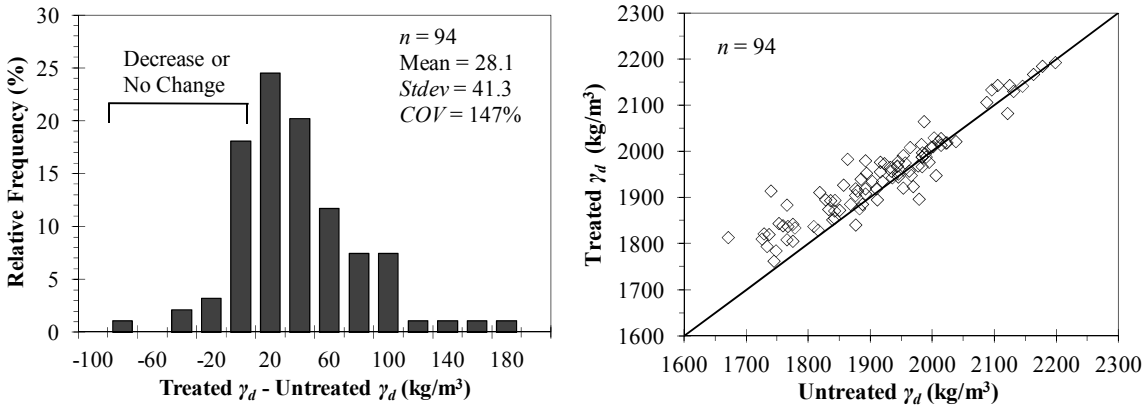

(a) Distribution of Treated γ_d - Untreated γ_d (b) Treated γ_d vs. Untreated γ_d

Figure 3.5. Maximum Dry Density Decrease with Cement Addition

Twenty-four percent of the database mix designs experienced a decrease or no change in the maximum dry density (γ_d) when cement was added to the mixture. This behavior could be caused by an accelerated cement hydration rate and/or prolonged time between cement addition and compaction. An accelerated hydration rate could be caused by the type of soil, cement source, or their interaction. ACI (2009) attributes this behavior to the flocculating action of the cementitious materials. In addition, three or four mix designs show a dramatic increase in γ_d with cement addition; these data points are believed to be testing error.

3.5 Summary of Database Findings

A concise list has been compiled to summarize aspects of the soil-cement mixture design procedures, test methods, and database results. The list also includes recommendations for enhancement based on information and data presented.

- Mississippi Test Methods 8 and 9 are not in agreement with respect to mold sizes used for material having greater than 10 percent retained on the 4.75 mm sieve. MT-8 specifies a 152.4 mm diameter mold having a volume of $2124e^{-6}$ m^3, and MT-9 specifies a 152.4 mm diameter mold having a volume of $2832e^{-6}$ m^3. A review of the database also showed that the mold size specified in MT-9 was not used once during the design process, and the mold specified in MT-8 is always used if Case 2 protocols were required.

- The sample calculations contained in Mississippi Test Method 9 that are used to determine the appropriate amount of cement for specimens made in MT-9 and MT-25 need to be updated.
- Review of Mississippi Test Methods and the soil-cement database revealed the cement index (cement by volume) calculations could be confusing and possibly misunderstood by some end users. Recommended design cement contents range from 3 to 7 percent under the current terminology, but this range is actually 2.7 to 6.3 percent by dry soil mass. It is strongly recommended that cement contents by weight (C_w) be used for laboratory operations and testing. If a cement index is desired for field control, then the design cement content by weight can easily be converted to a cement index at the conclusion of laboratory testing. Field control, however, can also be performed using mass proportions. The PCA calculation (PCA 1992) is recommended for converting cement content by weight to an equivalent cement index in the field, if this approach is desired.
- Mississippi Test Method 25 provides guidance for estimating the design cement content for soils using the untreated maximum dry density and plasticity index, but the guidance is not clearly defined. The database revealed that there is no correlation between the estimated cement content or the design cement content and the untreated maximum dry density and plasticity index. Nevertheless, the estimated cement content was equal to the ultimate design cement content for 96 percent of the database mix designs.
- Mississippi Test Methods and the database constantly switch back and forth between English and Metric units. A consistent system of units would be more beneficial for data analysis.
- Analysis of the soil-cement database revealed no correlation between soil properties and design cement content or compressive strength.
- Analysis of batch weights used for MT-25 testing disclosed some batching discrepancies. The discrepancy lies with accounting for moisture within the batched soil. In most cases, this discrepancy is relatively small since the soils tested contain little moisture, but mixture proportions should be closely controlled and monitored in a laboratory environment since it is feasible to do so.
- Twenty-four percent of the database mix designs exhibited a drop in maximum dry density (γ_d) with the addition of cement. This behavior is believed to be associated with the compaction time and re-use of material in MT-9. It is recommended that a time-frame relative to cement and water combination be set in which compaction must be completed for MT-9 and MT-25. Additional tests with known longer time frames might be a useful addition to MT-9 for quality control purposes.
- The MDOT soil-cement database proved to be extremely insightful to the practice of soil-cement mixture design for the state of Mississippi. Continual archiving of soil-cement mix designs in a manner conducive to quick retrieval and analysis would be of great benefit for future monitoring, research, and practice enhancements.

3.6 MDOT Soil-Cement Construction Practices

Section 308 of MDOT (2004), i.e. the *Red Book*, describes soil-cement construction requirements for MDOT projects. Figures 3.6 and 3.7 illustrate construction practices for the two soil-cement base course projects observed for this report. These projects vary significantly with respect to size and amount of treated material, and these projects exemplify the range of acceptable soil-cement construction practices within the state of Mississippi.

Figure 3.6. Soil-Cement Base Course Construction on State Route 9 (April 2012)

Figure 3.6 illustrates construction of State Route 9 (SR9) in north Mississippi which encompassed approximately 68,000 m^3 (88,900 yd^3) of mixed in-place soil-cement base material. First, the required amount of cement was spread onto the roadway using a mechanical cement-spreader attached to the back of the cement transport truck. The cement spread rate was monitored using spot and overall checks. The first mixing pass pulverized the soil and mixed the cement into the soil. If required, additional mixing water was added to the roadway to achieve optimum moisture content, and the second mixing pass incorporated the water into the layer. After mixing, the soil-cement layer was immediately compacted with sheeps-foot and vibratory steel-wheel rollers. Then, the layer was checked for proper density. The compacted surface was milled and shaped to the proper grade. A rubber-tire roller compacted the graded soil surface. Finally, the soil-cement layer was moistened and sealed with a bituminous membrane for curing.

Figure 3.7 illustrates construction of State Route 475 (SR475) in central Mississippi which required approximately 12,200 m^3 (16,000 yd^3) of mixed in-place soil-cement base material. First, the required amount of cement was spread onto the roadway using a pipe cement-spreader attached to the back of the cement transport truck. Cement spread was monitored using overall checks. One or two mixing passes were performed to pulverize the soil and mix the cement into the soil. The mixture was checked for proper pulverization. Additional mixing water was added to the mixture to achieve optimum moisture content, and a final mixing pass was performed. After mixing, the layer was immediately compacted with sheeps-foot and vibratory sheeps-foot rollers. After compaction, the surface was graded and shaped. A rubber-tire roller compacted the graded surface. Then, the layer was checked for proper density. Finally, the soil-cement layer was periodically moistened for 24 hrs before being sealed with a bituminous membrane for curing.

Figure 3.7. Soil-Cement Base Course Construction on State Route 475 (June 2012)

3.7 DOT Survey

A survey was developed and made available in order to gather information pertaining to stabilized soil design procedures, testing approaches, results evaluation, and pending concerns within the practice. This survey, found in Anderson (2013) Appendix D, was available at the 98th AASHTO Subcommittee Meeting on Materials (August 2012) in Biloxi, MS. Also, individuals were given the opportunity to find, complete, and submit the survey via the Construction Materials Research Center (CMRC) webpage found on the MSU Department of Civil and Environmental Engineering website for approximately four months. Responses were compiled and are summarized herein, while not disclosing sensitive information.

Twenty responses were collected, each from a different state department of transportation. The sectors (or divisions) of the departments of transportation included, but were not limited to, construction, materials, geotechnical, research, and testing. The following list contains all states that responded in alphabetical order. Questions as they appeared in the survey are italicized in the following sections, followed by a summary of the received responses.

Alabama	Louisiana	New Mexico	Pennsylvania
Colorado	Maine	North Carolina	South Carolina
Connecticut	Maryland	North Dakota	Tennessee
Delaware	Nebraska	Ohio	Texas
Georgia	Nevada	Oklahoma	Utah

Does your state utilize chemically stabilized (i.e. portland cement, fly ash, lime, slag cement, etc) pavement layers for roadway construction?

Most of the responses received indicated that the state DOT, to some extent, utilized chemically stabilized pavement layers for roadway construction. However, two of the twenty responses indicated states do not use chemically stabilized pavement layers because subgrade soils are adequate or there is an abundance of good aggregate sources for economical use on projects. One of these states used chemically stabilized pavement layers in some research, but no use as far as commercial projects.

Those responses that specified a state uses chemically stabilized pavement layers showed a variety of chemicals used. Nine of the eighteen responses said that cement was used or frequently used in the state. The most used of the chemical stabilizers seemed to be cement, lime, fly ash, and lime/fly ash. Other chemical stabilizers that were mentioned by a few respondents are cement kiln dust, lime kiln dust, calcium chloride, and sodium chloride. According to the survey, the southern region of the U.S. (per U.S. Census Bureau) seems to use chemically stabilized materials more frequently; however, this is not a strong trend because the use of chemically stabilized pavement layers seems to be widespread. The general trend for the northeast, Midwest, and west regions is the infrequent use of chemically stabilized pavement layers.

How is the design stabilizer (e.g. portland cement) content determined? Please list any test types (e.g. unconfined compression), specimen sizes (e.g. 3 in by 6 in), and test requirements (e.g. 200 psi after 7 day cure) that are used to determine the design stabilizer content.

Responses providing information pertaining to the aforementioned question all indicated that the unconfined compression test is used in the design of chemically stabilized pavement layers. A few responses showed that no design is required, but a predetermined amount of stabilizer is used per material type. The specimen size and design strength requirements were not consistent between states that responded. A general range of 689 kPa to 5171 kPa was observed. Table 3.3 gives specimen sizes, strength requirements, and curing descriptions for respondents sorted by h/d ratio.

At least ten of the departments use the standard proctor size specimen (102 by 116 mm) for compression strength testing. Depending on the material being used for a stabilizer, the strength requirement range generally falls between 700 and 3500 kPa for the h/d ratio of 1.15. Geographically, there seems to be no trend to required compressive strength with respect to region. There are states that share a boarder with differing compressive strength requirements.

Table 3.3. Specimen Size, Strength and Curing for Stabilized Design from DOT Survey

h/d Ratio	Req'd σ (kPa)	Curing Description
0.76	2068 or 4137	7 day moist, 24 hr soak
1.00	5171	7 days
1.15	1103 to 3447	5 days @ 38 C
	1379 to 2068	7 days
	3103 psi	---
	1034 or 2068	7 days
	1724	---
	No Minimum	---
	345 to 2068	7 days
	2068 to 2758	7 days
	689	7 day + 1 day moist cure
	2068 to 3447	7 days
1.33	1724 to 2620	7 days
1.50	1379 to 3447	7 days
2.00	1724 to 4137	---

Once determined, how is the design stabilizer content referenced? Examples might include percent of dry soil mass, by volume…..

When referencing the design amount of stabilizer, two methods are generally used: by volume and by mass. Of the eighteen responses, three states specify the design amount of stabilizer by volume. Thirteen out of eighteen respondents said their institution specifies the design amount of stabilizer on a by mass basis. One state institution gives a recommendation of the amount of stabilizer in pounds per square yard per project and one state did not specify.

What compaction method(s) are used to make specimens for Question 2?

There were seventeen out of twenty responses that gave information pertaining to the compaction method used to make specimens for designing stabilized pavement layers. The one response that did not give compaction information but still uses stabilization for pavement layers has a predetermined percentage by weight of stabilizer for specific material types.

The compaction efforts mostly refer back to AASHTO T99 and AASHTO T180. Some reference these specifications specifically while some states have their own specifications based on these test methods. One state uses the Harvard Miniature Compaction effort and specimen size (ASTM D4609).

Is there any replication of the tests performed in Question 2? For example, are three replicate unconfined compression tests averaged to compare to the design strength requirement?

Responses indicate that most state DOTs have some form of replication of testing specimens when designing chemically stabilized pavement layers. Eleven of the eighteen responses that utilize chemical stabilization have some form of replication. Two indicated that only one specimen was made for each stabilizer dosage. Seven entities did not provide information on this question. One indicated using two replicates in the design process. Eight of the responses use an average of three replicates in the design process, while two use five replicates. A respondent explained that they create five specimens per stabilizer amount and after testing all five, omit the highest and lowest, averaging the three remaining values.

Is there a maximum time allowed between mixing the chemical stabilizer, soil, and water until compaction must be completed?

Twelve respondents provided information indicating that there was a time limit placed on the amount of time between mixing the chemical stabilizer, soil, and water and completed compaction. There was a wide range in maximum allowable time between mixing and compaction. This time ranged from 30 minutes to 240 minutes. These responses were most likely referring to field times. One response indicated a time allowance of five minutes, and is assumed to be enforced during the design process.

Briefly describe any quality control measures that are taken with regard to chemically stabilized pavement layers in your state.

Quality control measures that are used do not seem to diverge from a few core checks. Respondents usually provided multiple quality control measures in answers. Six of the eighteen respondents indicated that field proctors are performed to confirm the compaction of the field mixed material compared to that performed in the laboratory. Eleven of the eighteen respondents shared that the spread rate of the chemical stabilizer is verified in the field, either by the tarp method or by distance covered per truck. The nuclear method of verifying density on the compacted pavement layer was mentioned by seven of the eighteen

responses. One of the responses even indicated that a small test strip must be constructed in order to verify that designs can be met by the construction crew before the job continues.

The formation of field specimens/cores was mentioned by five of the respondents. Three of these make specimens in the field, cure them in the laboratory, and obtain a compressive strength to compare to the design. Mold sizes were not specified in answers, but one of these responses indicated a split proctor mold was used. Two respondents indicated after an amount of time, actual cores were taken from the layer and tested for compressive strength; strengths had to meet design specifications. Coring procedures were not noted in responses, but one of these respondents indicated that 152 mm cores were taken from the job site.

Please list any problems or concerns with chemically stabilized pavement layers, their design, or their quality control. Also provide any feedback on areas of needed improvement in design or quality control.

From the survey, there seem to be several problems and concerns about stabilized pavement layers, their design, and quality control efforts and practices. The problems and concerns are summarized in the following bulleted list:

- Difficulty to achieve and verify uniform mixing of materials on site.
- Inconsistent spread rates caused by allowing spreading by blow tubes of tanker can lead to low or high concentrations of chemical stabilizer.
- Need for extensive sampling of borrow pit or in-situ material to ensure mix design properly represents material to be stabilized.
- Crucial to use exact same cement source in design and in field.
- Difficulty in balance between strength and cracking potential (cement content)
- Field strengths may achieve much higher strengths than in design.
- Variability in stabilization based only on soil classification; possibly include other tests for better performance prediction.
- Concern related to duration of required curing before traffic opening.
- Determination of appropriate stabilizer based on in-situ soil conditions.

CHAPTER 4 – MATERIALS TESTED

4.1 Overview of Materials Tested

Five soils, five cementitious materials, and one water source (laboratory tap water) were tested. The soils were sampled from borrow pits (referred to hereafter as pit soils). With exception of proctor compaction results that are presented in chapter 6, this chapter presents all properties of the materials tested. Four portland cement sources and one portland-slag cement blend were tested.

4.2 Pit Soils Tested

Five borrow pit soils were tested. The majority of lab efforts focus on three pit soils which were taken from highway construction sites utilizing soil-cement as base course. Pit soils *A*, *B*, and *C* were sampled from the first available MDOT base course project sites located in central, north, and south Mississippi after State Study 206 commenced. Samples were obtained from: 1) US Interstate 20 interchange project near Meridian, MS (*Pit A*); 2) US Hwy 45 interchange project near Saltillo, MS (*Pit B*); and 3) expansion of US Hwy 84 near Prentiss, MS (*Pit C*). Pit A was in MDOT District 5 in Lauderdale County (Central MS). Pit B was in MDOT District 1 in Lee County (North MS). Pit C was in MDOT District 7 in Jefferson Davis County (South MS). Approximately 2000 kg of material was obtained from each project. Pit soils *D* and *E* were sampled from: 4) State Route 9 project near Tupelo, MS (*Pit D*) and 5) State Route 475 relocation in Rankin County, MS (*Pit E*). Approximately 300 kg was obtained from each project. *Pit D* and *Pit E* were sampled from the roadway prior to construction; whereas, *Pit A*, *B*, and *C* were sampled from the project borrow pit. Figure 4.1 provides photos of pit soil acquisition.

4.2.1 Pit Soil Processing

Pit soils *A*, *B*, and *C* were sampled from a borrow pit using a backhoe or front-end loader that mixed the soil prior to loading into the trailer (Figure 4.1). Soil from *Pit A* was sampled below optimum moisture content while *Pit B* and *Pit C* were sampled near optimum moisture content. Soils *D* and *E* were sampled near optimum moisture content.

A detailed procedure was used to process all pit soils (Figure 4.2) to preserve the original raw material gradation. Each pit soil was sampled (and subsequently processed) entirely at one time. The following paragraphs describe each soil processing step.

Material was first spread onto tarps and allowed to air dry under fans until the soil reached a consistent moisture content (Figure 4.2a). While drying, the soil was stirred and thoroughly mixed. Stirring and mixing of the soil was implemented to speed up the drying process as well as provide sample uniformity. After drying, the soil was divided into several sections (Figure 4.2b). All material in each section was passed through a 4.75 mm sieve (Figure 4.2c). Material passing the 4.75 mm sieve was placed into a barrel, and material not passing the 4.75 mm sieve was placed into buckets for further processing (Figure 4.2d). Sections were processed one at a time to ensure that all of the material in each section remained in the same barrel with the exception of the plus 4.75 mm material.

(a) Borrow *Pit A*

(b) *Pit A* Sample Location

(c) Borrow *Pit B*

(d) *Pit B* Sample Location

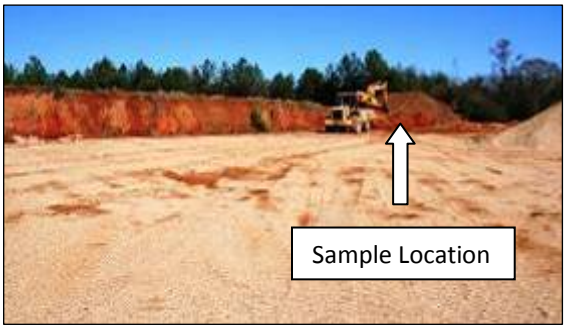

(e) Borrow *Pit C*

(f) *Pit C* Sample Location

(g) *Pit D* sampled from roadway

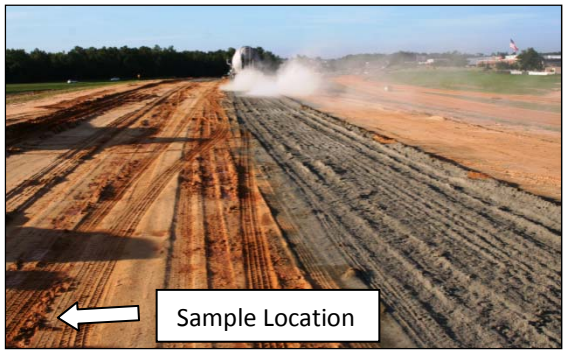

(h) *Pit E* sampled from roadway

Figure 4.1. Photos of Pit Soil Acquisition

(a) Air Drying of Soil

(b) Dividing Soil into Sections

(c) Portable Bin and 4.75 mm Sieve

(d) All Plus 4.75 mm Material

(e) Tamping of Plus 4.75 mm Material

(f) Soil after Processing

(g) Remixing Barrel of Soil

(h) Placing Soil into Buckets

Figure 4.2. Photos of Soil Processing (*Pit C* shown)

The plus 4.75 mm material consisted mostly of fine particles (i.e. silt and clay) which tended to cluster together in clumps. These large silt/clay clumps had a tendency to segregate during acquisition and initial handling of the raw material. Therefore, the research team decided to process the silt/clay clumps separately and equally distribute the fine material to each barrel at a later stage of processing. Each soil yielded approximately 14 buckets of silt/clay clumps that did not initially pass through the 4.75 mm sieve. The material was placed on a tarp and was lightly tamped until the material would pass through a 4.75 mm sieve (Figure 4.2e). The fine material was then redistributed equally to each barrel based on weight. The contents of each barrel were dumped, thoroughly remixed, and sealed in barrels for storage (Figure 4.2f). As the fully processed material was being placed into barrels, a sample was taken from the top, middle, and bottom of each barrel. This sample was taken to perform water content and gradation tests to ensure consistency among and between barrels. Seven barrels were available per pit soil *A*, *B*, and *C*.

Long term storage and subsequent batching from barrels poses the potential for segregation, particularly for soils with multiple particle sizes. For precaution, each barrel was emptied onto a tarp and remixed before batching test specimens (Figure 4.2g). To minimize the potential for segregation (especially during batching) the remixed soil was placed into 18.9 liter plastic buckets for temporary storage (Figure 4.2h). A barrel of soil typically yielded ten 18.9 liter buckets of material. Each bucket was labeled with the Pit ID (e.g. *A*, *B*, *C*, *D*, *E*), barrel number of origin, and a bucket number. Pit soils post processing are show in Figure 4.3.

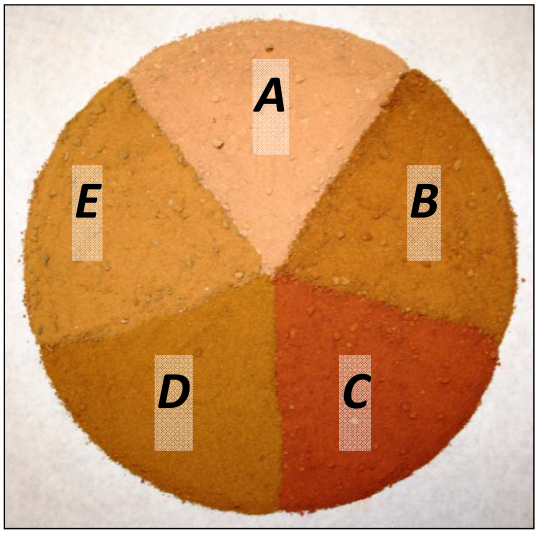

Figure 4.3. Pit Soils Tested (Post Processing)

4.2.2 Pit Soil Fundamental Properties

After pit soils were processed (see Section 4.2.1), pit soil samples were tested for fundamental properties (Table 4.1). A sample of pit soils *A*, *B*, and *C* was sent to MDOT Central Laboratory to perform a soil-cement mix design (non-fundamental property results from the mix designs are provided in Chapter 6). Data reported include results determined by MDOT Central Laboratory, Mississippi State University (MSU), and Burns, Cooley,

Dennis, Inc (BCD). Table 4.1 also contains data from the soil-cement mix designs used for the corresponding projects from which each pit soil was sampled (non-fundamental property results from the mix designs are provided in Chapter 6). Since pit soils *D* and *E* were part of a field study, only the project soil property results are reported.

As shown in Table 4.1, soil properties for pit soils *A*, *B*, and *C* are similar to the results for each corresponding project. All of the soil samples were non-plastic (*NP*) with the exception of the project mix design for *Pit C* (PI = 9). *Pit A* and *Pit B* have a slightly finer gradation than the project results, and *Pit C* has a noticeably coarser gradation than the corresponding project results.

Table 4.1. Fundamental Properties of Pit Soils

	Pit A		***Pit B***		***Pit C***		***Pit D***	***Pit E***
Soil Property	**Res.**[a]	**Proj.**[b]	**Res.**[a]	**Proj.**[b]	**Res.**[a]	**Proj.**[b]	**BCD** [c]	**Proj.**[b]
$\omega_{natural}$ (%)	≈ 9.4	--	≈ 13.4	--	≈ 11.0	--	≈ 11.1	≈ 18.6
$\omega_{air\text{-}dried}$ (%)	0.6 - 0.8	0.5	1.3 - 1.7	0.3	0.7 - 0.9	1.1	0.8	1.1
Plasticity Index	*NP*	*NP*	*NP*	*NP*	*NP*	9	*NP*	*NP*
% Pass 2 mm	99 - 100	100	100	100	98 - 100	100	100	100
% Pass 425 µm	77 - 83	66	95 - 96	97	89 - 93	95	98	100
% Pass 250 µm	57 - 64	41	61 - 65	62	53 - 59	67	71	80
% Pass 150 µm	24 - 27	--	25 - 29	--	30	--	--	--
% Pass 105 µm	21 - 22	--	22 - 26	--	27 - 28	--	--	--
% Pass 75 µm	19 - 21	14	21 - 25	11	26 - 29	40	19	16
G_s	2.65	2.66	2.65	2.66	2.65	2.67	--	2.65
Soluble SO_4 (%)	0.00	0.03	0.00	0.01	0.00	0.00	--	0.00
USCS	SM	SM	SM	SM	SM	SM	SM	SM
AASHTO Class.	A-2-4	A-2-4	A-2-4	A-2-4	A-2-4	A-4	A-2-4	A-2-4
MDOT Class.	*9C*	*9C*	*9C*	*9C*	*9C*	*9C*	*9C*	*9C*

Note: Three natural moisture contents ($\omega_{natural}$), forty air-dried moisture contents ($\omega_{air\text{-}dried}$), and 9 or 10 gradations were conducted for Pits A, B, and C for Res. samples.

a: Results from pit soil samples tested for the current research study.

b: Results from mix design performed by MDOT for the corresponding construction project.

c: Results from a mix design (MT-25) performed by BCD laboratory for the project (Station No. 219+00).

4.3 Cementitious Materials Tested

Five cementitious blends were used in this research: four ASTM C150 Type I portland cements and one Ground Granulated Blast Furnace Slag (GGBFS) blend (Tables 4.2 and 4.3). Certain testing procedures at MDOT central laboratory require that cements be identified only by type, therefore data acquired by these tests is identified only as type I, with no differentiation of source. The majority of testing was performed with TH cement. The GGBFS met requirements for Grade 100 according to ASTM C989 and AASHTO M302.

Table 4.2. Properties of Portland Cements Tested

Source[1]	***TH***	***GV***	***NC***	***TH_{SR475}***
SiO_2 (%)	19.9	20.0	20.3	19.9
Al_2O_3 (%)	4.7	4.5	4.5	4.8
Fe_2O_3 (%)	3.4	3.1	3.3	3.6
CaO (%)	64.5	64.2	63.1	64.0
MgO (%)	1.2	2.3	2.6	1.0
SO_3 (%)	3.7	3.2	3.1	3.5
C_3S (%)	60	62	60	61
C_2S (%)	11	9	13	11
C_3A (%)	7	6	6	7
C_4AF (%)	10	9	10	11
Limestone (%)	2.5	3.3	--	0.8
LOI (%)	2.2	2.7	2.2	1.4
Blaine (m^2/kg)	379	383	386	395
Initial Vicat (min.)	101	90	180	100
Air (%)	7	7	9	8
1-day strength (MPa)[3]	16	16	13	--
3-day strength (MPa)[3]	26	30	24	23
7-day strength (MPa)[3]	33	36	29	31
HoH, 7-day (kJ/kg)	353	344	--	328

1: TH = Holcim Cement Theodore, AL
GV = Holcim Cement Saint Genevieve, MO
NC = National Cement (SR9 field cement)
TH_{SR475} = Holcim Cement Theodore, AL (SR475 field cement)
2: 1, 3 and 7 day compressive strengths according to ASTM C109

Table 4.3. Properties of Slag Cement Tested

Property	**Result**
Sulfide-S (%)	0.6
Sulfate Ion-SO_3 (%)	0.3
Blaine Fineness (m^2/kg)	582
Plus 45 um (No. 325) (%)	1
Air Content (%)	5
Activity Index (%), 7-day	88
Activity Index (%), 28-day	126
7-day strength (MPa)	25
28-day strength (MPa)	43

Note: GGBFS (i.e. slag cement)source was Holcim Birmingham, AL.

CHAPTER 5 – EXPERIMENTAL PROGRAM

5.1 Experimental Program Overview

This study was experimentally focused and included soil-cement testing related to: thermal profile measurement with corresponding compressive strength, strength gain with time, strength variability, wheel tracking, and elastic modulus. A total of 2,101 tests were performed. The remainder of this chapter provides the terminology used to identify specimens, equipment and tools used, specimen preparation, and testing methods. Detailed descriptions of specimens tested are provided at the beginning of each results chapter.

5.2 Terminology

Testing was grouped into 10 different sub-categories. Specimens were identified by an equation that was three to five terms long (Tables 5.1 and 5.2). All specimen equations include the specimens testing category, material source, cement index (C_I), and either a series number, specimen number, or both. Testing category is identified by an alphabetical prefix and is always presented first in the equations. Series numbers, specimen numbers, and C_I are identified numerically.

Testing Categories incorporated include Strength Versus Time (ST), Elastic Modulus (EM), PURWheel (PW), Asphalt Pavement Analyzer (APA), Design Strength Variability (SV), Design Strength Variability Using the MDOT Curing Method (SVM), and Thermal Profile Quality Control (TP, FW, MA, PR). Specimen type and material source are identified by a designation for brevity. These designations are shown in Table 5.1. Equations for specimen identification and descriptions of terms are given in Table 5.2. Terminology and specimen identifiers used were identical to Sullivan (2012) and Anderson (2013) with the exception of some new specimens not included in those documents.

As an example the specimen identified by the equation ST-7-PA-5-12 is a strength versus time specimen of type 76 by 152 mm plastic mold. The material used was from pit soil A at a cement index of 5%. Numerically the specimen was the 12th replicate.

5.3 Testing Equipment and Tools

This section describes relevant equipment and tools used herein. Equipment and tools that could be used interchangeably at different laboratories are not discussed. Examples include, but are not limited to, storage containers, scales, ovens, and thermometers. Note that calibration and measurement precision applied in typical soil-cement operations is required.

5.3.1 Compaction Equipment

Five methods were used for compaction. Most specimens were compacted between 98 and 101 percent of wet density (γ) corresponding to standard proctor maximum dry density (γ_d). Target moisture contents were ± 0.5% of OMC. Two specimens were usually made from each mixed batch. On some occasions, single specimen sets were used. Single specimen sets are noted when they occur in the raw Appendix data files in Sullivan (2012) or Anderson (2013). Compaction method details are discussed in the following sections.

Table 5.1. Commonly Used Designations Within Terminology Equations

Specimen Type	Explanation	Material Source	Explanation
1	102 by 116 mm Standard Proctor	PA	Pit Soil A
2	100 by 114.6 mm Superpave Gyratory Compactor	PB	Pit Soil B
3	150 by 75 mm Superpave Gyratory Compactor	PC	Pit Soil C
4	76 by 152 mm Plastic Mold in Compaction Frame	PD	Pit Soil D
5	293 by 624 mm Linear Asphalt Compactor Slab	PE	Pit Soil E
6	150 by 62 mm Superpave Gyratory Compactor		
7	76 by 152 mm Plastic Mold		

Table 5.2. Terminology Equations for Specimen Identification

Equation Number	Equation	Test Category	Term 1	Term 2	Term 3	Term 4
5.1	ST-1-2-3-4	Strength Versus Time	Specimen Type	Material Source	C_I	Specimen Number
5.2	EM-1-2-3-4	Elastic Modulus	Specimen Type	Material Source	C_I	Specimen Number
5.3	PW-1-2-3-4	PURWheel	Specimen Type	Material Source	C_I	Specimen Number
5.4	APA-1-2-3-4	Asphalt Pavement Analyzer	Specimen Type	Material Source	C_I	Specimen Number
5.5	SV-1-2-3-4	Design Strength	Specimen Type	Material Source	C_I	Specimen Number
5.6	SVM-1-2-3-4	Design Strength (MDOT Method)	Specimen Type	Material Source	C_I	Specimen Number
5.7	TP-1-2-3	Phase 1 Thermal Profile QC	Series Number	Material Source & C_I	Specimen Number	---
5.8	FW-1-2-3	Phase 2 Thermal Profile QC	Series Number	Material Source & C_I	Specimen Number	---
5.9	MA-1-2	Phase 2 Thermal Profile QC	Material Source & C_I	Specimen Number	---	---
5.10	PR-1-2-3	Phase 3 Thermal Profile QC	Series Number	Material Source & C_I	Specimen Number	---

5.3.1.1 Plastic Mold Compaction Set

Equipment and protocols were developed during State Study 206 to allow soil-cement to be compacted in a plastic mold, as a result of this type of equipment not being found commercially. The equipment developed can be used in multiple combinations, and has the versatility to be used in the laboratory or the field. The remainder of this section describes the equipment and accessories used to compact soil-cement in a plastic mold.

Specimen molds were constructed from standard 76.2 by 152.4 mm plastic molds which meet the requirements of ASTM C470 for single-use concrete molds. The plastic molds were modified and utilized as a single-use specimen mold (Figure 5.1). The modified molds cost approximately $1.25 each and allow thermal profile and strength measurement on the same specimen. This project used each mold once prior to disposal for consistency, but a retrospective evaluation suggests the molds could be re-used.

Molds were modified by sanding the bottoms to remove the plastic ridge around the edge to provide a flush surface for compaction. Sanding was performed with a belt-sander and by hand. After sanding, a drill-press was used to produce a 35 mm diameter hole through the center of the mold bottoms. The 35 mm hole allows for the specimens to be manually extruded without damage for strength testing. An aluminum plate (76.2 mm diameter and 1.6 mm thick) was inserted into the bottom of the mold to cover the hole and provide a rigid surface for manual extrusion. The aluminum plate thickness changed the aspect ratio from 2:1 to 1.98:1, which was considered insignificant. The plastic cut-outs from the drilling process were used to fill the gap between the metal plate and the exterior bottom of the mold to provide a solid compaction surface. The drilling process made a small hole in the plastic cut-out which was filled with Bondo® Body Filler. Tape was used to hold the plastic cut-out in place and help seal the bottom of the mold.

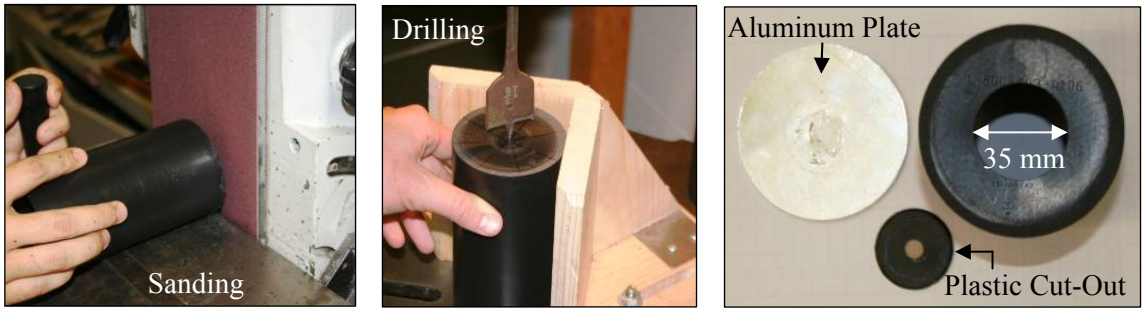

Figure 5.1. 76.2 by 152.4 mm Plastic Mold Modifications

A steel mold was designed and fabricated that allowed 76.2 mm diameter by 150.8 mm tall specimens (1.98:1 h/d aspect ratio) to be compacted inside the plastic molds modified as described previously. Figure 5.2 provides photos of the split mold and collar, and detailed drawings are provided in Appendix C of Sullivan (2012). The split mold concept is similar to the molding apparatus described in ASTM C1435. The split mold inner diameter is the same as the plastic mold outer diameter, while the collar and plastic mold have the same inner diameter to facilitate alignment and to prevent the plastic mold from being struck during compaction. The collar also helps contain the soil during compaction. The split mold is referred to hereafter as *PM* for plastic molded specimen.

Figure 5.2. Split Mold and Collar (Referred to as *PM*)

The *PM* split mold was used in two manners. The first was as the lower assembly of a compaction frame (*CF*) designed and fabricated during this research (Figure 5.3). Specimens compacted in the *PM* mold by the compaction frame were referred to as *PM-CF*, with details provided in the following paragraph and drawings provided in Appendix C of Sullivan (2012).

(a) Compaction Frame (*CF*)

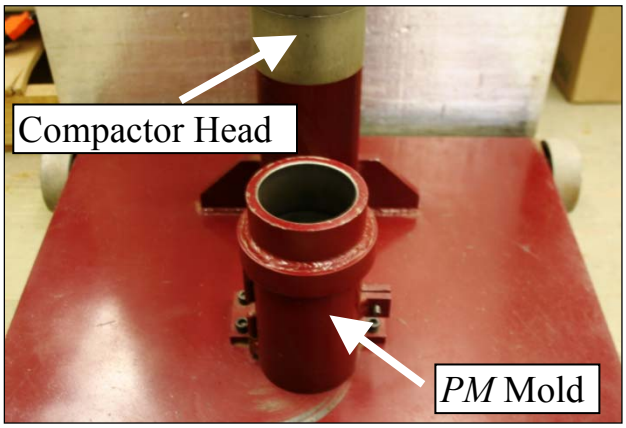

(b) PM Mold Attached to *CF* Base (mold closed)

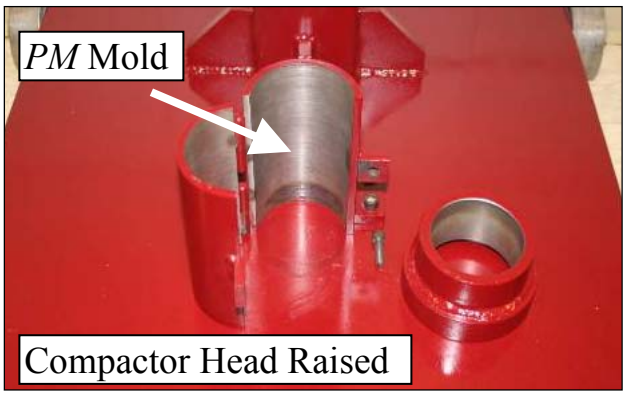

(c) *PM* Mold Attached to *CF* Base (mold open)

Figure 5.3. Compaction Frame and *PM* Mold (*PM-CF* Approach)

The second use of the *PM* mold was alongside a modified proctor hammer (4.54 kg mass falling 45.72 cm) when bolted to a 28.9 by 24.1 by 1.3 cm steel plate (Figure 5.4). Specimens compacted in the *PM* mold by a modified proctor hammer were referred to as *PM-P*. The *PM-P* compaction approach can easily be performed in the laboratory or the field. The total cost for one *PM-CF* split mold and compaction assembly was approximately $3,000 (materials and fabrication), while the total cost of one *PM-P* split mold and base plate minus the proctor hammer was approximately $900 (materials and fabrication).

The *CF* was designed to compact a known amount of material to a prescribed height, thus achieving a target specimen density. The *CF* fabricated for State Study 206 was very similar conceptually to the dropping-weight compacting machine described in ASTM D1632. The compaction head is connected to a guide rod and is placed on top of the soil to be compacted. Compaction is performed by dropping a 6.8 kg weight from a height of 30.5 cm and hitting a striker plate which transfers the compaction energy to the soil. The striker plate has a robust weld to withstand repeated striking from the 6.8 kg weight. Compaction heights for each layer were etched into the compaction head for consistency.

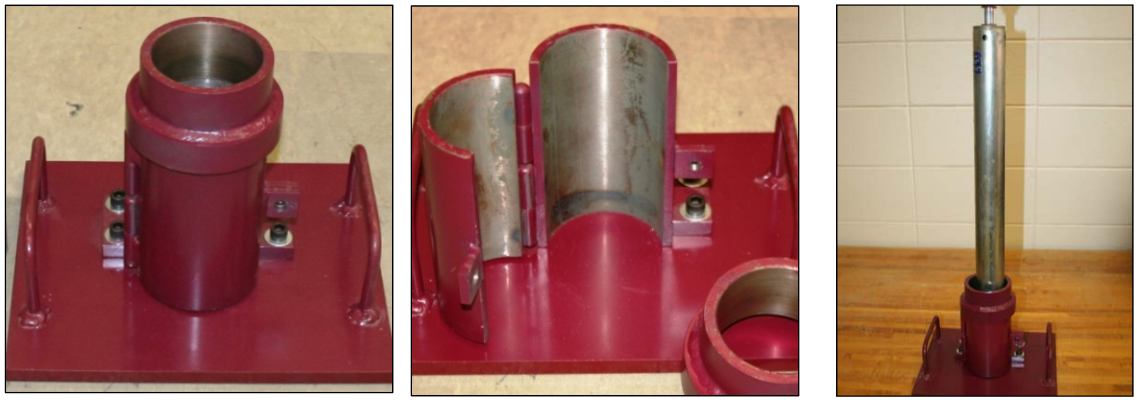

(a) *PM-P* (closed) (b) *PM-P* (open) (c) *PM-P* w/ Mod. Hammer

Figure 5.4. *PM* Mold with Modified Proctor Hammer (*PM-P* Approach)

5.3.1.2 Mechanical Standard Proctor Hammer

A mechanical standard Proctor hammer (photo is shown later in this document in Figure 5.14a) was used to compact most proctor specimens. In a few instances a standard proctor hammer operated by a technician was used; there was no differentiation between these approaches. In general, the same compaction procedure used in MT-8, a modification of AASHTO T99, was used to compact specimens with a mechanical hammer. A typical proctor compaction mold was used with a diameter of 101.6 mm and volume of $943e^{-6}$ m^3. The hammer had a weight of 2.5 kg and was dropped from a height of 30.5 cm above the top of the soil. These specimens were denoted specimen type 1 in Equation 5.1 through 5.10.

5.3.1.3 Linear Asphalt Compactor

The Linear Asphalt Compactor (LAC) was used to produce soil-cement slabs for PURWheel testing. Operation and features, including a more detailed procedural description,

of the LAC in use at MSU can be found in Doyle and Howard (2011). The LAC produces rectangular slabs that are 29.3 by 62.4 cm and between 3.8 and 10.2 cm thick.

5.3.1.4 Superpave Gyratory Compactor

A Pine AFGC 125X Superpave Gyratory Compactor (SGC) was used to compact specimens. Specimens with types 2, 3, and 6 (Equation 5.1 through equation 5.6) were compacted using the SGC. The SGC compacted the material to a height of 114.6, 75 or 62 mm, depending on specimen type.

5.3.2 Mixing Tools

Mixing operations were conducted in the following manner, which is slightly different than some common practices. Traditionally, soil-cement is often mixed by hand, but many specifications state that a suitable mechanical mixing device is acceptable and often preferred. For this study, mixing was performed using a stationary mechanical bucket mixer for consistency (Figure 5.5a). A 19 L capacity mixer was used for most mixing, though a 38 L capacity mixer of the same style as the 19 L mixer was used in a few instances. A mixing paddle was used to mix the materials and a hand trowel was used to aid in mixing (Figure 5.5b).

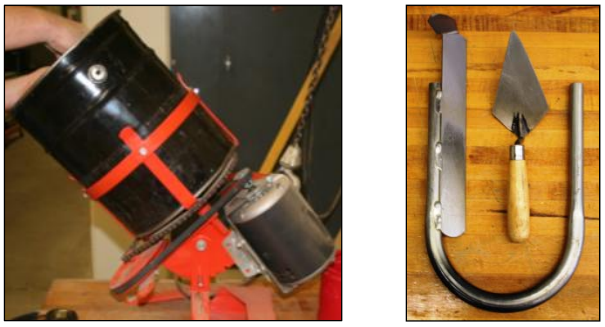

(a) Bucket Mixer (b) Mixing Tools

Figure 5.5. Mixing Tools (19 L Mixer Shown)

5.3.3 Wheel Tracking Devices

The PURWheel Laboratory Wheel Tracker was used to test soil cement slabs under multiple loading and environmental conditions. Four loading configurations were used during PURWheel testing. Lead weights were fabricated to simulate four different downward forces applied to the surface of the LAC compacted slabs (Figure 5.6). The manual for traditional bituminous material testing (Howard et al. 2010) specifies a 176 kg applied load for default PURWheel testing. This was referenced as 100% load. Weights were fabricated to apply a load to the specimen of approximately 86.4 kg (50% load), 110.6 kg (65% load), and 138.7 kg (80% load). Herein, load configurations are identified by percent referencing the suggested load in Howard et al. (2010). Wheel tracking tests were also performed using the Asphalt Pavement Analyzer (APA) and Hamburg Loaded Wheel Tester (HLWT). Testing with these devices was conducted according to common practice.

(a) 50% load (b) 65% load (c) 80% load (d) 100% load

Figure 5.6. Masses for PURWheel Loading Configurations

5.3.4 Compressive Strength and Elastic Modulus Testing Devices

Compressive strength and elastic modulus testing was conducted using a screw type load frame (4,500 kg capacity) with adjustable load rate shown in Figure 5.7a. A proving ring with a swiveling load head was used to measure the applied force. An H-2919 Compressometer/Extensometer (Comp/Ext) with dial gages supplied by Humboldt Manufacturing Company was used to measure horizontal and vertical deflections and determine elastic modulus (Figure 5.7b).

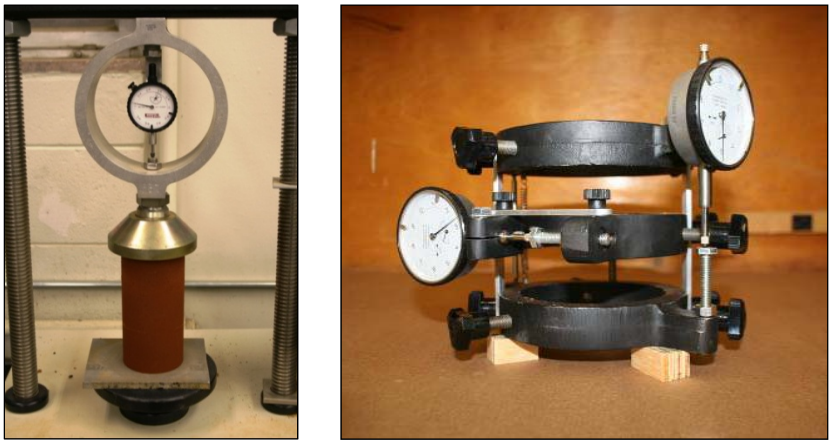

(a) Load Frame (b) Compressometer

Figure 5.7 Compressive Strength and Elastic Modulus Devices

5.3.5 Thermal Measurements Equipment

Two thermal measurement devices were built from Expanded Polystyrene (*EPS*) blocks (R_{SI} = 0.775) and are referred to as Blocks A and B or *EPS* devices. One thermal measurement device was built from 48 kg/m^3 density chemically Cross Linked Polyethylene (*XLPE*) foam blocks ($R_{SI} \approx 0.564$) and is referred to as Block C or *XLPE* device. The exact R_{SI} value for the tested *XLPE* block was unavailable, but an equivalent chemically cross linked polyethylene foam product from another producer was found to have an R_{SI} value of 0.564. Since additional information was not readily available, the R_{SI} value of the tested *XLPE* was considered be approximately 0.564. The *EPS* and *XLPE* devices are the same

except for amount of insulation and sensor type. A higher R_{SI} value indicates greater insulation. Device designs were based on Sullivan et al. (2012). One device is capable of testing eight specimens. A Channel ID was given to each device slot and denotes the Block type (e.g. A, B, or C) and slot position (e.g. 1 through 8). A list of the materials needed to construct one *EPS* device is given below:

1. One 15 by 38 by 66 cm *EPS* block (32 kg/m^3 density)
2. Two 5 by 38 by 66 cm *EPS* blocks (32 kg/m^3 density)
3. Six 0.64 by 20.32 cm carriage bolts
4. Twelve 1.11 cm diameter flat washers
5. Six 0.64 cm wing nuts
6. One 8-channel data logger (Pico Technology model *TC-08*)
7. Eight K-type thermocouples with fiberglass insulation and 1 m leads
8. Eight 0.79 by 4.13 cm fender washers
9. Aluminum foil tape and clear packing tape

Item 1 is the main block of the device which holds and insulates the specimens. One *EPS* block from Item 2 is the bottom of the device and accommodates the thermocouple instrumentation. The second *EPS* block from Item 2 is the lid for the device. Items 3 through 5 are the hardware needed to fasten the *EPS* blocks together. Items 6 through 8 are the instrumentation components. Tape needed to finish the device construction is Item 9. The following paragraphs describe the *EPS* device fabrication, and Figure 5.8 contains drawings and photos of the *EPS* device.

Eight 76.2 mm diameter holes and six 64 mm diameter holes were drilled through the main *EPS* block (Item 1). The six 64 mm diameter holes extend through the bottom *EPS* block (Item 2). The 76.2 mm holes house the specimens while the 64 mm holes are for the carriage bolts and other hardware (Items 3 through 5) that fasten the blocks together. Figure 5.8a is a schematic of the device which shows hole locations for the main and bottom blocks. Holes were drilled using a 76.2 mm (3 in) diameter hole-saw bit and a 64 mm (0.25 in) diameter drill bit. A drill press was used to perform cuts to ensure the precise vertical and horizontal alignment of each hole. Interior walls of the 76.2 mm diameter holes were lightly sanded until the plastic molds (described in Section 5.3.1.1) fit tightly inside without becoming lodged. The edges and exposed sides of the *EPS* blocks were wrapped with aluminum foil tape for added durability (Figure 5.8b).

By design, approximately 10 mm of the specimens extended beyond the top of the main block for easy specimen removal after testing. A lid was constructed to cover and insulate the exposed specimen tops during testing (Figure 5.8d). Circular recesses were cut into the bottom of the lid to provide a tight fit around the specimen tops and the fastening hardware. The indentions allowed for a flush seal between the main block and lid. Edges, exposed sides, and cut indentions were wrapped in aluminum foil tape.

The thermal measurement device was fastened together using carriage bolts, washers, and wing nuts (Items 3 through 5). The carriage bolts were inserted from the bottom of the bottom block through the 64 mm drilled holes, and were fastened with wing nuts. The head of each bolt was counter sunk so the device can rest on a flat surface. Washers were used to prevent the bolt head and wing nut from ripping through the *EPS* blocks. Wing nuts were hand tightened. Figures 5.8g and 5.8h show the completed device. One thermal measurement device costs approximately $700 (materials and data logger), and takes about 8 hours to fabricate. Cost estimate does not include the computer or data logging software.

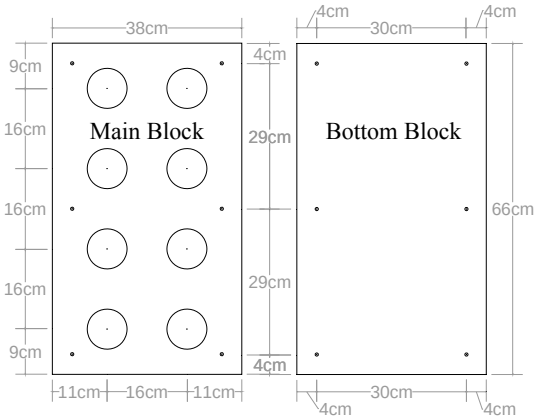

(a) Thermal Measurement Device Schematic

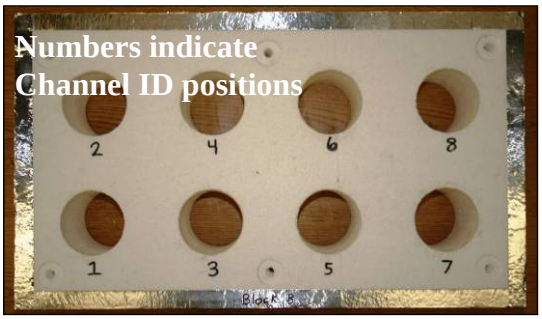

(b) Main Block

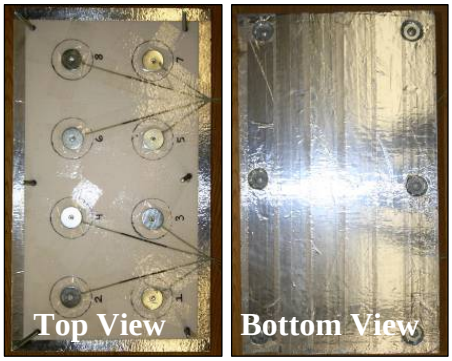

(c) Bottom Block

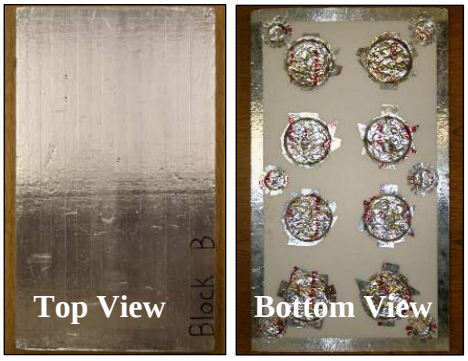

(d) Device Lid

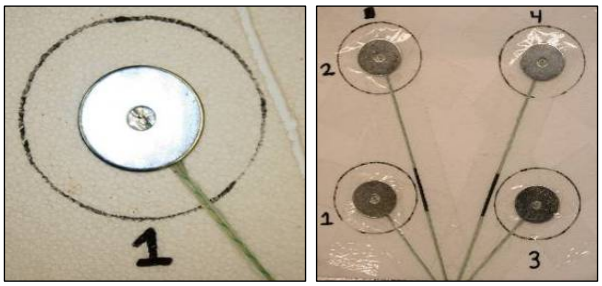

(e) Thermocouple Instrumentation

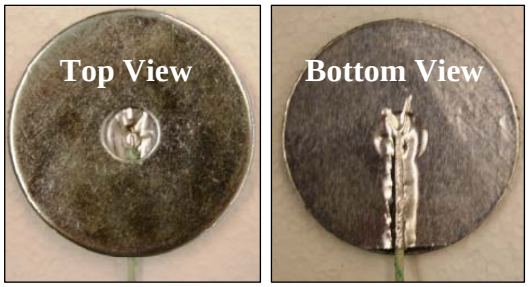

(f) Thermocouple Sensor

(g) Disassembled Device and Data Logger

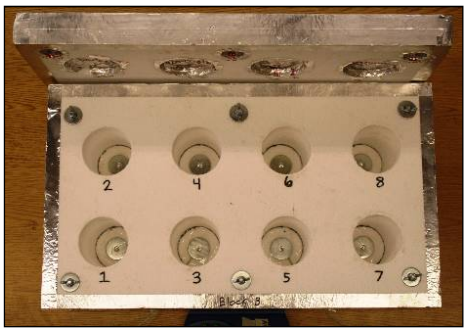

(h) Assembled Device and Lid

Figure 5.8. Schematic and Photos of Thermal Measurement Equipment (*EPS* shown)

The thermal measurement device described in Figure 5.8 was complimented with external insulation for some experiments. An external insulated enclosure was constructed of 2.5 cm thick sheets of honeycomb walled aluminum alloy insulation provided by Plascore. An R_{SI} was not available for the composite sheet of material, but could be estimated given that the aluminum alloy had an r-value of 0.03 (h*ft^2*°F/BTU). Figure 5.9 illustrates the external insulated enclosure, which is referred to as HC for honeycomb.

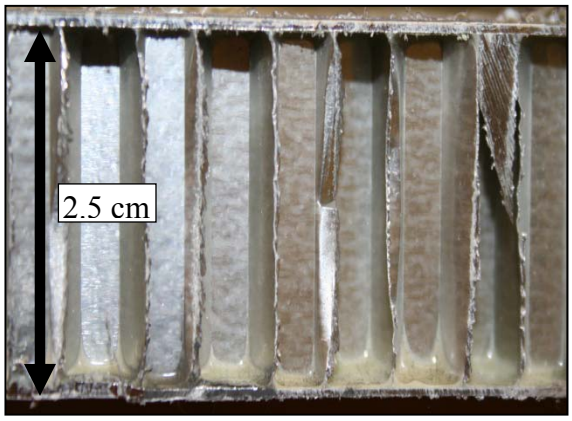

a) Aluminum Honeycomb Insulation

b) External Insulated Enclosure (Empty)

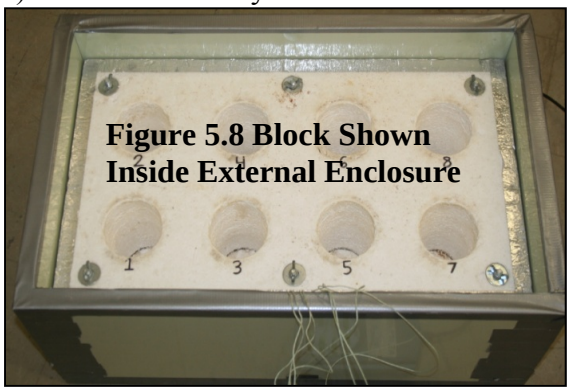

a) External Insulated Enclosure (Open)

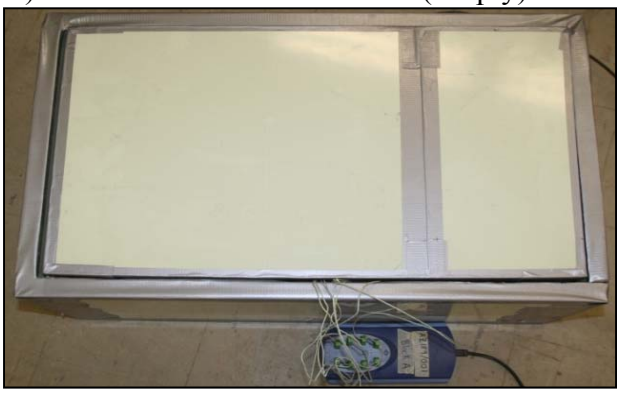

b) External Insulated Enclosure (Closed)

Figure 5.9. External Insulated Honeycomb (HC) Enclosure

5.3.6 Curing Devices

The environmental chamber used for the current work is commercially available and designed to cure concrete cylinders according to ASTM C31. The chamber is capable of cooling and heating a water bath to temperatures of 7 to 43°C with a precision of ±1°C. Testing protocols utilized the curing chamber to regulate the ambient air temperatures inside the chamber by heating and cooling the water bath. A metal rack was placed just above the water surface to accommodate thermal measurement equipment, and a small submersible pump was used to circulate the bath water and help minimize temperature variations in the chamber. Thermocouple wires were directed out the front of the chamber through the lid seal. Figure 5.10 is a photo of one of the two identical curing chambers with two Figure 5.8 devices inside. One environmental chamber was used to precondition materials, and a second chamber was used to house the thermal measurement devices.

Curing chamber water temperature did not directly correlate to the ambient temperature above the water. The discrepancy occurs because the environmental chamber is not perfectly insulated, and air temperatures inside the chamber are influenced by the air temperatures outside the chamber. Adjustments were made by placing a thermocouple inside the curing chamber and adjusting the controls to achieve the desired air temperature.

Figure 5.10. Environmental Curing Chamber with Devices

A moisture curing room was also used for some testing. Moisture room shelves were covered with sheets of flattened stainless steel expanded metal (12.7 mm number 18 style) that was mounted on wooden dowels to prevent soil-cement specimens from resting in very shallow standing water. The moisture room maintained humidity between 99.5 and 100%. A *SPER Scientific Model 800024* data logger was used to monitor the ambient air temperature of the moisture room every 60 minutes. Figure 5.11 shows a photo of the moisture curing room and a relative frequency histogram of the curing room ambient temperatures observed throughout testing.

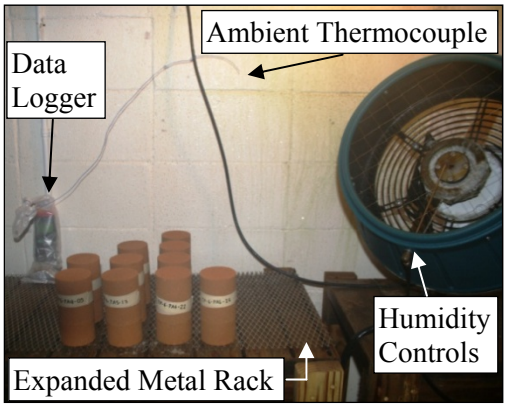

(a) Moisture Curing Room

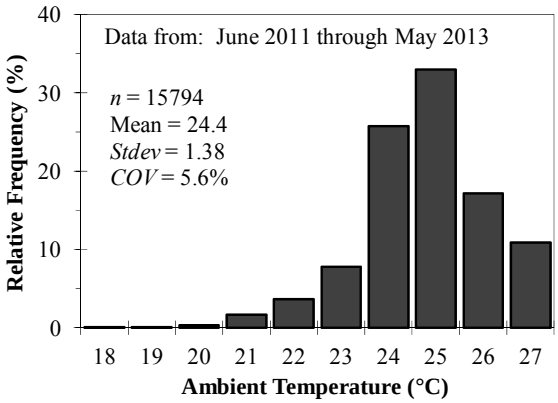

(b) Ambient Temperature Distribution

Figure 5.11. Moisture Curing Room and Ambient Temperature Distribution

5.4 Specimen Preparation

The raw materials (pit soils, cementitious materials, and water) described in Chapter 4 were made into test specimens using the tools and equipment described in Section 5.3. The remainder of this section describes specimen practices, and concludes with specimens that have been pre-conditioned, batched, mixed, compacted, and cured that are ready for testing.

5.4.1 Material Pre-Conditioning

Pre-conditioning of materials was performed for all thermal profile specimens and select other specimens before cement addition. Figure 5.12 is an example of phase 1 thermal profile pre-conditioning. The soil and water were mixed prior to pre-conditioning (see Section 5.4.2), and all materials were sealed during pre-conditioning. Cement was stored separately from the soil and water mixture. At the end of pre-conditioning initial material temperatures (T_i) for further specimen preparation had been achieved.

Figure 5.12. Example Material Pre-Conditioning

The majority of phase 1 thermal profile materials were pre-conditioned overnight in the Figure 5.10 environmental chamber at a prescribed temperature. Some phase 1 materials were pre-conditioned outside overnight, and in these instances weather conditions were monitored to ensure materials did not freeze (cooler conditions were being investigated). Some phase 1 materials were placed in a small room where air temperature was regulated with multiple space heaters (warmer conditions were being investigated). In these instances ambient temperature was recorded and monitored during pre-conditioning.

Phase 2 mold adjustment materials were pre-conditioned overnight in the Figure 5.10 environmental chamber at a prescribed temperature. For most of phase 2 thermal profile testing, T_i was not controlled, rather was the onsite temperature at the construction site. Phase 3 materials were pre-conditioned outdoors sitting on a concrete slab on grade while in sealed plastic cylinders (same cylinder types as in Figure 5.12).

Thermal profile foam blocks and mixing tools were also pre-conditioned in several instances. The thermal profile foam blocks (Figure 5.8) were at a device temperature (T_{BL}) at the time a specimen was first introduced into them that was recorded and is presented as appropriate during discussion of results. In phase 3, mixing and compaction tools were pre-conditioned outdoors prior to use for at least 30 minutes in the same location as the materials.

5.4.2 Batching and Mixing

Batching operations were conducted, when possible, in the same manner as MDOT standard practice discussed in Chapter 3. Equations 3.13 through 3.18 (Section 3.4.3) were used to calculate the amount of soil, water, and cement required for each mixture. Batch water adjustments were required to achieve the appropriate optimum moisture content as measured by MT-9. Excess batch water is needed due to losses on mixing tools and to evaporation. An experiment was conducted to determine the amount of additional batch

water needed to achieve the optimum moisture content as measured in MT-9; an additional 0.7 percent batch water achieved the appropriate moisture content in all soils.

Mixing was performed in two stages, and all specimens except those for LAC slabs were mixed in the 19 L bucket mixer (Figure 5.5). A paddle and a hand trowel were the mixing tools. The trowel was used by hand to assist mixing with the paddle. The first stage involved mixing of the soil and water, and the second stage entailed mixing the cement with the soil/water mixture (Figure 5.13a and 5.13b). Water was added while the mixer was running at approximately 90 grams per second in order to combat material clumping.

In both stages, mixing was performed for two minutes, which was determined to be an adequate amount of mixing time to ensure uniformity. In some cases, these stages occurred within a few minutes of each other, and in other cases several hours elapsed between these stages (material was sealed during storage to prevent evaporation and hydration). In some cases where pre-conditioning was performed, the soil/water mixture was remixed for 30 seconds prior to cement mixing to allow a more representative temperature to be recorded. A quality control measure was conducted to check moisture contents based on measured wet and dry soil masses throughout the process. Upon complete mixing of soil, water, and cement, a sample was taken from the bucket and used as a moisture content check.

(a) Mixing Soil and Water (b) Mixing Cement

Figure 5.13. Mixing Equipment and Operations

Material for LAC slabs was mixed in a similar fashion as described above. However, because of the large amount of material needed (i.e. approximately 30 kg), mixing was handled by two separate mixers. Mixers included the aforementioned 19 L bucket mixer as well as a 38 L bucket mixer. Material was divided between the two mixers, approximately 40% in the 19 L mixer and 60% in the 38 L mixer. Material from each mixer was then evenly divided to accommodate a two lift compaction procedure.

5.4.3 Specimen Compaction

5.4.3.1 Proctor Compaction for Density Evaluation Purposes

When compacted for density evaluation (i.e. Chapter 6 data), Proctor compaction was identified as being according to MT-8, MT-9, a modified version of MT-9 (MT-9-Mod), or specimens compacted after a fixed time delay. When following MT-9-Mod, each proctor point was batched, mixed, and compacted separately. No material was reused, and each point was compacted within 7 minutes of cement addition. MT-9 batched all soil and cement together and some specimens were compacted several minutes after cement addition.

5.4.3.2 Proctor Compaction for Producing Strength Specimens

The typical Proctor compaction protocol used to produce specimens for subsequent strength testing is illustrated in Figure 5.14. After material was mixed, compaction occurred in three equal lifts. Each lift was compacted with 25 equally distributed blows with a 2.5 kg hammer dropped 30.5 cm. Before the second and third lifts, a scarifying tool (produced for this study) was used to partially break up the previous layer to produce a uniform specimen. Once compaction was complete for both specimens (within 20 minutes of cement contact with water), a straightedge was used to strike off excess material before the specimen was extruded. After extrusion, specimens were labeled and placed under a damp towel for 2 $\pm$ 0.5 hours. Thereafter, measurements of height, diameter, and weight were recorded before a curing protocol was initiated. Because the mechanical standard Proctor hammer applied a given compaction energy rather than compacting to a density, some densities fell outside 98 to 101% of γ. When this occurred, specimens were still used.

(a) Hammer (b) Adding Material (c) Scarifying Surface (d) Extrusion (e) Striking off Surface

Figure 5.14. Example Proctor Compaction Photos

5.4.3.3 Slab Compaction

The Linear Asphalt Compactor (LAC) was used to produce soil cement slabs for PURWheel testing. There were 6 soil cement slabs made for this portion of the study. Slabs are referred to as a type 5 specimen in Equations 5.1 through 5.6. For soil cement slabs, a thickness of 7.6 cm was targeted. Two separately compacted lifts were needed to achieve

compaction. Before material was added, a piece of paper was placed in the bottom of the mold. The first lift of material was added and spread to an even uncompacted height. Compaction plates were set in place. Hydraulic system pressure was set at 2413 kPa; 18 passes were applied to each lift (a pass is defined as compaction energy applied once to a given point). After compaction of the first lift, compaction plates were removed, along with the top release paper and thin sheet of metal. The surface was scarified to produce the most uniform specimen possible. The second lift followed the same approach as the first lift. After compaction, the slab was removed from the mold on an aluminum plate and transported immediately to the curing environment (Section 5.4.4). Because the LAC applied a given compaction energy rather than compacting to a density, some densities fell outside 98 to 101% of wet density (γ). When this occurred, specimens were still used.

5.4.3.4 Gyratory Compaction

A Pine AFGC 125X Superpave Gyratory Compactor (SGC) was used to compact multiple specimen types. After material was mixed, a specified amount of material was placed in the SGC mold (100 mm or 150 mm diameter) to achieve 100% of wet density (γ). In most cases, a small amount (e.g. 10 grams) above the design weight was added to counter any lost mass (e.g. soaking of water into spacer paper, etc.). Spacer papers, as well as a thin piece of aluminum foil, were placed between the material and plates to assist in the removal of the top and bottom compaction plates. Specimen type 2 (Equation 5.1 through equation 5.6) was compacted to 114.6 mm tall to attain the same h/d ratio as specimen type 1 (Equation 5.2 through equation 5.6). The specimen was then extruded from the mold; and the top plate, foil, and spacer paper were removed. The specimen was carefully loosened from the bottom plate using a slight shearing action, followed by the removal of the bottom spacer paper and foil. After extrusion, specimens were labeled and placed under a damp towel for 2 $\pm$ 0.5 hours. Thereafter, measurements of height, diameter, and weight were recorded before a curing protocol was initiated.

5.4.3.5 *PM-CF* Compaction

Figure 5.15 illustrates the plastic mold and compaction frame (*PM-CF*) protocol. A single plastic mold was securely clamped to the compactor lower assembly and the collar was placed on top. Then each specimen was compacted in three equal lifts. Material for each lift was pre-batched using Equation 5.11. Equation 5.12 is a simplified form of Equation 5.11 where a single constant accounts for the mold volume, unit conversion, number of lifts, and 1 percent material increase.

$$W_{S-C} = \left(\frac{VPM \times \gamma_d \times 453.5924 \times \left(\frac{100 + OMC}{100} \right)}{3} \right) \times 1.01 \qquad \text{(Eq 5.11)}$$

$$W_{S-C} = 3.75 \times \gamma_d \times \left(\frac{100 + OMC}{100} \right) \qquad \text{(Eq 5.12)}$$

Where:

$W_{S\text{-}C}$ = Weight of soil-cement material per lift (g)

$V\,PM$ = Volume of the plastic mold (ft^3)

γ_d = Maximum dry density of soil-cement mixture (lb/ft^3)

453.5924 = Unit conversion from pounds to grams

OMC = Optimum moisture content of soil-cement mixture (%)

3 = Division for the three separate lifts

1.01 = Increase amount of material to account for material left on compacting hammer

3.75 = Constant value for mold volume, units, lift division, and material increase

(a) Measuring Each Lift (b) Compactor Hammer (c) Compactor Head at Height

(d) Scarifying Surface (e) Finish Compaction (f) Striking off Surface

Figure 5.15. Specimen Compaction as per *PM-CF* Approach

All laboratory specimens were compacted within 20 minutes of cement addition. As shown elsewhere, soil-cement specimens can be influenced by compaction delay, and 20 minutes appears to be a reasonable threshold for the pit soils tested in this study. All laboratory specimens were compacted between 98 and 101 percent of target γ and moisture contents were within 0.5 percent of target OMC. During specimen preparation, the number of blows (N_b) required to compact each specimen was recorded.

Material for each lift was placed into the mold (Figure 5.15a) and compacted to a height to replicate proctor density (Figure 5.15b, 5.15c). Before compaction of the second and third layers, the previous layer surface was scarified to produce a uniform specimen (Figure 5.15d). After compaction (Figure 5.15e), the top of the specimens was struck off level with the top of the mold (Figure 5.15f) and sealed with a plastic lid to complete preparation. Specimens were immediately taken to thermal profile measurement or curing.

5.4.3.6 *PM-P* Compaction

Plastic mold with modified Proctor hammer (*PM-P*) compaction was performed with the equipment shown in Figure 5.4c. Figure 5.16 is an example field compaction; this same approach was also incorporated during outdoor thermal profile and laboratory experiments. Specimens were compacted in three pre-weighed lifts with the field compactor and modified proctor hammer. Equation 5.13 was used to calculate the appropriate amount of material for each lift. Equation 5.13 is the same as Equation 5.12, but the amount of material for each layer was increased to account for a larger amount of material left on the compaction hammer.

Figure 5.16. Specimen Compaction as per *PM-P* Approach

$$W_{S-C} = 3.8 \times \gamma_d \times \left(\frac{100 + OMC}{100} \right) \quad \text{(Eq 5.13)}$$

Where:
W_{S-C} = Weight of soil-cement material per lift (g)
3.8 = Constant value for mold volume, units, lift division, and material increase
γ_d = Maximum dry density of soil-cement mixture (lb/ft^3)
OMC = Optimum moisture content of soil-cement mixture (%)

Each lift was compacted with 5 blows with a 4.54 kg hammer dropping from a height of 45.7 cm (modified Proctor hammer). This method of compaction produced specimens with densities between 92 and 100 percent of target max dry density (γ_d). Between lifts, the surface was scarified in the same manner as laboratory specimens.

5.4.4 Specimen Curing

A variety of curing protocols were employed in this research, with the equipment shown in Figures 5.10 and 5.11 being central to curing activities. Thermal profile specimens were cured for the first 24 hours inside plastic molds that were inside the Figure 5.8 foam blocks. In some cases the foam blocks were inside the Figure 5.10 environmental chamber (temperature controlled), while in other cases the foam blocks were exposed to other environments. Specific thermal profile environments are provided with test results as appropriate. After 24 hr of thermal profile measurement, specimens were either tested or placed into another type of curing protocol. The remaining paragraphs describe the additional categories of curing that were used in this report, with exception of field curing. Field curing protocols are described in Section 5.4.5

Specimens subjected to the Mississippi State University (MSU) curing protocol were placed under a damp towel for 2 ± 0.5 hours after compaction. This allowed the specimens to mature enough to prevent damage during measuring and handling. Some specimens could be handled immediately without damage, but the two hour hold time was kept consistent throughout the study. After 2 ± 0.5 hours, the specimens were measured for density immediately placed uncovered in the Figure 5.11 moist curing room for a prescribed amount of time before testing.

Specimen curing according to the MDOT protocol was performed as follows. After density measurements were taken, specimens were placed into 3.8 L plastic bags, then allowed to cure in the moist curing environment while in the plastic bags. Five hours before testing, the specimens were removed from the plastic bags and submerged in water stored in the moist curing environment. After five hours submerged in water, the specimens were ready to be tested.

All specimens used for wheel tracking were subject to the same curing protocol referred to as WTP for Wheel Tracking Protocol. Cylindrical specimens (types 3, 5, and 6 of Equation 3.1) were compacted and then placed under a damp towel for two hours before being moved to the moist curing room; specimens remained in the moisture curing room for 56 to 63 days. Thereafter, wheel tracking was performed. LAC slabs (type 5 of Equation 3.1) were placed in the moist curing room immediately after being compacted. Slabs were removed from the curing room to be sawn in half and measured for density after seven days. Slabs remained in the moist curing room for a total of 56 to 63 days. Thereafter, wheel tracking was performed.

Specimens investigated for mold effects were cured in the Figure 5.10 environmental chamber absent Figure 5.8 foam blocks. Temperature was regulated during curing. Some specimens cured inside plastic molds, while paired specimens produced in the same manner were cured out of plastic molds. Specimens cured out of mold were extracted immediately after compaction, while specimens cured in mold were extracted immediately before testing. Humidity was maintained at 100% for all specimens; in a few cases damp towels were used inside the environmental chamber for humidity control.

5.4.5 Phase 2 Thermal Profile Field Specimen Preparation

5.4.5.1 Loose Mix Specimen Preparation

Field work was conducted on State Route 9 near Tupelo, MS (*Pit D*) and State Route 475 in Rankin County, MS (*Pit E*). Three trials were conducted on each project with each trial conducted at a different location. Each field trial included 8 thermal profile specimens utilizing one thermal measurement device. One specimen was an inert reference which consisted of the project soil compacted near optimum moisture content with no cement. Two control specimens were prepared at the design moisture and cement content. The control specimens consisted of premeasured soil, water, and cement which were mixed using the mechanical laboratory bucket mixer using Section 5.4.2 protocols. Five thermal profile specimens were prepared using field mixed materials. After final mixing operations were complete, samples were taken from the roadway before compaction operations began.

Figure 5.17a shows the positions from which samples were taken. At each position, the full depth of freshly mixed soil-cement was sampled (Figure 5.17b) and mixed for 10 seconds with the Figure 5.5a bucket mixer. Two specimens were prepared using material sampled from Position 1; one specimen was prepared using material sampled from Position 2; and two specimens were prepared using material sampled from Position 3. Additionally, 6 specimens were compacted with material from Positions 4, 5, and left over material from other positions. These additional specimens were placed on the side of the roadway and were tested for compressive strength to assess early traffic opening assessment potential.

In general, field thermal profile specimens were prepared in the same manner as laboratory specimens. Field specimens were compacted as quickly as possible after completion of field mixing operations, and timing between mixing and compaction was recorded for each specimen. Compaction followed *PM-P* protocols in Section 5.4.3.6.

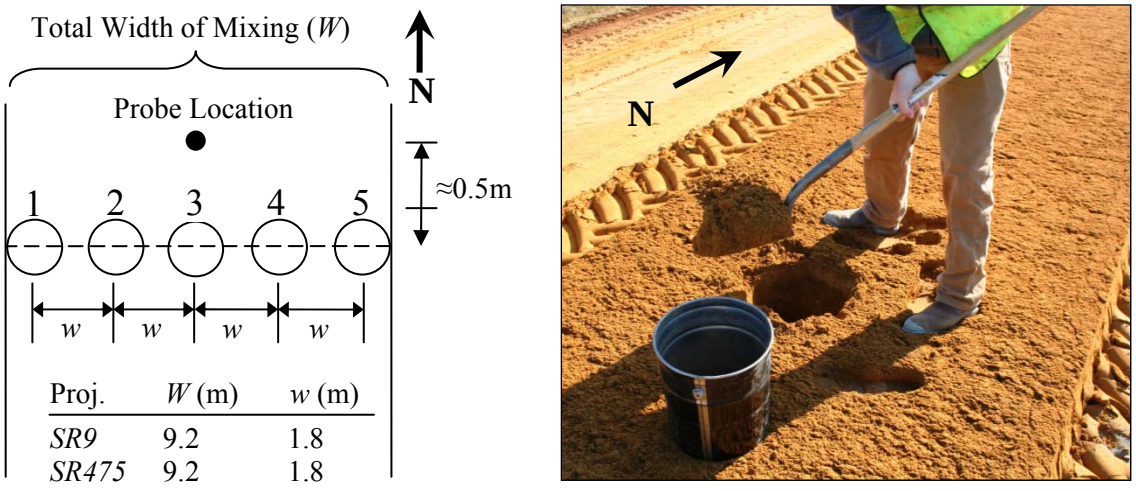

(a) Plan View of Sampling Positions (b) Sampling Position 1 from Roadway

Figure 5.17. Field Sampling Positions and Sampling Field Mixed Soil-Cement

5.4.5.2 Soil-Cement Core Specimen Preparation

After curing 7 days, field cores were cut from select roadways. At each field trial location, six 78.8 mm diameter cores were cut around the location of the in-situ probe discussed later in this chapter (Figure 5.18a). Field cores were cut using an ordinary wet-bit coring device where air pressure was used instead of water to remove cut material and cool the bit during cutting. This method was effective for cutting soil-cement field cores at early cure times with minimal specimen damage. Field cores were sealed in plastic bags to preserve the in-situ moisture content. In the lab, cores were trimmed to the proper height using a dry cut saw (Figure 5.18c).

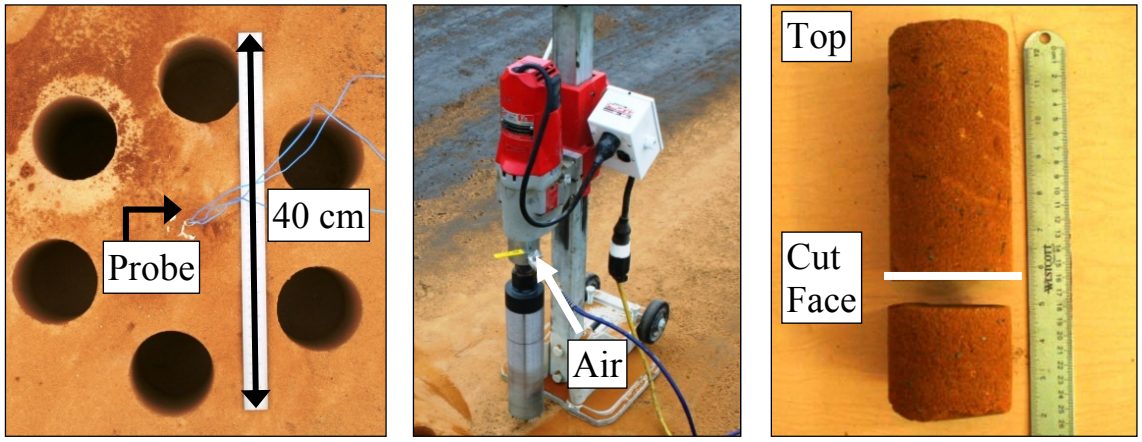

(a) Coring Pattern (b) Modified Coring Device (c) Trimmed Core Specimen

Figure 5.18. Soil-Cement Field Cores

5.4.6 Phase 3 Thermal Profile Outdoor Specimen Preparation

All phase 3 thermal profile quality activities occurred within an outdoor area on the order of 6 m square. Phase 3 activities consisted of outdoor off-site tests to determine the ability of field thermal profile testing to match that of laboratory testing. After mixing, cylinders were compacted using the *PM-P* approach (Section 5.4.3.6). Compaction was conducted either immediately after mixing or after a 30 minute delay period to more closely simulate field conditions. A control soil and water mixture was used for reference and tested alongside the soil-cement mixes. Each batch produced two specimens; two *PM* molds and modified proctor hammers were used to compact both specimens concurrently.

5.5 Testing Methods

Multiple testing methods were utilized in this report. These test methods utilized the equipment and tools in Section 5.3. Test methods were applied to specimens that had been prepared according to Section 5.4.

5.5.1 Density Measurement

Density was measured on the majority of specimens produced. The specimen diameter was taken to be the average of four diameter readings (two top and two bottom), and the specimen height was taken to be the average of four height readings. Figure 5.19 is an example of density measurement. After plastic mold removal, specimen weight and dimensions were measured to determine specimen density. Typically, density measurements were performed after 24 hours of curing inside the sealed plastic molds, or after two hours under a damp towel, though for some specimens other timing was applied and is noted as appropriate. For example, field prepared and field core specimens were measured shortly prior to strength testing.

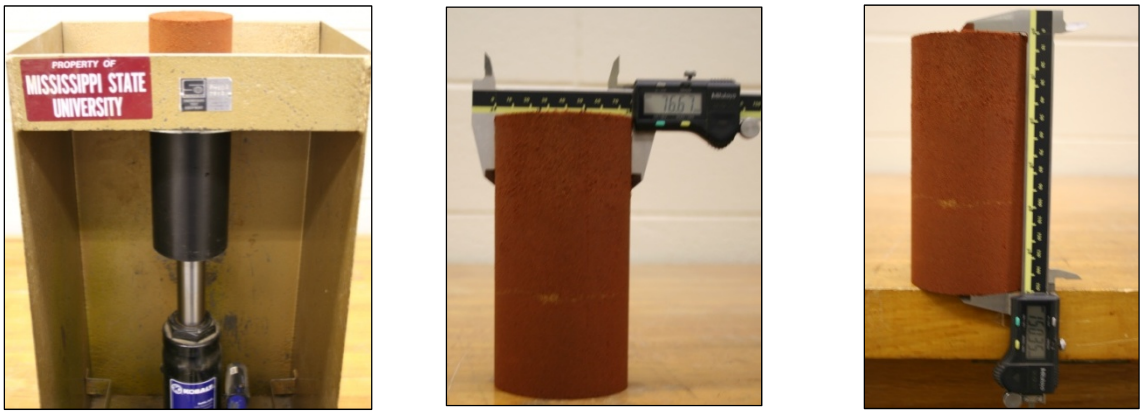

(a) Specimen Extraction (b) Diameter Measurement (c) Height Measurement

Figure 5.19. Specimen Dimension Measurements

5.5.2 Compressive Strength Testing

After curing, Unconfined Compression (UC) testing (Figure 5.20) was performed in accordance with ASTM D1633 Method B and MT-26. Tested specimens had height to diameter (h/d) ratios of 1.98:1 or 1.15:1. Typically, soil-cement specimens have a h/d ratio of 1.15 (101.6 mm diameter and 116.4 mm height). For this study, an approximate 2:1 h/d ratio was used for some testing to better interface thermal measurement and compressive strength testing. According to ASTM D1633, 2:1 ratio compressive strengths can be adjusted to 1.15:1 ratio strengths by multiplying by 1.10.

Unless denoted otherwise, UC testing occurred immediately after removing from the moisture curing room or soon after removing from plastic molds. None of the soil-cement specimens tested required capping to meet smoothness requirements. Specimens were loaded at a constant rate of 1.27 mm/min (0.05 in/min), and max load was recorded to the nearest 40 N.

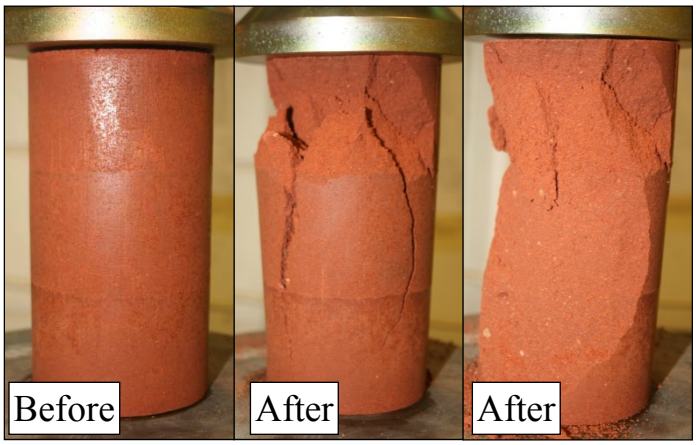

Figure 5.20. Unconfined Compression Testing Before and After

5.5.3 Elastic Modulus Testing

Elastic modulus testing was performed on cured specimen types 4 and 7 of Equation 5.2. ASTM C469 was used as a basis for elastic modulus testing. The Figure 5.7b apparatus was placed on three wooden spacer blocks. These spacers allowed the instrument to be placed so the effective gauge length would be comprised of the middle 101.6 mm of the specimen. A specimen was lowered into the instrument and centered. Seven set screws used to hold the compressometer to the specimen were evenly tightened as to not move the specimen from the center of the instrument (Figure 5.21a). Care was taken not to harm the specimen by only tightening set screws approximately 1.25 rotations after initial specimen contact. Bracing screws on the compressometer were then removed.

Specimens with the instrument securely attached were placed in the Figure 5.7 load frame configuration. Each specimen had a preload applied in order to set the instrumentation. This preload was approximately 40% of the ultimate stress. No data was recorded for this loading. Specimens were preloaded and loaded during testing at a constant rate of 1.27 mm/min. However, specimens were unloaded at a faster rate after the preload because of equipment limitations. Three technicians were used to accurately record load, vertical displacement, and horizontal displacement from dial gauges. Readings were taken every 10 seconds throughout testing. The elastic modulus from the compressometer, denoted E_{Comp}, was reported for the behavior through 40% of σ_{max} for each specimen. The number of points used to calculate E_{Comp} is denoted n_{Comp}.

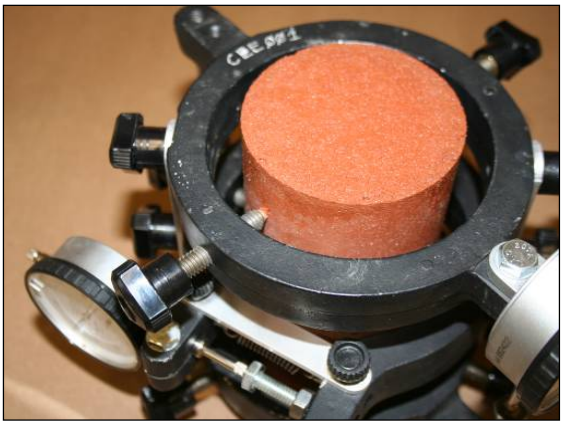

(a) Centered Specimen and Set Screws

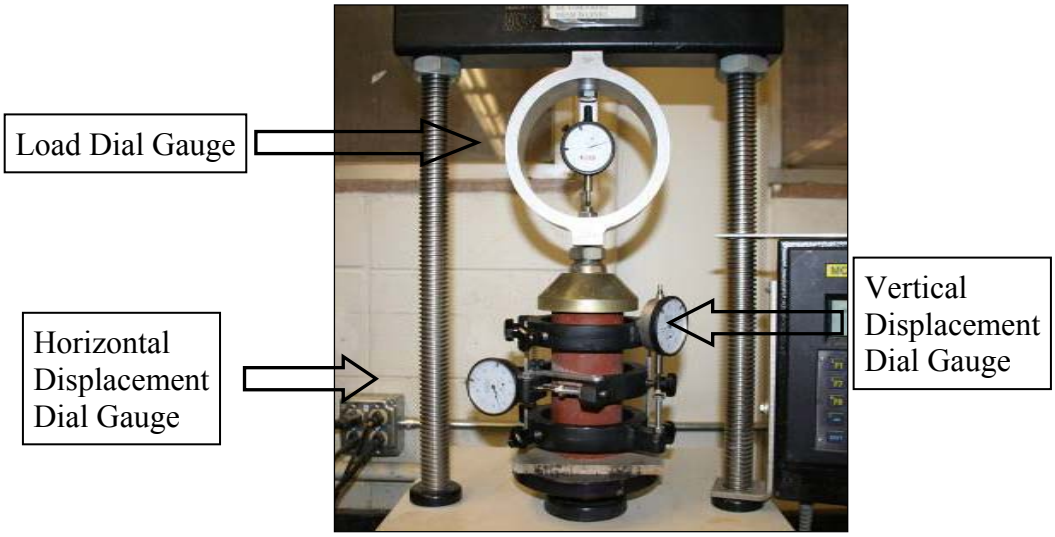

(b) Load Frame and Dial Gauges

Figure 5.21. Elastic Modulus Testing

5.5.4 Wheel Tracking

The PURWheel Laboratory Wheel Tracker was used to test soil cement slabs under multiple loading and environmental conditions. Tests were conducted at 64˚C according to the protocols in Howard et al. (2010), except for the items described as follows. Each slab was first subjected to a dry test. Thereafter, the same slab was tested in either a submerged or soaked condition test. These two tests (dry test and either submerged or soaked test) were conducted within 24 hours of each other. For the submerged condition, slabs were submerged for six hours and also during the test as described by the wet test procedure in Howard et al. (2010). For the soaked condition, slabs were submerged for six hours as described by the wet test procedure, however before tracking, water was drained below the slabs. Water was left in the bottom of the PURWheel to maintain 100% humidity in the chamber during soaked testing.

Wheel tracking tests were also conducted in the Asphalt Pavement Analyzer (APA) using type 3 specimens at design cement index and optimum moisture content. Each test

consisted of 8,000 cycles, at a temperature of 64 ˚C. Hose pressure was 690 kPa with a downward force of 445 N, typical 100% loading conditions. The testing procedure applied to specimens included a dry test followed by a submerged test. Tests were conducted within 24 hours of each other.

A trial run was performed with a Hamburg Loaded Wheel Tester (HLWT) that was based loosely on AASHTO T324. Tests consisted of 20,000 passes. Air temperature for the test was 50 ^{o}C. Before being subject to the 705 N wheel load, specimens were soaked under water at 50 ^{o}C for 30 minutes.

5.5.5 Phase 1 Thermal Profile Quality Control: Feasibility

Thermal measurement devices and software were first configured. ThermoCal data logging software was utilized in phase 1 to record thermal profiles, but other logging software packages are also available. Before each experiment, the thermal measurement equipment was calibrated. This was performed by allowing the equipment to equalize in a closed environmental chamber for at least 12 hours and running the sensor calibration routine in the ThermoCal software. The calibration reference temperature was taken as the average temperature reading from all sensors. This calibration procedure removed the slight temperature variation (±1 °C) among the thermocouple sensors.

Specimens prepared and sealed as described in Figure 5.15 (or sometimes other protocols) were immediately inserted into the calibrated thermal measurement device (Figure 5.22a). Data collection on any particular channel was started as soon as a specimen was inserted into the corresponding slot in the device (Figure 5.22b). The Channel ID notes the block and channel number for each specimen. Time zero for each specimen was taken to be the time when thermal data was first collected. After 24 hr of thermal profile logging, specimens were removed from plastic molds to be further cured and tested as described in Section 5.5.2.

(a) Inserting into Device

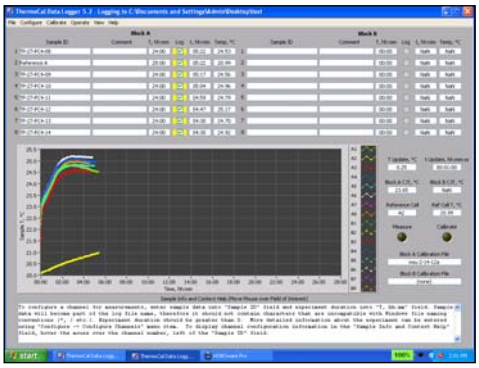

(b) Starting Data Collection (software screenshot)

Figure 5.22. Phase 1 Thermal Profile Testing

5.5.6 Phase 2 Thermal Profile Quality Control: SR9 and SR 475

5.5.6.1 Phase 2 Thermal Profile Testing

After compaction, procedures were the same as phase 1 thermal profile specimens in that specimens were immediately inserted into the foam block slots after compaction to begin

measurements. Thermal measurement devices were kept in the back of an air-conditioned van during specimen preparation and transit. A notable difference with respect to phase 1 activities was the specimen temperature and initial thermal profile block temperature differed. Thermal profile devices were transported to the laboratory and allowed to complete their 24 hr cycle in the laboratory. Thermal profiles were measured for 24 hours, and thereafter the thermal profile specimens were cured inside the sealed plastic molds for the remaining cure time. After curing, specimens were extracted from the plastic molds and tested using the same protocols as laboratory specimens.

5.5.6.2 Specimen Density Correction

Pit D and *E* were batched, conditioned to 21 °C, and treated with the corresponding project cement and *TH* cement. Specimens were compacted using the *PM-P* approach to densities varying from 90 to 105 percent of target γ_d by varying the number of hammer blows. Specimen thermal profiles were measured for 24 hours, and thereafter specimens were cured inside plastic molds. After 7 days, specimens were measured and tested according to Sections 5.5.1 and 5.5.2.

5.5.6.3 In-Situ Temperature Measurement

Probes were used to measure in-situ soil-cement layer temperature. The probes were made from wooden dowel rods and thermocouples (Figure 5.23a). After final compaction and finishing operations, a 6.4 mm diameter hole was drilled into the constructed soil-cement layer. The thermocouple probe was inserted, and the top of the probe was sealed with Plaster of Paris. The internal probe (Figure 5.23a) was positioned on the centerline of the roadway approximately 0.5 m from sample Position 3 (Figure 5.18a). Temperature was recorded at three depths within the constructed pavement layer (Figure 5.23b points T-2, T-3, and T-4), and ambient air temperature was recorded above probe location (Figure 5.23b point T-1).

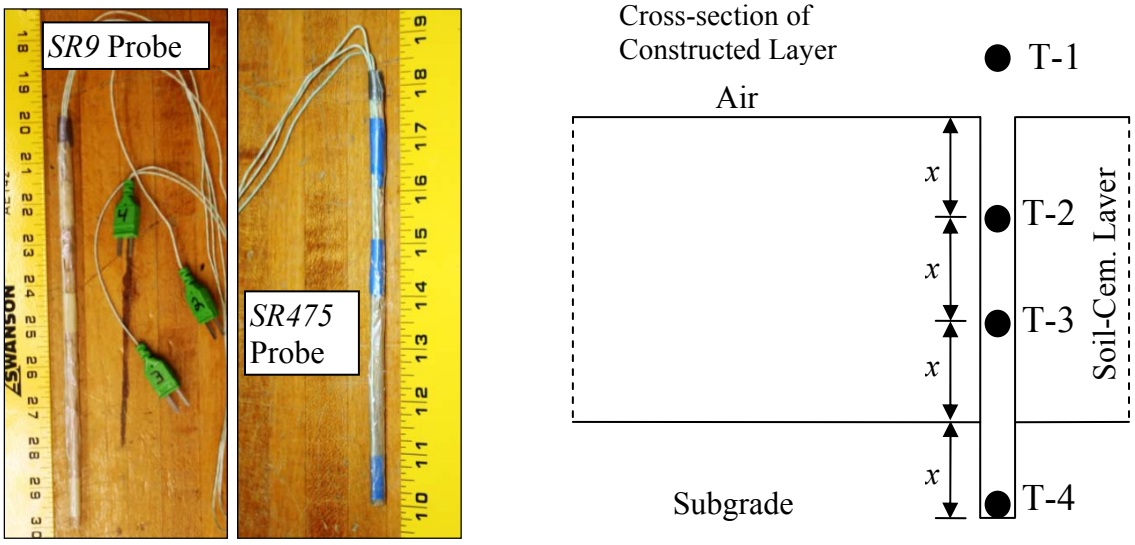

(a) Internal Thermocouple Probes (b) Internal Probe and Sensor Locations

Figure 5.23. Photos of In-Situ Probes and Probe Sensor Locations

5.5.6.4 Specimen Time Delay Correction

Tests conducted examined time delay effects between cement addition and specimen preparation on compressive strength and thermal profiles of field prepared specimens. *Pit D* and *E* were batched, pre-conditioned, and mixed with the corresponding project cement. Specimens were compacted using the *PM-P* approach (5 blows per layer). Thermal profiles were measured for 24 hr; thereafter, specimens were cured inside the plastic molds. After 7 days of curing, specimens were measured and tested according to Sections 5.5.1 and 5.5.2.

5.5.6.5 Mold Adjustment Factor

Tests were conducted to evaluate the effect of specimen curing in mold versus out of mold. *Pit D* and *E* were batched, pre-conditioned, and mixed with the corresponding project cement. Specimens were compacted using the *PM-P* approach (5 blows per layer). Two identical specimens were created per batch, one cured inside a plastic mold and one cured outside the mold. In and out of mold specimens were cured simultaneously in the Figure 5.10 chamber where humidity was 100%; damp towels were placed over the specimens in some cases to allow adequate humidity. At 1 and 7 days, specimens were measured and tested according to Sections 5.5.1 and 5.5.2. Three different temperatures were considered.

5.5.6.6 Cement Content Determination

Six field cores (3 from SR9 and 3 from SR475) were selected for cement content measurement using ASTM C114 and D806. One core was selected from each of the three test locations per project. Selected cores represented the strength for the given location. Each field core was processed to pass the No. 4 sieve, thoroughly mixed, quartered, and processed further to pass the No. 50 sieve. A representative sample was taken from each core to perform C114 and D806. Cement contents are reported as a percentage of dry soil mass.

5.5.7 Phase 3 Thermal Profile Quality Control: Protocol Refinement

The two concurrent specimens prepared in Section 5.4.6 were immediately placed in the insulated EPS thermal profile blocks (Figure 5.8), one in each of two blocks. Variables included conducting the test using no covering, clear plastic covering, and an external insulated enclosure (Figure 5.9) around the thermal profile block. Clear plastic covering was obtained by enclosing the block in a commercially available clear trash bag. Thermal profiles were observed for approximately 24 hours using Picolog Software, (free Pico Technology software). Density measurements and UC testing were conducted after thermal profiles had concluded as per sections 5.5.1 and 5.5.2, respectively.

The outdoor testing site used was a concrete slab on grade between two buildings on the MSU campus. It was not protected from direct sunlight, wind, or other weather effects. However, testing was not conducted during inclement weather (i.e. rain). To isolate weather effects from thermal profile data, the foam blocks used during testing were allowed to run without specimens to record ambient temperatures at the thermal measurement points inside the enclosure. These non-specimen runs were also conducted to evaluate temperature differences inside the testing apparatus caused by different coverings.

CHAPTER 6 – PROCTOR COMPACTION AND MT-25 MIX DESIGN TEST RESULTS

6.1 Overview of Compaction and Mix Design Results

Proctors were performed: 1) raw Proctor according to MT-8; 2) cement Proctor according to MT-9; 3) cement Proctor according to a modified version of MT-9; and 4) single Proctor points after varying delay times post mixing. A total of 46 Proctor curves and 35 individual Proctor points were established. These specimens were used only for density investigation; compressive strength testing was not performed. All Proctor compaction results are provided in Section 6.2. Compaction results were required to perform MT-25 soil-cement mix designs, the results of the 10 mix designs performed are provided in Section 6.3.

6.2 Proctor Compaction Test Results

Proctor compaction tests were performed for two purposes. The first purpose was to measure soil-cement densities to allow specimens to be re-compacted using these values as a reference. The second purpose was to examine MDOT's MT-9 protocols to determine if areas of improvement could be identified.

6.2.1 MT-8 Raw Proctor Test Results

Raw (i.e. no cement) Proctors (MT-8) were performed multiple times, and Table 6.1 provides the test results. The values provided in this section are primarily for batch calculations. Batch calculations were performed using bold and italic rows.

Table 6.1. Summary of MT-8 Pit Soil Standard Raw Proctor Results

Material	γ_d (kg/m^3)	OMC (%)	Performed By	Material
Pit A	1863	11.9	MDOT Central Lab	Project Sample
	1910[a]	12.1[a]	MDOT Central Lab	SS 206 Sample
	1862	11.1	Burns Cooley Dennis	SS 206 Sample
	1859	12.1	MSU Lab	SS 206 Sample
	1860	***11.6***	***Multiple Labs***	***SS 206 Sample***
Pit B	1725	15.5	MDOT Central Lab	Project Sample
	1852	13.4	MDOT Central Lab	SS 206 Sample
	1823	14.5	MSU Lab	SS 206 Sample
	1826	13.9	MSU Lab	SS 206 Sample
	1834	***13.8***	***Multiple Labs***	***SS 206 Sample***
Pit C	1963	11.3	MDOT Central Lab	Project Sample
	1956	11.1	MDOT Central Lab	SS 206 Sample
	1938	11.2	MSU Lab	SS 206 Sample
	1963	10.8	MSU Lab	SS 206 Sample
	1930	11.0	MSU Lab	SS 206 Sample
	1946	***11.0***	***Multiple Labs***	***SS 206 Sample***
Pit D	1772	14.5	MDOT Central Lab	Project Sample
	1772	***14.5***	***MDOT Central Lab***	***Project Sample***
Pit E	1756	15.1	MDOT Central Lab	Project Sample
	1756	***15.1***	***MDOT Central Lab***	***Project Sample***

a: data questionable and omitted.

6.2.2 MT-9 Cement Proctor Test Results

Proctor tests conducted according to MT-9 were performed using all five pit soils and multiple cements (Table 6.2). The Project Sample Proctor values in Table 6.2 were only reported for comparison to Proctor values determined for pit soils A to C. Project Sample Proctor values were used for *Pit D* and *E* in actual calculations.

Table 6.2 also provides change in maximum dry density and optimum moisture content values of MT-9 relative to MT-8, using Table 6.1 bold and italic rows as a reference. Only SS 206 samples were considered. *Pit A* density values increased for each of the thirteen curves of interest, with increases ranging from 18 to 90 kg/m^3 and having an average increase of 59 kg/m^3. Linear Regression Through Origin (RTO) of Table 6.2 *Pit A* $\Delta\gamma_d$ data resulted in an average increase in $\Delta\gamma_d$ of 10 kg/m^3 per 1% increase in cement index (C_I) with an R^2 value of 0.61.

Table 6.2. Summary of MT-9 Proctor Results

Pit	C_I	Cement	γ_d (kg/m^3)	OMC (%)	$\Delta\gamma_d$ (kg/m^3)	ΔOMC (%)	Performed By	Material
A	2	TH	1906	11.6	46	0.0	MSU Lab	SS 206 Sample
	4	TH	1878	11.8	18	0.2	MSU Lab	SS 206 Sample
	5	Type I	1983	10.6	---	---	MDOT Central Lab	Project Sample
	5	Type I	1920	11.8	60	0.2	MDOT Central Lab	SS 206 Sample
	6	TH	1910	11.8	50	0.2	MSU Lab	SS 206 Sample
	7	TH	1922	12.0	62	0.4	MSU Lab	SS 206 Sample
	8	TH	1943	10.9	83	-0.7	MSU Lab	SS 206 Sample
	10	TH	1949	11.0	89	-0.6	MSU Lab	SS 206 Sample
	3	TH, GGBFS	1905	11.7	45	0.1	MSU Lab	SS 206 Sample
	4	TH, GGBFS	1891	11.5	31	-0.1	MSU Lab	SS 206 Sample
	5	TH, GGBFS	1895	11.7	35	0.1	MSU Lab	SS 206 Sample
	6	TH, GGBFS	1939	11.2	79	-0.4	MSU Lab	SS 206 Sample
	7	TH, GGBFS	1942	11.2	82	-0.4	MSU Lab	SS 206 Sample
	8	TH, GGBFS	1950	10.9	90	-0.7	MSU Lab	SS 206 Sample
B	4	TH	1830	14.4	-4	0.6	MSU Lab	SS 206 Sample
	4	TH	1770	14.1	-64	0.3	MSU Lab	SS 206 Sample
	5	Type I	1873[a]	14.2[a]	39[a]	0.4[a]	MDOT Central Lab	SS 206 Sample
	5	TH	1778	15.0	-56	1.2	MSU Lab	SS 206 Sample
	5	TH	1793	14.0	-41	0.2	MSU Lab	SS 206 Sample
	6	TH	1759	14.8	-75	1.0	MSU Lab	SS 206 Sample
	6	TH	1775	13.6	-59	-0.2	MSU Lab	SS 206 Sample
	6.5	Type I	1810	15.2	---	---	MDOT Central Lab	Project Sample
C	3	TH	1959	10.9	13	-0.1	MSU Lab	SS 206 Sample
	4	Type I	1958	11.7	---	---	MDOT Central Lab	Project Sample
	4	TH	1935	11.4	-11	0.4	MSU Lab	SS 206 Sample
	5	Type I	1975	11.1	29	0.1	MDOT Central Lab	SS 206 Sample
D	7	NC	1796	14.7	---	---	MDOT Central Lab	Project Sample
E	7	TH_{SR475}	1737	13.6	---	---	MDOT Central Lab	Project Sample

- Change (Δ) values are MT-9 minus MT-8.
a: data questionable and omitted.

Pit B density values decreased for six of the seven curves considered. When all seven curves were considered, $\Delta\gamma_d$ values ranged from a 75 kg/m^3 decrease to a 39 kg/m^3 increase, with an average decrease of 37 kg/m^3. When the one curve from MDOT Central Lab was removed, $\Delta\gamma_d$ values for the six remaining curves ranged from a 75 kg/m^3 decrease to a 4 kg/m^3 decrease, with an average decrease of 50 kg/m^3. Values with the one seemingly outlier curve removed seem more reasonable.

Pit C density values increased for two of the three curves considered. None of the three curves seemed to be outliers so all three were utilized. Values ranged from a decrease of 11 kg/m^3 to an increase of 29 kg/m^3, with an average increase of 10 kg/m^3.

Overall, MT-9 testing resulted in one soil considerably increasing density from cement addition (*Pit A*), one soil considerably decreasing density from cement addition (*Pit B*), and one soil's density not being considerably affected by cement addition (*Pit C*). Erratic behavior from three randomly sampled soils aligns with Figure 3.5 produced from the MDOT soil-cement database and supports the position that there is room for enhancement in MT-9 compaction protocols.

6.2.3 MT-9-Mod Cement Proctor Test Results

Considerable density decrease in *Pit B* due to cement addition prompted full Proctor curves to be constructed with this soil using MT-9-Mod protocols, and the results are provided in Table 6.3. One curve each was produced at C_I values of 4, 5, and 6. Comparing these curves to MT-9 values in Table 6.2, γ_d increased 14, 26, and 46 kg/m^3, respectively, or 29 kg/m^3 on average. This value is still 21 kg/m^3 lower than the raw Proctor MT-8 value in Table 6.1, but the density decrease is considerably less than with MT-9.

Single Proctor points were performed with *Pit A* and *Pit C* to determine the effect of MT-9-Mod relative to MT-9. As would be expected based on Section 6.2.2 data, neither γ_d value was greatly affected. Both soil's γ_d values increased, but the increase was modest at 9 kg/m^3 for *Pit A*, and 13 kg/m^3 for *Pit C*.

Table 6.3. Summary of MT-9-Mod Proctor Test Results

Material	C_I	Cement	γ_d (kg/m^3)	OMC (%)	Type
Pit A	5	GV	1909	11.7	Single Checkpoint
	5	TH	1930	11.7	Single Checkpoint
	5	TH	1928	11.8	Single Checkpoint
Pit B	5	GV	1814	13.8	Single Checkpoint
	4	TH	1814	14.6	Full Curve
	5	TH	1812	14.0	Full Curve
	6	TH	1813	14.2	Full Curve
Pit C	4	GV	1937	11.5	Single Checkpoint
	5	TH	1947	11.4	Single Checkpoint
	5	TH	1948	11.4	Single Checkpoint

--All data in this table was performed by MSU Lab on SS 206 Sample.

For reference purposes in the remainder of this report, single Proctor points were produced with the *GV* cement source and compared to results with the *TH* cement source (Table 6.3). Values differed by 2 to 21 kg/m^3 and less than 0.2% moisture, indicating no

drastic differences with respect to the cement sources in this paper. As a result, the same Proctor values were used for specimens with *TH* and *GV* cement sources. Overall, Proctor reference values for *Pit A* and *Pit C* were those from MT-9 protocol, and Proctor reference values from *Pit B* were from MT-9-Mod protocol.

6.2.4 Compaction Delay Proctor Test Results

Additional Proctor testing was performed to evaluate the affect of compaction delay on density. A single pit soil (*Pit B*), cement (*TH*), and C_I (5%) were chosen for these tests. *Pit B* was chosen based on behavioral characteristics presented previously in this section. Results are provided in Figure 6.1, and show a pronounced density decrease when compaction was delayed for *Pit B*. This behavior is not expected to be this pronounced for all soils, or for all soil and cement combinations, but Figure 6.1 clearly shows time delay from cement and water mixing to beginning compaction can be a first order concern for some projects.

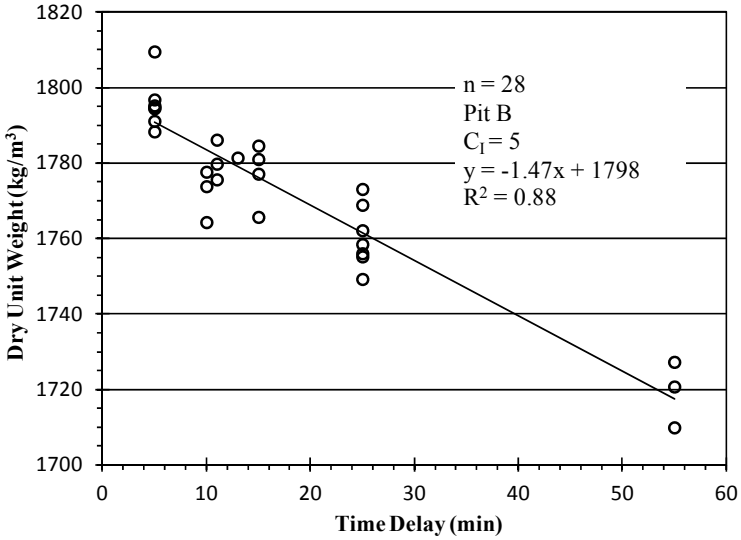

Figure 6.1. Proctor Compaction Time Delay Test Results

6.3 MT-25 Soil-Cement Mix Design Results

Table 6.4 contains results for the 10 soil-cement mix designs performed according to MT-25. A sample of pit soils A, B, and C was sent to MDOT Central Laboratory to conduct MT-25. For *Pit B* and *Pit C*, test results were reasonable as compared to results from the corresponding projects. Therefore, 5 percent and 4 percent cement index's was considered the design cement content for *Pit B* and *Pit C*, respectively. For *Pit A*, the results from MDOT Central Laboratory indicated a failure to reach strength criterion at 4, 5, and 6 percent cement indexes. Additional MT-25 tests were conducted by MSU at 4, 5, 6, 7, and 8 percent cement indexes. These additional results indicated that the design cement index for *Pit A* was 5 percent which agreed with the results from the corresponding project. Also, MT-25 was conducted on *Pit A* using a slag-cement blend (TH 25%, GGBFS 75%). Results

indicated the design cement content for the slag-cement blend was 4 percent. Design cement indexes for *Pit D* and *Pit E* were taken to be the same as the project mix design.

Table 6.4. Mississippi Test Method 25 Results

Pit	Cement Type	C_I (%)	7-Day σ_{max} (kPa)	14-Day σ_{max} (kPa)	Source[1]
A	Type I	5	1269	1517	MDOT
	TH	5[3]	2451[2]	2828[2]	MSU
	Type I	5	2710	2689	Proj.
	TH, *GGBFS*	4[3]	1560[2]	2477[2]	MSU
B	Type I	5[3]	2117	2448	MDOT
	Type I	6.5	2523	--	Proj.
C	Type I	4[3]	2372	3027	MDOT
	Type I	4	2613	3178	Proj.
D[4]	Type I	5	2275	2620	BCD
E	Type I	7[3]	2110	2648	Proj.

Note: Compressive strength criterion is 2070 kPa at or before 14-days.

1: MDOT = Results from MDOT Central Lab on SS 206 sampled soils
MSU = Results from MSU Lab on SS 206 sampled soils
Proj. = Results from MDOT Central Lab for the corresponding project mix design
BCD = Results from BCD lab for the corresponding project

2: Average of two specimens.

3: Selected design cement index for the current study.

4: Cement Index of ≈ 7% was used on the SR9 project; therefore, 7% was also used to prepare laboratory specimens.

CHAPTER 7 – STRENGTH VERSUS TIME TEST RESULTS

7.1 Overview of Strength Versus Time Test Results

This chapter contains unconfined compression (UC) strength test results versus time reported in terms of maximum compressive strength (σ_{max}). Eight strength versus time curves were produced. Seven of these curves are also in Anderson (2013), while the eighth curve that contains slag cement (GGBFS) has not been used elsewhere to date.

A total of 360 laboratory compacted specimens were evaluated for strength gain versus time (Table 7.1). A minimum of three UC specimens were tested at each curing time. The curing times were: 1, 3, 7, 14, 21, 28, 42, 56, 90, 120, 180, 240, 360, and 540 days. Extra specimens were used as needed to obtain the necessary replication, and all remaining specimens were tested at 540 days.

Table 7.1. Test Matrix for Strength Gain with Time

Material	Cement Type	Cement Index	Specimen Type	Tests	Cure Method
PA	*TH*	Design (5%)	1	45	MSU
PB	*TH*	Design (5%)	1	45	MSU
PC	*TH*	Design (4%)	1	45	MSU
PA	*TH*	Design (5%)	4	45	MSU
PB	*TH*	Design (5%)	4	45	MSU
PC	*TH*	Design (4%)	4	45	MSU
PC	*TH*	Design (5%)	2	45	MSU
PA	*25% TH, 75% GGBFS*	Design (4%)	4	45	MSU

**Raw data for all but TH, GGBFS is provided in Anderson (2013) Appendix A in Tables A.1 to A.7.*

7.2 Strength Gain Versus Time Results: Portland Cement

Figures 7.1 to 7.3 provide strength gain with time results organized by specimen type and cementitious material. All data in Figures 7.1 to 7.3 used TH cement at design cement index, while cured with the MSU protocol. All data sets in Figures 7.1 to 7.3 seem to demonstrate generally similar compressive strength behavior with increasing time. A logarithmic trendline and regression equations were fitted to each set of data. The trendlines shown are from the average compressive strength value per curing time. Figures 7.1 to 7.3 also show the logarithmic equation when individual data points are considered.

Most of the strength gain occurred within the first 56 days of curing. Using the trendlines shown, data sets achieved 75% to 85% of the highest compressive strength (540 days) at 56 days. After 56 days, the compressive strengths began to level off with increasing curing time. This was also seen in literature for soils stabilized with cement only (Felt and Abrams 1957, George 2006, Okyay and Dias 2010).

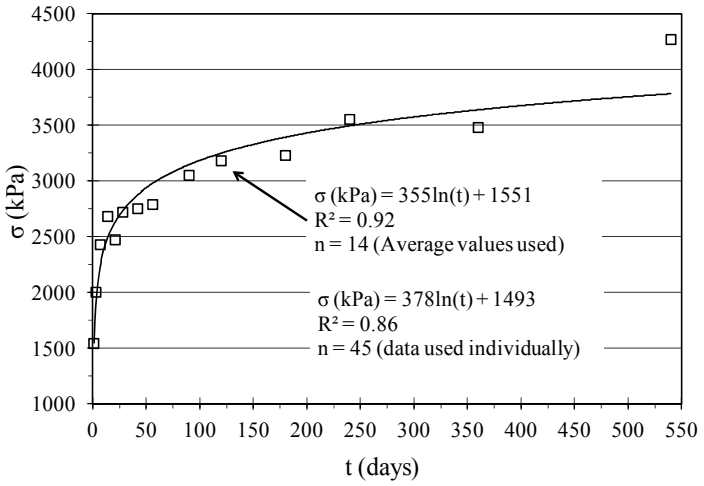

(a) ST1-PA5

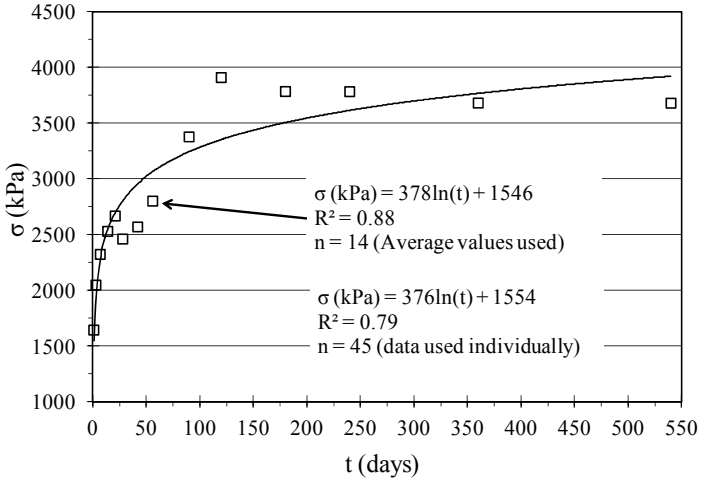

(b) ST1-PB5

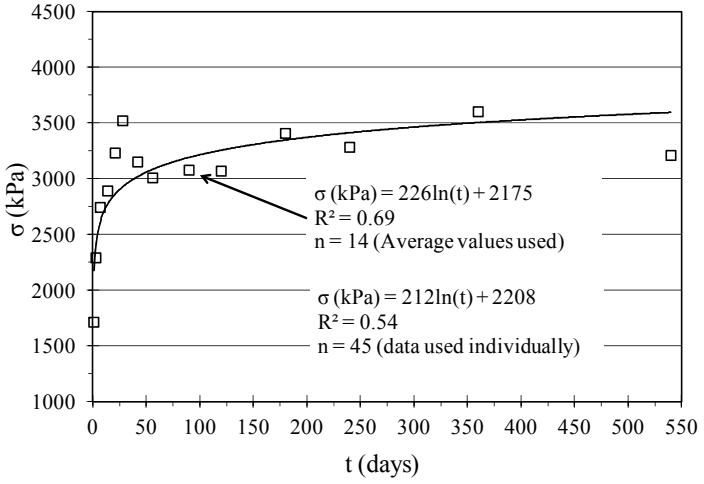

(c) ST1-PC4

Figure 7.1. Strength Gain with Time – Specimen Type 1

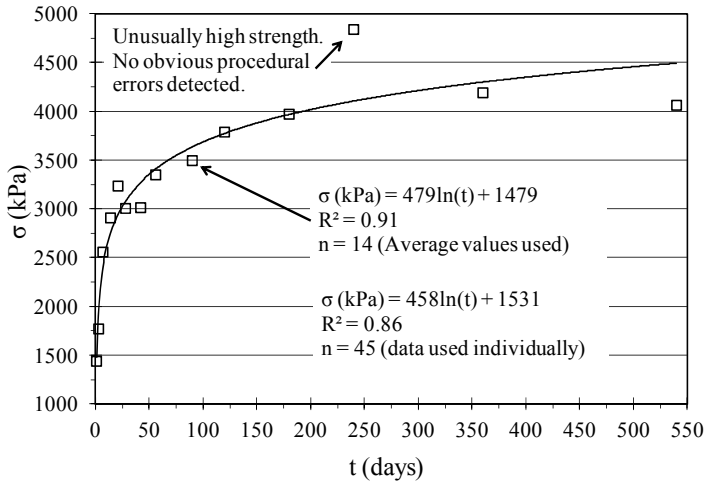

(a) ST4-PA5

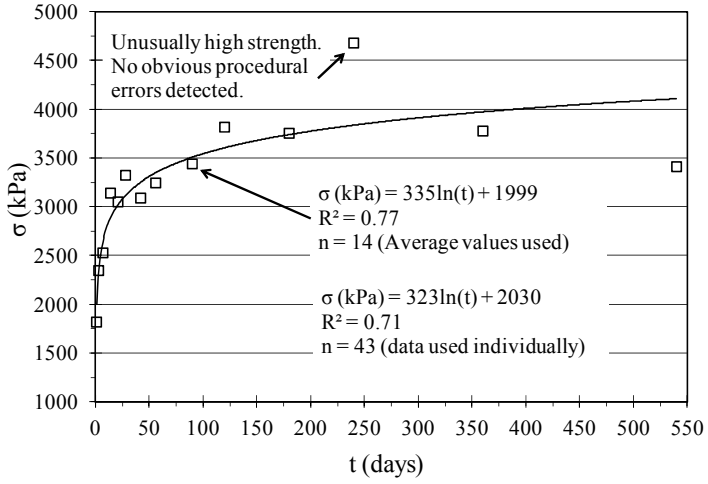

(b) ST4-PB5

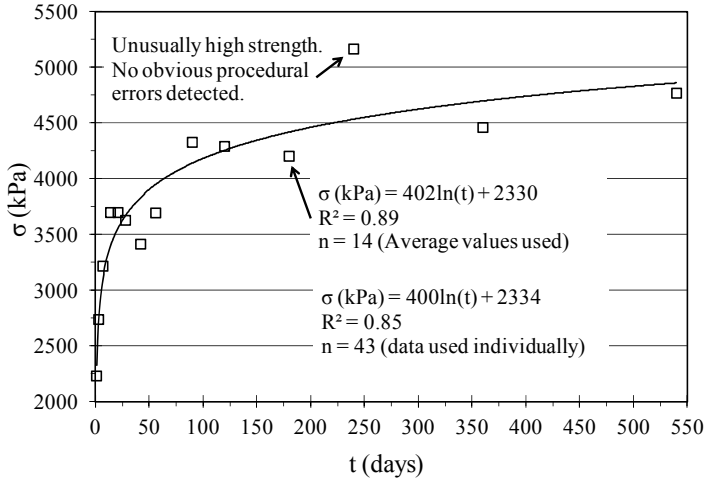

(c) ST4-PC4

Figure 7.2. Strength Gain with Time – Specimen Type 4

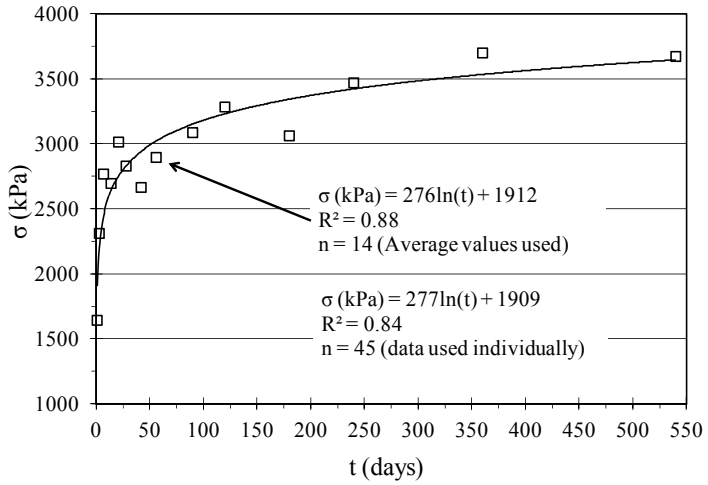

Figure 7.3. Strength Gain with Time – *Pit C* Specimen Type 2 (ST2-PC4)

Specimen type 1 (1.15:1 Proctor compacted) strength gain with time trendlines do not achieve double their design strength within 540 days, which is desirable as long term strength gain can be an indicator of a crack prone layer. Note that design strengths were selected with 1.15:1 Proctor compacted specimens. Figure 7.1 data suggests that MDOT's current cement contents are in a reasonable range and that enhancements to current practices should not result in large overall upward or downward shifts in cement content. There may, however, still be room for enhancement within the overall range of values currently being used (see Chapter 8).

Unconfined compressive strength measured at a 2:1 aspect ratio is typically multiplied by 1.1 to equate to compressive strength measured at a 1.15:1 aspect ratio (i.e. taller specimens should be weaker than shorter specimens when all other factors are equal). Interestingly, specimens compacted with the *PM-CF* approach (1.98:1) seemed to produce higher compressive strengths from the trendlines than those specimens compacted with a Proctor hammer at a 1.15:1 aspect ratio.

Figure 7.4 is a series of equality plots produced from Figures 7.1 through 7.3 where specimen types 1, 2, and 4 are compared using strength gain with time data where soil type, cement source, and cement content are the same for each individual point. Specimen type 1 is the standard method currently used by MDOT (1.15:1 Proctor compacted), specimen type 2 has the same aspect ratio as type 1 (1.15:1), but uses the SGC for compaction, and specimen type 3 has a different aspect ratio (1.98:1) and also uses a different compaction approach (*PM-CF*). Gyratory compaction had little to no impact on strength gain versus time based on Figure 7.4 as Regression Through Origin (RTO) resulted in a trendline slope of 0.97. *PM-CF* compaction at a 1.98:1 aspect ratio, on the other hand, was 14%, 9%, and 27% stronger, on average, than Proctor compaction at a 1.15:1 aspect ratio for soils A, B, and C, respectively.

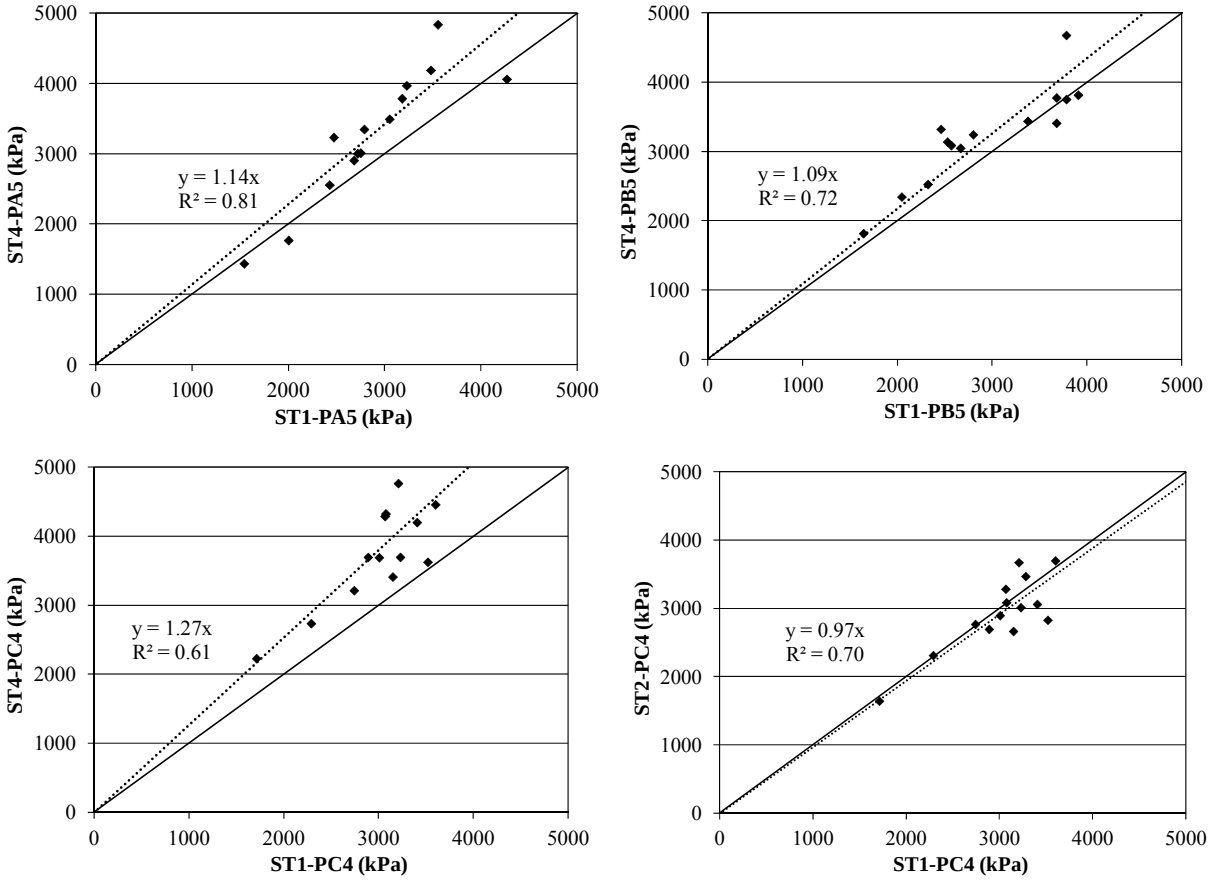

Figure 7.4. Compressive Strength Equality Plots Comparing Compaction Methods

7.3 Strength Gain Versus Time Results: Portland and Slag Cement Blend

A single series of tests was conducted with *Pit A* soil and GGBFS (Figure 7.5). Figure 7.5 used 75% GGBFS and 25% TH cement, and was also cured with the MSU protocol. Figure 7.5 did not produce the expected shape at later ages, so the Figure 7.6 equality plot was produced to compare the 25% TH and 75% GGBFS blend to the 100% TH blend presented in Section 7.2. Aside from cement type and dosage, these two strength versus time curves experienced identical conditions; both were design cement content. Specimens containing slag (GGBFS) were weaker than specimens only containing portland cement up to 21 days (i.e. they were below the Figure 7.6 equality line), which is not unusual as slag tends to gain strength at a slower rate in some conditions. From 28 to 180 days behavior is also not surprising with slag blends having higher strengths (slag blends often have higher strength at later ages relative to only portland cement blends). After 180 days, slag blends lose strength progressively up to 540 days, and fall back below the equality line indicating specimens with only portland cement were stronger after 180 days. The data collected was investigated and no outliers or other unusual behavior was found to explain strength decreasing at later ages in slag specimens. Further explanation of decreasing late age strengths in these specimens warrants additional investigation. Whether or not this behavior is reasonable or is some sort of anomaly or laboratory error is unknown.

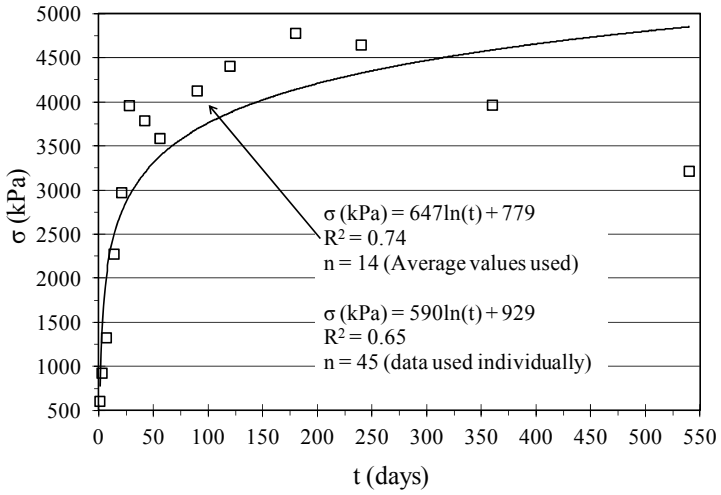

Figure 7.5. Strength Game with Time – ST4-PA4S – Specimen Type 4

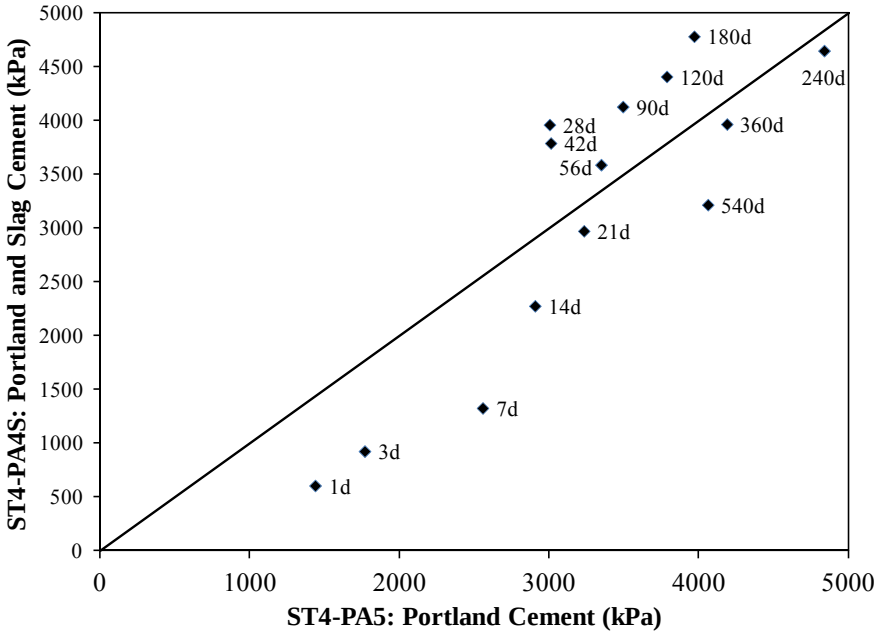

Figure 7.6. Comparison of Portland and Blended Cement Compressive Strength

CHAPTER 8 – MIX DESIGN EVALUATION VIA STRENGTH VARIABILITY TEST RESULTS

8.1 Overview of Strength Variability Results

Parameters investigated in this chapter include variability and normality; reliability design; and cement source, compaction method, and curing method effects on compressive strength. Outliers were removed before analysis was conducted. The number of outliers in a data set was denoted n_0; the number of data points used in analysis per data set was denoted *n.* To Identify outliers, Tukey's Method uses the distance between data and the Inter Quartile Range (*IQR*). The distance between data's 25th (Q_1) and 75th (Q_3) percentiles is the *IQR*. Data falling outside the range of $Q_1 - 1.5IQR$ to $Q_3 + 1.5IQR$ were considered outliers and were not included in the analysis.

A total of 750 laboratory unconfined compression (UC) tests were conducted for strength variability (Table 8.1). Twenty-five sets of 30 specimens each were tested. Maximum compressive strength (σ_{max}), was evaluated.

Table 8.1. Test Matrix for Pit Soil Strength Variability

Identifier	Material	Cement Type	Cement Index	Specimen Type	Tests	Cure Method
SV1-PA5	PA	*TH*	Design	1	30	MSU
SV1-PA6	PA	*TH*	+1%	1	30	MSU
SV1-PA4	PA	*TH*	-1%	1	30	MSU
SV1-PB5	PB	*TH*	Design	1	30	MSU
SV1-PB6	PB	*TH*	+1%	1	30	MSU
SV1-PB4	PB	*TH*	-1%	1	30	MSU
SV1-PC4	PC	*TH*	Design	1	30	MSU
SV1-PC5	PC	*TH*	+1%	1	30	MSU
SV1-PC3	PC	*TH*	-1%	1	30	MSU
SV2-PA5	PA	*TH*	Design	2	30	MSU
SV2-PB5	PB	*TH*	Design	2	30	MSU
SV2-PC4	PC	*TH*	Design	2	30	MSU
SV4-PA5 (1)	PA	*TH*	Design	4	30	MSU
SV4-PB5 (8a)	PB	*TH*	Design	4	30	MSU
SV4-PC4 (13)	PC	*TH*	Design	4	30	MSU
SV4-PA5 (2)	PA	*GV*	Design	4	30	MSU
SV4-PB5 (9)	PB	*GV*	Design	4	30	MSU
SV4-PC4 (14)	PC	*GV*	Design	4	30	MSU
SVM1-PA5	PA	*TH*	Design	1	30	MDOT
SVM1-PB5	PB	*TH*	Design	1	30	MDOT
SVM1-PC4	PC	*TH*	Design	1	30	MDOT
SV7-PA5	PA	*TH*	Design	7	30	MSU
SV7-PB5	PB	*TH*	Design	7	30	MSU
SV7-PC4	PC	*TH*	Design	7	30	MSU
SV4-PA4S (18)	PA	75% GGBFS, 25% TH	Design	4	30	MSU

**Raw data is provided in Anderson (2013) Appendix A in Tables A.8 to A.31 with the exception of GGBFS data. Numbers in parenthesis signify the Series number as this data was used in both Chapters 8 and 11. All data is 7 day compressive strengths.*

8.2 Variability and Normality

For all sets of strength variability specimens in this study, variability was evaluated using relative histograms and normality plots. A method developed by Filliben (1975) and presented by Ott and Longnecker (2010) was used to analyze the normality plots for each data set. In this method, the correlation coefficient (r) is used to estimate a *P-value*, which is then used to determine the certainty that the data is normally distributed. Table 8.2 summarizes variability and normality findings; histograms and normality plots are presented in Anderson (2013) Appendix B Figures B.1 to B.8.

In general, *Pit A* seemed to have the least variability with respect to compressive strength (σ_{max}) of the soils tested; averaging the eight Table 8.2 COV values incorporating only portland cement resulted in a value of 5.7%. Pit B seemed to have the next highest variability; averaging the eight Table 4.1 COV values resulted in a value of 7.9%. *Pit C* generally seemed to have the most variability; averaging the eight Table 8.2 COV values resulted in a value of 9.3%. All sets of data seem to be at least somewhat normally distributed, except for SV4-PB5 (8a). This set of data exhibits a poor level of certainty that the data is normally distributed. As part of Sullivan (2012), this set was remade. Results were similar in nature with respect to the normality fit.

Table 8.2. Compressive Strength Variability and Normality

Soil Set	Cement Type	*n*	n_0	Mean (kPa)	Stdev (kPa)	COV (%)	*P Value*	Normality Fit
SV1-PA4	*TH*	29	1	1605	67	4.2	0.41	Good ($0.10 \leq P \leq 0.50$)
SV1-PA5	*TH*	30	0	2201	131	5.9	0.72	Excellent ($P \geq 0.50$)
SV1-PA6	*TH*	30	0	2508	112	4.5	0.71	Excellent ($P \geq 0.50$)
SVM1-PA5	*TH*	30	0	1982	132	6.7	0.80	Excellent ($P \geq 0.50$)
SV2-PA5	*TH*	27	3	2239	77	3.4	0.77	Excellent ($P \geq 0.50$)
SV7-PA5	*TH*	30	0	2077	244	11.7	0.09	Acceptable ($0.05 \leq P \leq 0.10$)
SV4-PA5 (1)	*TH*	29	1	2430	128	5.3	0.41	Good ($0.10 \leq P \leq 0.50$)
SV4-PA5 (2)	*GV*	29	1	2317	95	4.1	0.48	Good ($0.10 \leq P \leq 0.50$)
SV4-PA4S (18)	75% GGBFS	30	0	1696	90	5.3	0.50	Excellent ($P \geq 0.50$)
SV1-PB4	*TH*	30	0	1795	117	6.5	0.08	Acceptable ($0.05 \leq P \leq 0.10$)
SV1-PB5	*TH*	30	0	2293	158	6.9	0.11	Good ($0.10 \leq P \leq 0.50$)
SV1-PB6	*TH*	30	0	2590	216	8.3	0.25	Good ($0.10 \leq P \leq 0.50$)
SVM1-PB5	*TH*	30	0	1766	205	11.6	0.29	Good ($0.10 \leq P \leq 0.50$)
SV2-PB5	*TH*	30	0	2720	168	6.2	0.31	Good ($0.10 \leq P \leq 0.50$)
SV7-PB5	*TH*	28	2	2085	135	6.5	0.43	Good ($0.10 \leq P \leq 0.50$)
SV4-PB5 (8a)	*TH*	30	0	2461	243	9.9	0.04	Poor ($0.01 \leq P \leq 0.05$)
SV4-PB5 (9)	*GV*	30	0	2831	200	7.1	0.25	Good ($0.10 \leq P \leq 0.50$)
SV1-PC3	*TH*	30	0	1766	209	11.8	0.28	Good ($0.10 \leq P \leq 0.50$)
SV1-PC4	*THI*	30	0	2165	218	10.1	0.49	Good ($0.10 \leq P \leq 0.50$)
SV1-PC5	*TH*	30	0	2557	372	14.6	0.22	Good ($0.10 \leq P \leq 0.50$)
SVM1-PC4	*TH*	30	0	1875	205	10.9	0.41	Good ($0.10 \leq P \leq 0.50$)
SV2-PC4	*TH*	30	0	2705	143	5.3	0.23	Good ($0.10 \leq P \leq 0.50$)
SV7-PC4	*TH*	29	1	2279	118	5.2	0.42	Good ($0.10 \leq P \leq 0.50$)
SV4-PC4 (13)	*TH*	30	0	3181	179	5.6	0.41	Good ($0.10 \leq P \leq 0.50$)
SV4-PC4 (14)	*GV*	30	0	2668	297	11.1	0.40	Good ($0.10 \leq P \leq 0.50$)

Note: Data shown is after removal of all outliers. Numbers in parenthesis signify the Series number as this data was used in both Chapters 8 and 11. All data is 7 day compressive strengths. 75% GGBFS was mixed with 25% TH.

A single set of 30 specimens was conducted using a 75% GGBFS and 25% *TH* cement blend. Variability and normality for GGBFS specimens was not meaningfully different than other cementitious additives (average value for all portland cement tests was 5.7% and COV with GGBFS was 5.3%). The data was mostly normally distributed based on the chosen normality test. Therefore, statistical tests were performed assuming a normal distribution for all data sets. Statistics contained in Table 8.2 were used as a basis for all statistical data analysis. Adjustments for h/d ratios are noted in analysis.

8.3 Reliability Design - Compressive Strength Variability

To investigate potential advantages of a reliability based design, the number of replicates required to achieve some level of confidence (75, 85, or 95%) was found with a predetermined margin of error. Margins of error chosen originated from the relationship between compressive strength and cement index. From Table 8.2, the difference in mean compressive strength over a 1% change in cement index was approximately 300 to 600 kPa. Margins of error of 150, 225, and 300 kPa were chosen to reasonably bound a $\pm$ ½% cement index change of the tested indices. The margin of error is evenly distributed on either side of the mean, so, for example, an error margin of 150 kPa equates to the lower end difference resulting from a 1% change in cement content of 300 kPa.

The confidence interval equation (Ott and Longnecker 2010) and shown in Equation 8.1 was used to find the number of replicates (n_{reps}) needed in order to obtain a desired level of confidence with a prescribed margin of error. The margin of error portion of the equation (Eq 8.2) was rearranged to find the number of replicates (Eq. 8.3). Also, Equation 8.2 was used to find the margin of error from existing MDOT practice in MT-25 (n_{reps} = 1) for comparison with the reliability analysis. An example is provided of the procedure used.

$$\bar{x} \pm z_{\alpha/2} * \frac{Stdev}{\sqrt{n_{reps}}} \qquad \text{(Eq. 8.1)}$$

$$ME = z_{\alpha/2} * \frac{Stdev}{\sqrt{n_{reps}}} \qquad \text{(Eq. 8.2)}$$

$$n_{reps} = \left(\frac{z_{\alpha/2} * Stdev}{ME} \right)^2 \qquad \text{(Eq. 8.3)}$$

Where:
$\bar{x}$ = Mean of the sample set (kPa)
$z_{a/2}$ = Z-score for a specified confidence level
For 75% = 1.15
For 85% = 1.44
For 95% = 1.96
n_{reps} = Number of replicates needed to obtain desired level of confidence
Stdev = Standard deviation
ME = Margin of error (kPa)

For example, take the set of data from SV1-PB4; this data set had a mean of 1795 kPa, a standard deviation of 117, and a COV of 6.5%. Using Equation 8.2, the standard deviation (117 kPa), z-score from an 85% level of confidence (1.44), and one replicate (n_{reps} = 1), the margin of error for the common practice of testing one replicate was 168 kPa.

To find the number of replicates needed for a 150 kPa margin of error at 75, 85, and 95% confidence levels, Equation 8.3 was used. This equation yielded 0.80, 1.26, and 2.34, respectively, for a 150 kPa margin of error. The values were rounded to the nearest 0.25. The procedure was again conducted for margins of error of 225 and 300 kPa.

Table 8.3 contains the results from the reliability analysis. The procedure summarized in the previous paragraph was conducted for each data set and each margin of error. Each row represents a single data set. Analysis included determination of replicates based on reliability and margin of error as well as the present design procedure margin of error. An average number of replicates for each reliability level and margin of error is also shown.

General obvious trends hold true in the reliability analysis table. These trends are that 1) more replicates are needed to achieve a higher level of confidence regardless of the margin of error and 2) a larger margin of error requires less replication of tests. The current design practice of testing one replicate gave an average margin of error for all sets of approximately 250 kPa at 85% reliability. Based on the averages of replicates of all data sets (bottom row of Table 8.2), if the number of replicates was increased to two, then the reliability of design would be as follows: 75% reliability that the mean is contained within a margin of error of 150 kPa; 85% reliability that the mean is contained within a margin of error of 225 kPa; and 95% reliability that the mean is contained within a margin of error of 300 kPa. If the number of replicates was increased, the reliability within each specified margin of error would increase accordingly.

8.4 Cement Source Effect on Compressive Strength

To determine if the cement source (e.g. *TH* or *GV*) affected the mean compressive strength (σ_{max}), t-tests were performed at a level of significance (α) of 0.05. Tests were performed assuming unequal variances with a two-tailed approach. The null hypothesis (H_0) was set as $\mu_1 = \mu_2$, and the alternative hypothesis (H_a) was $\mu_1 \neq \mu_2$. Compared specimen sets were of the same type (i.e. equal h/d ratios); therefore, no adjustments were conducted. Table 8.4 provides the results.

The t-tests for all soils show that the cement source had a significant effect on the mean compressive strength. *Pit A* and *Pit C* materials treated with *TH* cement produced a higher mean compressive strength than did *Pit A* and *Pit C* treated with *GV*. However, *Pit B* material treated with *GV* cement yielded a mean compressive strength higher than *Pit B* treated with *TH* cement. This indicates that the cement source had a significant effect on the mean compressive strength of the class 9C soils investigated. It is noteworthy the results differed in directionality between different pit soils.

Table 8.3. Compressive Strength Reliability Analysis for Design Purposes

Set	Mean (kPa)	COV (%)	*ME*[1] when n_{reps} =1 (kPa)	n_{reps} with 150 kPa *ME*			n_{reps} with 225 kPa *ME*			n_{reps} with 300 kPa *ME*		
				75%	85%	95%	75%	85%	95%	75%	85%	95%
SV1-PA4	1605	4.2	96	0.25	0.50	0.75	<0.25	0.25	0.25	<0.25	<0.25	0.25
SV1-PA5	2201	5.9	189	1.00	1.50	3.00	0.50	0.75	1.25	0.25	0.50	0.75
SV1-PA6	2508	4.5	161	0.75	1.25	2.25	0.25	0.50	1.00	0.25	0.25	0.50
SVM1-PA5	1982	6.7	190	1.00	1.50	3.00	0.50	0.75	1.25	0.25	0.50	0.75
SV2-PA5	2239	3.4	111	0.25	0.50	1.00	0.25	0.25	0.50	0.00	0.25	0.25
SV7-PA5	2077	11.7	351	3.50	5.50	10.25	1.50	2.50	4.50	0.75	1.25	2.50
SV4-PA5 (1)	2430	5.3	184	1.00	1.50	2.75	0.50	0.75	1.25	0.25	0.50	0.75
SV4-PA5 (2)	2317	4.1	137	0.50	0.75	1.50	0.25	0.25	0.75	0.25	0.25	0.50
SV4-PA4S (18)	1696	5.3	130	0.48	0.75	1.38	0.21	0.33	0.62	0.12	0.19	0.35
SV1-PB4	1795	6.5	168	0.75	1.25	2.25	0.25	0.50	1.00	0.25	0.25	0.50
SV1-PB5	2293	6.9	228	1.50	2.25	4.25	0.75	1.00	2.00	0.25	0.50	1.00
SV1-PB6	2590	8.3	311	2.75	4.25	8.00	1.25	2.00	3.50	0.75	1.00	2.00
SVM1-PB5	1766	11.6	295	2.50	3.75	7.25	1.00	1.75	3.25	0.50	1.00	1.75
SV2-PB5	2720	6.2	242	1.75	2.50	4.75	0.75	1.25	2.25	0.50	0.75	1.25
SV7-PB5	2085	6.5	194	1.00	1.75	3.00	0.50	0.75	1.50	0.25	0.50	0.75
SV4-PB5 (8a)	2461	9.9	350	3.50	5.50	10.00	1.50	2.50	4.50	0.75	1.25	2.50
SV4-PB5 (9)	2831	7.1	288	2.25	3.75	6.75	1.00	1.75	3.00	0.50	1.00	1.75
SV1-PC3	1766	11.8	301	2.50	4.00	7.50	1.25	1.75	3.25	0.75	1.00	1.75
SV1-PC4	2165	10.1	314	2.75	4.50	8.00	1.25	2.00	3.50	0.75	1.00	2.00
SV1-PC5	2557	14.6	536	8.25	12.75	23.75	3.50	5.75	10.50	2.00	3.25	6.00
SVM1-PC4	1875	10.9	295	2.50	3.75	7.25	1.00	1.75	3.25	0.50	1.00	1.75
SV2-PC4	2705	5.3	206	1.25	2.00	3.50	0.50	0.75	1.50	0.25	0.50	0.75
SV7-PC4	2279	5.2	170	0.75	1.25	2.50	0.25	0.50	1.00	0.25	0.25	0.50
SV4-PC4 (13)	3181	5.6	258	2.00	3.00	5.50	0.75	1.25	2.50	0.50	0.75	1.25
SV4-PC4 (14)	2668	11.1	428	5.25	8.25	15.00	2.25	3.50	6.75	1.25	2.00	3.75
			Average	1.75	2.75	5.25	0.75	1.25	2.25	0.50	0.75	1.25

75, 85, and 95% refer to level of confidence. n_{reps} values rounded to nearest 0.25. Avg. taken without highest and lowest value of original data; then rounded.
[1]Margin of error with 85% reliability.

Table 8.4. Effects of Cement Source on Compressive Strength

Term 1	μ_1 (kPa)	Term 2	μ_2 (kPa)	*df*	t_{crit}	t_{stat}	H_0 Conclusion
SV4-PA5 (1)	2430	SV4-PA5 (2)	2317	52	2.01	3.83	Reject
SV4-PB5 (8a)	2461	SV4-PB5 (9)	2831	56	2.00	-6.43	Reject
SV4-PC4 (13)	3181	SV4-PC4 (14)	2668	48	2.01	8.11	Reject

Note: Number in parenthesis are series numbers.

8.5 Compaction Method Effect on Compressive Strength

Statistical t-tests were utilized to investigate how the compaction method affected the mean compressive strength of similar specimens. Specimens were made with *TH* cement. Specimens were made with design cement contents compacted to maximum dry density and optimum moisture content. Tests were conducted at a level of significance of 0.05, assuming unequal variances with a two-tailed approach. The null hypothesis (H_0) was $\mu_1 = \mu_2$, and the alternative hypothesis (H_a) was $\mu_1 \neq \mu_2$. Compared specimen sets were not of the same type (i.e. equal h/d ratios); therefore, adjustments were conducted to compare all strengths at a h/d ratio of 2:1. Tables 8.5 to 8.7 show t-test results.

The t-tests showed different results for each pit soil while a few trends were consistent with all materials. The difference in compressive strength means for type 1 and 2 specimens was significant for *Pit B* and *Pit C* while not significant for *Pit A*. For type 1 and type 4 specimens, the difference in compressive strength means was significant for all pit soils. The difference in compressive strength means for type 1 and type 7 specimens was not significant for *Pit A* and *Pit B* but was significant for *Pit C*. Although *Pit C* showed a significant difference in mean compressive strengths, there seems to be a possible significant trend that specimen type 1 adjusted compressive strength mean is comparable to specimen type 7 compressive strength mean.

The difference in compressive strength means for type 2 and type 4 specimens was not significant for *Pit B* and significant for *Pit A* and *Pit C*. For type 2 and type 7 specimens, the difference in compressive strength means significant for *Pit B* and *Pit C* while not significant for *Pit A*. For type 4 and type 7 specimens, the difference in compressive strength means was significant for all pit soils.

Table 8.5. Effect of Compaction Method on Compressive Strength: *Pit A*

Term 1	μ_1 (kPa)	Term 2	μ_2 (kPa)	*df*	t_{crit}	t_{stat}	H_0 Conclusion
SV1-PA5	2001*	SV2-PA5	2036*	48	2.01	-1.37	Accept
SV1-PA5	2001*	SV4-PA5 (1)	2430	56	2.00	-13.36	Reject
SV1-PA5	2001*	SV7-PA5	2077	42	2.02	-1.54	Accept
SV2-PA5	2036*	SV4-PA5 (1)	2430	44	2.02	-14.46	Reject
SV2-PA5	2036*	SV7-PA5	2077	34	2.03	-0.89	Accept
SV4-PA5 (1)	2430	SV7-PA5	2077	44	2.02	7.01	Reject

** Adjusted compressive strengths to 2:1 h/d ratio, see Section 5.5.2.*
Note: Number in parenthesis are Series numbers.

Table 8.6. Effect of Compaction Method on Compressive Strength: *Pit B*

Term 1	μ_1 (kPa)	Term 2	μ_2 (kPa)	*df*	t_{crit}	t_{stat}	H_0 Conclusion
SV1-PB5	2085*	SV2-PB5	2472*	58	2.00	-10.11	Reject
SV1-PB5	2085*	SV4-PB5 (8a)	2461	47	2.01	-7.30	Reject
SV1-PB5	2085*	SV7-PB5	2085	56	2.00	0.00	Accept
SV2-PB5	2472*	SV4-PB5 (8a)	2461	49	2.01	0.21	Accept
SV2-PB5	2472*	SV7-PB5	2085	56	2.00	10.25	Reject
SV4-PB5 (8a)	2461	SV7-PB5	2085	46	2.01	7.36	Reject

** Adjusted compressive strengths to 2:1 h/d ratio, see Section 5.5.2.*
Note: Number in parenthesis are Series numbers.

Table 8.7. Effect of Compaction Method on Compressive Strength: *Pit C*

Term 1	μ_1 (kPa)	Term 2	μ_2 (kPa)	*df*	t_{crit}	t_{stat}	H_0 Conclusion
SV1-PC4	1969*	SV2-PC4	2459*	50	2.01	-11.32	Reject
SV1-PC4	1969*	SV4-PC4 (13)	3181	57	2.00	-24.85	Reject
SV1-PC4	1969*	SV7-PC4	2279	48	2.01	-7.32	Reject
SV2-PC4	2459*	SV4-PC4 (13)	3181	53	2.01	-17.85	Reject
SV2-PC4	2459*	SV7-PC4	2279	57	2.00	5.57	Reject
SV4-PC4 (13)	3181	SV7-PC4	2279	50	2.01	22.92	Reject

** Adjusted compressive strengths to 2:1 h/d ratio, see Section 5.5.2.*
Note: Number in parenthesis are Series numbers.

8.6 Curing Method Effect on Compressive Strength

Statistical t-tests were utilized to investigate how the curing method affected the mean compressive strength of similar specimens. Tests were conducted at a level of significance of 0.05, assuming unequal variances with a two-tailed approach. The null hypothesis (H_0) was $\mu_1 = \mu_2$, and the alternative hypothesis (H_a) was $\mu_1 \neq \mu_2$. Compared specimen sets were of the same type (i.e. equal h/d ratios); therefore, no adjustments were conducted. Table 8.8 shows t-test results.

Table 8.8. Effects of Curing Method on Compressive Strength

Term 1	μ_1 (kPa)	Term 2	μ_2 (kPa)	*df*	t_{crit}	t_{stat}	H_0 Conclusion
SV1-PA5	2201	SVM1-PA5	1982	58	2.00	6.46	Reject
SV1-PB5	2293	SVM1-PB5	1766	55	2.00	11.15	Reject
SV1-PC4	2165	SVM1-PC4	1875	58	2.00	5.31	Reject

The t-tests for all soils show that the method of curing had a significant effect on the mean compressive strength. The MSU curing method yielded a higher mean compressive strength than the MDOT curing method. For *Pit A*, the MSU curing method produced a mean compressive strength of 219 kPa (11%) higher than the MDOT curing method. For *Pit B*, the MSU curing method produced a mean compressive strength of 527 kPa (30%) higher than the MDOT curing method. For *Pit C*, the MSU curing method produced a mean compressive strength of 290 kPa (15%) higher than the MDOT curing method. The curing method had a different relative effect on mean compressive strength between materials.

The MDOT design requirement for soil cement pavement layers (MT-25) specifies the minimum cement content that will produce a compressive strength of 2070 kPa in 14 days. Designs based on MT-25 for the three pit soils were used in this study and specified the design cement index for each pit soil. Specimens made in accordance with MDOT making and curing protocols (testing category SVM) were replicated; Term 2 in Table 8.7 shows the mean value of the compressive strengths for each pit soil. It was noted that the mean value for all three pit soils at design cement index fell below the required compressive strength for design. Since similar making and curing protocols were used, there seems to be no immediate explanation for the discrepancy. However, the results confirm that curing method has a significant effect on the mean compressive strength.

8.7 Cement Index to Compressive Strength Relationship

Proctor compacted specimens (type 1) were tested at three cement indices (-1% of design, design, and +1% of design) with all three pit soils. Thirty replicate tests were performed per combination, for a total of 270 tests. Table 8.9 provides linear regression results for each pit soil to determine the effect of changing the cement index (C_I) on maximum compressive strength (σ_{max}). As seen in Table 8.9, relationships were reasonably linear with R^2 values being 0.97 or higher. Slopes ranged from 396 to 452, which could loosely be interpreted that increasing the cement index by 1% increased compressive strength by 396 to 452 kPa (57 to 66 psi). The data in Table 8.9 suggests a design method could test pre-determined cement contents, fit a linear trendline to the data, and use the trendline to calculate the cement content needed to achieve a design compressive strength.

Table 8.9. Cement Index to Compressive Strength Correlations

Specimen Set	Equation	R^2
SV1-PA	σ_{max} (kPa) = 452 (C_I) - 153	0.97
SV1-PB	σ_{max} (kPa) = 398 (C_I) + 239	0.98
SV1-PC	σ_{max} (kPa) = 396 (C_I) + 581	0.99

8.8 Design Guidance

Based on the analysis presented in this chapter, laboratory mix design guidance has been developed. Cement source effects were statistically significant on mean compressive strength, and differences were not consistently higher or lower between soil types. It is recommended to use portland cement from the same source that will be used on the project whenever possible (especially for large projects).

With regard to testing variability and MT-25 protocols, a protocol is suggested that should reduce variability with modest additional effort. Note there may be slight variations of the suggested protocol that can fit more seamlessly into MDOT Central Laboratory operations, and if that is the case making those adjustments shouldn't be problematic so long as the fundamental components remain in the method. By far, the most important component is to use the Figure 5.2 mold (i.e. the *PM* split mold) during laboratory mix design.

Ideally laboratory mix design and field quality control operations would be performed using the same mold and compaction equipment. At present, the *PM* split mold has been successfully used in the laboratory and in the field, though the compaction method was different. The *PM-CF* and *PM-P* approaches were both investigated a fair amount during

State Study 206, though the *PM-CF* approach was the one investigated the most for purposes of laboratory mix design. Ultimately the *PM-P* approach (or a deviation that also uses the *PM* mold and a Proctor hammer) is probably the most appropriate long term choice, though at present implementation of the *PM-CF* approach is probably more efficient as it can occur with less complications. Once the *PM-CF* approach is implemented for laboratory mix design and the *PM* mold is also implemented into quality control operations, steps to further synchronize these two activities should be more straightforward.

This chapter investigated *PM-CF* (type 4) and *PM-P* (type 7) prepared specimens and found their compressive strengths were significantly different. Table 8.10 summarizes behavior of each compactor. On average, specimens were 25% stronger and had 1% higher density when compacted with the *PM-CF* approach relative to the *PM-P* approach. As seen, *PM-CF* specimens can be accurately compacted to a reference density, which is advantageous for laboratory mix design. *PM-P* specimen densities were more variable, which can be attributed to applying a fixed number of blows (5) with a Proctor hammer. A trial and error procedure could be implemented to determine the number of blows to achieve the desired density, but in the interest of simplicity to assist in implementation, further discussion in this chapter uses the *PM-CF* compaction protocol. Chapter 12 provides additional information related to field quality control options where the *PM-P* approach was utilized.

Table 8.10. Strength and Density Comparison of Specimen Types 4 and 7

Pit	Cement	***PM-CF* (Type 4)**		***PM-P* (Type 7)**		**%**
Soil	**Index**	**% γ**	**σ_{max} (kPa)**	**% γ**	**σ_{max} (kPa)**	**Diff**
A	5	98.8 to 100.2 (99.3)	2430	96.9 to 99.8 (98.6)	2077	17
B	5	98.0 to 100.4 (99.3)	2461	95.7 to 100.1 (97.7)	2085	18
C	4	98.3 to 100.2 (99.3)	3181	97.5 to 100.1 (98.8)	2279	40

Note: % γ values are min to max with average in parenthesis.
Note: % Diff values are percent *PM-CF* specimens are stronger than *PM-P* specimens.

The following procedure is suggested to replace the current protocols in MT-25, and relies on two replicate tests (n_{reps} = 2) as opposed to the current MT-25 protocol (n_{reps} = 1). Use the *PM-CF* approach and prepare two specimens at 4% cement index, four specimens at 5% cement index, and two specimens at 6% cement index (eight specimens total). Current MT-25 protocols make six total specimens.

Cure all eight specimens (curing protocols discussed later in this section) and test two of the 5% cement index specimens at 7 days. If these specimens meet, exceed, or are within 345 kPa (50 psi) of the design strength criteria (discussed later in this section), test the 4% and 6% cement index specimens at 7 days and test the remaining two 5% cement index specimens at 14 days. The trendline slope at 7 days from the 4, 5, and 6% specimens can be used to adjust the 5% cement index specimens tested at 14 days to other cement contents if needed. If the two 5% cement index specimens tested at 7 days are more than 345 kPa (50 psi) lower than the design strength criteria, test the remaining six specimens at 14 days. The trendline slope at 14 days from the 4, 5, and 6% specimens can be used to adjust the 5% cement index specimens tested at 7 days to other cement contents if needed.

Once all specimens have been tested, plot average compressive strength as a function of cement content, and use a linear trendline fit to calculate the cement content needed to achieve the design strength to one decimal place on a dry mass basis. The procedure is similar to that performed in Section 8.7. Note this approach could slightly lower design

cement contents as the current procedure has an inherent overdesign; for example if design is 2070 kPa, and test result at 5% cement index is 2210 kPa, 5% is used. The current approach would pick (for example) 4.8% as the cement index. After the cement content is calculated to one decimal place, MDOT can use their judgment to determine the cement content to use as the value during construction. For example, if the value is calculated at 4.8%, MDOT could elect to use 5%, but if the value is calculated at 4.2%, MDOT could elect to use 4.5%.

At this juncture, all design procedure components have been addressed except the curing protocols and design strength requirement. These components are interrelated. The baseline for discussion is MT-25's current requirements of 2070 kPa (300 psi) when specimens are prepared with a Proctor hammer (specimen type 1 in Table 5.1) and cured according to MDOT's current protocol (cured in plastic bags until five hours before testing, then submerged in water until testing).

At a minimum, replacing Proctor compaction (type 1) with *PM-CF* compaction (type 4) is recommended. Replacing MDOT's current curing protocol with the MSU protocol (specimens placed uncovered in 100% humidity ambient temperature curing room until tested) is suggested. Guidance is provided in the remaining paragraphs related to adjusting the current MT-25 strength requirement of 2070 kPa to other values depending on the combination MDOT elects to implement. In an overall sense the goal is to provide similar cement contents to those already being used based on favorable findings in Chapter 7.

Table 8.11 provides suggested design compressive strength values for combinations that could be useful. These suggested design values are provided as minimum to maximum, with an average value in parenthesis. Note that the suggested design values have not been rounded; e.g. 2463 kPa (357 psi) would probably be rounded to 2413 kPa (350 psi) for use as a design requirement. The upper end of the suggested design strengths was from *Pit C*, which had a fairly high *PM-CF* value when cured according to the MSU method of 3181 kPa. As an initial recommendation, values between the minimum and average suggested design strength seem reasonable. The *PM-CF* specimens cured with the MSU protocol are the suggested approach to implement with an initial design strength requirement of 2758 kPa (400 psi). As stated previously, using the aforementioned conditions and a 2758 kPa (400 psi) strength requirement is not expected to shift overall design cement contents appreciably from their current state. The recommended approach, however, is expected to refine values for individual projects within the range of currently used values, and also provide enhanced interfacing with pavement layer thickness design and construction quality control.

Table 8.11. Suggested Design Compressive Strength Values

Specimen Type	Curing Protocol	% Difference[b]	Suggested Design Strength (kPa)
Proctor (Type 1)	MDOT	---[a]	2070 (current MT-25 value)
Proctor (Type 1)	MSU	+ 11 to 30 (19)	2298 to 2691 (2463)
PM-CF (Type 4)	MDOT	+7 to 47 (21)	2215 to 3043 (2505)[c]
PM-CF (Type 4)	MSU	+ 23 to 70 (44)	2546 to 3519 (2981)

a: All % Difference values in this table are relative to Proctor specimens and MDOT curing protocol.

b: (+) indicates specimens were stronger than Proctor specimens and MDOT curing. Values provided are min to max with average in parenthesis

c: Experiments were not conducted for this combination of conditions, rather data from specimen types 1 (Proctor) and 4 (*PM-CF*) cured with the MSU method were compared and the differences reported. The assumption with this data is that the relative effects between Proctor and *PM-CF* compaction would be the same for MDOT or MSU curing protocols. Note that strength versus time testing presented in Chapter 7 resulted in *PM-CF* specimens being + 9 to 27 (17) than Proctor compacted specimens cured with the MSU protocol.

CHAPTER 9 – ELASTIC MODULUS TEST RESULTS

9.1 Elastic Modulus Results Overview

A total of 54 laboratory compacted specimens were tested for elastic modulus (Table 9.1). Three specimens were tested at each cure time, totaling nine tests per material per specimen type. Specimens were evaluated for maximum compressive strength (σ_{max}), and elastic modulus from a compressometer (E_{Comp}). Specimens were tested at cure times of 7, 28, and 60 days.

Table 9.1. Test Matrix for Elastic Modulus

Identifier	Material	Cement Type	Cement Index	Specimen Type	Cure Method	Tests (per Cure Time)
EM4-PA5	PA	*TH*	Design (5%)	4	MSU	3
EM4-PB5	PB	*TH*	Design (5%)	4	MSU	3
EM4-PC4	PC	*TH*	Design (4%)	4	MSU	3
EM 7-PA5	PA	*TH*	Design (5%)	7	MSU	3
EM7-PB5	PB	*TH*	Design (5%)	7	MSU	3
EM7-PC4	PC	*TH*	Design (4%)	7	MSU	3

**Raw data is provided in Anderson (2013) Appendix A in Tables A.32 to A.37.*

9.2 Elastic Modulus Results

Tables 9.2 to 9.4 provide elastic modulus results organized by pit soil. All data in Tables 9.2 to 9.4 used *TH* cement at design cement index, while cured with the MSU protocol (Section 5.4.4). The modulus value reported is the value using strain measured with the compressometer (E_{Comp}), values are reported in gigapascals (GPa), and average values reported are of three test replicates.

The range of values for average elastic modulus was 3.3 GPa (EM7-PB5 7 day) to 10.8 GPa (EM4-PC4 90 day). Results from the elastic modulus testing using the compressometer show that modulus seems to increase with an increase in cure time. This was well documented in the literature with cement stabilized materials (Felt and Abrams 1957 and James et al. 2009) and lime stabilized soils (Thompson 1966). Elastic modulus values for *Pit A* seemed to plateau (type 4) or slightly decrease (type 7) after 28 days. *Pit B* elastic modulus values also seemed to plateau. *Pit C* showed a different behavioral trend than *Pit A* and *Pit B*. For both specimen types (type 4 and type 7), the elastic modulus was still increasing between 28 and 90 day cures. However, the increase in elastic modulus between 28 and 90 day cures for *Pit C* was not as dramatic as increases between 7 and 28 days.

Table 9.2. Elastic Modulus Values for *Pit A*

Set ID	Time (days)	Avg. σ_{max} (kPa)	Avg. E_{Comp} (GPa)
EM4-PA5	7	2484	4.6
	28	3111	6.2
	90	3576	6.4
EM7-PA5	7	2312	5.2
	28	2939	6.6
	90	3098	6.5

Table 9.3. Elastic Modulus Values for *Pit B*

Set ID	Time (days)	Avg. σ_{max} (kPa)	Avg. E_{Comp} (GPa)
EM4-PB5	7	2555	4.4
	28	3080	5.4
	90	3794	5.5
EM7-PB5	7	2237	3.3
	28	2768	4.5
	90	3005	4.5

Table 9.4. Elastic Modulus Values for *Pit C*

Set ID	Time (days)	Avg. σ_{max} (kPa)	Avg. E_{Comp} (GPa)
EM4-PC4	7	2671	6.6
	28	3501	9.0
	90	3991	10.8
EM7-PC4	7	2640	5.3
	28	2952	7.0
	90	3407	8.4

9.3 Elastic Modulus Correlations

Figure 9.1 plots maximum unconfined compression strength, σ_{max}, (kPa) by measured elastic modulus, E_{Comp}, (GPa). A linear regression line was fitted to the data (LF) with the intercept forced to zero (i.e. RTO) and is shown on the plot. Also, lines encompassing most of the data are provided with the linear fit; these lines are referred to as the upper boundary (UB) and the lower boundary (LB). 98% of the data was contained within the upper and lower boundary lines; one data point was above the upper boundary line.

Relationships for the LF, LB, and UB lines in Figure 9.1 are given in general form in Equation 9.1. This equation resembles Equation 2.7, though in Equation 2.7 a compressive strength was multiplied by a constant to calculate an elastic modulus value, given both are in the same units. Input for Equation 9.1 was compressive strengths in kPa. Output for Equation 9.1 was elastic modulus in GPa. In order to convert between customary units, the constant (C_i) for each line equation was multiplied by 10^{-6}, as shown in Equation 9.1.

$$E_{Comp}\ (GPa) = C_i * 10^{-6} * \sigma_{max}\ (kPa) \qquad \text{(Eq. 9.1)}$$

Where:
E_{Comp} = Elastic modulus (GPa)
σ_{max} = Maximum compressive strength (kPa)
C_i = Equation constant for *i* line
C_U = 2900, Constant for Upper Boundary Line
C_F = 2000, Constant for Linear Fit Line
C_L = 1300, Constant for Lower Boundary Line

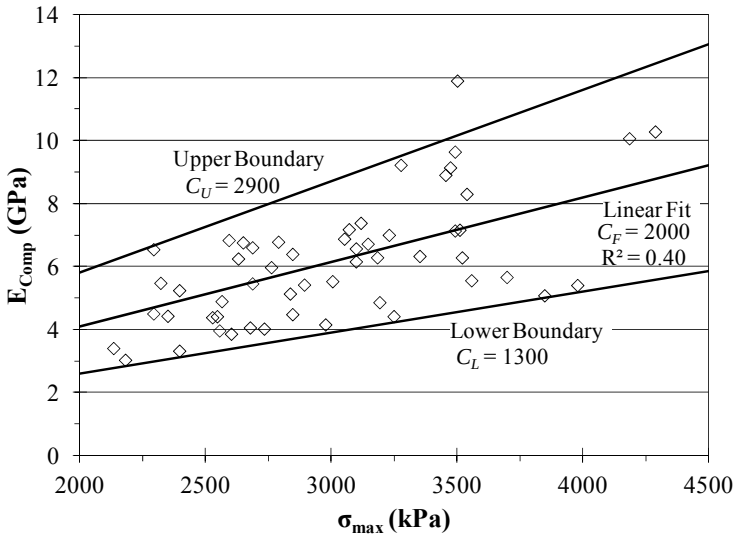

Figure 9.1. Elastic Modulus versus Compressive Strength

Table 9.5 shows the measured elastic modulus distribution based on soil type and specimen type. There were no data points that fell below the lower boundary. *Pit A* seemed to be more evenly distributed between the upper and lower boundaries with 61% between the lower boundary (LB) and linear fit (LF), and 39% between the LF and the upper boundary (UB). *Pit B* was mostly between the lower boundary and the linear fit lines (89%), with the other 11% between the linear fit and upper boundary lines. On the contrary, *Pit C* had more between the linear fit and upper boundary lines (83%), with 11% between the lower boundary and linear fit lines. Specimen type seemed to be more evenly distributed between the lower and upper boundary lines. The distribution showed different pit soils had slightly different trends when comparing unconfined compression strength and elastic modulus. C_i values for *Pit A* (C_A), *Pit B* (C_B), and *Pit C* (C_C) when considering only one pit soil at a time were 2000, 1600, and 2500, respectively.

Table 9.5. Distribution of Elastic Modulus Given Parameters

		Percentage in Region (%)			
Parameter	***n***	**< LB**	**LB-LF**	**LF-UB**	**> UB**
Pit A	18	0	61	39	0
Pit B	18	0	89	11	0
Pit C	18	0	11	83	6
Type 4	27	0	52	44	4
Type 7	27	0	56	44	0

Type 4 and Type 7 refer to the specimen type as per Section 5.2.

Correlations found in literature were investigated with the data obtained from elastic modulus testing. Figure 9.2 shows the relationship between these correlations and the data collected. Equations 2.5 to 2.7 were used to calculate elastic modulus with σ_{max} and/or gradation modulus; then units were converted for plotting consistency. Equation 2.5 from Thompson (1966) was derived to find elastic modulus given unconfined compression strength of lime stabilized materials. The calculated elastic modulus from the compressive strength test data using Equation 2.5 severely under predicted elastic modulus values measured herein. This was explained because the equation was developed for a separate stabilized material. Equation 2.7 referenced in James et al. (2009) finds elastic modulus of cement stabilized base layers from the unconfined compressive strength for the MEPDG. The MEPDG uses this equation as a level 2 input. The calculated elastic modulus from the compressive strength test data using Equation 2.7 predicts values that somewhat align with the lower boundary of the tested specimens; i.e. the equation predicted a conservative elastic modulus value.

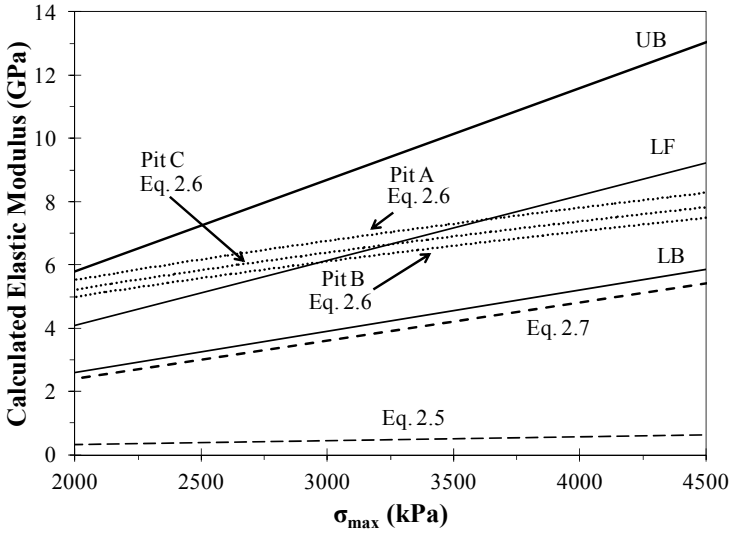

Figure 9.2. Elastic Modulus Correlations from Literature (Dashed Lines) with Present Study (Solid Lines)

Equation 2.6 from Kolias and Williams (1984) used the compressive strength and a gradation modulus to find the elastic modulus. A gradation modulus was determined for *Pit A*, *Pit B* and *Pit C*; the gradation modulus values were 8.92, 9.21, and 9.09, respectively. The calculated elastic modulus from the compressive strength and the respective gradation modulus using Equation 2.6 seems to predict relatively accurate elastic modulus values compared to the best linear fit of the test data. Although the equation seems to slightly over predict modulus values for the design strength region (i.e. strengths between 2000 and 2500 kPa), the equation better predicts elastic modulus values when strengths reach those seen during the performance of the pavement layer (i.e. greater than around 2500 kPa that occur at later ages). Equation 2.6 from Kolias and Williams (1984) seems to better predict the actual elastic modulus of the materials while Equation 2.7 yields a conservative elastic modulus value typically used for design.

CHAPTER 10 – WHEEL TRACKING TEST RESULTS

10.1 Wheel Tracking Results Overview

Wheel tracking was performed on soil-cement to investigate material performance under simulated traffic loading. Testing was performed with the PURWheel, APA, and HLWT. Results and discussion related to each method are provided in the following sections.

A total of 6 HLWT specimens (specimen type 6), 6 LAC slabs (specimen type 5), and 8 APA specimens (specimen type 3) were tested (Table 10.1). Each LAC slab and APA specimen was tested twice. The first test was dry and the second test was either submerged or soaked. One LAC slab produces two PURWheel specimens (one specimen was used for each test), for a total of 12 PURWheel tests. Note that one PURWheel test evaluated multiple conditions and collected a considerable amount of data. Two APA specimens used for each test, for a total of 4 APA tests. Note that one APA test also evaluated multiple conditions.

Table 10.1. Wheel Tracking Test Matrix

Material	Cement Index (%)	Specimen Type	Loading Conditions (%)	Test Conditions
PA	Design (5%)	5	50/100	PURWheel Dry PURWheel Submerged
PB	Design (5%)	5	50/100	PURWheel Dry PURWheel Submerged
PB	Design (5%)	5	65/80	PURWheel Dry PURWheel Submerged
PB	Design (5%)	5	50/100	PURWheel Dry PURWheel Soaked
PB	Design (5%)	5	65/80	PURWheel Dry PURWheel Soaked
PC	Design (4%)	5	50/100	PURWheel Dry PURWheel Submerged
PA	Design (5%)	3	100	APA-Dry APA-Submerged
PA	+1% of Design (6%)	3	100	APA-Dry APA-Submerged
PB	Design (5%)	3	100	APA-Dry APA-Submerged
PC	Design (4%)	3	100	APA-Dry APA-Submerged

Notes: Cement used was TH, all specimens were cured according to Section 5.4.4 WTP, and raw data is provided in Anderson (2013) Appendix C. HLWT specimens were also tested, but as seen in Section 10.2, no specific data was collected.

10.2 HLWT Test Results

Initial HLWT soil-cement testing in typical bituminous material conditions proved too harsh. Specimens failed after a small fraction of the passes were completed, and material

debris covered the inside of the equipment. No useful data was collected and further testing was not performed to avoid equipment damage.

10.3 APA Test Results

APA data obtained from each test was fitted with a logarithmic trend line (Figure 10.1). The trend lines are labeled with the soil, cement index, trend line equation, and the R^2 value for each test. Dry and submerged test results are shown in Figure 10.1a and 10.1b, respectively. Each plot shows rutting for that test only; the total rut measurement after both tests would be the sum of the two final rut depths (d_{fr}). For example, *Pit B* specimens rutted 1.5 mm during the dry test and 8.2 mm during the submerged test; therefore, *Pit B* had a total rut depth of approximately 9.7 mm after 16,000 cycles.

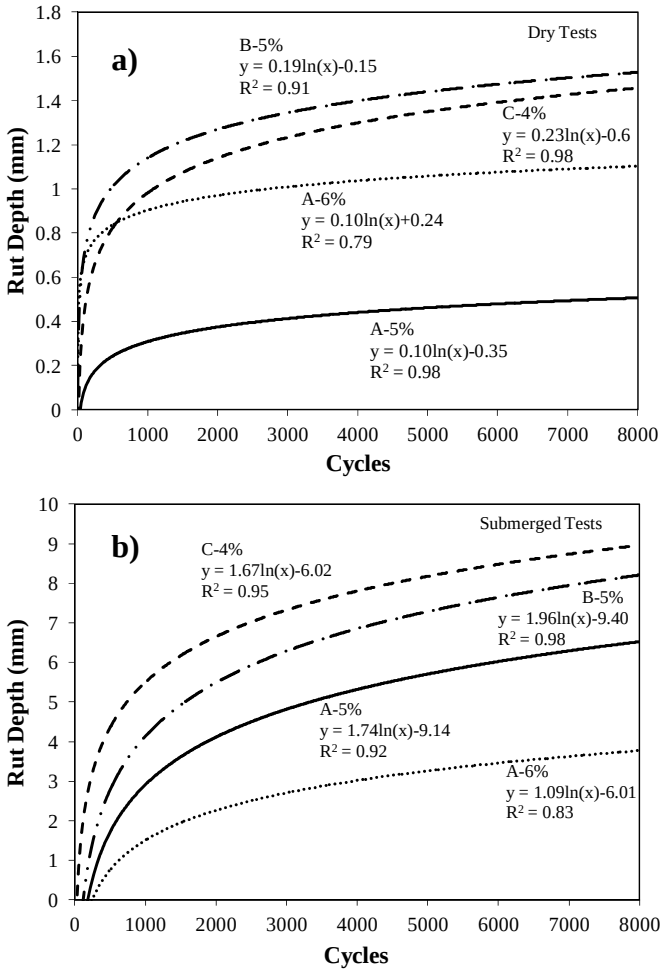

Figure 10.1. APA Results - Dry and Submerged Tests

Data shows that for all the dry tests, there is minimal rutting (e.g. a maximum of 1.5 mm rut). *Pit B* exhibited the most rutting in the dry test, followed closely by *Pit C*. Both cement indexes tested with *Pit A* provided less rutting than *Pit B* or *Pit C*. Interestingly, *Pit A* specimens with a cement index of 6% rutted approximately 0.6 mm more than specimens with 5% cement index. Again, the difference in final rut depths of all materials in the dry

tests was within one millimeter and less than 1.5 mm; this shows that for the dry condition, these materials are not susceptible to rutting at the given loading.

Higher APA rutting was observed in the data from the submerged tests. Table 10.2 shows final rut depths (d_{fr}) of the four tested materials, along with a rutting rate (mm/1000 cycles) from 0 to 2000 cycles and 2000 to 8000 cycles. Trendlines are used to obtain values at 2000 and 8000 cycles; it was assumed that there was no rutting at zero cycles. These values were then used to calculate the slope between 0 and 2000 cycles and 2000 and 8000 cycles by subtracting the calculated rut values and dividing by the number of thousand cycles. This procedure yields mm per 1000 cycles. Intervals were chosen based on observed changes in behavior (e.g. noticeable change in slope).

Table 10.2. APA Submerged Test Results

Soil	C_I (%)	d_{fr} (mm)	Rutting Rate (mm/1000 cycles)	
			0-2000	2000-8000
A	5	6.5	2.0	0.8
A	6	3.8	1.1	0.5
B	5	8.2	2.7	0.9
C	4	9.0	3.3	1.0

The different behaviors under wheel load testing are evident even with a small test matrix. *Pit A*, with both the 5 and 6% cement indexes, exhibited the least rut deformation, and followed by *Pit B* and then *Pit C*. *Pit C* had the highest final rut depth of 9 mm. This indicates that rutting behavior in a wet condition is dependent on the material, even when the cement content meets the design requirement. Also, *Pit A* at 6% C_I has less final rut depth and lower rutting rates than *Pit A* at 5% C_I. Most rutting occurred within the first 2000 cycles. The rutting rate noticeably decreased in the last three quarters of the test.

Figure 10.2 shows a post-testing specimen photograph. The rutting in soil-cement specimens appeared to be an abrasive carving or displacement/removal of material rather than shear or densification that typically ruts bituminous materials. The environment in which the materials are subjected to during testing had a considerable effect on the rutting behavior.

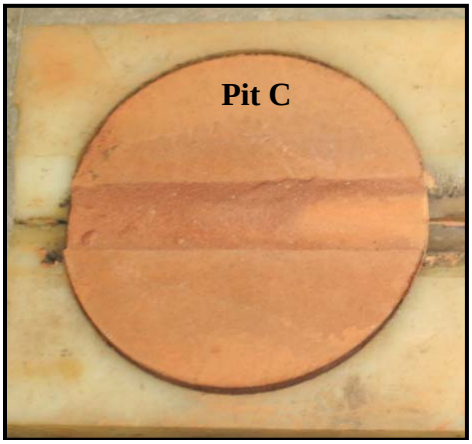

Figure 10.2. Soil-Cement Specimen Post APA Submerged Testing

10.4 PURWheel Test Results

Table 10.3 summarizes PURWheel test results. Final rut depths, and/or passes to failure are used for analysis. The maximum rut depth measured for a dry test was 2.0 mm at 20,000 passes. This was during 100% loading of *Pit A* and *Pit B*. In all dry tests, minimal rutting was observed. Dry conditions seem to be somewhat resistant to permanent rut deformation and are not discussed further. Remaining discussion focuses on rutting from the soaked and submerged condition tests, which is the focus of Table 10.3.

Table 10.3. PURWheel Soaked/Submerged Results

Pit Soil	C_I (%)	Test Conditions	Loading (%)	Final Rut Depth (mm)	Passes to Failure
A	5	Submerged	50	0.1	
			100	---	8,774
B	5	Submerged	50	2.6	
			65	11.2	
			80	---	16,938
			100	---	6,356
C	4	Submerged	50	0.3	
			100	3.4	
B	5	Soaked	50	0.4	
			65	0.3	
			80	0.0	
			100	-1.5*	

(---) signifies failure (actual rut depth ≥23 mm) according to Howard et al. (2010).
Final rut depths taken after 20,000 passes (full test) unless failure occurred.
Maximum rut depth of 2 mm for dry testing.
** Data collection error, but minimal rutting observed (<2mm).*

Results show that for all 50% loadings, submerged and soaked, there was essentially no rutting. *Pit B* had the highest rut measurement with a 50% loading of 2.6 mm. *Pit A* and *Pit B* specimens, when submerged and subjected to the 100% loading, failed between 6000 and 9000 passes. This was less than half the length of a full test. *Pit C* had 3.4 mm of rutting under submerged conditions with a 100% applied load. However, as seen in Anderson (2013) Appendix C Figure C.6b, *Pit C* may have been beginning to fail towards the end of the test. It started to demonstrate similar behaviors to *Pit A* and *Pit B* just before failure.

Pit B submerged testing with the 65% and 80% loadings further demonstrated the progression of material damage. The 65% submerged loading showed a higher final rut depth than the 50% loading while the 80% submerged loading failed with a higher number passes to failure than the 100% loading. The progression of damage with increased load suggests that with given environmental conditions, there was a loading threshold up to which materials could perform satisfactorily.

Results from the *Pit B* soaked tests with 50, 65, 80 and 100% loadings showed essentially no rutting for the scope of this study. To experience considerable damage, specimens had to be submerged in water during testing. Soaked testing did not result in meaningful amounts of damage.

CHAPTER 11-PHASE 1 THERMAL PROFILE QUALITY CONTROL TEST RESULTS: FEASIBILITY

11.1 Overview of Laboratory Specimen Analysis

This chapter focuses on analysis of laboratory prepared thermal profile specimens. A total of 534 laboratory prepared specimens were analyzed in this chapter for thermal profiles, with raw data provided in Sullivan (2012) Appendix B. Of these 534 specimens, 324 are unique to this chapter, while 210 of these specimens were also used for compressive strength analysis in Chapter 8. Additionally, specimen compaction evaluation provided in this chapter used specimens whose other data was used throughout multiple chapters in this report.

Table 11.1 shows the test matrix for phase 1 thermal profile specimens and gives a brief description of the analysis purpose. The number of replicate σ_{max} tests and the time at which σ_{max} was tested ($t_{\sigma max}$) are also provided. A few specimens are used in multiple series of data (these specimens are noted in Sullivan (2012) Appendix B).

Before analysis, data outliers were identified for each data set using Tukey's Method, which distinguishes outliers by measuring the data's distance from the Inter Quartile Range (*IQR*). The *IQR* is the distance between the data set's 25th (Q_1) and 75th (Q_3) percentile. Data points falling outside the range of Q_1 - 1.5**IQR* and Q_3 + 1.5**IQR* were considered to be outliers and were not included in analysis. The number of outliers was denoted n_o.

11.2 Analysis Terminology

Seven variables were considered in analysis (Figure 11.1). Five variables correspond to thermal profiles and two variables correspond to compressive strength. The Nurse-Saul maturity function also known as the Temperature-Time Factor (*TTF*) was used to express specimen maturity. Areas beneath or between thermal profile curves are considered to essentially be the same maturity approach as the Nurse-Saul maturity function or the *TTF*.

11.3 Specimen Preparation Characteristics

The specimen preparation protocol (e.g. compaction in plastic molds) presented herein is a relatively new concept; therefore, an analysis was performed to examine the number of hammer blows (*PM-CF* approach) required to achieve a target density, and specimen volumes post compaction. All laboratory prepared specimens were used to analyze the post compaction specimen dimensions and specimen volumes.

11.3.1 Number of Hammer Blows

Pit soils *A*, *B*, and *C* were compacted using the *PM-CF* approach. Relative frequency histograms were constructed of the blow count distribution (Table 11.2 summarizes the results). Blow count variability per lift can be attributed to varying target densities for each mixture, but in general, the average blow counts were 10 to 13 per lift for the pit soils.

Table 11.1. Summary of Phase 1 Thermal Profile Tests

Series	Soil	Compaction Type	Additive	T_i (°C)	T_{BL} (°C)	Target ω (%)	C_I (%)	Description	$t_{\sigma max}$ (day) 1	3	7	14
1	*A*	*PM-CF*	*TH*	≈ 21	≈ 21	Optimum	5	Profile Variability	--	--	30	--
2	*A*	*PM-CF*	*GV*	≈ 21	≈ 21	Optimum	5	Profile Variability	--	--	30	--
18	*A*	*PM-CF*	*TH*, *GGBFS*	≈ 21	≈ 21	Optimum	4	Profile Variability	--	--	30	--
3	*A*	*PM-CF*	*TH*	≈ 10	≈ 21	Optimum	2, 4, 6, 8, 10	Effect of Cement Content	--	--	15	--
22	*A*	*PM-CF*	*TH*	≈ 21	≈ 21	Optimum	2, 4, 6, 8, 10	Effect of Cement Content	--	--	15	--
23	*A*	*PM-CF*	*TH*	≈ 32	≈ 21	Optimum	2, 4, 6, 8, 10	Effect of Cement Content	--	--	15	--
4	*A*	*PM-CF*	*TH*	≈ 21	≈ 21	Opt. ± 2	4, 5, 6	Effect of Cement & Water	--	--	21	--
5	*A*	*PM-CF*	*TH*	≈ 10	≈ 21	Optimum	4, 5, 6	Effect of Initial Temperature	9	9	9	--
6	*A*	*PM-CF*	*TH*	≈ 21	≈ 21	Optimum	4, 5, 6	Profile Correlation to σ_{max}	9	9	9	--
7	*A*	*PM-CF*	*TH*	≈ 32	≈ 21	Optimum	4, 5, 6	Effect of Initial Temperature	9	9	9	--
49	*A*	*PM-CF*	*TH*	≈ 32	≈ 32	Optimum	5	Effect of T_i and T_{BL}	6	6	6	--
20	*A*	*PM-CF*	*TH*, *GGBFS*	≈ 10	≈ 21	Optimum	3, 4, 5	Effect of Initial Temperature	--	--	9	--
19	*A*	*PM-CF*	*TH*, *GGBFS*	≈ 21	≈ 21	Optimum	3, 4, 5	Profile Correlation to σ_{max}	--	9	9	9
21	*A*	*PM-CF*	*TH*, *GGBFS*	≈ 32	≈ 21	Optimum	3, 4, 5	Effect of Initial Temperature	--	--	9	--
8a	*B*	*PM-CF*	*TH*	≈ 21	≈ 21	Optimum	5	Profile Variability	--	--	30	--
8b	*B*	*PM-CF*	*TH*	≈ 21	≈ 21	Optimum	5	Profile Variability	--	--	30	--
9	*B*	*PM-CF*	*GV*	≈ 21	≈ 21	Optimum	5	Profile Variability	--	--	30	--
10	*B*	*PM-CF*	*TH*	≈ 21	≈ 21	Optimum	4, 5, 6	Profile Correlation to σ_{max}	9	9	9	--
13	*C*	*PM-CF*	*TH*	≈ 21	≈ 21	Optimum	4	Profile Variability	--	--	30	--
14	*C*	*PM-CF*	*GV*	≈ 21	≈ 21	Optimum	4	Profile Variability	--	--	30	--
27	*C*	*PM-CF*	*TH*	≈ 21	≈ 21	Optimum	4	Equip. Configuration	--	--	30	--
15	*C*	*PM-CF*	*TH*	≈ 21	≈ 21	Optimum	3, 4, 5	Profile Correlation to σ_{max}	9	9	9	--

-- Series numbers correspond to Sullivan (2012).

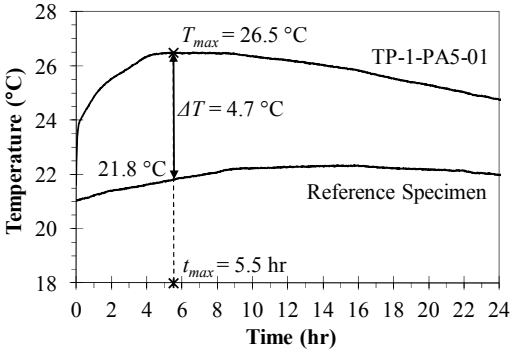

(a) t_{max} and ΔT

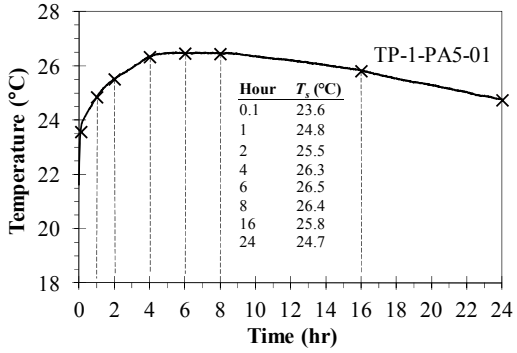

(b) Profile Temperature Points

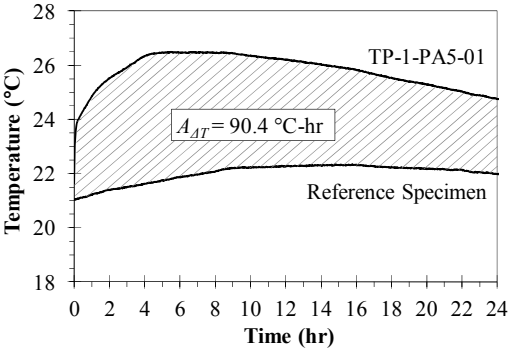

(c) Area of T_s minus T_r ($A_{\Delta T}$)

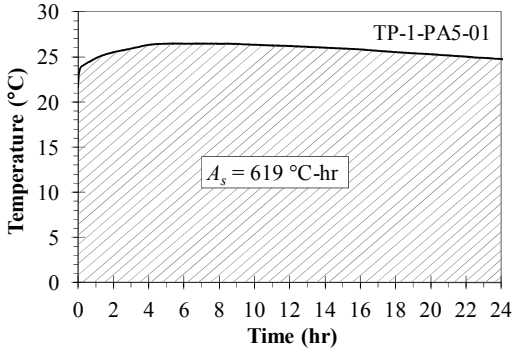

(d) Area Under T_s Profile (A_s)

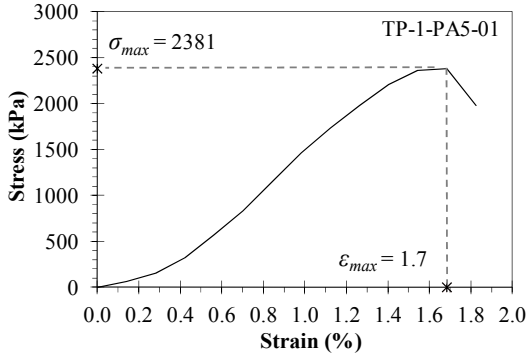

(e) Specimen Stress-Strain Curve

Figure 11.1. Analysis Terminology

Table 11.2. Summary of *PM-CF* Blow Count Data

	Total	Blows per lift		
Soil	**Lifts**	**Mean**	***Stdev***	***COV* (%)**
Pit A	900	12.8	3.0	23.6
Pit B	351	12.1	1.9	15.7
Pit C	351	10.3	2.2	21.3

Note: Three lifts per specimen.

11.3.2 Specimen Dimensions

The plastic molds used to compact specimens may have slight variations with respect to dimensions that are allowed by ASTM C 470, and the plastic molds have the potential to deform during compaction. Specimen density measurements were used to evaluate the volumetric variability of specimens after compaction in the *PM* compactor assembly. This investigation encompassed all laboratory compacted specimens using both the *PM-CF* and *PM-P* compaction approaches.

Specimen dimensional measurements of interest include the average of two top diameter, average of two bottom diameter, overall average specimen diameter (average of top and bottom measurements), and the average height. From these measurements, the specimen h/d ratio and volume were calculated. Variability was evaluated by constructing relative frequency histograms and normality plots. Figure 11.2 shows the overall relative frequency histogram and an example normality plot used to assess specimen volumetric variability, while Table 11.3 summarizes all results.

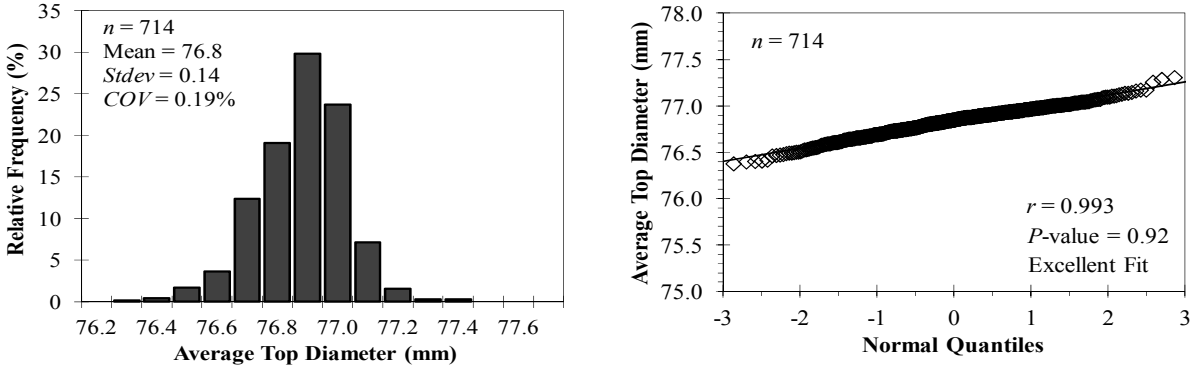

(a) Example Histogram (b) Example Normality Plot

Figure 11.2. Examples of Constructed Histogram and Normality Plot

Table 11.3. Specimen Volumetric Variability

Variable	*n*	Mean	*Stdev*	*COV* (%)	*P*-value	Normality Fit
Avg. Top Diameter (mm)	714	76.8	0.14	0.19	0.92	Excellent
Avg. Bottom Diameter (mm)	714	76.4	0.19	0.25	0.98	Excellent
Overall Avg. Diameter (mm)	714	76.6	0.15	0.20	0.99	Excellent
Avg. Height (mm)	714	150.6	0.23	0.16	0.11	Good
h/d Ratio	714	1.97	0.005	0.24	0.99	Excellent
Percent of Expected Volume[1]	714	100.9	0.45	0.45	0.98	Excellent

1: The expected theoretical specimen volume is 687.8 cm^3 (diameter = 76.2 mm; height = 150.8 mm).

The Table 11.3 data demonstrates acceptable specimens can be compacted inside a plastic mold with the *PM* compactor assembly. The average overall diameter was 0.4 mm larger than the 76.2 mm target, and the specimen tapers 0.4 mm from the top to the bottom. A small taper is intuitive given the plastic molds are closed at the bottom and open at the top. Overall, the average specimen volume was 0.9% above the target and the h/d aspect ratio was 1.97. As per ASTM C 470 requirements, no two specimen diameter measurements differ by more than 2 percent.

11.4 Comparison of Compressive Strength and Thermal Measurement Variability

Compressive strength and thermal measurement variability was compared in this section. The evaluation mostly followed the statistical approach used in Section 8.2. Data used in the evaluation was from Series 1, 2, 8a, 8b, 9, 13, 14, and 18.

11.4.1 Compressive Strength Variability

Variability of *PM-CF* compaction σ_{max} readings was used for thermal profile comparison, and most of this data was presented in Table 8.2, albeit in a condensed form. Figure 11.3 is an example frequency histogram and normality plot used for analysis and represented in Table 8.2 for Soil Set SV4-PA5 (1).

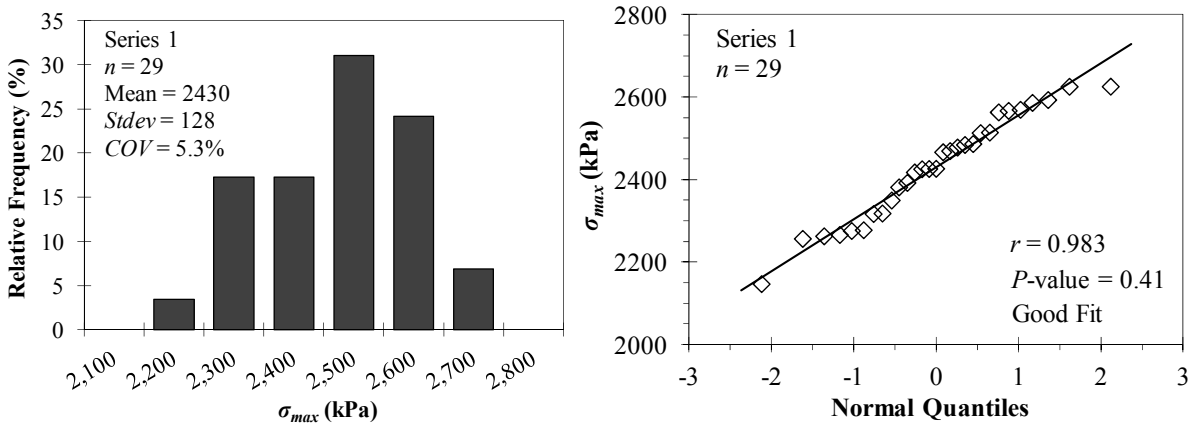

(a) Relative Frequency Histogram Series 1 (b) Normality Plot Series 1

Figure 11.3. Examples of σ_{max} Histograms and Normality Plots

SV4-PB5 (8a) from Table 8.2 produced an average compressive strength of 2461 kPa with a *COV* of 9.9% and a poor normality fit. This series was repeated to investigate the poor normality fit, and the repeated series is denoted Series 8b. Series 8b produced an average 7 day compressive strength of 2672 kPa with a *COV* of 9.5% and a *P-Value* of 0.03 (Poor normality fit). These results were approximately 200 kPa greater than Series 8a data with approximately the same amount of variability, verifying the poor normality fit.

11.4.2 Thermal Measurement Variability

Tables 11.4 through 11.13 show the results from relative frequency histograms, normality plots, and statistical t-tests for the five thermal measurement variables in Figure 11.1. All t-tests were performed at $\alpha = 0.05$ assuming unequal variances. Tables 11.4 and 11.5 show results for the recorded maximum temperature (T_{max}). The T_{max} measurement for all three soils stabilized with portland cement (i.e. *TH* and *GV*) was fairly consistent with mean values ranging from 25.7 to 27.2 °C and *COV*'s ranging from 1.1 to 3.5 %. *Pit A* stabilized with GGBFS recorded a lower mean T_{max} (22.9 °C) than portland cement mixtures, but the mixture was also less variable (*COV* = 0.8%). *Pit B* appears to be slightly more variable than *Pit A* and *Pit C* with respect to T_{max}. All soil and cement combinations, except for *Pit B* with *GV*, have a good to excellent normality fit.

Results from t-tests (Table 11.5) show no significant difference in mean T_{max} between cement sources for *Pit A* or one of the *Pit B* comparisons (Series 8b and Series 9). Results do show a significant difference in mean T_{max} for *Pit C* as well as one of the *Pit B* comparisons (Series 8a and Series 9). Also, there is a significant difference in mean T_{max} between the two Series 8 data sets.

Table 11.4. Thermal Profile Variability: T_{max}

Series	Pit	Cement Source	C_I (%)	n	n_o	Mean (°C)	*Stdev* (°C)	*COV* (%)	*P*-Value	Normality Fit
1	*A*	*TH*	5	30	0	25.9	0.4	1.6	0.13	Good
2	*A*	*GV*	5	30	0	25.7	0.3	1.3	0.14	Good
18	*A*	*TH,GGBFS*	4	30	0	22.9	0.2	0.8	0.41	Good
8a	*B*	*TH*	5	30	0	27.2	0.5	1.9	0.37	Good
8b	*B*	*TH*	5	30	0	25.8	0.7	2.5	0.68	Excellent
9	*B*	*GV*	5	30	0	25.9	0.9	3.5	0.03	Poor
13	*C*	*TH*	4	30	0	26.6	0.4	1.6	0.87	Excellent
14	*C*	*GV*	4	30	0	25.7	0.3	1.1	0.72	Excellent

Table 11.5. Statistical t-test Results for Cement Source: T_{max}

Term 1	μ_1 (°C)	Term 2	μ_2 (°C)	H_a	df	t_{crit}	t_{stat}	H_0 Conclusion
Pit A-TH (1)	25.9	*Pit A-GV* (2)	25.7	$\mu_1 \neq \mu_2$	55	2.00	1.66	Accept
Pit B-TH (8a)	27.2	*Pit B-TH* (8b)	25.8	$\mu_1 \neq \mu_2$	55	2.00	9.50	Reject
Pit B-TH (8a)	27.2	*Pit B-GV* (9)	25.9	$\mu_1 \neq \mu_2$	46	2.01	7.10	Reject
Pit B-TH (8b)	25.8	*Pit B-GV* (9)	25.9	$\mu_1 \neq \mu_2$	53	2.01	-0.46	Accept
Pit C-TH (13)	26.6	*Pit C-GV* (14)	25.7	$\mu_1 \neq \mu_2$	52	2.01	9.47	Reject

Notes: Series numbers are noted in parentheses; $\alpha = 0.05$; H_0 was $\mu_1 = \mu_2$ for all t-tests; and unequal variances was assumed for all t-tests.

Tables 11.6 and 11.7 contain results for the recorded change in temperature (ΔT) at the time T_{max} occurs. The mean ΔT range for portland cement mixtures (i.e. *TH* and *GV*) was 4.2 to 5.5 °C and the *COV*'s ranged from 7.0 to 13.3 percent. The mean ΔT for the GGBFS mixture was noticeably lower (2.0 °C) with a *COV* of 8.5 percent. *Pit B* was noticeably more variable than *Pit A* and *Pit C* with respect to ΔT. All soil and cement combinations have a good to excellent normality fit. Table 11.7 shows t-test results which indicate a significant difference in mean ΔT between cement sources for all comparisons except for one *Pit B* comparison (Series 8b and 9).

Table 11.6. Thermal Profile Variability: ΔT

Series	Pit	Cement Source	C_I (%)	n	n_o	Mean (°C)	*Stdev* (°C)	*COV* (%)	*P*-Value	Normality Fit
1	*A*	*TH*	5	30	0	4.4	0.3	7.0	0.41	Good
2	*A*	*GV*	5	30	0	4.2	0.3	7.3	0.87	Excellent
18	*A*	*TH,GGBFS*	4	30	0	2.0	0.2	8.5	0.75	Excellent
8a	*B*	*TH*	5	30	0	5.5	0.4	6.7	0.62	Excellent
8b	*B*	*TH*	5	30	0	4.8	0.6	13.3	0.62	Excellent
9	*B*	*GV*	5	30	0	5.0	0.5	10.1	0.42	Good
13	*C*	*TH*	4	30	0	4.8	0.4	7.2	0.77	Excellent
14	*C*	*GV*	4	30	0	4.5	0.3	7.0	0.42	Good

Table 11.7. Statistical t-test Results for Cement Source: ΔT

Term 1	μ_1 (°C)	Term 2	μ_2 (°C)	H_a	*df*	t_{crit}	t_{stat}	H_0 Conclusion
Pit A-TH (1)	4.4	*Pit A-GV* (2)	4.2	$\mu_1 \neq \mu_2$	58	2.00	2.46	Reject
Pit B-TH (8a)	5.5	*Pit B-TH* (8b)	4.8	$\mu_1 \neq \mu_2$	47	2.01	5.75	Reject
Pit B-TH (8a)	5.5	*Pit B-GV* (9)	5.0	$\mu_1 \neq \mu_2$	53	2.01	5.06	Reject
Pit B-TH (8b)	4.8	*Pit B-GV* (9)	5.0	$\mu_1 \neq \mu_2$	55	2.00	-1.32	Accept
Pit C-TH (13)	4.8	*Pit C-GV* (14)	4.5	$\mu_1 \neq \mu_2$	57	2.00	3.93	Reject

Notes: Series numbers are noted in parentheses; $\alpha = 0.05$; H_0 was $\mu_1 = \mu_2$ for all t-tests; and unequal variances was assumed for all t-tests.

Tables 11.8 and 11.9 contain results for the recorded time (t_{max}) where T_{max} occurs. The t_{max} was noticeably more variable than other thermal profile variables. The mean t_{max} for portland cement mixtures ranged from 3.0 to 7.1 hours with *COV*'s ranging from 10.2 to 23.4 percent. The t_{max} for the GGBFS mixture was more variable than portland cement mixtures with a mean value of 3.4 hours and a *COV* of 30.4 percent. All soil and cement combinations have an acceptable to excellent normality fit. Results from t-tests (Table 11.9) show a significant difference in t_{max} between cement sources for all comparisons with exception of one *Pit B* comparison (Series 8b and 9).

Table 11.8. Thermal Profile Variability: t_{max}

Series	Pit	Cement Source	C_I (%)	*n*	n_o	Mean (hr)	*Stdev* (hr)	*COV* (%)	*P*-Value	Normality Fit
1	*A*	*TH*	5	30	0	4.9	0.5	10.2	0.65	Excellent
2	*A*	*GV*	5	30	0	7.1	1.3	18.8	0.16	Good
18	*A*	*TH,GGBFS*	4	30	0	3.4	1.1	30.4	0.07	Acceptable
8a	*B*	*TH*	5	30	0	3.4	0.5	14.3	0.20	Good
8b	*B*	*TH*	5	30	0	4.0	0.9	23.4	0.10	Good
9	*B*	*GV*	5	30	0	4.4	1.0	22.8	0.05	Acceptable
13	*C*	*TH*	4	30	0	3.0	0.5	15.3	0.16	Good
14	*C*	*GV*	4	30	0	3.3	0.4	11.2	0.92	Excellent

Table 11.9. Statistical t-test Results for Cement Source: t_{max}

Term 1	μ_1 (hr)	Term 2	μ_2 (hr)	H_a	*df*	t_{crit}	t_{stat}	H_0 Conclusion
Pit A-TH (1)	4.9	*Pit A-GV* (2)	7.1	$\mu_1 \neq \mu_2$	37	2.03	-8.30	Reject
Pit B-TH (8a)	3.4	*Pit B-TH* (8b)	4.0	$\mu_1 \neq \mu_2$	44	2.02	-2.90	Reject
Pit B-TH (8a)	3.4	*Pit B-GV* (9)	4.4	$\mu_1 \neq \mu_2$	42	2.02	-4.80	Reject
Pit B-TH (8b)	4.0	*Pit B-GV* (9)	4.4	$\mu_1 \neq \mu_2$	58	2.00	-1.68	Accept
Pit C-TH (13)	3.0	*Pit C-GV* (14)	3.3	$\mu_1 \neq \mu_2$	56	2.00	-3.02	Reject

Notes: Series numbers are noted in parentheses; $\alpha = 0.05$; H_0 was $\mu_1 = \mu_2$ for all t-tests; and unequal variances was assumed for all t-tests.

Tables 11.10 and 11.11 show results for the recorded area beneath the thermal profile curve (A_s). The mean values of A_s for portland cement mixtures range from 585 to 616 °C-hr, and *COV*'s range from 0.9 to 2.8 percent. The mean value of A_s for the GGBFS mixture was lower than portland cement mixtures at 537 °C-hr with a *COV* of 0.6 percent. All soil and cement combinations have a good to excellent normality fit. Table 11.11 shows t-test results indicating no significant difference in mean A_s between cement sources for *Pit A* or one of the *Pit B* comparisons (Series 8b and Series 9). Although, t-test results indicate a significant difference in mean A_s between cement sources for the other *Pit B* comparisons and *Pit C* comparison.

Table 11.10. Thermal Profile Variability: A_s

Series	Pit	Cement Source	C_I (%)	n	n_o	Mean (°C-hr)	*Stdev* (°C-hr)	*COV* (%)	*P*-Value	Normality Fit
1	*A*	*TH*	5	30	0	602	9.1	1.5	0.77	Excellent
2	*A*	*GV*	5	30	0	601	7.8	1.3	0.33	Good
18	*A*	*TH,GGBFS*	4	30	0	537	3.5	0.6	0.87	Excellent
8a	*B*	*TH*	5	30	0	616	10.1	1.6	0.68	Excellent
8b	*B*	*TH*	5	30	0	591	11.7	2.0	0.75	Excellent
9	*B*	*GV*	5	30	0	594	16.6	2.8	0.15	Good
13	*C*	*TH*	4	30	0	602	8.6	1.4	0.33	Good
14	*C*	*GV*	4	30	0	585	5.4	0.9	0.42	Good

Table 11.11. Statistical *t*-test Results for Cement Source: A_s

Term 1	μ_1 (°C-hr)	Term 2	μ_2 (°C-hr)	H_a	df	t_{crit}	t_{stat}	H_0 Conclusion
Pit A-TH (1)	602	*Pit A-GV* (2)	601	$\mu_1 \neq \mu_2$	57	2.00	0.50	Accept
Pit B-TH (8a)	616	*Pit B-TH* (8b)	591	$\mu_1 \neq \mu_2$	57	2.00	8.61	Reject
Pit B-TH (8a)	616	*Pit B-GV* (9)	594	$\mu_1 \neq \mu_2$	48	2.01	6.01	Reject
Pit B-TH (8b)	591	*Pit B-GV* (9)	594	$\mu_1 \neq \mu_2$	52	2.01	-0.75	Accept
Pit C-TH (13)	602	*Pit C-GV* (14)	585	$\mu_1 \neq \mu_2$	49	2.01	8.96	Reject

Notes: Series numbers are noted in parentheses; $\alpha = 0.05$; H_0 was $\mu_1 = \mu_2$ for all t-tests; and unequal variances was assumed for all t-tests.

Tables 11.12 and 11.13 provide results for the recorded area difference between the measured thermal profile and the reference specimen ($A_{\Delta T}$). The mean values of $A_{\Delta T}$ for portland cement mixtures ranged from 66.6 to 88.0, and *COV*'s range from 9.4 to 13.2 percent. The mean value of $A_{\Delta T}$ for the GGBFS mixture was lower at 31.4 °C-hr, and the *COV* was 9.9 percent. All soil and cement combinations have an acceptable to excellent normality fit. Results from t-tests (Table 11.12) show a significant difference in mean $A_{\Delta T}$ between the two *Pit B* data sets treated with *TH* cement (Series 8a and 8b), but all other comparisons were found to not be significantly different with respect to mean $A_{\Delta T}$.

Table 11.12. Thermal Profile Variability: $A_{\Delta T}$

Series	Pit	Cement Source	C_I (%)	n	n_o	Mean (°C-hr)	*Stdev* (°C-hr)	*COV* (%)	*P*-Value	Normality Fit
1	*A*	*TH*	5	30	0	81.3	7.7	9.4	0.85	Excellent
2	*A*	*GV*	5	30	0	81.8	6.9	8.5	0.39	Good
18	*A*	*TH,GGBFS*	4	30	0	31.4	3.1	9.9	0.85	Excellent
8a	*B*	*TH*	5	30	0	88.0	9.0	10.3	0.80	Excellent
8b	*B*	*TH*	5	30	0	79.6	10.5	13.2	0.65	Excellent
9	*B*	*GV*	5	30	0	84.0	8.3	9.9	0.82	Excellent
13	*C*	*TH*	4	30	0	69.3	8.3	11.9	0.07	Acceptable
14	*C*	*GV*	4	30	0	66.6	6.9	10.3	0.39	Good

Table 11.13. Statistical t-test Results for Cement Source: $A_{\Delta T}$

Term 1	μ_1 (°C-hr)	Term 2	μ_2 (°C-hr)	H_a	df	t_{crit}	t_{stat}	H_0 Conclusion
Pit A-TH (1)	81.2	*Pit A-GV* (2)	81.8	$\mu_1 \neq \mu_2$	57	2.00	-0.30	Accept
Pit B-TH (8a)	88.0	*Pit B-TH* (8b)	79.6	$\mu_1 \neq \mu_2$	56	2.00	3.11	Reject
Pit B-TH (8a)	88.0	*Pit B-GV* (9)	84.0	$\mu_1 \neq \mu_2$	58	2.00	1.77	Accept
Pit B-TH (8b)	79.6	*Pit B-GV* (9)	84.0	$\mu_1 \neq \mu_2$	55	2.00	-1.82	Accept
Pit C-TH (13)	69.3	*Pit C-GV* (14)	66.6	$\mu_1 \neq \mu_2$	56	2.00	1.42	Accept

Notes: Series numbers are noted in parentheses; $\alpha = 0.05$; H_0 was $\mu_1 = \mu_2$ for all t-tests; and unequal variances was assumed for all t-tests.

11.4.3 Variability Comparison

Figure 11.4 presents equality plots comparing the *COV*'s of thermal measurement variables to those of compressive strength.

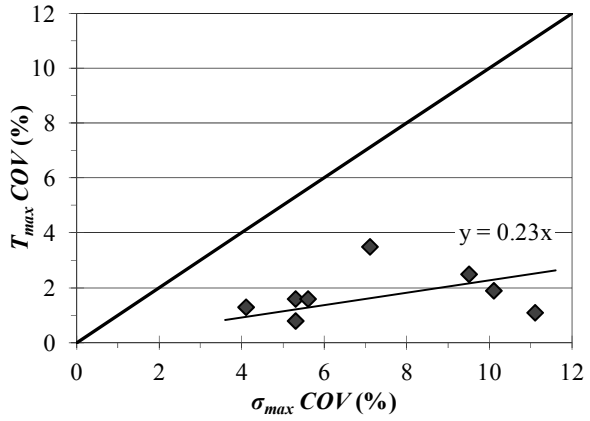

(a) T_{max} *COV* Comparison

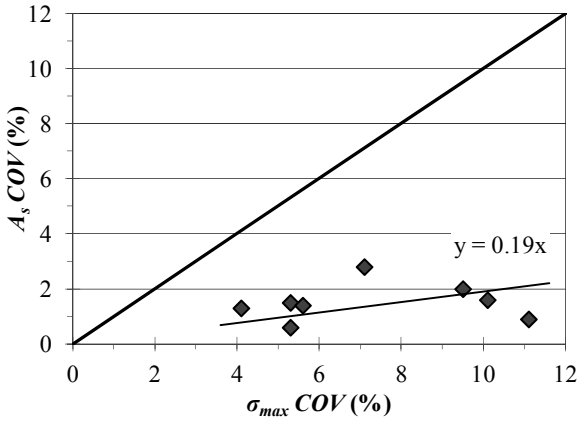

(b) A_s *COV* Comparison

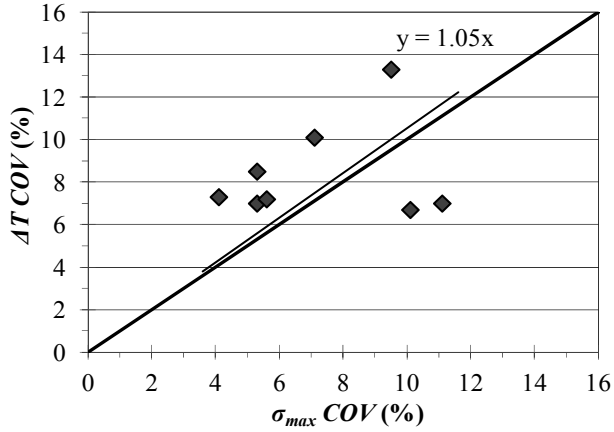

(c) ΔT *COV* Comparison

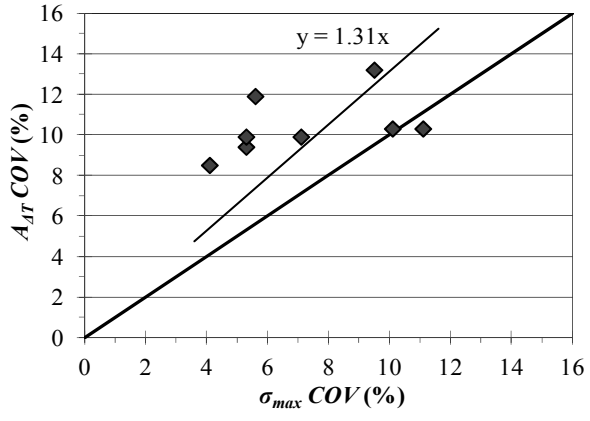

(d) $A_{\Delta T}$ *COV* Comparison

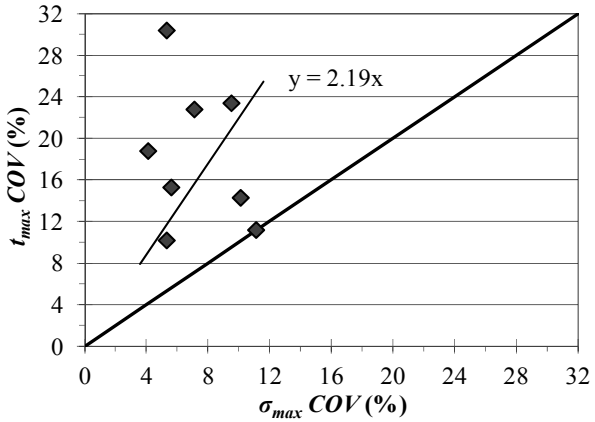

(e) t_{max} *COV* Comparison

Figure 11.4. Variability Comparisons of Measured Variables

Both T_{max} and A_s values demonstrate lower variability when compared to compressive strength. T_{max} and A_s (Figure 11.4a and 11.4b) have slopes of 0.23 and 0.19 which means that, generally speaking, variability was on the order of 20% that of compressive strength. ΔT (Figure 11.4c) had approximately the same amount of variability as compressive strength. $A_{\Delta T}$ and t_{max} both appear to have more variability than compressive strength with slopes of 2.19 and 1.31, respectively. Based on the variability analysis in this section, the thermal profile variables T_{max}, A_s, and ΔT were selected for further analysis in the following sections in this chapter.

11.5 Effects of Equipment Configuration

An experiment was conducted to evaluate: 1) the effects of using different insulation for the thermal measurement device; and 2) the effects of using different sensor types. The thermal measurement device constructed with *XLPE* foam and different sensors is identified as Block C or *XLPE* device. Dimensions and fabrication are the same as discussed in Section 5.3.5. Each slot within Block C contained a thermocouple (*TC*) and a thermistor (*TM*) sensor without an attached metal washer. Thirty tests were conducted on *Pit C* treated with *TH* cement (Series 27). Series 27 testing was compared to Series 13 which tested the same mixture with the *EPS* devices (i.e. Blocks A and B). Table 11.14 contains a summary of the results from Series 27 and Series 13.

Table 11.14. Variability Comparison of *XLPE* device and *EPS* devices

Variable	Series[1]	Sensor Type	C_I (%)	n	n_o	Mean	*Stdev*	*COV* (%)	*P*-Value	Normality Fit
σ_{max}	27	*TC*	4	28	2	3215	153	4.8	0.14	Good
σ_{max}	27	*TM*	4	28	2	3215	153	4.8	0.14	Good
σ_{max}	13	*TC* with washer	4	30	0	3181	179	5.6	0.42	Good
T_{max}	27	*TC*	4	30	0	24.8	0.5	1.8	0.77	Excellent
T_{max}	27	*TM*	4	30	0	24.4	0.4	1.7	0.82	Excellent
T_{max}	13	*TC* with washer	4	30	0	26.6	0.4	1.6	0.87	Excellent
ΔT	27	*TC*	4	29	1	4.1	0.3	7.8	0.41	Good
ΔT	27	*TM*	4	29	1	4.0	0.3	6.4	0.92	Excellent
ΔT	13	*TC* with washer	4	30	0	4.8	0.4	7.2	0.77	Excellent
t_{max}	27	*TC*	4	30	0	3.4	0.8	22.6	0.17	Good
t_{max}	27	*TM*	4	29	1	3.1	0.4	12.8	0.54	Excellent
t_{max}	13	*TC* with washer	4	30	0	3.0	0.5	15.3	0.16	Good
A_s	27	*TC*	4	30	0	571	9.3	1.6	0.75	Excellent
A_s	27	*TM*	4	30	0	563	9.0	1.6	0.84	Excellent
A_s	13	*TC* with washer	4	30	0	602	8.6	1.4	0.33	Good
$A_{\Delta T}$	27	*TC*	4	30	0	62.7	6.2	9.9	0.82	Excellent
$A_{\Delta T}$	27	*TM*	4	30	0	60.4	6.6	10.9	0.17	Good
$A_{\Delta T}$	13	*TC* with washer	4	30	0	69.3	8.3	11.9	0.07	Acceptable

Notes: All test specimens are Pit C treated with TH cement source; and results reflect values after outlier removal.

1: Series 27 was tested using XLPE device (i.e. Block C) which has an $R_{SI} \approx 0.564$, and Series 13 was tested using EPS devices (i.e. Blocks A and B) which have an $R_{SI} = 0.775$.

The variability and data distribution of the measured results was about the same between both types of devices, but the *XLPE* device (Block C) produced slightly different results when compared to the *EPS* devices (Blocks A and B). The *XLPE* device measured a lower T_{max} (≈ 2 °C less), a lower ΔT (≈ 0.7 °C less), a lower A_s (≈ 35 °C-hr less), a lower $A_{\Delta T}$ (≈ 6 °C-hr less), and slightly higher t_{max} (≈ 0.3 hour higher) when compared to *EPS* devices. These differences in measured thermal profiles are likely due to the decreased amount of insulation provided by the *XLPE* block. In general, thermocouple (*TC*) and thermistor (*TM*) sensors have the same amount of variability, but *TM* sensors tended to record slightly lower temperatures than *TC* sensors. Table 11.15 contains results from *t*-tests performed to evaluate if there is a significant difference between *TC* and *TM* sensors. Table 11.15 shows there are significant differences in mean values of T_{max} and A_s between thermocouple (*TC*) and thermistor (*TM*) sensors.

Table 11.15. Statistical *t*-test Results for *XLPE* device Analysis (Series 27)

Term 1	μ_1	Term 2	μ_2	H_a	*df*	t_{crit}	t_{stat}	H_0 Conclusion
T_{max} (*TC*)	24.8	T_{max} (*TM*)	24.4	$\mu_1 \neq \mu_2$	57	2.00	3.81	Reject
ΔT (*TC*)	4.1	ΔT (*TM*)	4.0	$\mu_1 \neq \mu_2$	53	2.01	1.50	Accept
t_{max} (*TC*)	3.4	t_{max} (*TM*)	3.1	$\mu_1 \neq \mu_2$	50	2.01	1.45	Accept
A_s (*TC*)	571	A_s (*TM*)	563	$\mu_1 \neq \mu_2$	58	2.00	3.62	Reject
$A_{\Delta T}$ (*TC*)	62.7	$A_{\Delta T}$ (*TM*)	60.4	$\mu_1 \neq \mu_2$	58	2.00	1.39	Accept

Notes: Sensor type is noted in parentheses; $\alpha = 0.05$; H_0 was $\mu_1 = \mu_2$ for all t-tests; and unequal variances was assumed for all t-tests.

11.6 Effect of Initial Material Temperature on Thermal Profiles

Series 5, 6, 7, 19, 20, and 21 investigated initial material temperature (T_i) effects on measured thermal profiles at varying cement contents. Before testing, materials were pre-conditioned as described in Section 5.4.1, and the thermal measurement block was kept at a constant 21°C (T_{BL}) during testing. T_i effects were evaluated by plotting T_i on the x-axis, plotting T_{max}, ΔT, or A_s on the y-axis, and fitting a linear trendline. For brevity, Table 11.16 shows all of the linear trendline equations and R^2 values for the plotted data. Overall, R^2 values for trendline equations ranged from 0.78 to 0.99. For *Pit A*, the slope of the trendline equation for T_{max} correlation to T_i was approximately 0.40; the slope for ΔT correlation was approximately 0.13; and the slope for A_s correlation was approximately 9.8 to 12.0.

As shown in Table 11.16, the initial material temperature (T_i) has a considerable effect on T_{max}, ΔT, and A_s values. Almost all trendlines have high R^2 values. Upon closer examination of the measured thermal profiles, it was clear that not only is T_i having a major effect on the thermal measurement results but also the initial temperature of the devices (T_{BL}) is having a large effect on the results. Both the cold T_i (≈10 °C) and hot T_i (≈32 °C) tests were affected by the T_{BL} temperature, which was 21 °C in every case. For the cold T_i tests, the T_{BL} contributed to hydration heat from the specimens, thus masked some of the heat generation. For the hot T_i tests, the T_{BL} cooled off the hydrating specimens, thus reducing the measured temperatures. The high R^2 values noted in Table 11.16, as well as data collected in Sections 11.7 and 11.10, could be misleading because the contributions of T_{BL} to the cold and hot tests were consistent for every test. To gain a better understanding of the effects of T_{BL} on the thermal profiles, an experiment was conducted which varied the T_{BL} during thermal measurement testing. Data was taken from Series 7 and 49. Figure 11.5 shows the effects of T_{BL} for specimens with $T_i \approx 32$ °C.

Table 11.16 Summary of Effects of Initial Material Temperature (T_i)

Soil	Cement	C_I (%)	n	Trendline Equation	R^2
Pit A	*TH*	4	27	$T_{max} = 0.40T_i + 17.74$	0.96
Pit A	*TH*	5	27	$T_{max} = 0.39T_i + 18.55$	0.96
Pit A	*TH*	6	27	$T_{max} = 0.40T_i + 19.24$	0.92
Pit A	*TH,GGBFS*	3	15	$T_{max} = 0.42T_i + 14.34$	0.84
Pit A	*TH,GGBFS*	4	15	$T_{max} = 0.39T_i + 15.57$	0.83
Pit A	*TH,GGBFS*	5	15	$T_{max} = 0.43T_i + 15.02$	0.86
Pit A	*TH*	4	27	$\Delta T = 0.15T_i + 0.19$	0.78
Pit A	*TH*	5	27	$\Delta T = 0.16T_i + 0.66$	0.87
Pit A	*TH*	6	27	$\Delta T = 0.13T_i + 1.65$	0.84
Pit A	*TH,GGBFS*	3	15	$\Delta T = 0.12T_i$ -1.49	0.97
Pit A	*TH,GGBFS*	4	15	$\Delta T = 0.11T_i$ - 0.68	0.89
Pit A	*TH,GGBFS*	5	15	$\Delta T = 0.09T_i$ - 0.03	0.78
Pit A	*TH*	4	27	$A_s = 11.89T_i + 321$	0.99
Pit A	*TH*	5	27	$A_s = 12.00T_i + 338$	0.99
Pit A	*TH*	6	27	$A_s = 11.36T_i + 367$	0.97
Pit A	*TH,GGBFS*	3	15	$A_s = 10.70T_i + 287$	0.98
Pit A	*TH,GGBFS*	4	15	$A_s = 10.40T_i + 308$	0.97
Pit A	*TH,GGBFS*	5	15	$A_s = 9.78T_i + 327$	0.99

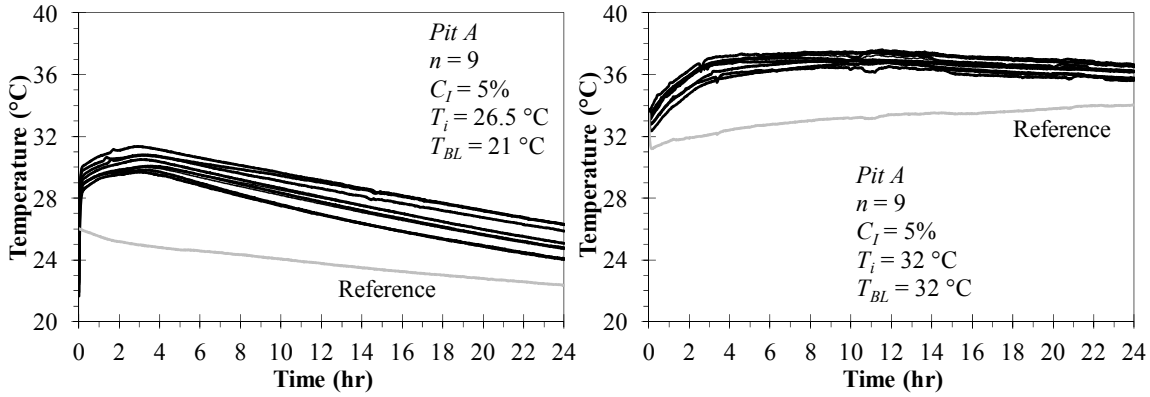

(a) Devices remained at 21 °C (b) Devices remained at 32 °C

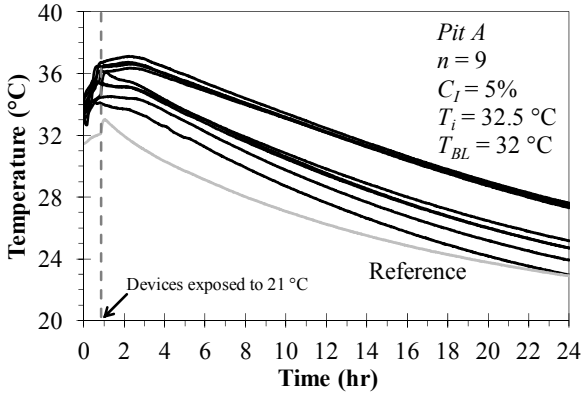

(c) Devices moved from 32 °C to 21 °C after data start

Figure 11.5. Effects of T_{BL} on Thermal Profiles with $T_i \approx 32$ °C

For Figure 11.5a, the initial material temperature (T_i) was approximately 26.5 °C and the initial temperature of the device (T_{BL}) was 21 °C. Thermal profiles in Figure 11.5a have an average T_{max} of about 30 °C. In Figure 11.5b, the T_i was 32 °C and the T_{BL} was also 32 °C. For Figure 11.5b specimens, the devices were exposed to ambient air temperatures of 32 °C for the duration of testing, and the average T_{max} was approximately 36 °C. In Figure 11.5c, the materials and devices were conditioned the same as Figure 11.5b specimens. After all specimens were prepared and inserted into the devices, the devices were removed from the 32 °C ambient air temperatures and exposed to 21 °C air temperatures. For Figure 11.5c, the average T_{max} was still approximately 36 °C, but there was a dramatic change to the thermal profiles after the devices were placed into the 21 °C environment. The implications of the effects of T_i and T_{BL} on the measured thermal profiles are as they relate to quality control are meaningful based on findings in this section. Table 11.16 and Figure 11.5 provide general evidence concerning the effects of T_i and T_{BL}, but additional investigation is needed to understand how to account for temperature effects. Chapters 12 and 13 provide more information in this regard.

11.7 Effect of Cement and Moisture Content on Thermal Profiles

The effects of cement content and the combined effects of cement and moisture content on thermal profiles were evaluated using data from Series 3, 4, 22, and 23. The effect of cement content was evaluated over a range of initial material temperatures (10, 21, and 32 °C) where the initial *EPS* block temperature (T_{BL}) was 21 °C. The combined effects of cement and moisture content were evaluated at 21 °C where the initial block temperature was 21 °C. Figure 11.6 shows the effects of varying C_I and the combined effects of cement content and moisture content on observed values of T_{max}, ΔT, and A_s.

Figure 11.6a shows the influence of cement content (C_I) on T_{max}. The overall increasing trend is consistent (i.e. similar trendline slopes) for all three initial material temperatures, and the trendline R^2 values range from 0.92 to 0.97. These results suggest that T_{max} is directly affected by the cement content and initial material temperature (T_i). Figure 11.6c shows the influence of C_I on ΔT. There is a clear increase in ΔT with increase in C_I for all three T_i with R^2 values ranging from 0.95 to 0.96. Figure 11.6e shows the influence of cement content on A_s. Again, the overall trend for all three T_i was an increase in cement content caused an increase in A_s. Trendline R^2 values for cement content and A_s range from 0.83 to 0.99. Statistical *t*-tests at $\alpha = 0.05$ and assuming unequal variances were performed on each incremental change in C_I to determine significant differences in values of T_{max}, ΔT, and A_s, and *t*-test results are shown in Figure 11.6. *S* denotes a significant change and *NS* denotes no significant change in mean value.

Figures 11.6b, 11.6d, and 11.6f show the combined effects of cement content and moisture content on T_{max}, ΔT, and A_s. These plots show no strong influence from moisture content change and only slight influences from small changes in cement content. Note the range of moisture contents tested only covers ±2% of *OMC*, which is a common acceptable moisture range in most soil-cement specifications. Also note T_{BL} at a constant value of 21˚C is very likely affecting Figure 11.6 results in a manner that limits the usefulness of the data that does not have T_i at 21 ^{o}C.

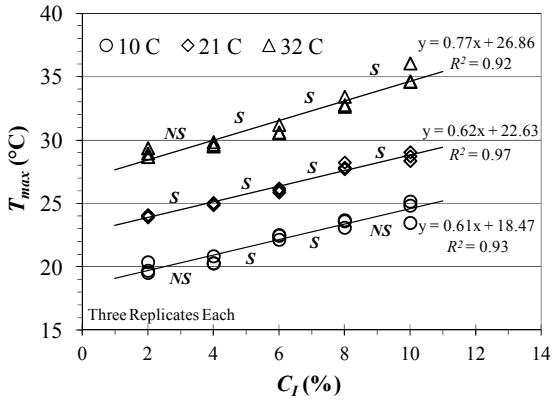

(a) C_I Effects on T_{max}

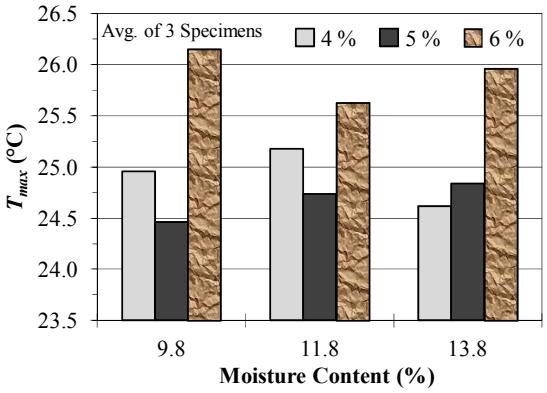

(b) C_I and Moisture Content Effects on T_{max}

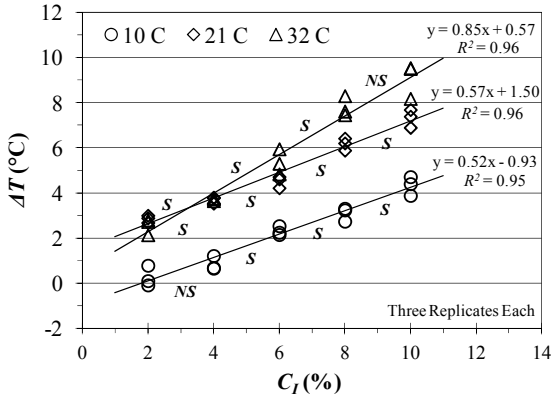

(c) C_I Effects on ΔT

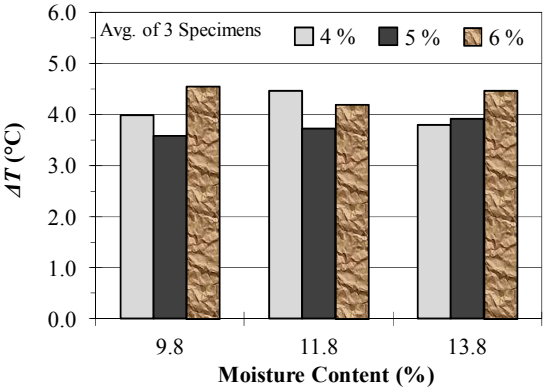

(d) C_I and Moisture Content Effects on ΔT

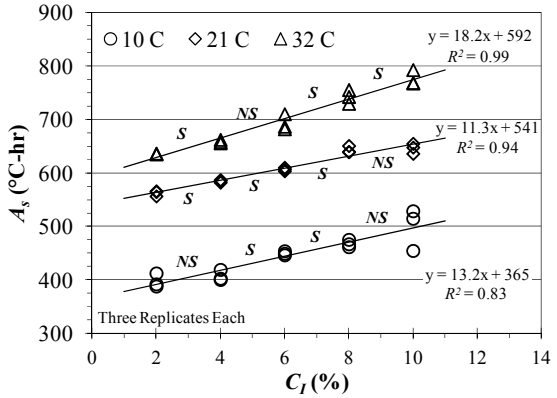

(e) C_I Effects on A_s

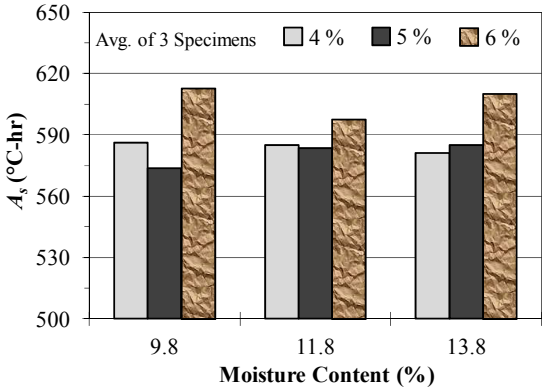

(f) C_I and Moisture Content Effects on A_s

Figure 11.6. Effects of Cement and Moisture Content on Thermal Profiles

11.8 Thermal Profile Correlation to σ_{max} and C_I

Series 5, 10, 15, and 19 examined thermal profile behaviors when C_I was varied by 1 percent from design. This data was also used to determine how thermal measurements relate to σ_{max}.

Figure 11.7 shows the compressive strength gain of *Pits A*, *B*, and *C* treated at design C_I and ± 1% C_I. All specimens had a T_i of approximately 21 °C and were compacted using the *PM-CF* approach. Each column represents an average of 3 replicates. According to *MT-25* results, the design cure time to reach a σ_{max} of 2070 kPa for *Pits A*, *B*, and *C* treated with portland cement (*TH*) was 7 days, and the design cure time for *Pit A* treated with GGBFS blend was 14 days. Note the compressive strengths for specimens compacted using the *PM-CF* approach were noticeably higher than similar specimens compacted using standard proctor compaction effort. For *Pits A*, *B*, and *C* (Figure 11.7a, 11.7b, and 11.7c), there is a noticeable difference in σ_{max} when the C_I is varied by 1% from the design C_I, particularly at the design cure time. This trend also holds true with the GGBFS blend mixture (Figure 11.7d). Also, σ_{max} gain of the GGBFS blend mixture is slow at early ages, but the strength gain between 7 and 14 days is considerable.

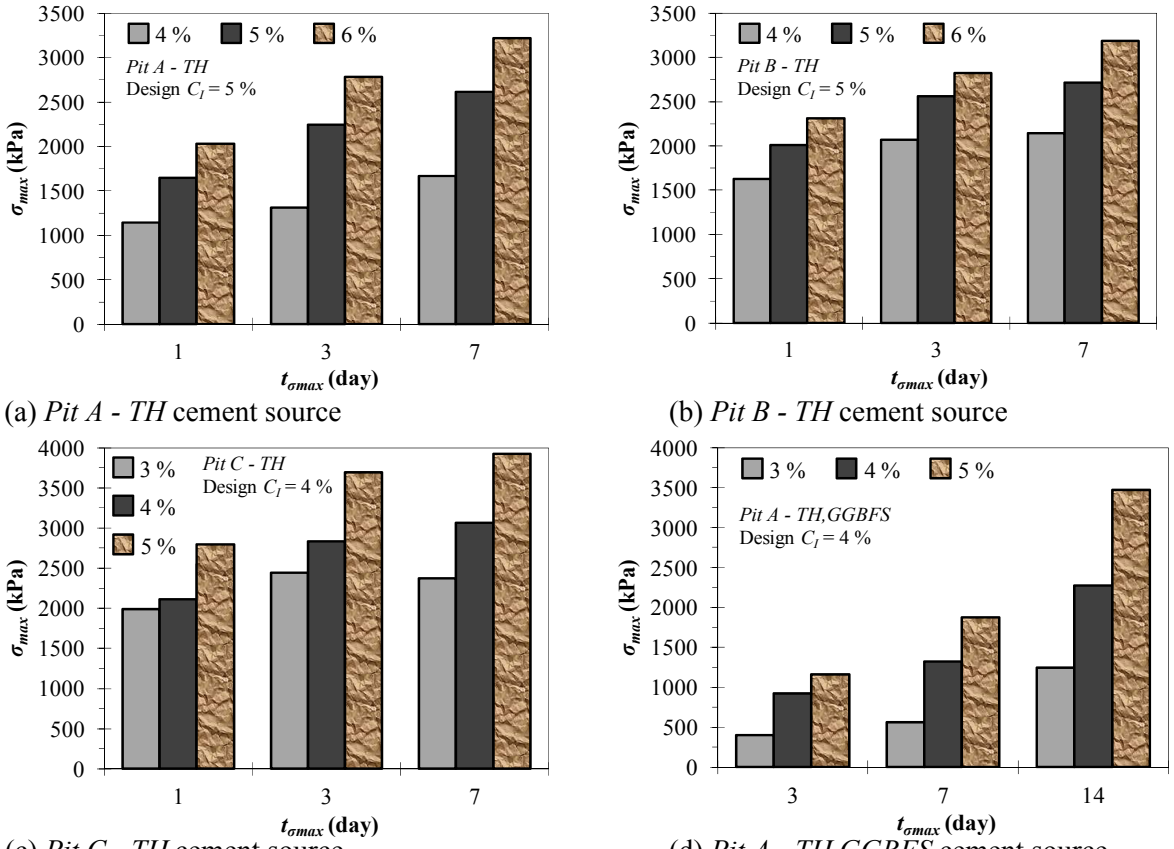

(a) *Pit A - TH* cement source (b) *Pit B - TH* cement source

(c) *Pit C - TH* cement source (d) *Pit A - TH,GGBFS* cement source

Figure 11.7. Compressive Strength Gain of Pit Soils (*PM-CF* Approach)

Statistical t-tests were conducted for T_{max}, ΔT, and A_s to determine if there were significant differences between 1 percent increments of C_I. Tables 11.17 through 11.19 provide t-test results. As shown in Table 11.17 with exception to *Pit C*, a 1% decrease in C_I from the design C_I produced a lower value for T_{max}, and a 1% increase in C_I from the design C_I did not produce a significantly different T_{max} value. For *Pit C*, a 1% incremental change in C_I did not produce a significantly different T_{max}, but a 2% incremental change did produce a

significant change in T_{max}. For ΔT (Table 11.18), a 1% decrease in C_I from the design C_I produced a lower ΔT for pit soil *A*, *B*, and *C* stabilized with portland cement. For *Pits A* and *C*, there was no significant change in ΔT with a 1% increase in C_I from the design C_I, but for *Pit B* there was an increase in ΔT. For *Pit A* stabilized with GGBFS blend, there was no change in ΔT with a 1% decrease in C_I from the design C_I, and there was an increase in ΔT with a 1% increase in C_I from the design C_I. Statistical *t*-test results for A_s were the same as T_{max} results (Table 11.19).

Table 11.17. Statistical *t*-test Results for Varying C_I: T_{max}

Term 1	μ_1 (°C)	Term 2	μ_2 (°C)	*df*	t_{crit}	t_{stat}	H_0 Conclusion
Pit A-TH 4%	25.0	*Pit A-TH* 5%	25.7	15	2.13	-6.72	Reject
Pit A-TH 5%	25.7	*Pit A-TH* 6%	25.9	9	2.26	-0.84	Accept
Pit B-TH 4%	26.3	*Pit B-TH* 5%	26.9	16	2.12	-3.71	Reject
Pit B-TH 5%	26.9	*Pit B-TH* 6%	27.3	11	2.20	-1.35	Accept
Pit C-TH 3%	25.6	*Pit C-TH* 4%	25.9	13	2.16	-1.92	Accept
Pit C-TH 4%	25.9	*Pit C-TH* 5%	26.2	13	2.16	-1.42	Accept
Pit C-TH 3%	25.6	*Pit C-TH* 5%	26.2	16	2.12	-4.62	Reject
Pit A-TH,GGBFS 3%	21.6	*Pit A-TH,GGBFS* 4%	22.5	9	2.26	-3.81	Reject
Pit A-TH,GGBFS 4%	22.5	*Pit A-TH,GGBFS* 5%	22.7	16	2.12	-0.39	Accept

Notes: Data from Series 5, 10, 15, and 19; $\alpha = 0.05$; H_0 was $\mu_1 = \mu_2$ and H_a was $\mu_1 \neq \mu_2$ for all t-tests; and unequal variances was assumed for all t-tests.

Table 11.18. Statistical *t*-test Results for Varying C_I: ΔT

Term 1	μ_1 (°C)	Term 2	μ_2 (°C)	*df*	t_{crit}	t_{stat}	H_0 Conclusion
Pit A-TH 4%	4.21	*Pit A-TH* 5%	4.71	13	2.16	-4.16	Reject
Pit A-TH 5%	4.71	*Pit A-TH* 6%	4.53	9	2.26	0.70	Accept
Pit B-TH 4%	5.14	*Pit B-TH* 5%	5.66	16	2.12	-3.29	Reject
Pit B-TH 5%	5.66	*Pit B-TH* 6%	6.25	12	2.18	-2.48	Reject
Pit C-TH 3%	4.28	*Pit C-TH* 4%	4.71	13	2.16	-2.27	Reject
Pit C-TH 4%	4.71	*Pit C-TH* 5%	5.1	14	2.14	-2.03	Accept
Pit A-TH,GGBFS 3%	1.64	*Pit A-TH,GGBFS* 4%	1.83	16	2.12	-0.88	Accept
Pit A-TH,GGBFS 4%	4.21	*Pit A-TH,GGBFS* 5%	4.71	13	2.16	-4.16	Reject

Notes: Data from Series 5, 10, 15, and 19; $\alpha = 0.05$; H_0 was $\mu_1 = \mu_2$ and H_a was $\mu_1 \neq \mu_2$ for all t-tests; and unequal variances was assumed for all t-tests.

Table 11.20 summarizes thermal profile test results. For all portland cement mixtures, the design C_I produced an average T_{max} that ranged from 25.7 to 26.9 °C, an average ΔT that ranged from 4.7 to 5.7 °C, and an average A_s that ranged from 591 to 613 °C-hr. For the GGBFS blend mixture, the design C_I produced an average T_{max} of 22.5 °C, an average ΔT of 1.6 °C, and an average A_s of 530 °C-hr. When the C_I is varied by plus or minus 1% C_I, the resultant average values for T_{max}, ΔT, and A_s change as shown in Table 11.20. Changes for *Pit A* values loosely follow the cement content effects trend line equations ($T_i \approx 21$°C) developed in Section 11.6, but changes in values for *Pits B*, *C*, and the GGBFS blend are different.

Table 11.19. Statistical *t*-test Results for Varying C_I: A_s

Term 1	μ_1 (°C-hr)	Term 2	μ_2 (°C-hr)	*df*	t_{crit}	t_{stat}	H_0 Conclusion
Pit A-TH 4%	579	*Pit A-TH* 5%	601	14	2.14	-6.55	Reject
Pit A-TH 5%	601	*Pit A-TH* 6%	604	11	2.20	-0.76	Accept
Pit B-TH 4%	601	*Pit B-TH* 5%	613	16	2.12	-3.20	Reject
Pit B-TH 5%	613	*Pit B-TH* 6%	620	12	2.18	-1.27	Accept
Pit C-TH 3%	583	*Pit C-TH* 4%	591	14	2.14	-2.04	Accept
Pit C-TH 4%	591	*Pit C-TH* 5%	594	16	2.12	-0.69	Accept
Pit C-TH 3%	583	*Pit C-TH* 5%	594	15	2.13	-3.11	Reject
Pit A-TH,GGBFS 3%	512	*Pit A-TH,GGBFS* 4%	530	9	2.26	-3.47	Reject
Pit A-TH,GGBFS 4%	530	*Pit A-TH,GGBFS* 5%	532	16	2.12	-0.32	Accept

Notes: Data from Series 5, 10, 15, and 19; $\alpha = 0.05$; H_0 was $\mu_1 = \mu_2$ and H_a was $\mu_1 \neq \mu_2$ for all t-tests; and unequal variances was assumed for all t-tests.

Table 11.20. Summary of Thermal Profile Results

		Design C_I - 1%		Design C_I		Design C_I + 1%	
Series	**Variable**	**Mean**	***COV* (%)**	**Mean**	***COV* (%)**	**Mean**	***COV* (%)**
5	T_{max} (°C)	25.0	1.0	25.7	0.7	25.9	2.7
5	ΔT (°C)	4.2	7.4	4.7	3.7	4.5	16.7
5	A_s (°C-hr)	579	1.4	601	0.9	604	2.3
10	T_{max} (°C)	26.3	1.2	26.9	1.3	27.3	3.0
10	ΔT (°C)	5.1	6.6	5.7	5.9	6.2	9.9
10	A_s (°C-hr)	601	1.1	613	1.3	620	2.4
15	T_{max} (°C)	25.6	1.2	25.9	1.9	26.2	1.1
15	ΔT (°C)	4.3	6.9	4.7	10.3	5.1	6.1
15	A_s (°C-hr)	583	1.0	591	1.6	594	1.4
19	T_{max} (°C)	21.6	0.9	22.5	3.1	22.7	3.4
19	ΔT (°C)	1.0	20.5	1.6	25.8	1.8	26.2
19	A_s (°C-hr)	512	0.5	530	2.7	532	2.3

CHAPTER 12 – PHASE 2 THERMAL PROFILE QUALITY CONTROL TEST RESULTS: SR9 AND SR475

12.1 Overview of SR9 and SR475 Specimen Analysis

Two soil-cement base course projects (MS State Route 9 and MS State Route 475) were selected to further evaluate performing field thermal measurements. Laboratory thermal profile testing was conducted on a total of 126 SR9 and SR475 specimens as illustrated in Table 12.1. All specimens were compacted using the *PM-P* method, targeted the optimum moisture content for the specimen, and were tested for compressive strength at 7 days. Initial material temperature (T_i) values are listed in Table 12.1; initial temperatures for the thermal profile block (T_{BL}) were constant for all specimens at 21˚C.

Table 12.1. SR9 and SR475 Thermal Profile Tests

Series	Soil	Cement	T_i (˚C)	C_I (%)	Description	Replicates
11	*D*	*NC*	≈ 21	6.9	Specimen Density Correction	22
28	*D*	*TH*	≈ 21	6.9	Specimen Density Correction	18
29	*E*	TH_{SR475}	≈ 21	7	Specimen Density Correction	18
30	*E*	*TH*	≈ 21	7	Specimen Density Correction	18
31	*D*	*NC*	≈ 21	6.9	Specimen Time Delay	8
32	*D*	*NC*	≈ 32	6.9	Specimen Time Delay	10
33	*E*	TH_{SR475}	≈ 21	7	Specimen Time Delay	10
34	*E*	TH_{SR475}	≈ 32	7	Specimen Time Delay	10
47	*D*	*NC*	≈ 26	4, 6, 8	C_I Comparison for Field Work	6
48	*E*	TH_{SR475}	≈ 26	4, 6, 8	C_I Comparison for Field Work	6

Table 12.2 is the test matrix of 114 field work specimens and their sampling position. Table 12.5 contains the text matrix of 48 specimens used to investigate mold adjustments. In addition, 14 cement content tests were conducted with more traditional ASTM methods, 24 temperature with time curves were measured with thermocouples, and 18 moisture contents were collected as part of a measurement delay experiment. A total of 344 tests were performed. Raw field data is in Sullivan (2012) Appendix B.

Table 12.2. Field Work Test Matrix

					Position						Specimen	Total	
Series	Soil	Additive	C_I (%)	Location	C	1	2	3	4	5	Type	Tested	$t_{\sigma max}$ (day)
35	*D*	*NC*	7	1	2	2	3	2	2	2	Molded	13	7
36	*D*	*NC*	7	1	-	-	-	6	-	-	Core	6	7
37	*D*	*NC*	7	2	2	2	2	3	2	2	Molded	13	7
38	*D*	*NC*	7	2	-	-	-	6	-	-	Core	6	7
39	*D*	*NC*	7	3	2	2	2	3	2	2	Molded	13	7
40	*D*	*NC*	7	3	-	-	-	6	-	-	Core	6	7
41	*E*	TH_{SR475}	7	1	2	2	2	3	2	2	Molded	13	7
42	*E*	TH_{SR475}	7	1	-	-	-	6	-	-	Core	6	7
43	*E*	TH_{SR475}	7	2	2	2	2	3	2	2	Molded	13	7
44	*E*	TH_{SR475}	7	2	-	-	-	6	-	-	Core	6	7
45	*E*	TH_{SR475}	7	3	2	2	2	3	2	2	Molded	13	7
46	*E*	TH_{SR475}	7	3	-	-	-	6	-	-	Core	6	7

Table 12.3. Mold Adjustments Test Matrix

Soil	Additive	Temperature	Test Days	Cured in Mold
D	NC	Warm	1 and 7	Yes
D	NC	Room	1 and 7	Yes
D	NC	Cold	1 and 7	Yes
D	NC	Warm	1 and 7	No
D	NC	Room	1 and 7	No
D	NC	Cold	1 and 7	No
E	TH_{SR475}	Warm	1 and 7	Yes
E	TH_{SR475}	Room	1 and 7	Yes
E	TH_{SR475}	Cold	1 and 7	Yes
E	TH_{SR475}	Warm	1 and 7	No
E	TH_{SR475}	Room	1 and 7	No
E	TH_{SR475}	Cold	1 and 7	No

This chapter provides data that can be used for many purposes. One key purpose was to further refine understanding of using thermal profile techniques during field quality control operations. In addition, data was collected that can be useful for traffic opening, understanding in-situ temperature profiles, and for adjusting properties such as compressive strength for density, preparation time delay, and curing within or out of molds.

Unless specifically stated otherwise, compressive strength data presented in this chapter was adjusted for density according to the protocols in Section 12.3 (Eq 12.1 in particular), and also adjusted for specimen size according to ASTM D1633 (i.e. h/d = 2.00 measured strengths were multiplied by 1.10 to adjust to equivalent h/d = 1.15 strengths). This was performed since target σ_{max} values are currently defined by MDOT with h/d = 1.15 specimens. The term $\sigma_{max\ adj}$ refers to specimens that have had their measured compressive strength (σ_{max}) adjusted for density, and in the case of the data in this chapter, these values have also been adjusted for specimen size unless specifically stated otherwise.

12.2 Relevant SR9 and SR475 Construction Properties

Tables 12.4 and 12.5 detail SR9 and SR475 sampling and construction timing, and additional information is provided in Section 3.6. SR9 encompassed a large amount of treated material (68,000 m^3) and was constructed in a paving train fashion. Typically, 10 to 12 truckloads of cement were mixed and compacted per day. Cement was mixed into the soil within an hour of being spread, and mixing was performed in two passes. Sheeps-foot and vibratory compaction was completed within 1.5 hours after the first mixing pass. Shaping and finishing was performed in two phases (milling and grading) and final compaction was completed within 2 hours of the end of vibratory compaction.

SR475 had a smaller amount of treated material (12,200 m^3) and was constructed using less equipment. Typically, 3 to 4 truckloads of cement were mixed and compacted per day. Unlike SR9, all truckloads of cement were spread onto the roadway at the beginning of the work day. In some cases the cement was mixed within an hour of being spread, but in other cases several hours passed before the cement was mixed. Mixing was performed with 2 or 3 passes. Sheeps-foot and vibratory compaction was typically completed within 1.5 hours of the first mixing pass. Shaping and finishing was performed with a motor grader, and final compaction was completed within an hour of end vibratory compaction.

Table 12.4. Summary of Field Work Sampling

Project	Location	Station No.	Lane	Date
SR9	1	122 + 00	North bound	04/20/2012
	2	145 + 37	North bound	04/20/2012
	3	171 + 01	North bound	04/23/2012
SR475	1	98 + 21	North bound	06/19/2012
	2	93 + 12	South bound	06/19/2012
	3	24 + 00	Southeast exit ramp	06/21/2012

Table 12.5. Summary of Construction Timing for Field Work Projects

Project	T_i (˚C)	t_c	t_m	N_p	T_{vib}	t_{comp}
SR9-1	22.0	8:50 AM	9:45 AM	2	11:00 AM	12:30 PM
SR9-2	26.3	1:25 PM	2:20 PM	2	3:50 PM	5:00 PM
SR9-3	11.0	7:20 AM	8:14 AM	2	9:35 AM	11:31 AM
SR475-1	24.0	7:25 AM	8:18 AM	3	9:40 AM	10:54 AM
SR475-2	32.1	7:25 AM	12:29 PM	2	1:42 PM	2:15 PM
SR475-3	26.3	6:57 AM	7:47 AM	2	9:20 AM	10:10 AM

Notes: t_c is the time of start cement spread; t_m is the time of first mixing pass; N_p is the total number of mixing passes for each sample position: t_{vib} is the time of end vibratory compaction; and t_{comp} is the time of end compaction with rubber-tire roller.

12.3 Density Correction

In the field, specimens compacted with the *PM-P* approach did not always achieve 98 to 101 percent of the target maximum dry density (γ_d) due to the need for simplicity. Therefore, laboratory specimens were made to correlate percentage of target γ_d to σ_{max} and thermal profile measurements. Data for this analysis is contained in Series 11, 28, 29, and 30 which consist of *Pits D* and *E* treated with the corresponding field cement (*NC* or TH_{SR475}) and *TH* cement. Overall, specimen density appeared to have more of an effect on the compressive strength (7 day cure) than the thermal profile measurements.

Figure 12.1 shows the effect of density on compressive strength (σ_{max}) for each combination of soil and cement. The measured σ_{max} was normalized so that σ_{max} of 1.0 corresponds to 100 percent of target γ_d. The σ_{max} at 100 percent of target γ_d was determined by plotting the measured σ_{max} (y-axis) versus the percentage of γ_d (x-axis) for each data series (not shown for brevity), and linear regression equations (R^2 ranged from 0.89 to 0.96) were used to calculate the predicted σ_{max} at 100 percent of target γ_d. Figure 12.1 shows a strong correlation (R^2 from 0.89 to 0.96) between the percentage of target γ_d and the normalized σ_{max} for all combinations of soil and cement source. Trendline slopes ranged from 0.048 to 0.059 for all four mixtures, and trendline slopes were very similar when *Pits D* and *E* were treated with the same cement source (i.e. *TH* cement).

Figure 12.2 combines the data from Figure 12.1 to generalize the overall trend between percentage of γ_d and normalized σ_{max}. This allows for an overall correction for density which could be applied to any combination of soil type or cement source. Figure 12.2a combines the data from Figures 12.1a and 12.1c which includes *Pit D* treated with *NC* and *TH* cement sources. Figure 12.2b combines the data from Figures 12.1b and 12.1d which includes *Pit E* treated with TH_{SR475} and *TH* cement sources. Figure 12.2c combines Figures 12.2a and 12.2b to include all data points. Also shown in Figure 12.2c are the 95%

confidence interval (dotted line) and 95% prediction interval (dashed line). The confidence interval (*CI*) indicates, with $\alpha = 0.05$, the estimated mean value will fall between the dotted lines, and the prediction interval (*PRI*) indicates, with $\alpha = 0.05$, any individual value will fall between the dashed lines. Figure 12.2d is an equality plot comparing the predicted normalized σ_{max} using the overall trendline (Figure 12.2c) and each individual trendline (Figures 12.1a, 12.1b, 12.1c, and 12.1d). All four trendlines fall close to the equality line which indicates that the overall average trendline equation closely depicts the strength-density relationship for all four mixtures tested. Until additional information becomes available, the Figure 12.2c approach appears to be reasonable for density adjustment. Equation 12.1 is the compressive strength adjustment used for field prepared specimens in this report.

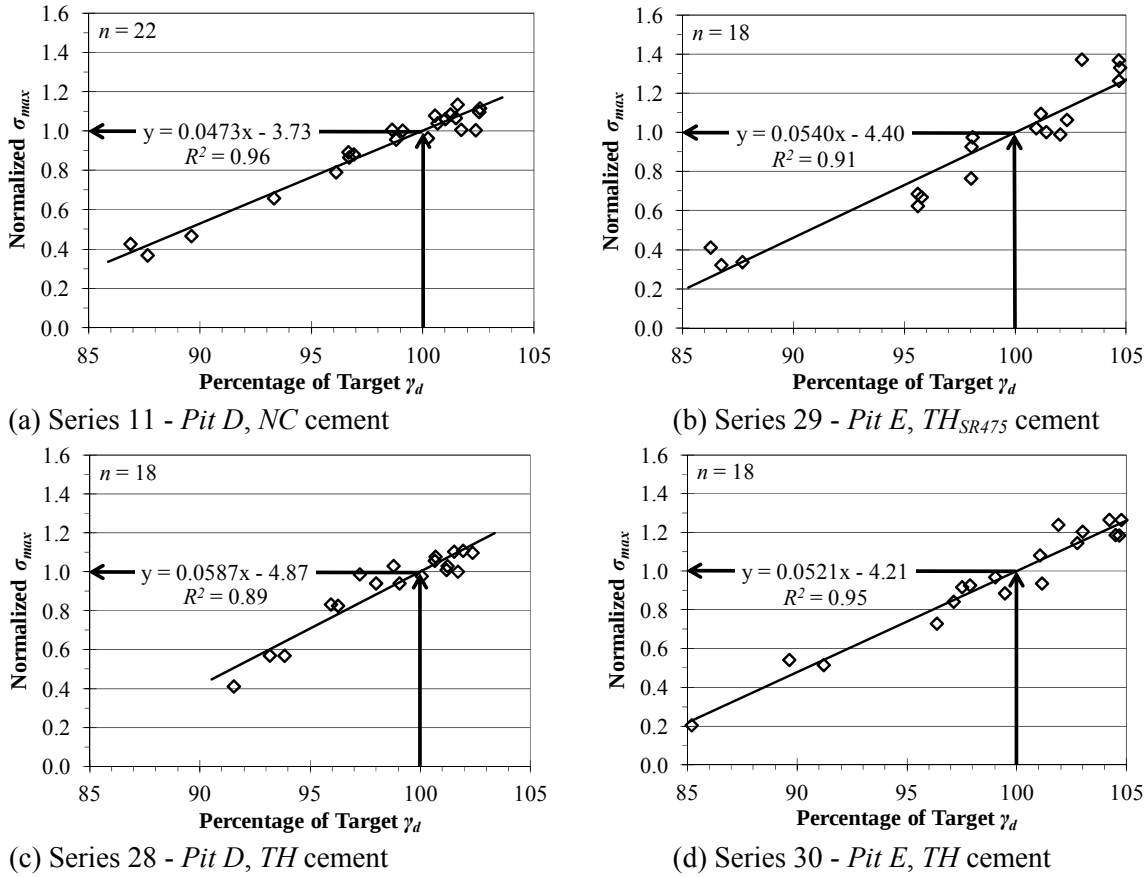

(a) Series 11 - *Pit D*, *NC* cement

(b) Series 29 - *Pit E*, TH_{SR475} cement

(c) Series 28 - *Pit D*, *TH* cement

(d) Series 30 - *Pit E*, *TH* cement

Figure 12.1. Specimen Density Effects on Compressive Strength (σ_{max})

$$\sigma_{\max adj} = \sigma_{\max} \times \left(1 + \left(1 - \left(P_{\gamma d} \times 0.0521 - 4.21\right)\right)\right) \quad \text{(Eq 12.1)}$$

Where:

$\sigma_{max\ adj}$ = Adjusted compressive strength (kPa)

σ_{max} = Measured compressive strength (kPa)

$P_{\gamma d}$ = Percentage of target maximum dry density (%)

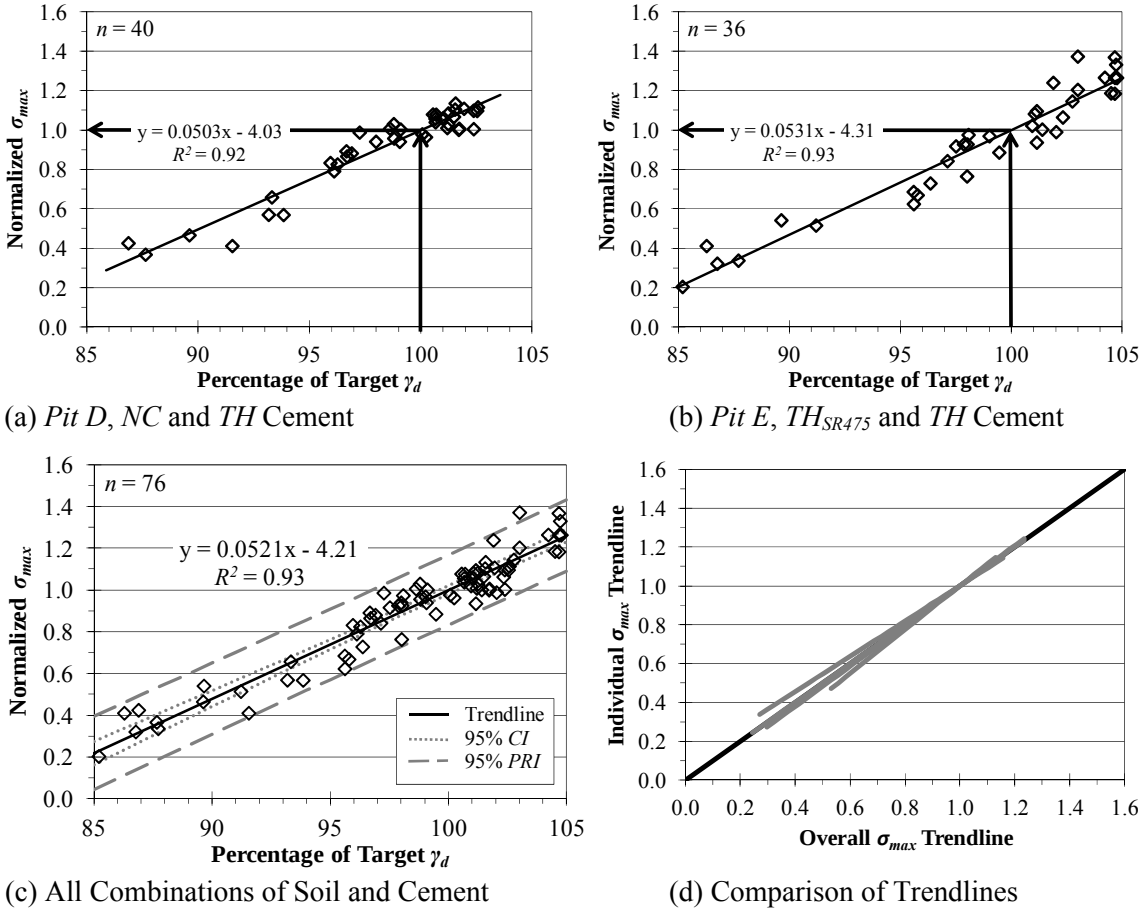

(a) *Pit D*, *NC* and *TH* Cement (b) *Pit E*, TH_{SR475} and *TH* Cement

(c) All Combinations of Soil and Cement (d) Comparison of Trendlines

Figure 12.2. Generalization of Specimen Density Effects on σ_{max}

Table 12.6 correlates density and thermal measurements. Overall, there were no strong trends between percentage of target γ_d ($P_{\gamma d}$) and any thermal measurement variable, but there is a weak trend showing that increasing density will slightly increase T_{max}, ΔT, and A_s values. Little to no correction is likely needed to adjust thermal measurements for density.

Table 12.6. Correlation of Specimen Density and Thermal Measurements

Variable	Pit	Cement	Trendline Equation	R^2
T_{max}	*D*	*NC*	$T_{max} = 0.03P_{\gamma d} + 23.3$	0.13
ΔT	*D*	*NC*	$T_{max} = 0.03P_{\gamma d} + 1.87$	0.15
A_s	*D*	*NC*	$T_{max} = 0.67P_{\gamma d} + 551$	0.13
T_{max}	*D*	*TH*	$T_{max} = 0.08P_{\gamma d} + 19.2$	0.43
ΔT	*D*	*TH*	$T_{max} = 0.05P_{\gamma d} - 0.06$	0.35
A_s	*D*	*TH*	$T_{max} = 1.88P_{\gamma d} + 445$	0.44
T_{max}	*E*	TH_{SR475}	$T_{max} = 0.08P_{\gamma d} + 19.3$	0.62
ΔT	*E*	TH_{SR475}	$T_{max} = 0.03P_{\gamma d} + 1.93$	0.38
A_s	*E*	TH_{SR475}	$T_{max} = 2.07P_{\gamma d} + 416$	0.65
T_{max}	*E*	*TH*	$T_{max} = 0.05P_{\gamma d} + 22.6$	0.45
ΔT	*E*	*TH*	$T_{max} = 0.02P_{\gamma d} + 3.65$	0.14
A_s	*E*	*TH*	$T_{max} = 1.06P_{\gamma d} + 521$	0.40

12.4 Time Delay Corrections

In the field, some specimens could not be compacted immediately after completion of cement mixing because of construction practices (i.e. multiple mixing passes, and similar); therefore, an analysis was conducted to take into account the effects of compaction delay time (t_d) between cement mixing and specimen preparation. Tested compaction delay times (i.e. the time from cement addition to the end of specimen compaction) varied from 5 to 65 minutes as this is similar to the time frame experienced in the field. Tests were performed with *Pits D* and *E* at two initial material temperatures (21 and 32°C). Overall, t_d appeared to have more of an effect on the thermal profile measurement than it did on compressive strength. Figures 12.3 and 12.4 show the effects of compaction delay on T_{max}, ΔT, and A_s.

Trends between compaction delay time and T_{max}, ΔT, or A_s were low to reasonable (R^2 = 0.28 to 0.69) in Figures 12.3 and 12.4 due to data variability; therefore, further investigation may be needed to investigate the issue of compaction delay. In every case, the observed values of T_{max}, ΔT, and A_s decrease as the compaction delay time increases. With exception of one case (*Pit D* at 32°C), the T_{max} decreases approximately 0.02°C for every minute of delay. For *Pit D* at 32°C, the T_{max} decreases approximately 0.01°C for every minute of delay. With exception to one case (*Pit E* at 32°C), the ΔT decreases approximately 0.015°C every minute of delay. For *Pit E* at 32°C, the ΔT decreased approximately 0.04°C for every minute of delay. For *Pit D*, A_s decreases approximately 0.43 °C-hr for every minute of delay. For *Pit E*, A_s decreases approximately 0.36 °C-hr every minute of delay.

The effects of compaction delay on the compressive strength (σ_{max}) were evaluated by plotting compaction delay time (x-axis) versus the measured compressive strength (y-axis). Table 12.7 summarizes the trendline equations developed from these plots. Results show no correlation between compaction delay time (t_d) and compressive strength (σ_{max}). All recorded σ_{max} values fall within the expected range of variability for both mixtures. Time delay specimens were compacted to, on average, $P_{\gamma d}$ of 100.3% so they were not adjusted and reported as σ_{max}.

Table 12.7. Effects of Compaction Delay on Compressive Strength

Soil	Cement	C_I (%)	T_i (°C)	Trendline Equation	R^2
Pit D	*NC*	7	21	$\sigma_{max} = 1.32t_d + 1587$	0.21
Pit D	*NC*	7	32	$\sigma_{max} = -0.05t_d + 1634$	0.00
Pit E	TH_{SR475}	7	21	$\sigma_{max} = 2.58t_d + 1884$	0.23
Pit E	TH_{SR475}	7	32	$\sigma_{max} = 1.71t_d + 2078$	0.87

A small experiment was performed with *Pit C* where a soil-cement mixture was prepared at design cement and optimum moisture contents. Specimens were oven dried after pre-scribed delay times of 0 to 8 hr in 1 hr increments; duplicate specimens were tested for a total of 18 experiments. The purpose of the experiments was to determine hydrations effect on moisture contents if specimens happen to be held in the field for a period of time and not dried immediately. Results of the experiment was the maximum difference in any two of the sixteen experiments was 0.21%, and a linear trendline with an R^2 value of 0.69 predicted approximately 0.02% decrease in moisture content per hour of measurement delay. This is a tolerable error, and 0.02% per hour seems like a reasonable correction factor for quality control purposes.

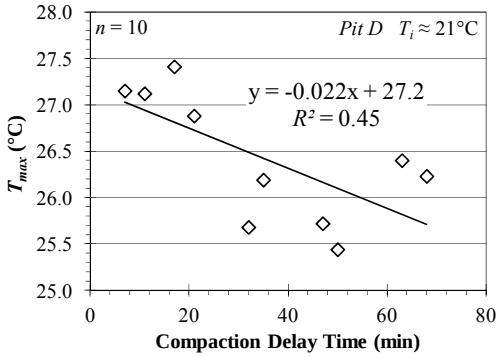

(a) *Pit D*, 21°C, T_{max}

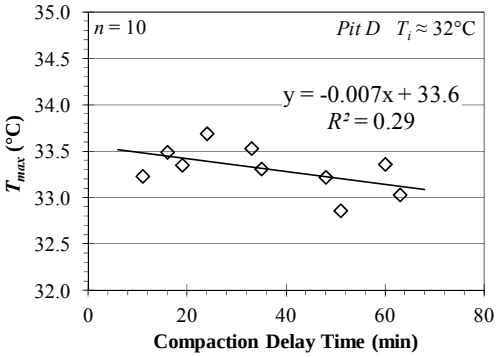

(b) *Pit D*, 32°C, T_{max}

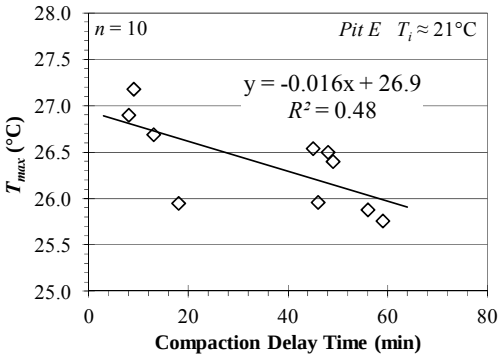

(c) *Pit E*, 21°C, T_{max}

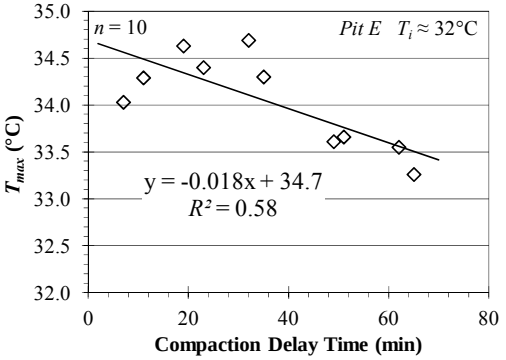

(d) *Pit E*, 32°C, T_{max}

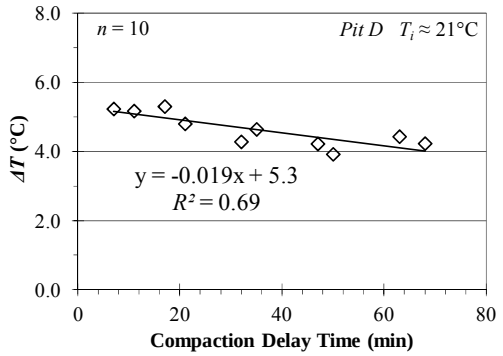

(e) *Pit D*, 21°C, ΔT

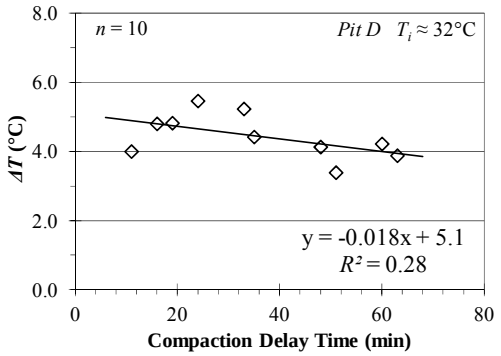

(f) *Pit D*, 32°C, ΔT

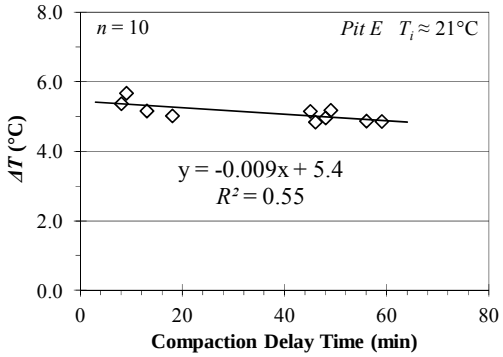

(g) *Pit E*, 21°C, ΔT

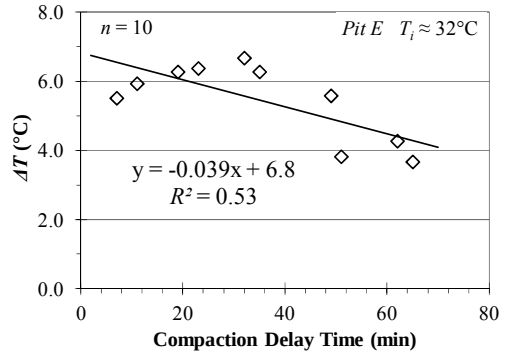

(h) *Pit E*, 32°C, ΔT

Figure 12.3. Effects of Compaction Delay Time (t_d) on T_{max} and ΔT

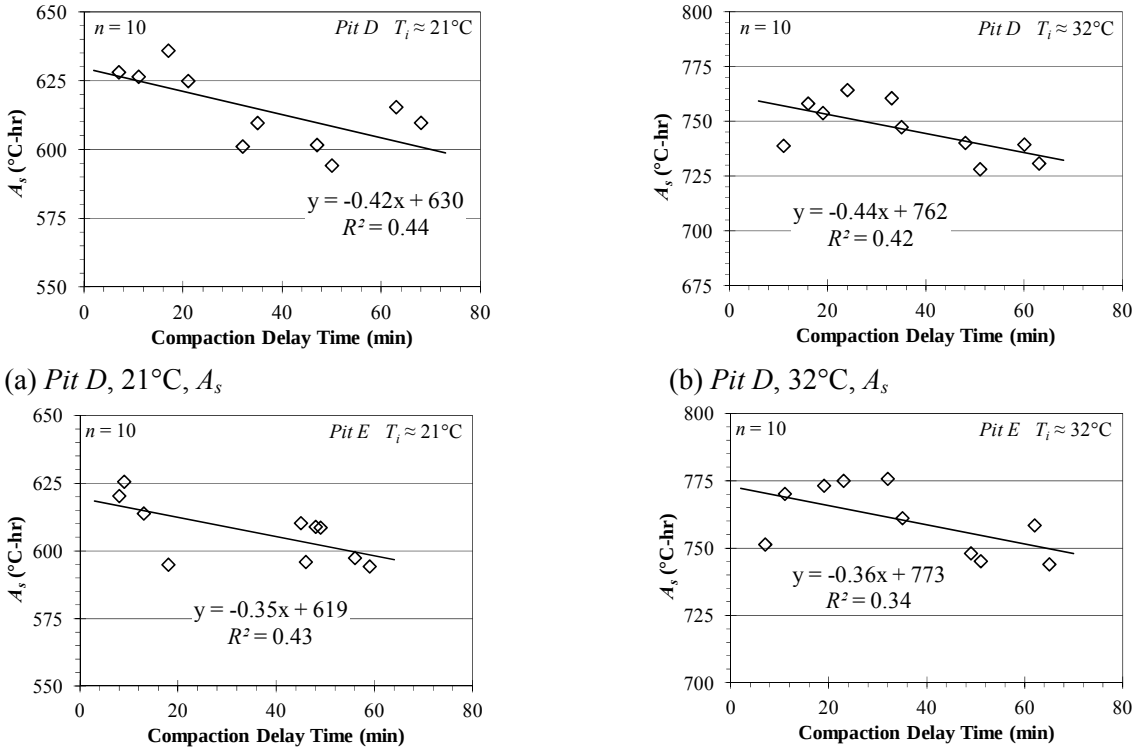

(a) *Pit D*, 21°C, A_s (b) *Pit D*, 32°C, A_s

(c) *Pit E*, 21°C, A_s (d) *Pit E*, 32°C, A_s

Figure 12.4 Effects of Compaction Delay Time (t_d) on A_s

12.5 Thermal Profiles Measured on Field Prepared Specimens

Field thermal profile specimens were prepared according to Section 5.4.5, and Figures 12.5 and 12.6 contain plots of thermal profiles alongside summary information and compressive strength results. Reported compressive strengths were adjusted for density using Equation 12.1 and specimen size as per ASTM D1633. In Figures 12.5 and 12.6, thermal profiles are plotted with time zero as the cement addition time. Each location has two cement addition times, one for the control mixtures and one for the field mixtures. For comparison, all profiles were plotted together which creates an offset for the reference specimen profile. The offset was alleviated by plotting the reference specimen twice with time zero referencing each cement addition time individually. For example, at Location 1 on SR475 (Figure 12.6a) the cement for the control mixture was added at 8:59 AM, and thermal measurements for that specimen and the reference specimen began at 9:04 AM. So 9:04 AM is Time = 0.08 hr on Figure 12.6a. The cement addition time for Position 1 was 8:18 AM, and thermal measurements began at 9:10 AM. So 9:10 AM for Position 1 specimens is Time = 0.9 hr on Figure 12.6a. Thermal measurements on all three specimens were started at approximately the same time, but the plot in Figure 12.6a shows a 0.68 hr shift between the control and position 1 specimens (because of the different cement addition times). The asterisked reference thermal profile shows the recorded reference specimen thermal profile synchronized with the cement addition time for the field mixed specimens (Positions 1, 2, and 3). For SR9, the reference and asterisked reference profiles are almost indistinguishable, but for SR475 the difference is noticeable.

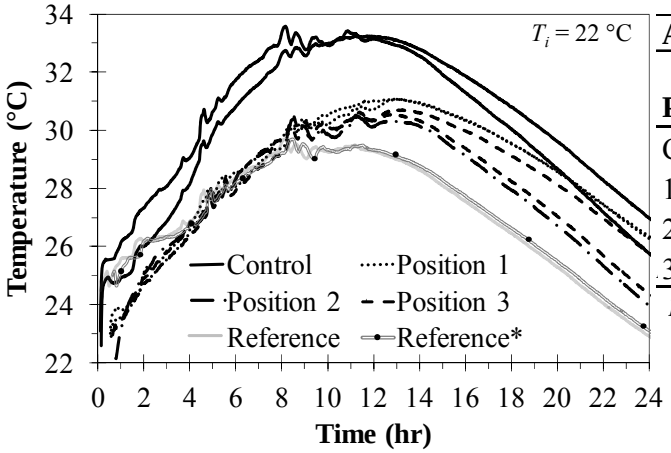

Average Test Results

Pos.	T_{max} (°C)	ΔT (°C)	A_s (°C-hr)	σ_{max} (kPa)	n
C	33.4	3.9	723	2273	2
1	31.1	1.9	672	1426	2
2	30.5	1.1	648	1528	1
3	30.7	1.4	657	1216	2

Note: σ_{max} was adjusted for specimen density.

(a) Thermal Profile - Location 1

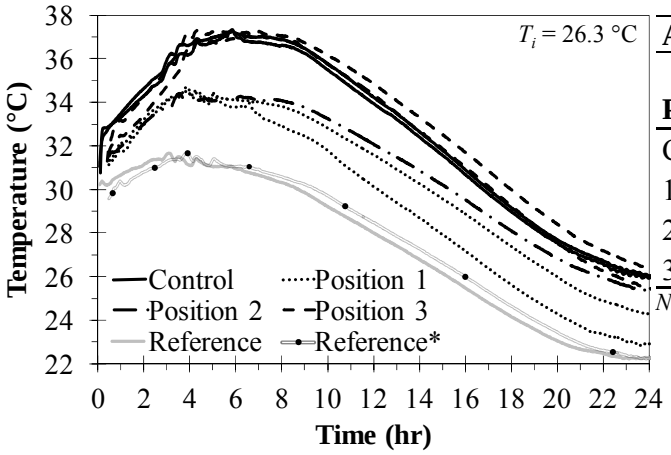

Average Test Results

Pos.	T_{max} (°C)	ΔT (°C)	A_s (°C-hr)	σ_{max} (kPa)	n
C	37.3	6.2	778	2226	2
1	34.6	3.0	707	893	2
2	34.4	2.8	726	910	1
3	37.2	6.0	771	1967	2

Note: σ_{max} was adjusted for specimen density.

(b) Thermal Profile - Location 2

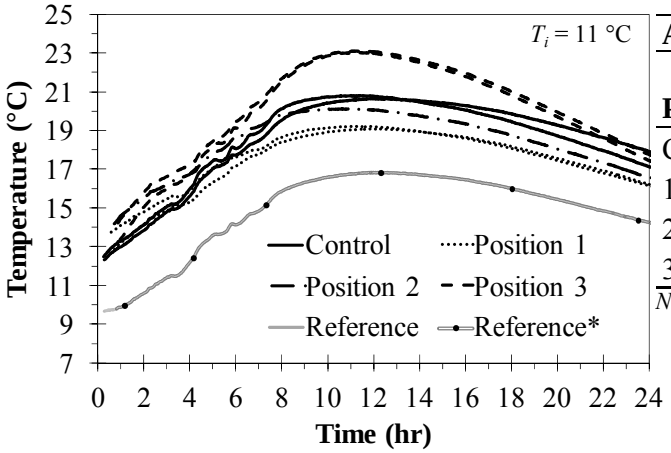

Average Test Results

Pos.	T_{max} (°C)	ΔT (°C)	A_s (°C-hr)	σ_{max} (kPa)	n
C	20.7	3.9	442	2590	2
1	19.2	2.4	413	875	2
2	20.1	3.4	431	1465	1
3	23.1	6.3	467	3728	2

Note: σ_{max} was adjusted for specimen density.

(c) Thermal Profile - Location 3

Figure 12.5. Measured Field Thermal Profiles for SR9

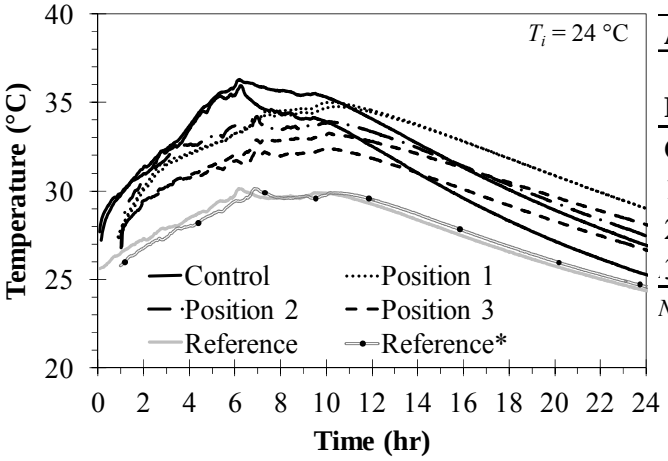

Average Test Results

Pos.	T_{max} (°C)	ΔT (°C)	A_s (°C-hr)	σ_{max} (kPa)	n
C	36.1	6.0	752	1854	2
1	34.9	5.0	749	2673	2
2	34.2	4.1	724	2162	1
3	32.8	2.9	705	1114	2

Note: σ_{max} was adjusted for specimen density.

(a) Thermal Profile - Location 1

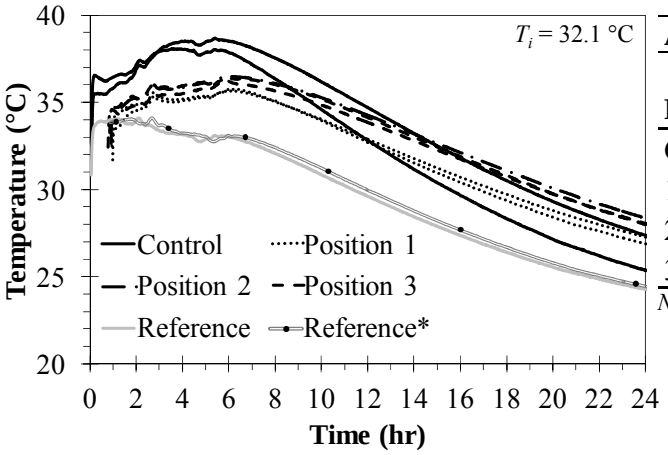

Average Test Results

Pos.	T_{max} (°C)	ΔT (°C)	A_s (°C-hr)	σ_{max} (kPa)	n
C	38.4	5.2	794	2275	2
1	35.7	2.6	739	1486	2
2	36.5	3.5	769	1606	1
3	36.3	3.2	766	1766	2

Note: σ_{max} was adjusted for specimen density.

(b) Thermal Profile - Location 2

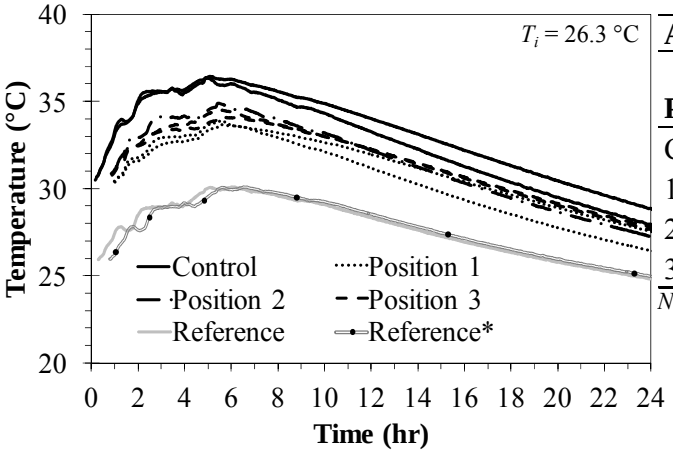

Average Test Results

Pos.	T_{max} (°C)	ΔT (°C)	A_s (°C-hr)	σ_{max} (kPa)	n
C	36.4	6.5	786	2118	2
1	33.8	3.7	713	1045	2
2	34.9	4.9	728	1531	1
3	34.3	4.3	734	1228	2

Note: σ_{max} was adjusted for specimen density.

(c) Thermal Profile - Location 3

Figure 12.6. Measured Field Thermal Profiles for SR475

Overall, thermal measurements produced suitable profiles for relative comparison to control mixture profiles. Generally speaking, the thermal profile results align and agree with measured compressive strength results (e.g. higher average values of T_{max}, ΔT, and A_s yielded a higher average σ_{max}). Some locations experienced a 4 to 6 °C increase in the reference specimen which may suggest outside influences from ambient temperatures inside the van. Note that the Figure 5.10 environmental chamber was taken to the project site and kept in an air conditioned van during the entire process; T_{BL} was 21 ^{o}C for all Figure 12.5 and 12.6 experiments.

For SR9 Location 1 (Figure 12.5a), the control specimen thermal profiles were much greater in magnitude than the field mixed thermal profiles, which may suggest a difference in cement content. The control specimens also have a greater average $\sigma_{max\ adj}$ which supports the thermal profile findings.

For SR9 Location 2 (Figure 12.5b), the control specimen thermal profiles and position 3 profiles were approximately the same while positions 1 and 2 profiles were noticeably lower. Profile and $\sigma_{max\ adj}$ data suggest position 3 and controls had about the same amount of cement and positions 1 and 2 contained less cement. For SR9 Location 3 (Figure 12.5c), the position 3 profiles were noticeably higher than the control profiles, and positions 1 and 2 profiles were a little lower than the controls. Overall, the cement content difference suggested by the profiles is supported with average $\sigma_{max\ adj}$ results.

For SR475 Location 1 (Figure 12.6a), control profiles peaked slightly higher than field mixed specimens, but field mixed and control specimens had similar A_s values. Average $\sigma_{max\ adj}$ values were also puzzling as positions 1 and 2 produced higher $\sigma_{max\ adj}$ than the control specimens. For SR475 Location 2 (Figure 12.6b), control profiles peaked higher than field mixed specimens, and field mixed profiles were all approximately the same magnitude. Average $\sigma_{max\ adj}$ results show all field mixed specimens to be about the same, and average control $\sigma_{max\ adj}$ was noticeable higher. For SR475 Location 3 (Figure 12.6c), control profiles and average $\sigma_{max\ adj}$ were greater than field mixed specimens. Field mixed profiles were closely grouped, and $\sigma_{max\ adj}$ values were approximately the same.

An attempt was made to recreate two of the field thermal plots (Figures 12.5b and 12.5c) in the laboratory. Thermal profile data from Series 47 and 48 was plotted on the same plot as Series 37 and 45 in hopes of bounding the field profiles with lab profiles of known cement content. Laboratory materials were conditioned to the same initial material temperature (T_i) as the field specimens and the thermal device temperature (T_{BL}) was a constant 21 °C throughout testing. Figure 12.7 displays the thermal profile results. The laboratory prepared thermal profiles (noted by C_I values in Figure 12.7) do not resemble the measured field thermal profiles. The field and laboratory profiles differ with respect to magnitude and shape. These results further support the discussion in Section 11.6 concerning the effects of T_i and T_{BL}. Based on these results, re-creating field thermal profiles in a laboratory setting using current equipment and protocols appears to be a daunting task.

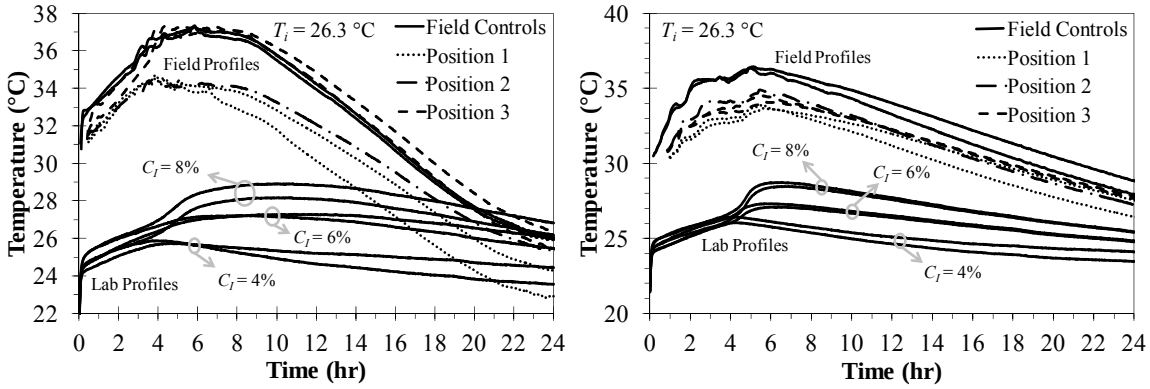

(a) *SR9* Location 1 (b) *SR475* Location 3

Figure 12.7. Field Thermal Profiles Overlaid with Lab Thermal Profiles

Linear Regression and Analysis of Variance (ANOVA) techniques were applied to the SR9 and SR 475 data presented in Figures 12.5 and 12.6. The variables of key interest were ΔT (x-value or independent variable) and $\sigma_{max\ adj}$ (y-value or dependent variable). The other thermal profile variables were casually and unproductively investigated as no correlations were evident. The investigation used ΔT with ^{o}C units and $\sigma_{max\ adj}$ with MPa units to provide outputs that were easier to understand absent scientific notation.

When interpreting the following results it is important to note that T_{BL} was a constant 21 ^{o}C through all testing, while T_i varied from 11 to 26 ^{o}C for SR9 and from 24 to 32 ^{o}C for SR475. Data presented in this report thus far suggests that T_{BL} values more closely resembling T_i values provides for improved thermal measurement data; i.e. that the correlations presented could likely be improved by changing T_{BL} values depending on field T_i values at the time of sampling.

Statistical investigation of SR9 resulted in an R^2 value of 0.51, an adjusted R^2 value of 0.46, and a p-value of 0.009 for the relationship between ΔT and $\sigma_{max\ adj}$. Statistically, the p-value can be viewed as the probability of observing a test statistic at least as extreme as that observed, and for a 95% confidence level, p-values below 0.05 indicate a statistically significant relationship (between ΔT and $\sigma_{max\ adj}$ in this case). The p-value determined for SR9 was well below 0.05 indicating a statistically significant relationship between ΔT and $\sigma_{max\ adj}$. For SR9, increasing ΔT by 1 ^{o}C resulted in an increase in $\sigma_{max\ adj}$ of 0.33 MPa based on a linear trendline. All factors considered, there was a respectable correlation between ΔT and $\sigma_{max\ adj}$ for SR9.

Statistical investigation of SR475 resulted in an R^2 value of 0.32, an adjusted R^2 value of 0.26, and a p-value of 0.054 for the relationship between ΔT and $\sigma_{max\ adj}$. The p-value determined for SR475 was just above the significance threshold. For SR475, increasing ΔT by 1 ^{o}C resulted in an increase in $\sigma_{max\ adj}$ of 0.24 MPa based on a linear trendline. All factors considered, there appears to be a weak but not statistically significant correlation at 95% confidence between ΔT and $\sigma_{max\ adj}$ for SR475.

When the findings of both pavements are considered, field data collection suggests ΔT to be a reasonably promising thermal profile output. For purposes of quality control for specification purposes, however, many additional matters must be addressed. For use as a guide on warranty projects (or equivalent), there could be some applications at present where outputs are used subjectively. At present, however, use of the linear trendline predictions

should not be expected to result in especially accurate results; i.e. using ΔT to predict $\sigma_{max\ adj}$ is not presently expected to be especially reliable, though it does seem reasonable to expect general trends to hold that could be useful during construction.

12.6 Comparing Thermal Profiles, Strength, and Cement Content Measurement

The data presented in Section 12.5 provides some interesting observations, but is not definitive regarding thermal profile use in soil-cement quality control. The data does further reinforce the importance of the equipment block temperature (T_{BL}), but also reinforces the potential of ΔT as the key thermal profile output for soil-cement purposes. This section compares thermal profile data to cement content measured in more customary manners. This section also compares thermal profile and traditionally measured cement content data to compressive strength adjusted for density (Eq 12.1) and specimen size (D1633).

Test results are provided in Table 12.8. The average increase in cement content from D806 (wet process) to C114 (X-Ray) was 0.47%, which based on a paired t-test was not statistically significant at a 95% confidence level (*p-value* of 0.145) when the mean difference was compared to zero. Differences within any one pair ranged from C114 being 1.1% higher than D806 to 0.5% lower than D806.

A check was performed where a sample of *Pit D* and *NC* cement was hand batched with a cement content C_w of 6.2% by weight. C114 and D806 were performed on the mixed sample and resulted in values of 9.1% and 8.5%, respectively. In essence, both methods resulted in cement content prediction that was much higher than the actual cement content. Over predicting cement content by 2.3 to 2.9% is meaningful.

Table 12.8. Cement Content Calculation

Project	Location	Individual Specimen $\sigma_{max\ adj}$ (kPa)	D806 C_w (%)	C114 C_w (%)	Position 3 ΔT (oC)
SR9	1	839	6.6	7.7	1.4
SR9	2	1108	7.1	8.1	6.0
SR9	3	2179	5.5	6.5	6.3
SR475	1	2050	6.7	6.9	2.9
SR475	2	1605	5.1	4.6	3.2
SR475	3	1270	6.9	6.9	4.3

--Reported cement contents are by dry soil mass and not cement index.

Table 12.8 test results contain Figure 5.17a position 3 ΔT values. Position 3 was used for comparisons since it was closest to the probe location where cores were taken that were ultimately used to measure cement content (Figure 5.18a). Position 3 was also used since it is parallel in the longitudinal (or traffic) direction to where cores were taken and would likely receive more consistent cement spread than any other position relative to the core location.

Position 3 in Figure 5.17a was used for cement content comparisons since it was closest to the probe location where cores were taken, but also since these two locations are parallel in the longitudinal or traffic direction and would most likely receive more consistent cement spread than any other position relative to the probe location.

The data set is limited for comparing to $\sigma_{max\ adj}$ since the comparison needs to be performed by pavement type. For SR9 and SR475, neither D806 or C114 measured cement contents agreed with $\sigma_{max\ adj}$ in terms of relative ranking; i.e. the lowest strength having the lowest cement content and so forth. For SR9, ΔT correctly ranked all three $\sigma_{max\ adj}$ values; i.e. lowest strength had lowest ΔT, mid range strength had mid range ΔT, and highest strength had highest ΔT. For SR475, ΔT did not correctly rank $\sigma_{max\ adj}$.

Cement content measurement for quality control purposes has many obstacles to overcome; existing ASTM or thermal profile methods. The findings in Sections 12.5 and 12.6 indicate it might be more fruitful for MDOT to implement the Figure 5.2 mold for a period of time and evaluate its effectiveness prior to considering implementing thermal profile measurements. Thereafter, thermal profile related implementation decisions could be made with more information.

12.7 In-Situ Temperature Measurement

Figure 12.8 plots in-situ probe temperatures over time for each of the 6 locations, and time was synchronized to the first mixing pass at each location. Refer to Figure 5.23 for a schematic of probe sensor locations. Overall, in-situ probes were unable to detect temperature profiles produced from cement hydration. The ambient air temperature (T-1) experienced the most dramatic swings in temperature, and each of the thermocouple sensors located within the soil-cement layer (T-2, T-3, and T-4) recorded smaller swings in temperature.

The magnitude of temperature swings recorded within the soil-cement layer was probably a function of the amount of insulation provided by the layer itself. For SR9 (Figures 12.8a, 12.8c, and 12.8e), temperatures generally ranged between 5 and 35°C. For SR475 (Figures 12.8b, 12.8d, and 12.8f), temperatures generally ranged between 20 and 45°C. The recorded ambient temperature (T-1) was used to calculate the *TTF* of molded field cured compressive strength specimens and field cores.

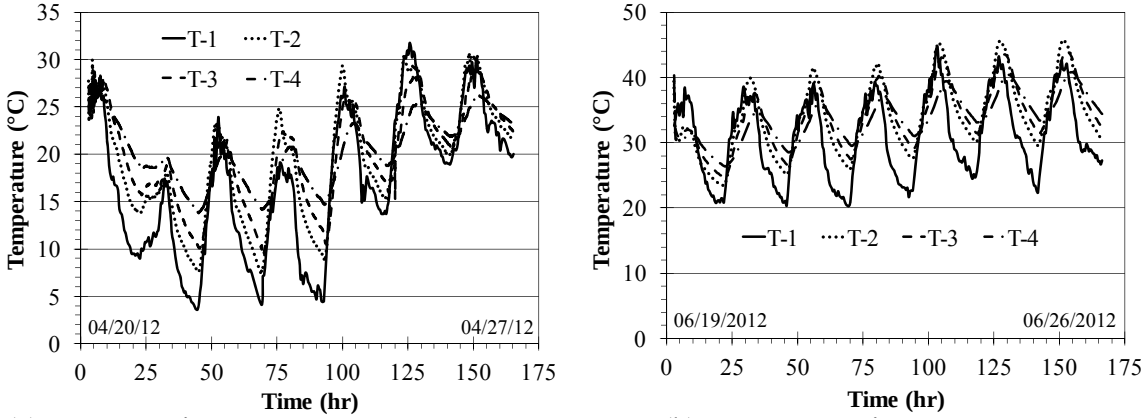

(a) *SR9* Location 1 (b) *SR475* Location 1

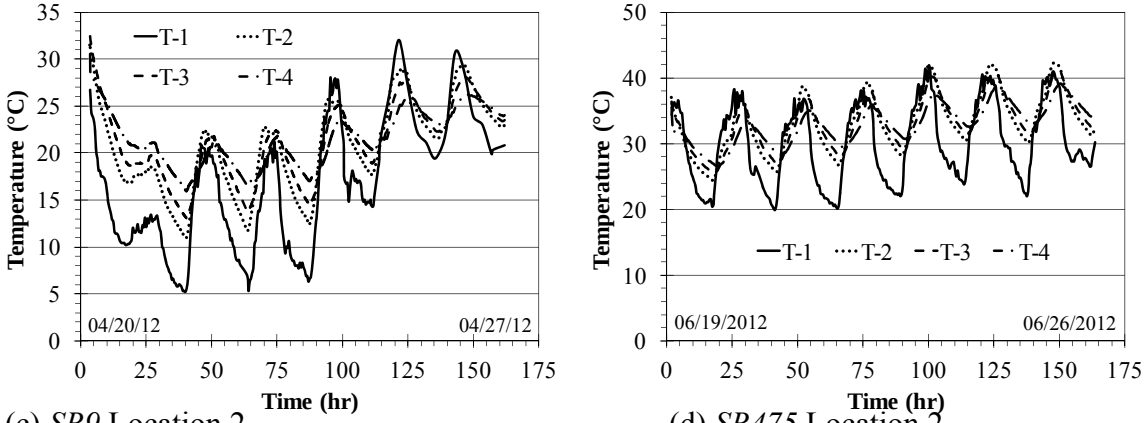

(c) *SR9* Location 2 (d) *SR475* Location 2

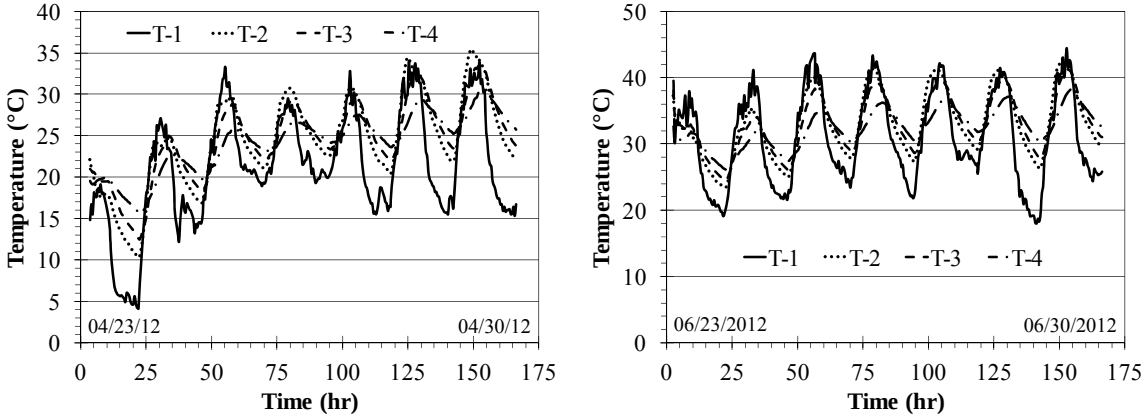

(e) *SR9* Location 3 (f) *SR475* Location 3

Figure 12.8. Temperature Plots of In-Situ Probes

12.8 Field Compressive Strength Specimens

Field compressive strength data analyzed in this section are from Series 35 through 46, and raw data is contained in Sullivan (2012) Appendix B. All field made specimens were tested for compressive strength after 7 days of curing. Compressive strength specimens

consist of thermal profile specimens (noted as lab cured), field cured specimens (molded using the *PM-P* hammer approach), and field cores cut from the roadway as described in Section 5.4.5.2. Figure 12.9 compares the average σ_{max} for lab cured, field cured, and field core specimens. The average *TTF* at the test time is reported in Figure 12.9. Reported $\sigma_{max\ adj}$ values were adjusted for density (Eq 12.1) and specimen size (as per ASTM D 1633); so that, $\sigma_{max\ adj}$ are comparable to the target σ_{max} of 2070 kPa. Table 12.9 expands upon the results shown in Figure 12.9 and presents a comparison between molded specimens and field cores. Both the field cured and field core specimens have approximately the same *TTF*.

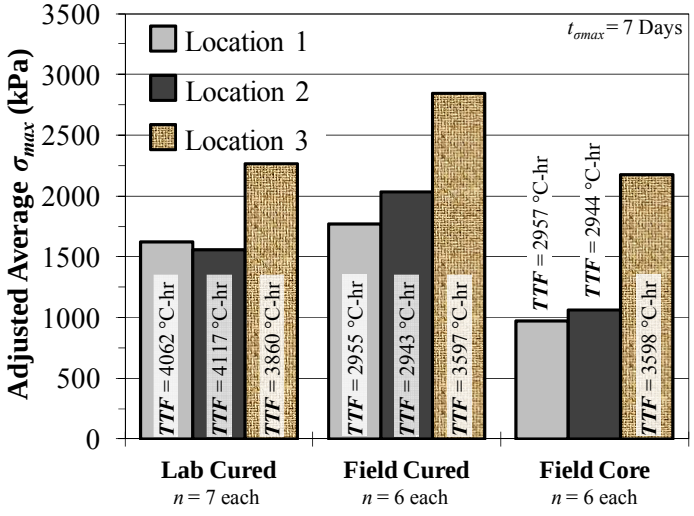

(a) *SR9* $\sigma_{max\ adj}$ Data

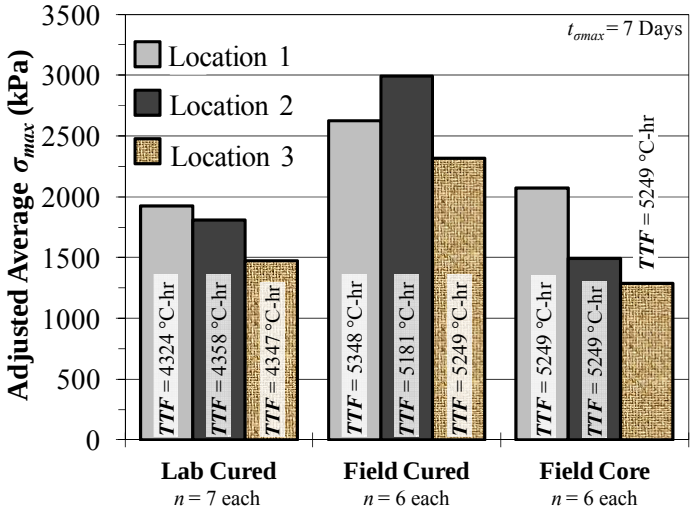

(b) *SR475* $\sigma_{max\ adj}$ Data

Figure 12.9. Field Compressive Strength Results

For both SR9 and SR475, the field cured specimens had a higher average σ_{max}, and with exception of one case, the field cores recorded average $\sigma_{max\ adj}$ lower than both the lab and field cured specimens. For SR9 (Figure 12.9a), the field cured specimens had a higher

average $\sigma_{max\ adj}$ with a lower *TTF* (≈ 3000 °C-hr) than the lab cured (≈ 4000 °C-hr), which is counter intuitive. Field cured specimens were prepared using mixed material from positions 4, 5, 3, and 2, and lab cured specimens were prepared using control mixtures and mixed material from positions 1, 2, and 3. Some discrepancy in Figure 12.9 could be attributed to varying cement contents among sample positions. For SR475, field cured specimens had a higher average σ_{max} and a higher *TTF*, which was expected.

As seen in Table 12.9, the SR9 field cured specimens have a noticeably high *COV* (18 to 38 %) suggesting a higher variability in $\sigma_{max\ adj}$. Thermal profile results in Section 12.5 indicate some variability in cement content for SR9 at Locations 2 and 3; therefore, high *COV*'s could be the result of variations in cement content among sample positions. SR9 field cores were less variable with *COV*'s from 7 to 22 %. On average, the SR9 field core compressive strengths were 33 to 48 percent less than the field cured specimens, which were molded with the *PM-P* hammer approach. For SR475, the field cured specimens and the field cores had approximately the same *COV*'s (6 to 19 %). On average, compressive strengths of SR475 field cores were 29 to 50 percent less than the molded field cured specimens.

Table 12.9. Molded Specimens and Field Cores $\sigma_{max\ adj}$ Comparison

		Field Cured		Field Cores	
Project	**Location**	**Mean (kPa)**	***COV* (%)**	**Mean (kPa)**	***COV* (%)**
SR9	1	1772	18.3	970	22.4
SR9	2	2032	37.9	1063	7.2
SR9	3	2844	32.7	2177	8.2
SR475	1	2627	6.0	2073	17.1
SR475	2	2993	18.1	1490	9.9
SR475	3	2315	19.2	1289	6.5

Note: Some SR475 cores required capping prior to testing (noted in Sullivan (2012) Appendix B), and no SR9 cores required capping.

12.9 Traffic Opening

This section provides general guidance for a potential method to determine when a soil-cement layer can be opened to traffic. The approach presented incorporates maturity methods coupled with conventional compressive strength testing. Laboratory specimens were used to develop generalized trendlines characterizing the strength gain of soil-cement mixtures having an MT-25 required 7 day cure time. These curves could be used to estimate a *TTF* in which the design σ_{max} is achieved. Compressive strength data from field specimens prepared using the *PM-P* compaction technique was used to evaluate the traffic opening approach.

Three trendline bands (Figure 12.10) were developed using data from Chapter 11 (Series 5, 6, 7, 10, and 15). These specimens were prepared using the *PM-CF* compaction approach; therefore, the measured σ_{max} was adjusted to equivalent strengths observed using the *PM-P* compaction approach. The multiplied adjustment factor for *Pit A*, *Pit B*, and *Pit C* was 0.94, 0.80, and 0.72, respectively. After adjusting the σ_{max} for compaction type and specimen size (ASTM D1633), the σ_{max} was normalized to reflect the percentage of the design σ_{max} (2070 kPa).

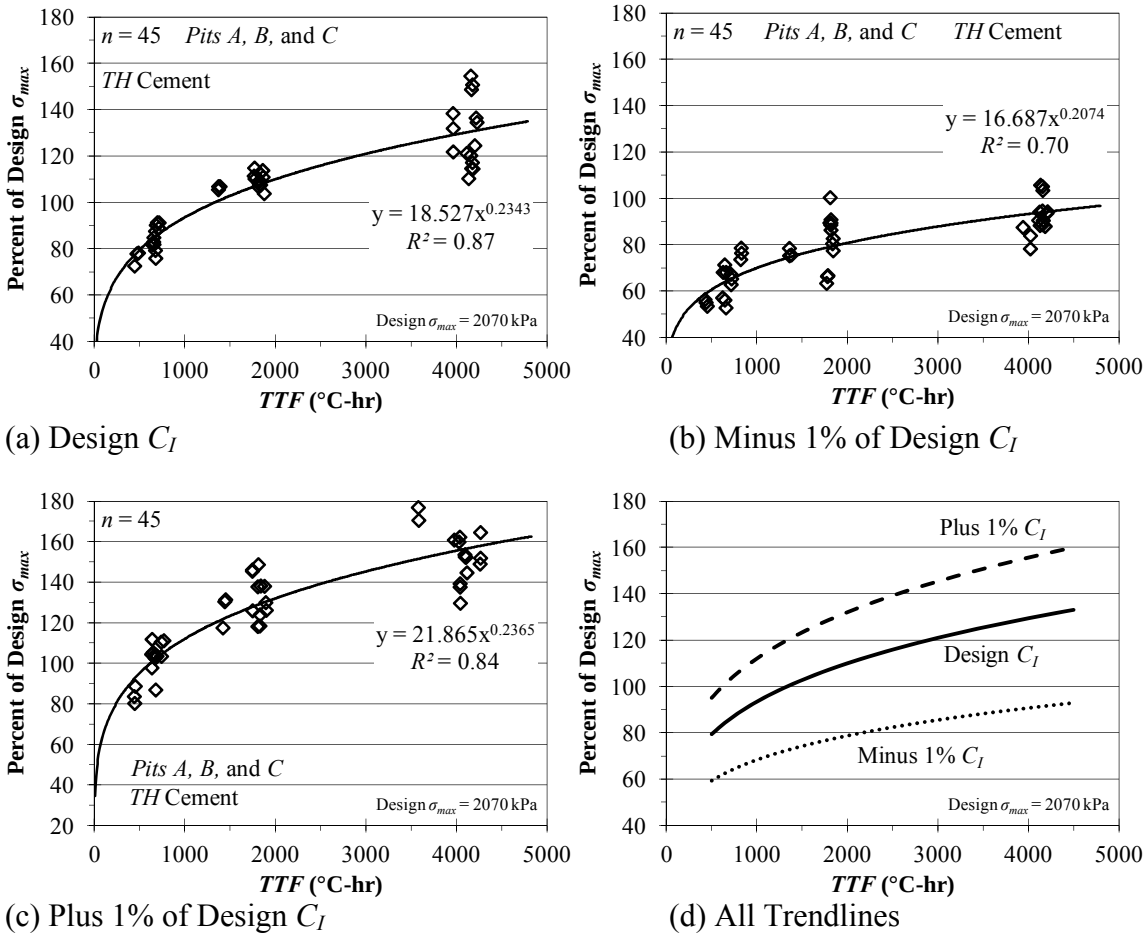

Figure 12.10. Development of Traffic Opening Guidance Trendlines

Figures 12.10a, 12.10b, and 12.10c show good power fits for the relationship between *TTF* and normalized σ_{max} (R^2 = 0.70 to 0.87). Figure 12.10d shows the trendlines from Figures 12.10a, 12.10b, and 12.10c. These three trendline bands are meant to provide insight to the level of maturity (*TTF*) required to achieve the design σ_{max}. Figure 12.11 shows the average σ_{max} of the lab cured and field cured specimens for SR9 and SR475 plotted against the trendline bands developed in Figure 12.10.

As seen in Figure 12.11, all six averaged field cured σ_{max} data points fall between the design $C_I \pm 1\%$ trendlines. Four of the six averaged lab cured σ_{max} data points fall below the minus 1% of design C_I trendline. Lower strengths observed with some of the averaged lab cured specimens is not fully understood and may require further investigation by means of additional analysis and/or further testing.

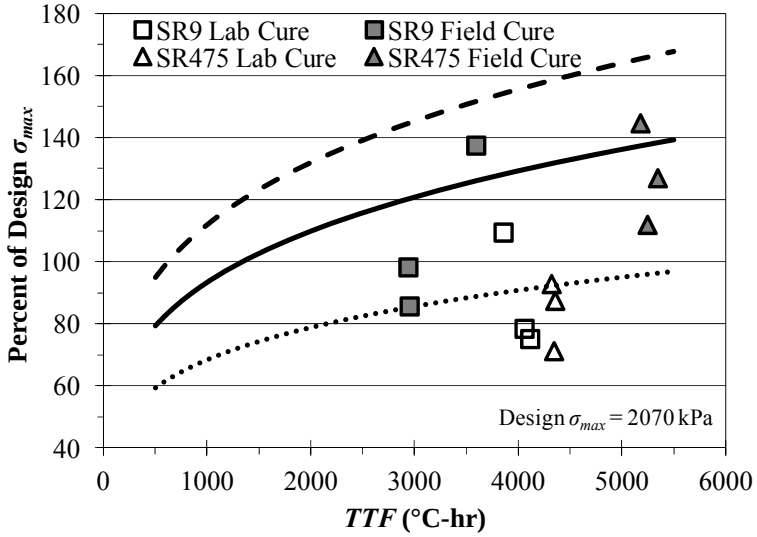

Figure 12.11. Traffic Opening Verification with Average *SR9* and *SR475* σ_{max} Results

12.10 Mold Adjustments

Some combinations of laboratory mix design and field quality control or traffic opening might benefit from curing some specimens inside their plastic compaction molds. Generally speaking, most of the testing in this report has cured specimens compacted in the *PM* assembly out of their plastic molds after 1 day of thermal profile measurements. The data presented in this section evaluates differences in specimen compressive strengths due to whether or not they are cured in 100% humidity out of the plastic mold, or are sealed in the mold during curing. Temperature of both specimens was the same.

The data set was assembled in a paired fashion for direct comparison. As a result, measured compressive strengths at h/d = 1.98 were used directly without any correction for specimen size or density. Note that density was evaluated statistically between the matched pairs. Test results are provided in Table 12.10.

Table 12.10. Mold Curing Effects Test Results

Soil	Curing Temperature	Compressive Strength (kPa)			
		1 Day In Mold	1 Day Out of Mold	7 Day In Mold	7 Day Out of Mold
D	≈32 °C	1048	1189	1958	2161
E	≈32 °C	1348	1397	2365	2717
D	≈22 °C	572	595	1090	1312
E	≈22 °C	603	615	1648	1166
D	≈8 °C	336	358	1345	1133
E	≈8 °C	321	326	1751	1737

--Testing was performed with each soil's project cement.
--Cement index values were 6.9% for *Pit D* and 7% for *Pit E*.
--Each compressive strength shown is the average of two specimens.

A paired t-test was performed on all 1 day results at a 95% confidence level. The average increase in compressive strength from being cured in the plastic mold to being cured

outside the plastic mold was 42 kPa, which was not statistically significant (*p-value* of 0.098) when the mean difference was compared to zero. The same comparison was performed on all 7 day results, and the average increase in compressive strength from being cured in the plastic mold to being cured outside the plastic mold was 12 kPa, which was not statistically significant (*p-value* of 0.932).

Even though there were no statistical differences in the data set, there were some practically meaningful differences between some of the pairs. At a 1 day cure, the difference within any pair ranged from 5 to 141 kPa (<1 to 20 psi) with specimens cured out of the mold being stronger in all cases. At a 7 day cure, the difference within any pair ranged from specimens cured out of molds being 482 kPa (70 psi) weaker to 352 kPa (51 psi) stronger. Since these specimens were compacted with the PM-P approach, density was not constant, which could explain some of these differences. Density effects were not explored in the interest of brevity. Overall, the data collected suggests curing specimens in their plastic molds for up to 7 days appears feasible.

CHAPTER 13-PHASE 3 THERMAL PROFILE QUALITY CONTROL TEST RESULTS: PROTOCOL REFINMENT

13.1 Overview of Phase 3 Thermal Profile Test Results

Phase 3 thermal profile testing was conducted to investigate the reliability and/or feasibility of multiple methods of thermal profile quality control. These experiments were performed outdoors to reasonably simulate activities at a construction site. All experiments were performed under the premise of using relatively simple experimental configurations that would not require sophisticated activities in the field. Chapter 11 indicated that using an environmental chamber allowed distinguishable cures to be obtained, and Chapter 12 showed that the differential of initial material and thermal profile block temperatures was of first order concern. The investigation in this chapter aimed to investigate whether the Chapter 12 issues could be mitigated with reasonable field procedures absent an environmental chamber.

In total 144 specimens (Table 13.1) were tested, alongside 15 temperature differential experiments, for a total of 159 tests. Each specimen had 6 replicates, and unless further noted results were reported as an average of the results of the six specimens. Cement indexes used were design plus or minus 1 and design plus or minus 2. In an attempt to ascertain the possibility to estimate cement content in newly constructed soil-cement based on on-site field results, thermal profile, density, and 1 day compressive strength data were collected.

Table 13.1. Phase 3 Thermal Profile Quality Control Test Matrix

Group	Pit Soil	Additive	Cement Indexes			Covering	Time Delay	Replicates
1	B	TH	4	5	6	None	None	6 per Index (18 Total)
	B	TH	4	5	6	Clear Bag	None	6 per Index (18 Total)
2	B	TH	4	5	6	None	30 Min	6 per Index (18 Total)
	B	TH	4	5	6	Clear Bag	30 Min	6 per Index (18 Total)
3	B	TH	4	5	6	HC	30 Min	6 per Index (18 Total)
	B	TH	3	5	7	HC	30 Min	6 per Index (18 Total)
4	D	NC	4	5	6	HC	30 Min	6 per Index (18 Total)
	D	NC	3	5	7	HC	30 Min	6 per Index (18 Total)

13.2 Phase 3 Thermal Profile Results: Evaluating Equipment Configurations

Trial runs (no specimens) of the EPS thermal profile block shown in Figure 5.8 were first conducted to evaluate the ability of the block to perform if left on-site. The block was placed outside with either no covering, a clear plastic bag, a black plastic bag, or the honeycomb insulated enclosure (HC) shown in Figure 5.9. These experiments were performed because if the EPS block is left on site, it will require covering for rainfall or dew protection, which can easily be accomplished by a thin plastic bag. Additionally, use of the HC enclosure provides additional insulation with minimal additional effort on site.

Temperature measurements were recorded for 4 to 24 hours at intervals of 5 minutes. Air measurements were based on the average of two thermocouples placed approximately 1 meter above the EPS device. EPS block temperatures were based on an average of two of the eight thermocouples present in the block that are used to measure specimen temperature (the

same two locations were used throughout). The device and covering was allowed to acclimate to temperature for 30 minutes prior to data collection.

Table 13.2 provides equipment configuration evaluation results. The average air temperature and average block temperature for the testing period were recorded for each test interval that is represented by a row in Table 13.2 (note that some of the fifteen experiments in Table 13.2 were performed on the same day). The difference between the two average temperatures (air and block) was calculated and is denoted as ΔT_b. A positive value for ΔT_b indicates that the block temperature was higher than the air temperature as this was the case for most the majority of test times. An average of the ΔT_b for each test day is also shown in the table along with the standard deviation of the ΔT_b values.

Table 13.2. Insulation Investigation Results

Covering	Avg. Air Temp. (˚C)	Avg. Block Temp. (˚C)	ΔT_b (˚C)	Average of ΔT_b (˚C)	Standard Deviation of ΔT_b (˚C)
None	33.8	35.5	1.7	1.1	1.6
None	37.9	36.7	-1.2		
None	29.9	32.5	2.6		
None	29.1	32.0	2.9		
None	30.8	31.2	0.4		
None	29.8	30.0	0.2		
Clear Bag	33.8	39.3	5.5	5.3	1.5
Clear Bag	37.9	41.6	3.7		
Clear Bag	29.9	36.6	6.7		
Black Bag	29.1	37.1	8.0	6.2	2.0
Black Bag	30.8	37.4	6.6		
Black Bag	29.8	33.9	4.1		
HC	27.1	28.4	1.3	1.0	0.3
HC	23.5	24.2	0.7		
HC	22.1	23.1	1.0		

There was no meaningful difference in no covering and the HC insulation with an increase in temperature in the block of 1 ^{o}C for practical purposes. This is not surprising as the HC block is not fully sealed and a slight amount of air flow can occur around the edges of the HC block lid. Black and clear plastic coverings caused temperatures in the EPS device to increase noticeably more than the HC honeycomb insulation. Both plastic coverings restrict air flow from the EPS device, so it stands to reason they would create more of a temperature differential. As expected a black plastic covering caused the highest temperature differential. Practically, use of a plastic covering is expected to increase temperature at the EPS measurement locations by 4 to 5 ^{o}C more than the EPS device alone, which is manageable.

The primary finding from Table 13.2 experiments is that use of the HC block nor a plastic bag covering (or likely even a combination as would be used on site) is prohibitive but that the configuration needs to be consistent for every experiment. Even if, for example, there is no chance of rain, the same plastic covering should be used in all cases to have the same baseline temperature configuration. Use of a plastic bag is expected to provide a slight

advantage as additional heat at the measurement locations should help detect cement contents. All remaining experiments were conservative and only used a bag or the HC covering. The recommendation from this research is to use the EPS thermal profile block inside a secondary insulation block (e.g. HC) covered with a black plastic bag when collecting on site thermal measurements data.

13.3 Phase 3 Thermal Profile Results: Evaluating Test Specimens

Results of the phase 3 thermal profile investigation are shown in Tables 13.3 through 13.6 on an individual specimen basis. Air temperatures are included for comparison purposes. Figure 11.1b was used as a guide for selecting test times for investigating change in temperature relative to the reference specimens at several intervals. The ΔT concept from Figure 11.1a was also investigated. Checkpoints were evaluated for no cover, clear plastic cover, and the honeycomb insulation (HC) device. Differences between a reference cylinder (Section 13.3.1) and the test cylinders temperature were reported as ΔT_i at time interval i. Positive values of ΔT_i indicate an increase in temperature of the specimen in the block compared to the reference specimen, while negative values of ΔT_i indicate the opposite. Compressive strengths were measured at 24 $\pm$ 1 hr, then adjusted for density using equation 12.1. Specimens were compacted either directly after mixing or after a 30 minute delay.

In a few cases the data used to calculate $\sigma_{max\ adj}$ was not available due to data recording omissions. Since the main purpose of this chapter was to evaluate thermal profile testing feasibility on site, the thermal results of these specimens were still used in data analysis. Section 13.3.2 compares 1 day compressive strengths with ΔT and ΔT_i.

13.3.1 Reference Specimens

There were two methods used to produce reference specimens for temperature results analysis. For specimens with no insulation or clear plastic insulation, a reference specimen was pre-mixed and compacted, then included with the test specimens in the block (Method 1). This specimen was allowed to acclimate to temperature in the same manner as the EPS device and insulation. It was later determined that a pre-mixed reference may not perform the same as a reference that is mixed and compacted at the same time as cylinder specimens (Method 2). In Method 2 the reference cylinder is prepared, conditioned at the same location as the materials used to produce soil-cement specimens, and compacted using the same procedure as the test specimens. For testing in the HC insulated block, both types of reference specimens were included with the test specimens.

Figure 13.1 is an equality plot comparing measured temperatures of Method 1 and Method 2 taken at 1, 2, 4, 6, 8, 16, and 24 hr. RTO analysis produced a slope of 0.99 indicating little average overall difference between the two methods. Early times (1 and 2 hr) largely represented the maximum and minimum temperature values, while later ages fell in between. Although the average behavior of these materials was similar, there is noticeable scatter in the data. Producing reference specimens is a potential obstacle in using change in temperature concepts (ΔT and ΔT_i) during field quality control. Use of temperature change concepts is likely a necessary component of using thermal measurements in the field. The key challenge is having a reference specimen and a soil-cement specimen in the EPS device at the same temperature at the beginning of the thermal measurement period.

Table 13.3. No Covering Soil B Thermal and Compressive Strength Individual Specimen Results

Specimen ID	Time Delay (min)	Air Temp. (˚C)				Thermal Profile Data ΔT_i (˚C) at Time (hr)							T_{max} and ΔT Data (°C)		
		Average	Std Dev	Max	Min	1	2	4	6	8	16	24	t_{max} (hr)	T_{max}	ΔT
PR-1-PB4-1N	0	27.9	6.6	47.1	20.2	8.3	8.0	7.2	5.9	4.8	1.7	0.2	0.7	38.0	9.8
PR-1-PB4-2N	0	24.6	4.7	43.6	20	6.2	5.8	5.2	4.4	3.7	1.3	0.0	0.0	35.4	5.3
PR-1-PB4-3N	0	30.5	5.4	44.7	24	1.3	2.3	5.0	6.3	7.3	5.1	0.2	4.0	35.1	4.6
PR-1-PB4-5N	0	31.8	7.8	56.7	23	1.5	1.9	2.2	2.0	1.8	0.7	-0.3	3.4	35.7	2.1
PR-1-PB4-7N	0	27.3	7.1	52.4	19	5.9	6.4	5.8	5.0	4.5	2.0	0.8	8.0	31.8	4.5
PR-1-PB4-8N	0	27.5	7.6	57.7	21	6.8	6.4	5.9	4.9	4.2	1.7	2.4	4.0	31.6	5.8
PR-1-PB5-1N	0	27.9	6.6	47.1	20	8.0	7.6	6.7	5.7	4.8	2.4	1.1	0.7	37.3	9.1
PR-1-PB5-2N	0	24.6	4.7	43.6	20	4.8	4.7	4.3	3.5	2.7	1.0	0.4	2.8	32.3	4.6
PR-1-PB5-3N	0	30.5	5.4	44.7	24	1.8	2.5	4.6	5.7	6.6	4.8	1.5	2.3	35.3	2.8
PR-1-PB5-5N	0	31.8	7.8	56.7	23	0.8	1.3	1.5	1.3	1.1	0.5	0.3	3.1	35.0	1.5
PR-1-PB5-7N	0	27.3	7.1	52.4	19	4.9	5.5	4.8	3.9	3.3	1.2	0.9	6.5	30.5	3.9
PR-1-PB5-8N	0	27.5	7.6	57.7	21	6.9	5.8	4.9	4.0	3.3	1.3	2.3	3.4	30.7	5.3
PR-1-PB6-1N	0	27.9	6.6	47.1	20	10.2	10.	9.0	7.7	6.5	3.2	1.2	1.9	39.2	10.1
PR-1-PB6-2N	0	24.6	4.7	43.6	20	5.5	6.3	6.2	5.5	4.8	2.7	1.3	0.0	36.3	6.2
PR-1-PB6-3N	0	30.5	5.4	44.7	24	2.4	3.7	6.3	7.6	8.5	6.3	1.1	3.8	36.8	5.7
PR-1-PB6-5N	0	31.8	7.8	56.7	23	1.7	2.5	3.0	2.9	2.7	1.8	0.6	3.8	36.5	2.9
PR-1-PB6-7N	0	27.3	7.1	52.4	19	7.3	8.2	7.5	6.1	5.3	2.8	1.7	6.3	32.7	6.1
PR-1-PB6-8N	0	27.5	7.6	57.7	21	8.7	7.8	7.1	6.1	5.3	2.8	1.6	3.3	32.9	7.5
PR-2-PB4-9N	30	25.4	4.2	37.6	21	2.5	2.5	4.5	3.0	2.9	1.4	0.5	10.2	28.3	2.6
PR-2-PB4-10N	30	25.4	4.2	37.6	21	2.2	2.6	4.1	2.5	2.4	1.6	0.9	9.3	28.7	3.1
PR-2-PB4-11N	30	23.8	3.0	33.2	20	4.8	5.1	4.4	3.8	3.1	1.1	0.5	2.8	32.5	4.9
PR-2-PB4-12N	30	23.8	3.0	33.2	20	4.0	4.1	3.7	3.2	2.9	1.3	1.0	3.3	31.6	3.9
PR-2-PB4-13N	30	22.6	5.1	36.5	16	2.4	2.8	2.9	2.7	2.7	1.4	0.4	9.0	27.2	2.6
PR-2-PB4-14N	30	22.6	5.1	36.5	16	2.3	2.9	3.1	2.3	2.0	1.2	1.0	8.9	26.6	1.9
PR-2-PB5-9N	30	25.4	4.2	37.6	21	5.0	6.7	7.9	2.8	1.7	-0.3	-0.7	3.9	30.1	8.5
PR-2-PB5-10N	30	25.4	4.2	37.6	21	3.3	4.1	7.7	3.8	3.4	1.8	1.0	4.1	29.8	8.3
PR-2-PB5-11N	30	23.8	3.0	33.2	20	1.0	0.7	-0.9	-1.9	-2.5	-2.5	0.3	1.4	28.8	1.7
PR-2-PB5-12N	30	23.8	3.0	33.2	20	3.7	3.9	3.3	2.8	2.4	0.9	1.0	2.4	31.3	3.8
PR-2-PB5-13N	30	22.6	5.1	36.5	16	1.9	2.4	2.9	2.3	2.1	0.9	0.4	8.2	26.6	2.1
PR-2-PB5-14N	30	22.6	5.1	36.5	16	3.1	4.0	4.5	3.6	3.0	1.3	0.9	7.6	27.6	3.2
PR-2-PB6-9N	30	25.4	4.2	37.6	21	3.5	3.0	6.4	3.7	3.4	2.1	1.3	8.9	28.7	3.2
PR-2-PB6-10N	30	25.4	4.2	37.6	21	4.6	5.8	9.6	5.4	4.8	2.1	0.8	3.8	32.3	10.7
PR-2-PB6-11N	30	23.8	3.0	33.2	20	3.9	4.4	4.3	3.9	3.6	2.0	1.0	4.2	32.1	4.3
PR-2-PB6-12N	30	23.8	3.0	33.2	20	4.4	4.7	4.0	3.3	2.7	0.6	0.8	2.4	32.1	4.6
PR-2-PB6-13N	30	22.6	5.1	36.5	16	3.3	3.9	3.9	3.1	2.9	1.9	1.2	8.7	27.4	2.8
PR-2-PB6-14N	30	22.6	5.1	36.5	16	3.7	5.0	5.5	4.5	3.9	1.5	0.6	6.5	28.5	4.3

--Method 1 references were used to calculate ΔT_i

Table 13.4. Clear Covering Soil B Thermal and Compressive Strength Individual Specimen Results

Specimen ID	Time Delay (min)	Air Temp. (˚C)				Thermal Profile Data ΔT_i (˚C) at Time (hr)							T_{max} and ΔT Data (°C)		
		Average	Std Dev	Max	Min	1	2	4	6	8	16	24	t_{max} (hr)	T_{max}	ΔT
PR-1-PB4-1B	0	27.9	6.6	47.1	20.2	10.5	9.5	8.1	7.2	6.1	3.2	2.6	3.0	38.6	9.3
PR-1-PB4-2B	0	24.6	4.7	43.6	20.3	7.1	7.0	6.3	5.6	4.8	2.6	1.5	0.0	34.6	4.6
PR-1-PB4-3B	0	30.5	5.4	44.7	24.2	2.8	3.3	3.6	3.5	3.2	2.0	1.2	20.3	36.2	4.6
PR-1-PB4-5B	0	31.8	7.8	56.7	23.8	0.7	1.3	1.9	2.0	1.9	1.3	1.5	4.2	36.1	1.9
PR-1-PB4-7B	0	27.3	7.1	52.4	19.1	6.5	6.7	6.5	5.3	4.7	2.7	1.4	7.3	32.8	5.0
PR-1-PB4-8B	0	27.5	7.6	57.7	21.0	-4.3	-0.2	3.7	4.9	5.3	6.2	-8.2	4.1	32.4	4.0
PR-1-PB5-1B	0	27.9	6.6	47.1	20.2	8.6	7.9	6.7	5.9	5.1	2.8	1.7	3.2	37.1	8.7
PR-1-PB5-2B	0	24.6	4.7	43.6	20.3	6.3	6.7	6.2	5.5	4.7	2.3	1.6	3.3	34.1	6.3
PR-1-PB5-3B	0	30.5	5.4	44.7	24.2	3.2	3.8	3.9	3.6	3.1	1.8	1.4	3.0	36.5	3.9
PR-1-PB5-5B	0	31.8	7.8	56.7	23.8	0.1	0.9	1.5	1.6	1.6	1.0	7.3	4.0	35.7	1.5
PR-1-PB5-7B	0	27.3	7.1	52.4	19.1	6.4	6.8	6.5	5.2	4.5	2.3	3.9	7.3	32.7	4.9
PR-1-PB5-8B	0	27.5	7.6	57.7	21.0	-5.0	-0.9	2.5	3.6	4.1	5.4	-7.6	3.91	31.3	2.39
PR-1-PB6-1B	0	27.9	6.6	47.1	20.2	11.2	10.	9.1	7.9	6.7	3.5	2.2	2.9	29.9	0.6
PR-1-PB6-2B	0	24.6	4.7	43.6	20.3	5.4	6.3	6.2	5.6	4.9	2.9	1.4	0.0	34.2	4.0
PR-1-PB6-3B	0	30.5	5.4	44.7	24.2	3.0	3.8	4.1	3.9	3.6	2.3	1.7	3.7	36.6	4.1
PR-1-PB6-5B	0	31.8	7.8	56.7	23.8	0.5	1.6	2.3	2.4	2.4	1.8	0.4	4.0	36.5	2.3
PR-1-PB6-7B	0	27.3	7.1	52.4	19.1	7.4	7.9	7.4	5.9	5.1	2.9	1.6	7.0	33.3	5.6
PR-1-PB6-8B	0	27.5	7.6	57.7	21.0	-3.8	0.6	4.3	5.3	5.7	6.5	-8.2	3.9	33.0	4.1
PR-2-PB4-9B	30	25.4	4.2	37.6	21.8	2.0	3.3	3.1	2.6	2.7	1.3	0.5	8.4	28.9	2.6
PR-2-PB4-10B	30	25.4	4.2	37.6	21.8	1.7	3.0	2.7	1.4	1.4	1.1	0.7	11.8	27.9	1.4
PR-2-PB4-11B	30	23.8	3.0	33.2	20.0	3.5	3.7	3.8	3.4	2.8	1.2	1.1	3.9	32.5	3.8
PR-2-PB4-12B	30	23.8	3.0	33.2	20.0	2.7	3.0	2.6	2.4	2.2	1.2	1.3	2.6	31.4	3.0
PR-2-PB4-13B	30	22.6	5.1	36.5	16.3	2.3	2.8	3.9	3.6	3.3	1.7	0.8	7.5	28.9	3.4
PR-2-PB4-14B	30	22.6	5.1	36.5	16.3	2.0	3.6	3.7	2.2	1.8	1.2	1.1	7.8	27.4	1.9
PR-2-PB5-9B	30	25.4	4.2	37.6	21.8	1.2	3.2	3.1	2.1	1.9	0.7	0.3	7.9	28.2	2.0
PR-2-PB5-10B	30	25.4	4.2	37.6	21.8	3.2	4.9	5.7	4.0	3.5	1.8	1.0	6.1	29.9	3.9
PR-2-PB5-11B	30	23.8	3.0	33.2	20.0	1.6	1.9	1.8	1.4	1.1	0.2	0.6	2.8	30.5	2.0
PR-2-PB5-12B	30	23.8	3.0	33.2	20.0	3.2	3.4	3.0	2.6	2.3	1.0	1.2	2.6	31.8	3.4
PR-2-PB5-13B	30	22.6	5.1	36.5	16.3	2.0	2.9	4.3	3.1	2.5	1.1	0.8	7.1	28.2	2.7
PR-2-PB5-14B	30	22.6	5.1	36.5	16.3	2.4	4.5	5.2	3.4	2.8	1.3	1.1	6.6	28.5	3.2
PR-2-PB6-9B	30	25.4	4.2	37.6	21.8	3.0	3.9	3.8	2.6	2.5	1.7	1.1	9.9	28.8	2.4
PR-2-PB6-10B	30	25.4	4.2	37.6	21.8	4.3	5.8	5.7	4.0	3.7	1.6	0.5	7.0	30.0	3.9
PR-2-PB6-11B	30	23.8	3.0	33.2	20.0	2.6	3.3	3.5	3.3	3.1	2.0	1.4	4.3	32.2	3.5
PR-2-PB6-12B	30	23.8	3.0	33.2	20.0	3.3	3.6	3.3	2.8	2.4	0.9	1.3	2.6	32.1	3.7
PR-2-PB6-13B	30	22.6	5.1	36.5	16.3	2.9	3.4	3.5	3.0	2.7	1.9	1.3	8.2	28.3	2.7
PR-2-PB6-14B	30	22.6	5.1	36.5	16.3	3.5	5.8	6.2	3.9	3.2	1.4	1.0	4.6	29.0	5.7

--Method 1 references were used to calculate ΔT_i

Table 13.5. HC Covering Soil B Thermal and Compressive Strength Individual Specimen Results

Specimen ID	Time Delay (min)	Air Temp. (˚C)				Thermal Profile Data ΔT_i (˚C) at Time (hr)							T_{max} and ΔT Data (^{o}C)		
		Average	Std Dev	Max	Min	1	2	4	6	8	16	24	t_{max} (hr)	T_{max}	ΔT
PR-3-PB4-23	30	20.8	3.2	29.5	16.3	2.9	3.3	3.4	3.3	3.1	2.1	1.3	0.0	28.4	-1.2
PR-3-PB4-24	30	20.8	3.2	29.5	16.3	3.0	3.4	3.7	3.8	3.7	3.1	1.8	0.0	27.6	0.2
PR-3-PB4-25	30	23.6	4.6	37.2	18.3	3.0	1.7	0.5	2.8	2.8	2.0	1.4	8.2	28.4	2.2
PR-3-PB4-26	30	23.6	4.6	37.2	18.3	2.4	5.2	0.0	2.3	2.2	2.4	2.2	8.2	27.3	1.1
PR-3-PB4-27	30	22.4	2.7	29.5	19.5	3.4	3.8	4.0	3.7	3.4	2.3	1.6	0.1	32.9	0.4
PR-3-PB4-28	30	22.4	2.7	29.5	19.5	2.8	3.3	3.6	3.7	3.6	3.0	2.4	0.1	32.2	-0.2
PR-3-PB5-23	30	20.8	3.2	29.5	16.3	2.7	3.3	3.4	3.2	2.9	1.8	1.2	0.0	28.6	-1.0
PR-3-PB5-24	30	20.8	3.2	29.5	16.3	2.7	3.2	3.5	3.5	3.3	2.5	1.4	0.0	28.5	-1.1
PR-3-PB5-25	30	23.6	4.6	37.2	18.3	2.6	2.5	0.3	3.9	3.5	2.1	1.2	7.8	29.3	3.1
PR-3-PB5-26	30	23.6	4.6	37.2	18.3	2.6	4.9	2.6	3.1	2.8	2.2	1.9	4.3	29.0	2.3
PR-3-PB5-27	30	22.4	2.7	29.5	19.5	3.1	3.8	4.0	3.7	3.4	2.1	1.3	0.1	32.8	0.4
PR-3-PB5-28	30	22.4	2.7	29.5	19.5	2.8	3.4	3.6	3.5	3.4	2.6	1.9	0.1	32.9	0.5
PR-3-PB6-23	30	20.8	3.2	29.5	16.3	3.3	4.1	4.3	4.3	4.1	3.3	1.9	0.0	28.2	-1.4
PR-3-PB6-24	30	20.8	3.2	29.5	16.3	3.0	3.8	4.0	3.8	3.4	2.3	1.3	0.0	28.7	-0.9
PR-3-PB6-25	30	23.6	4.6	37.2	18.3	3.3	3.5	-0.9	3.3	3.1	2.9	2.4	8.2	28.4	2.2
PR-3-PB6-26	30	23.6	4.6	37.2	18.3	2.9	5.3	3.0	3.4	3.1	2.2	1.5	4.3	29.9	3.2
PR-3-PB6-27	30	22.4	2.7	29.5	19.5	3.6	4.5	4.7	4.7	4.5	3.5	2.7	0.1	32.4	-0.8
PR-3-PB6-28	30	22.4	2.7	29.5	19.5	3.3	4.0	4.1	3.9	3.6	2.3	1.5	0.1	34.1	1.6
PR-3-PB3-17	30	24.5	3.4	34.1	20.6	2.5	2.7	2.8	2.7	2.6	1.8	1.0	2.7	30.7	2.2
PR-3-PB3-18	30	24.5	3.4	34.1	20.6	2.6	2.9	3.2	3.3	3.3	2.8	1.2	3.8	30.5	2.0
PR-3-PB3-19	30	17.2	5.0	30.3	11.1	2.9	1.7	0.9	2.1	2.0	1.1	0.5	6.6	24.1	1.5
PR-3-PB3-20	30	17.2	5.0	30.3	11.1	2.6	2.0	-1.5	1.7	1.8	2.2	1.7	8.8	23.4	0.8
PR-3-PB3-21	30	20.0	2.3	26.7	17.0	2.1	2.5	2.7	2.7	2.5	1.8	1.2	0.0	35.5	-1.9
PR-3-PB3-22	30	20.0	2.3	26.7	17.0	2.5	2.9	3.2	3.4	3.4	3.1	1.7	0.0	33.7	-3.8
PR-3-PB5-17	30	24.5	3.4	34.1	20.6	1.7	1.8	1.6	1.3	1.2	0.7	1.0	1.5	30.1	1.5
PR-3-PB5-18	30	24.5	3.4	34.1	20.6	2.8	3.3	3.5	3.4	3.3	2.5	1.2	2.7	31.5	3.0
PR-3-PB5-19	30	17.2	5.0	30.3	11.1	2.9	2.9	1.7	3.8	3.2	1.4	0.4	5.9	25.8	3.4
PR-3-PB5-20	30	17.2	5.0	30.3	11.1	2.4	3.2	1.9	3.0	2.6	2.0	1.4	6.6	24.9	2.4
PR-3-PB5-21	30	20.0	2.3	26.7	17.0	3.6	4.3	4.3	3.9	3.5	2.1	1.4	0.0	34.6	-2.8
PR-3-PB5-22	30	20.0	2.3	26.7	17.0	3.8	4.5	4.6	4.5	4.3	3.1	1.9	0.0	34.9	-2.5
PR-3-PB7-17	30	24.5	3.4	34.1	20.6	3.6	4.4	4.6	4.5	4.3	3.4	1.7	3.3	32.1	3.7
PR-3-PB7-18	30	24.5	3.4	34.1	20.6	3.0	3.8	4.0	3.8	3.4	2.2	1.3	2.8	32.1	3.6
PR-3-PB7-19	30	17.2	5.0	30.3	11.1	3.2	3.4	1.4	3.3	3.1	2.7	2.1	6.6	24.8	2.3
PR-3-PB7-20	30	17.2	5.0	30.3	11.1	3.0	4.5	3.0	3.2	2.8	1.7	1.1	4.3	25.5	3.0
PR-3-PB7-21	30	20.0	2.3	26.7	17.0	2.3	3.2	3.6	3.8	3.8	3.3	1.9	0.0	34.2	-3.2
PR-3-PB7-22	30	20.0	2.3	26.7	17.0	2.1	2.7	2.9	2.8	2.6	1.8	1.0	0.0	37.0	-0.4

--Method 2 references were used to calculate ΔT_i

Table 13.6. HC Covering Soil D Thermal and Compressive Strength Individual Specimen Results

	Time Delay	Air Temp. (˚C)				Thermal Profile Data ΔT_i (˚C) at Time (hr)							T_{max} and ΔT Data (^{o}C)		
Specimen ID	**(min)**	**Average**	**Std Dev**	**Max**	**Min**	**1**	**2**	**4**	**6**	**8**	**16**	**24**	t_{max} **(hr)**	T_{max}	ΔT
PR-4-PD4-29	30	16.0	2.6	21.7	12.6	1.4	1.9	2.4	2.6	2.5	2.2	1.7	5.3	22.1	2.0
PR-4-PD4-30	30	16.0	2.6	21.7	12.6	1.8	2.3	2.9	3.2	3.2	3.2	2.5	5.9	22.2	2.1
PR-4-PD4-31	30	18.1	2.5	23.8	14.9	1.0	1.6	2.3	2.6	2.6	2.3	1.6	6.0	22.8	2.0
PR-4-PD4-32	30	18.1	2.5	23.8	14.9	1.1	1.6	2.3	2.7	2.9	2.9	2.1	6.6	22.5	1.7
PR-4-PD4-33	30	17.6	2.8	23.2	13.3	1.1	1.2	1.3	1.6	1.6	1.5	1.4	9.7	20.9	1.5
PR-4-PD4-34	30	17.6	2.8	23.2	13.3	2.1	1.7	1.0	0.5	0.3	0.2	0.3	9.7	19.7	0.3
PR-4-PD5-29	30	16.0	2.6	21.7	12.6	1.2	1.7	2.3	2.6	2.6	2.2	1.7	6.2	22.3	2.2
PR-4-PD5-30	30	16.0	2.6	21.7	12.6	1.4	1.9	2.4	2.9	2.9	2.9	2.2	6.1	22.5	2.4
PR-4-PD5-31	30	18.1	2.5	23.8	14.9	0.6	1.2	2.0	2.4	2.5	2.3	1.7	6.6	22.8	2.1
PR-4-PD5-32	30	18.1	2.5	23.8	14.9	0.5	1.1	1.9	2.4	2.5	2.7	1.9	6.6	22.7	2.0
PR-4-PD5-33	30	17.6	2.8	23.2	13.3	1.1	1.4	1.8	2.1	2.1	1.8	1.5	9.6	21.4	2.0
PR-4-PD5-34	30	17.6	2.8	23.2	13.3	0.4	0.6	0.6	0.8	0.9	1.3	1.5	9.8	20.4	1.0
PR-4-PD6-29	30	16.0	2.6	21.7	12.6	1.7	2.3	2.9	3.5	4.0	4.2	3.1	7.3	22.9	3.0
PR-4-PD6-30	30	16.0	2.6	21.7	12.6	1.4	1.9	2.5	3.0	3.3	3.0	2.2	7.3	22.8	2.9
PR-4-PD6-31	30	18.1	2.5	23.8	14.9	1.0	1.6	2.5	3.2	3.6	3.9	2.7	7.8	28.3	2.7
PR-4-PD6-32	30	18.1	2.5	23.8	14.9	0.1	0.8	1.7	2.4	2.7	2.8	2.0	7.8	23.0	2.4
PR-4-PD6-33	30	17.6	2.8	23.2	13.3	1.1	1.2	1.2	1.5	2.0	2.5	2.5	14.1	21.6	2.5
PR-4-PD6-34	30	17.6	2.8	23.2	13.3	0.7	1.1	1.3	1.6	1.7	1.9	1.9	9.8	21.2	1.8
PR-4-PD3-35	30	16.1	4.7	28.9	10.4	0.1	-0.2	1.6	1.8	1.8	1.7	1.3	5.4	23.0	1.2
PR-4-PD3-36	30	16.1	4.7	28.9	10.4	1.2	-0.4	1.1	1.5	1.7	2.5	2.3	5.9	22.2	0.4
PR-4-PD3-37	30	13.9	5.6	31.0	8.5	0.6	1.4	2.0	2.1	2.1	1.9	-0.8	0.0	32.8	-1.9
PR-4-PD3-38	30	13.9	5.6	31.0	8.5	0.4	1.4	2.2	2.6	2.9	3.4	-0.2	0.0	32.6	-2.1
PR-4-PD3-39	30	9.8	4.0	23.0	4.2	3.1	2.6	0.7	1.0	1.2	0.5	-0.3	7.5	15.9	1.5
PR-4-PD3-40	30	9.8	4.0	23.0	4.2	-0.3	-0.7	-0.1	0.4	0.7	0.8	0.8	8.5	14.8	0.5
PR-4-PD5-35	30	16.1	4.7	28.9	10.4	0.0	-0.5	2.2	2.6	2.6	2.2	1.6	5.8	24.1	2.8
PR-4-PD5-36	30	16.1	4.7	28.9	10.4	1.4	0.6	1.9	2.5	2.6	3.0	2.5	6.1	23.8	2.0
PR-4-PD5-37	30	13.9	5.6	31.0	8.5	0.2	1.1	2.0	2.4	2.5	2.3	-1.0	0.0	28.8	-5.9
PR-4-PD5-38	30	13.9	5.6	31.0	8.5	-0.3	0.7	1.9	2.6	3.0	3.6	1.2	0.0	30.2	-4.4
PR-4-PD5-39	30	9.8	4.0	23.0	4.2	1.2	1.6	1.2	1.5	1.7	0.9	0.2	7.8	16.6	2.3
PR-4-PD5-40	30	9.8	4.0	23.0	4.2	0.5	1.1	0.7	1.1	1.3	1.1	0.7	8.6	16.1	1.9
PR-4-PD7-35	30	16.1	4.7	28.9	10.4	0.2	-1.2	1.5	2.7	3.5	4.5	3.9	8.3	24.1	2.7
PR-4-PD7-36	30	16.1	4.7	28.9	10.4	1.2	0.6	1.3	2.4	3.1	3.5	2.7	7.8	24.2	2.7
PR-4-PD7-37	30	13.9	5.6	31.0	8.5	-0.2	0.9	2.4	4.0	4.8	5.4	0.2	0.0	27.3	-7.4
PR-4-PD7-38	30	13.9	5.6	31.0	8.5	-0.7	0.2	1.4	2.8	3.3	3.5	1.7	0.0	30.5	-4.1
PR-4-PD7-39	30	9.8	4.0	23.0	4.2	0.7	0.3	-0.1	0.6	1.3	2.7	2.4	11.7	16.5	2.6
PR-4-PD7-40	30	9.8	4.0	23.0	4.2	0.7	1.1	-0.1	0.3	0.9	1.6	1.2	11.0	16.2	2.3

--*Method 2 references were used to calculate ΔT_i for all cases except those marked with "*" in which case Method 1 was used.*

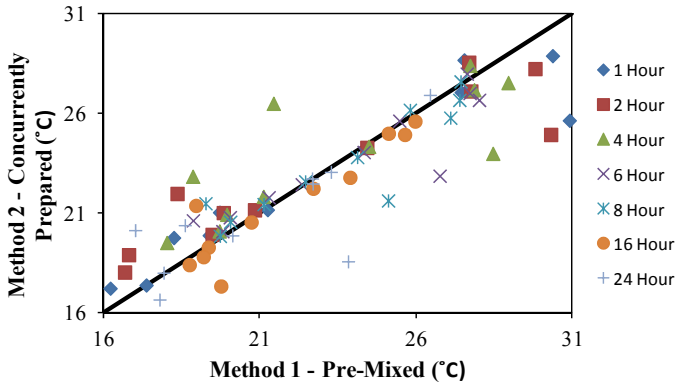

Figure 13.1. Comparison of Reference Specimen Methods

13.3.2 Comparison of 1 Day Strength and Thermal Measurement Outputs

Linear Regression and Analysis of Variance (ANOVA) techniques were applied to the data presented in Tables 13.3 to 13.6; each table was analyzed separately. The variables of interest were ΔT or ΔT_i (x-value) and $\sigma_{max\ adj}$ (y-value). The investigation used ΔT or ΔT_i with ^{o}C units and $\sigma_{max\ adj}$ with MPa units to provide outputs that were easier to understand absent scientific notation. Statistically significant relationships were identified with p-values below 0.05. Statistical results are provided in Table 13.7 and Figure 13.2.

There was no statistical correlation between ΔT and 1 day compressive strength for any of the four sets of cases investigated. In most cases, p-values were very high (0.590 to 0.877). These findings do not agree with those observed in Chapter 12 where ΔT correlated to 7 day compressive strength. One likely explanation for the difference was an environmental chamber was used in Chapter 12 (i.e. specimens were not left outside during their thermal measurement period), and in Chapter 13 specimens were left outside with different insulation levels. It should also be noted that 1 day compressive strengths are expected to be more variable than 7 day compressive strength, which could have some influence when interpreting the ΔT or ΔT_i correlations presented in this section.

Visual observation of Tables 13.3 to 13.6 reveals that t_{max} (i.e. the time at which ΔT occurred varies greatly and does not follow general expectations for an exothermic product such as portland cement). One example per table is provided in the bulleted list that follows where t_{max} varies from 0 hr (i.e. first measurement was the highest) to up to 20.3 hr within a group of six identically prepared specimens.

- Table 13.3: 0 hr (PR-1-PB4-2N) to 8 hr (PR-1-PB4-7N)
- Table 13.4: 0 hr (PR-1-PB4-2B) to 20.3 hr (PR-1-PB4-3B)
- Table 13.5: 0 hr (PR-3-PB4-23) to 8.2 hr (PR-3-PB-4-26)
- Table 13.6: 0 hr (PR-4-PD7-38) to 11.7 hr (PR-4-PD7-39)

Maximum temperatures immediately after preparation for specimens not flash setting is counter intuitive and likely indicates outside influences are reducing temperature at the bottom of the specimen faster than portland cement's hydration process is increasing temperature. With the amount of insulation provided in these experiments, this behavior seems plausible, and indicates that ΔT_i may be a more suitable indicator when no environmental chamber is present and specimens are left outside. The remainder of this chapter's investigation focuses on ΔT_i.

Table 13.7. Phase 3 Strength to Thermal Profile Correlations

Soil	Covering	*X*-Axis Value	R^2 adj.	*p-value*	Slope (MPa per ^oC)
B	None	ΔT	-0.04	0.877	---
B	None	$\Delta T_{i=1}$	-0.04	0.907	---
B	None	$\Delta T_{i=2}$	-0.03	0.779	---
B	None	$\Delta T_{i=4}$	-0.04	0.941	---
B	None	$\Delta T_{i=6}$	-0.04	0.955	---
B	None	$\Delta T_{i=8}$	-0.04	0.912	---
B	None	$\Delta T_{i=16}$	-0.04	0.985	---
B	None	$\Delta T_{i=24}$	0.12	0.035	0.22
B	Clear	ΔT	-0.03	0.750	---
B	Clear	$\Delta T_{i=1}$	0.09	0.057	---
B	Clear	$\Delta T_{i=2}$	0.02	0.203	---
B	Clear	$\Delta T_{i=4}$	-0.04	0.963	---
B	Clear	$\Delta T_{i=6}$	0.00	0.362	---
B	Clear	$\Delta T_{i=8}$	0.03	0.173	---
B	Clear	$\Delta T_{i=16}$	0.15	0.022	0.11
B	Clear	$\Delta T_{i=24}$	0.11	0.040	-0.05
B	HC	ΔT	-0.02	0.590	---
B	HC	$\Delta T_{i=1}$	-0.02	0.515	---
B	HC	$\Delta T_{i=2}$	0.13	0.030	---
B	HC	$\Delta T_{i=4}$	-0.02	0.476	---
B	HC	$\Delta T_{i=6}$	0.07	0.081	---
B	HC	$\Delta T_{i=8}$	0.11	0.040	0.21
B	HC	$\Delta T_{i=16}$	0.29	0.001	0.30
B	HC	$\Delta T_{i=24}$	0.26	0.002	0.38
D	HC	ΔT	0.05	0.113	---
D	HC	$\Delta T_{i=1}$	0.01	0.251	---
D	HC	$\Delta T_{i=2}$	0.00	0.355	---
D	HC	$\Delta T_{i=4}$	-0.04	0.981	---
D	HC	$\Delta T_{i=6}$	-0.03	0.642	---
D	HC	$\Delta T_{i=8}$	-0.01	0.452	---
D	HC	$\Delta T_{i=16}$	0.13	0.045	0.10
D	HC	$\Delta T_{i=24}$	0.02	0.200	---

--Slopes were only recorded in cases where the *p-value* was less than 0.05

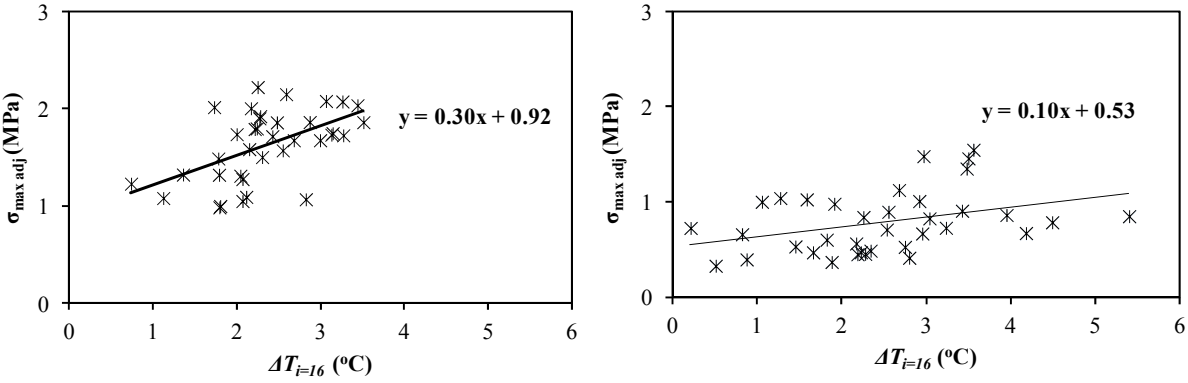

a) Soil B, HC, $\Delta T_{i=16}$ b) Soil D, HC, $\Delta T_{i=16}$

Figure 13.2. Strength to Thermal Measurement Correlations at 16 hr

Seven of the twenty-eight ΔT_i cases investigated detected a statistically significant correlation (i.e. *p-value* below 0.05) between ΔT_i and $\sigma_{max\ adj}$. The earliest a correlation was detected was 8 hours (i.e. $\Delta T_{i\ =\ 8}$), and correlations were also detected at 16 and 24 hours. One of the correlations detected produced a negative slope (i.e. that increased temperature indicated decreased strength), which is not intuitive and was dismissed a coincidence that led to the correlation.

Three of the four soil-covering type combinations investigated detected a statistically significant correlation at 16 hours. The HC configuration is of most interest for field quality control purposes, and at 16 hours *Pit B* and *Pit D* both detected correlations between $\Delta T_{i\ =\ 16}$ and $\sigma_{max\ adj}$. Figure 13.2 plots these correlations. The aforementioned Chapter 12 correlations between ΔT and $\sigma_{max\ adj}$ were 0.24 MPa per ^{o}C for SR475 (i.e. *Pit E*) and 0.33 MPa per ^{o}C for SR9 (i.e. *Pit D*). The *Pit B* HC correlation was 0.30 MPa per ^{o}C, which is bracketed by the Chapter 12 values, whereas the *Pit B* HC correlation was noticeably less at 0.10 MPa per ^{o}C.

Overall, detecting correlations between thermal measurements and compressive strength while specimens remained outdoors the entire time protected by easily portable insulation systems with no heating/cooling capabilities is promising. The work presented in this section supports concept feasibility. It is very likely that improved resolution could be obtained with larger specimen sizes and/or additional insulation. An environmental chamber pre-conditioned to the initial material temperature would very likely enhance data resolution even further. The remaining sections of this chapter investigate cement content detection at several ΔT_i time intervals by comparing thermal measurements to known cement contents.

13.3.3 No Covering Equipment Configuration

Table 13.8 provides no covering test results. Thermal values shown are averages of the 6 replicate specimens; in this case the first 6 rows of Table 13.3 are averaged to construct the first row of Table 13.8. Table 13.9 calculates the difference in temperature at each time interval compared to the change in C_I. For example, Table 13.9 row 1 indicates that as C_I increased from 4 to 5 the average temperature recorded decreased 0.5 ˚C at the 1 hour mark. Changes in ΔT_i should be positive and similar for changes in C_I of 4 to 5 and 5 to 6.

In both the delay and no delay specimens a change in C_I of 4 to 5 was not detected by thermal measurements. Cement index changes of 5 to 6 and 4 to 6 were detected at all measurement times, however the correct order of C_I was only predicted by thermal measurements on delay specimens at 2 and 4 hours. Considering no covering was used around the EPS block, these results were encouraging.

Table 13.8. Phase 3 Average Thermal Profile Results with No Covering

Specimen ID	Time Delay (min)	Overall Air Temp. (˚C)				ΔT_i (˚C) at Time (hr)						
		Mean	Std Dev	Max	Min	1	2	4	6	8	16	24
PR-1-PB4	0	28.3	6.5	50.4	21.4	5.0	5.1	5.2	4.8	4.4	2.1	0.5
PR-1-PB5	0	28.3	6.5	50.4	21.4	4.5	4.6	4.5	4.0	3.6	1.9	1.1
PR-1-PB6	0	28.3	6.5	50.4	21.4	6.0	6.4	6.5	6.0	5.5	3.3	1.2
PR-2-PB4	30	23.9	4.1	35.8	19.4	3.0	3.3	3.8	2.9	2.7	1.3	0.7
PR-2-PB5	30	23.9	4.1	35.8	19.4	3.0	3.6	4.2	2.2	1.7	0.4	0.5
PR-2-PB6	30	23.9	4.1	35.8	19.4	3.9	4.5	5.6	4.0	3.5	1.7	1.0

-- Overall Air Temp. was calculated as the average of the air temp values for the 6 replicate specimens

Table 13.9. Phase 3 Differential Thermal Profile Results with No Covering

Change in C_I	Time Delay (min)	Difference in Temperature (˚C) at Time (hr)						
		1	2	4	6	8	16	24
4 to 5	0	-0.5	-0.6	-0.8	-0.8	-0.7	-0.2	0.5
5 to 6	0	1.4	1.9	2.0	2.0	1.9	1.4	0.2
4 to 6	0	1.0	1.3	1.3	1.2	1.1	1.2	0.7
4 to 5	30	-0.1	0.3	0.5	-0.7	-1.0	-1.0	-0.3
5 to 6	30	0.9	0.9	1.4	1.8	1.8	1.3	0.5
4 to 6	30	0.9	1.1	1.8	1.1	0.9	0.4	0.3

13.3.4 Clear Covering Equipment Configuration

Tables 13.10 and 13.11 provide clear covering results, and these results were prepared in the same manner as Tables 13.8 and 13.9. These results somewhat mirrored the results for no covering, but did provide modestly better resolution. C_I change of 4 to 5 was the most difficult to detect, although the 30 minute delay specimens did detect cement content changes at times of 2, 4 and, 6 hours. Cement index changes of 5 to 6 and 4 to 6 were detected at all times except 24 hr. The correct order of C_I was detected in 30 minute delay specimens at 2, 4, and 6 hours. Modestly improved resolution from no covering to a clear covering is intuitive and encouraging for the feasibility of this concept. Interestingly, cement content detection was best at 2 to 6 hours, whereas Section 13.3.2 correlations of thermal measurements and compressive strength were best at 8 to 24 hours.

Table 13.10. Phase 3 Average Thermal Profile Results with Clear Covering

Specimen ID	Time Delay (min)	Overall Air Temp. (˚C)				ΔT_i (˚C) at Time (hr)						
		Mean	Std Dev	Max	Min	1	2	4	6	8	16	24
PR-1-PB4	0	28.3	6.5	50.4	21.4	3.9	4.6	5.0	4.7	4.3	3.0	0.0
PR-1-PB5	0	28.3	6.5	50.4	21.4	3.3	4.2	4.6	4.2	3.8	2.6	0.1
PR-1-PB6	0	28.3	6.5	50.4	21.4	3.9	5.1	5.6	5.2	4.7	3.3	-0.2
PR-2-PB4	30	23.9	4.1	35.8	19.4	2.4	3.2	3.3	2.6	2.4	1.3	0.9
PR-2-PB5	30	23.9	4.1	35.8	19.4	2.3	3.5	3.9	2.8	2.3	1.0	0.8
PR-2-PB6	30	23.9	4.1	35.8	19.4	3.3	4.3	4.3	3.3	2.9	1.6	1.1

-- Overall Air Temp. was calculated as the average of the air temp values for the 6 replicate specimens

Table 13.11. Phase 3 Differential Thermal Profile Results with Clear Covering

Change in C_I	Time Delay (min)	Difference in Temperature (˚C) at Time (hr)						
		1	2	4	6	8	16	24
4 to 5	0	-0.6	-0.4	-0.5	-0.5	-0.5	-0.4	0.1
5 to 6	0	0.7	0.9	1.0	1.0	0.9	0.7	-0.3
4 to 6	0	0.1	0.5	0.5	0.4	0.4	0.3	-0.2
4 to 5	30	-0.1	0.3	0.5	0.2	0.0	-0.3	-0.1
5 to 6	30	1.0	0.8	0.5	0.5	0.6	0.5	0.3
4 to 6	30	0.9	1.1	1.0	0.7	0.6	0.3	0.2

13.3.5 HC Covering Equipment Configuration

Tables 13.12, 13.13, and 13.14 provide HC covering results, and these results were prepared in the same manner as Tables 13.8 and 13.9. HC insulated results appear to have improved thermal clarity over the other options considered, with is intuitive. C_I change of 4 to 5 was still the most difficult to detect. However, a greater percentage of the times considered detected at least some positive thermal activity compared to no covering or clear covering specimens. Cement index changes of 5 to 6 and 4 to 6 were detected at all times but 1 hour with *Pit B* and all times after 6 hours with *Pit D*. The correct order of C_I was detected in *Pit B* specimens at 2, 4, 6, and 8 hours. The correct order of C_I was recorded in Pit D specimens at 8, 16, and 24 hours.

The earliest test time where the correct cement index order was predicted in both soils was 8 hours, which aligns reasonably well with compressive correlation timing presented in Section 13.3.2. When viewed in the context of compressive strength and cement content detection, using thermal measurements data at 8 to 16 hours seems to provide the best resolution for the data collected. In general, low cement index values may prove to be more difficult to detect, but cement content being too high (e.g. double spread over the same area) is generally of more concern.

As with compressive strength correlations, the ability to detect cement content with simplistic and portable insulation was modest. The findings of this chapter are encouraging for feasibility and proof of concept, but may need further enhancement prior to large scale implementation. As discussed previously, increased insulation and/or increased specimen size are options that should improve resolution.

Table 13.12. Phase 3 Average Thermal Profile Results with HC Covering

	Time Delay	Overall Air Temp. (˚C)				ΔT_i (˚C) at Time (hr)						
Specimen ID	(min)	Mean	Std Dev	Max	Min	1	2	4	6	8	16	24
PR-3-PB4	30	22.3	3.5	32.1	18.0	2.9	3.4	2.5	3.3	3.1	2.5	1.8
PR-3-PB5	30	22.3	3.5	32.1	18.0	2.8	3.5	2.9	3.5	3.2	2.2	1.5
PR-3-PB6	30	22.3	3.5	32.1	18.0	3.2	4.2	3.2	3.9	3.6	2.7	1.9
PR-3-PB3	30	20.6	3.6	30.4	16.2	2.5	2.5	1.9	2.7	2.6	2.1	1.2
PR-3-PB5	30	20.6	3.6	30.4	16.2	2.9	3.3	2.9	3.3	3.0	2.0	1.2
PR-3-PB7	30	20.6	3.6	30.4	16.2	2.9	3.7	3.3	3.6	3.4	2.5	1.5
PR-4-PD4	30	17.2	2.6	22.9	13.6	1.4	1.7	2.0	2.2	2.2	2.1	1.6
PR-4-PD5	30	17.2	2.6	22.9	13.6	0.9	1.3	1.8	2.2	2.3	2.2	1.8
PR-4-PD6	30	17.2	2.6	22.9	13.6	1.0	1.5	2.0	2.6	2.9	3.1	2.4
PR-4-PD3	30	13.3	4.8	27.6	7.7	0.8	0.7	1.2	1.6	1.7	1.8	0.5
PR-4-PD5	30	13.3	4.8	27.6	7.7	0.5	0.8	1.7	2.1	2.3	2.1	0.9
PR-4-PD7	30	13.3	4.8	27.6	7.7	0.3	0.3	1.1	2.1	2.8	3.5	2.0

Overall Air Temp. was calculated as the average of the air temp values for the 6 replicate specimens

Table 13.13. Phase 3 Differential Thermal Profile Results with HC Covering: Pit B

Change in C_I	Time Delay (min)	Difference in Temperature (˚C) at Time (hr)						
		1	2	4	6	8	16	24
4 to 5	0	-0.1	0.1	0.4	0.2	0.1	-0.3	-0.3
5 to 6	0	0.5	0.7	0.3	0.4	0.4	0.5	0.4
4 to 6	0	0.3	0.7	0.7	0.6	0.5	0.2	0.1
3 to 5	30	0.3	0.9	1.0	0.7	0.4	-0.2	0.0
5 to 7	30	0.0	0.3	0.3	0.3	0.4	0.6	0.3
3 to 7	30	0.3	1.2	1.4	0.9	0.8	0.4	0.3

Table 13.14. Phase 3 Differential Thermal Profile Results with HC Covering: Pit D

Change in C_I	Time Delay (min)	Difference in Temperature (˚C) at Time (hr)						
		1	2	4	6	8	16	24
4 to 5	0	-0.5	-0.4	-0.2	0.0	0.1	0.1	0.2
5 to 6	0	0.1	0.2	0.2	0.4	0.6	0.9	0.7
4 to 6	0	-0.4	-0.2	0.0	0.4	0.7	1.0	0.8
3 to 5	30	-0.3	0.1	0.4	0.5	0.5	0.3	0.3
5 to 7	30	-0.2	-0.4	-0.6	0.0	0.5	1.4	1.1
3 to 7	30	-0.5	-0.4	-0.2	0.5	1.1	1.7	1.5

CHAPTER 14-SUMMARY, CONCLUSIONS, AND RECOMMENDATIONS

14.1 Summary

Soil-cement practices within MDOT related to Class 9C soils used for base layers were evaluated in this report. The overall objective was to provide draft design and quality control guidance that could be incorporated and/or specified to improve performance of soil-cement base layers. This overall objective was met within the efforts of State Study 206.

While meeting the project's overall objective, conclusions and recommendations for enhancing and/or modifying existing design and quality control protocols were developed that are provided in the remaining sections of this chapter. In addition, guidance for incorporating parameters such as elastic modulus into the Mechanistic-Empirical Pavement Design Guide (MEPDG) was provided. Several of the items described in this report rely on equipment designed and fabricated during State Study 206. In particular, economical thermal profile test equipment and a compaction mold were developed that allow soil-cement mix design, elastic modulus measurement for M-E pavement layer thickness design, and construction to interface together more effectively.

14.2 Conclusions

The overall conclusion from State Study 206 was that MDOT soil-cement activities have many positive attributes, but there is room for enhancement in terms of laboratory mix design, M-E pavement design, and construction quality control. This study concluded that the mold described in Figure 5.2 should be able to improve MDOT's soil-cement practices. This approach allows specimens to be compacted inside a plastic mold at a 1.98:1 h/d aspect ratio for laboratory mix design, elastic modulus measurement, thermal profile measurements, and construction quality control. This study also concluded that using thermal profiles for construction quality has some promising attributes, but also has challenges that need further investigation before widespread use would be warranted. Specific conclusions are provided in the following list.

- *Practice Review:* The DOT survey practice review showed there to be no universal or standard criteria for stabilized soil design within the state DOT's who responded. Widespread use of compressive strength for design was noted; however, no standard strength requirement was used. The MDOT soil-cement database (Chapter 3) proved to be very insightful to the current practice of soil-cement in the state of Mississippi. Archiving data in a manner suitable for quick analysis can be of great benefit. Specific observations derived from the database are provided in Section 3.5.
- *Proctor Compaction:* Compaction delays can result in pronounced density decreases, though the extent of the density decrease appears to vary with soil type. In some cases, density decrease due to time delays between mixing and compaction can become a first order effect. When compared to Proctor compaction absent cement, density behavior measured with MT-9 protocols was erratic for the pit soils tested. The overall Proctor compaction conclusion was MT-9 protocols can be enhanced.

- *Strength Gain Versus Time:* Strength gain with time behavior was similar for all pit soils and all compaction methods. Most of the strength gain was seen in the first 56 days of curing (75 to 85% of 540 day strengths). Although designed with at least 2070 kPa strengths at 7 or 14 days, pit soils exhibited continued strength gain and achieved 3550 to 3950 kPa (Specimen type 1) after 540 days of curing based on regression equations. Strain gain with time data suggested that MDOT's current cement contents are in a reasonable range and that enhancements to current practices should not result in large overall upward or downward shifts in cement content.
- *Mix Design Evaluation:* Replicate testing and variability analysis results showed that using two replicates instead of one would increase the reliability of design and lower the margin of error with minimal additional effort relative to existing MT-25 practices. Cement source and curing method had a significant effect on soil-cement compressive strength. Compaction method had a significant effect on compressive strength for all soils when comparing specimen type 1 and 4 and specimen type 4 and 7. Significance of compaction method was dependent on soil type for all other comparisons.
- *Elastic Modulus:* A conservative value for elastic modulus was found by using the maximum compressive strength and Equation 2.7. Equation 2.6 gave elastic modulus values comparable to the actual measured elastic modulus values found in this study, especially during the performance period of a soil-cement pavement layer. Measured elastic modulus values seem to be at least somewhat dependent on soil type. Elastic modulus values measured using the compressometer/extensometer were reasonable relative to those found in literature for similar materials and cement contents.
- *Wheel Tracking:* Wheel tracking of soil-cement provided somewhat useful yet somewhat limited insight into evaluating performance of soil cement pavement layers. Rutting does not seem to be an issue with soil cement layers in Mississippi, even in unrealistically harsh conditions. Testing showed failure took place only when at least 80% of highway surface loading was directly applied and the specimen was submerged in hot water during testing.
- *Laboratory Thermal Profile Testing:* Thermal measurement analysis revealed that ΔT is a promising thermal profile measurement output. In most cases, thermal profile results were able to statistically differentiate between cement contents at 2% cement index intervals, and in some cases at 1% intervals. Although, practically speaking the recorded differences were modest. Laboratory testing also revealed the importance and potential implications revolving around the interaction of initial material temperature (T_i) and the initial temperature of the thermal measurement device (T_{BL}).
- *Field Thermal Profile Testing:* Incorporating thermal measurements into a field quality control program may be feasible. They have shown promise as a quality control tool for cement content measurement. Statistically significant correlations were detected between ΔT and density adjusted compressive strength for field applications when an environmental chamber was used. Statistically significant correlations were also detected between ΔT_i and field adjusted compressive strength when specimens were left outdoors in an insulated box absent temperature regulation capabilities. When left outdoors in this manner, differences detected were modest and could be difficult to implement into a quality control program.

14.3 Recommendations

Recommendations related to the design and performance of soil cement pavement layers are as follows. Several of these recommendations are directly related to implementation of the Figure 5.2 mold into MDOT's soil-cement operations, which is the primary recommendation from State Study 206. Over time, use of this mold should help to better interface laboratory mix design, M-E pavement design, and construction quality control. With regard to thermal profile use for soil-cement quality control, the overall recommendation at this time is not to implement the technique. Implementation of the Figure 5.2 mold should occur first, and once there is some understanding of its impact, thermal profile's optimal role within quality control operations should be better understood. Additional recommendations are provided in bullet form as follows.

- *Proctor Compaction:* Replacing MT-9 protocols with MT-9 Mod protocols is recommended. Specifically, it is recommended not to re-use material when performing cement Proctors, and to compact specimens within 7 minutes of mixing soil, cement, and water for laboratory design purposes. Once an optimum moisture content has been determined using MT-9 Mod protocols, it is recommended to determine dry density as a function of compaction delay (initial recommendations are hold times of 30 and 60 minutes) at optimum moisture content. Comparing the MT-9 Mod value with no compaction delay (i.e. compacted within 7 minutes of mixing) to the 30 and 60 minute compaction delay data points (i.e. compacted within 37 or 67 minutes of mixing) should be useful in determining field quality control plans for the soil and cement to be used on the project. Portland cement from the same source to be used on the project should be used during these compactions if possible.
- *Laboratory Mix Design:* The design guidance provided in Section 8.8 should be implemented into MT-25. There are a few manners which this information could be implemented, all of which utilize the Figure 5.2 mold. It is recommended for MDOT to continue performing MT-25 in its present form, but also use the Figure 5.2 mold in a side by side manner incorporating the Section 8.8 protocols in the most convenient manner for Central Laboratory operations. Over a relatively short time period (e.g. one construction season), it is likely that an optimal manner to implement the information in Section 8.7 will be obtained. In the assessment of the authors, how the Figure 5.2 mold is implemented is not nearly as important as that the Figure 5.2 mold is implemented. Implementation of this mold is envisioned to allow positive interaction between laboratory mix design, pavement design, and quality control.
- *Elastic Modulus:* Direct measurement of elastic modulus is recommended for large projects using specimens prepared with the Figure 5.2 mold. For smaller projects, Equation 2.6 or Equation 2.7 can be used. If MDOT prefers a conservative elastic modulus estimate, Equation 2.7 is recommended. If MDOT prefers a more precise elastic modulus estimate, Equation 2.6 is recommended.
- *Wheel Tracking:* It is recommended that further study not focus on wheel tracking of soil-cement pavement layers. The research found that soil-cement layers are only substantially influenced by combined loading and environmental effects not commonly seen in soil-cement layers (submerged and fully loaded direct contact). The information presented herein appears to be sufficient at the present time for Class 9C Mississippi soils from the perspective of wheel tracking.

- *Thermal Profile Testing:* Thermal measurements are not recommended for widespread implementation as a quality control tool at the present time absent sophisticated equipment. Future investigations that account more accurately for temperature measurement bias, provide additional insulation, investigate larger specimens, and similar are needed prior to widespread use. The concepts were demonstrated to be feasible, so widespread use may be more reasonable in the future.
- *Future Research:* Research performed as part of State Study 206 identified a few areas that could be fruitful areas of additional study. They are listed below.
  - Perform additional investigations to explore the strength and elastic modulus versus density behavior of soil cement mixtures. This could provide valuable information on how density affects the design and performance of soil cement pavement layers.
  - Perform additional Proctor compaction testing with several soil types to assess effects of cement content and compaction delay on dry density. This data should be used to evaluate MT-9-Mod protocols and to further refine compaction control quality operations during construction.
  - MDOT should consider further investigating the linearity relationship between average compressive strength and cement content. A suggestion is to expand the testing scope herein from ±1% cement index of design to ±2% cement index of design.
  - Perform additional testing with the *PM-P* compaction protocol to synchronize laboratory mix design and field quality control compaction protocols.
  - Investigate relative merits of testing fairly large samples of uncompacted or lightly compacted soil-cement to measure cement content using thermal profiles. An example would be instrumenting a cooler and filling it with soil-cement.
  - Perform further analysis and investigation to determine how thermal measurements can be effectively utilized in soil-cement practices.
  - Continue to investigate reasonably straightforward methods to use thermal profiles in field quality control operations. Three of the key items that need investigated further are: 1) the effects of more insulation on measured thermal profiles; 2) merits of increased soil-cement specimen size; and 3) implementable methods of minimizing initial temperature differences between reference specimens (i.e. no cement), soil-cement specimens, and the measuring block.

CHAPTER 15-REFERENCES

Abu-Farsakh, M.Y., Alshibli, K., Nazzal, M.D., and Seyman, E. (2004). *Assessment of In-Situ Test Technology for Construction Control of Base Courses and Embankments*. Report No. FHWA/LA.04/389, Louisiana Transportation Research Center, Baton Rouge, LA.

ACI. (2009). *Report on Soil Cement*. Report No. ACI 230.1R-09, ACI Committee 230, American Concrete Institute, Farmington Hills, MI.

Adaska, W.S. and Luhr, D.R. (2004). "Control of Reflective Cracking in Cement Stabilized Pavements." *Proceedings of 5th International RILEM Conference*, May 5-7, Limoges, France.

AHTD. (2003). *Standard Specification for Highway Construction*. Arkansas State Highway and Transportation Department, Little Rock, AR.

ALDOT. (2012). *Standard Specifications for Highway Construction*. Alabama Department of Transportation, Montgomery, AL.

Anday, M.C. (1963). "Curing Lime-Stabilized Soils." *Highway Research Record*, 29, 13-26.

Anderson, B.K. (2013). *Investigation of Factors Influencing Design and Performance of Soil Cement Pavement Layers.* Master's Thesis, Mississippi State University. http://sun.library.msstate.edu/ETD-db/ETD-search/search

Carino, N.J. and Lew, H.S. (2001). "The Maturity Method: From Theory to Application." *Proceedings of the 2001 Structures Congress and Exposition*, May 21-23, Reston, VA, 19-30.

Chanvillard, G. and D'Aloia, L. (1997). "Concrete Strength Estimation at Early Ages: Modification of the Method of Equivalent Age." *ACI Materials Journal*, 97(6), 520-530.

Chitambira, B., Al-Tabbaa, A., Perera, A.S.R., and Yu, X.D. (2005). "Accelerated Ageing of a Stabilised/Solidified Contaminated Soil Using Elevated Temperature." *Proceedings of the International Conference on Stabilisation/Solidification Treatment and Remediation*, April 12-13, Cambridge, UK, 149-158.

Chitambira, B., Al-Tabbaa, A., and Yu, X.D. (2006). "The Temperature Dependency of the Hardening of Stabilized/Solidified Contaminated Soil." *Journal of Land Contamination & Reclamation*, 14(1), 109-120.

Chitambira, B., Al-Tabbaa, A., Perera, A.S.R., and Yu, X.D. (2007). "The Activation Energy of Stabilised/Solidified Contaminated Soils." *Journal of Hazardous Materials*, 141, 422-429.

Circeo, J.J., Davidson, D.T., and David, H.T. (1962). "Strength-Maturity Relations of Soil-Cement Mixtures." *Highway Research Board Bulletin*, 353, 84-97.

Cost, T. and Ahlrich, R. (2005). "Use of Slag Cement in Soil Stabilization." Paper presented at *ACI Convention*, session sponsored by ACI committee 233 for Slag Cement, November 6-10, Kansas City, MO.

Cost, V.T. and Gardiner, A. (2009). "Practical Concrete Mixture Evaluation via Semi-Adiabatic Calorimetry." *Proceedings of 2009 Concrete Technology Forum*. National Ready Mixed Concrete Association, May 13-15, Cincinnati, OH, pp. 21.

Doyle, J.D., and Howard, I.L. (2011). *Linear Asphalt Compactor Operator's Manual*. Manual No. CMRC M 10-2 Version 2, Construction Materials Research Center, Mississippi State University, pp. 16.

FDOT. (2010). *Standard Specifications for Road and Bridge Construction*. Florida Department of Transportation, Tallahassee, FL.

Felt, E.J. and Abrams, M.S. (1957). "Strength and elastic properties of compacted soil-cement mixtures," *Papers on Soils*, STP 206, American Society for Testing and Materials, Philadelphia, pp. 152-178.

Felton, P.J. (1975). Unpublished research, University of Surrey, United Kingdom.

Filliben, J.J. (1975). "The Probability Plot Correlation Coefficient Test for Normality." *Technometrics*, 17, 111-117.

Fossberg, P.E., Mitchell, J.K., and Monismith, C.L. (1972). "Load deformation characteristics of a pavement with cement-stabilized base and asphalt surfacing," *Proceedings of the Third International Conference on the Structural Design of Asphalt Surfacing*, Vol. 1, pp. 795-811.

GDOT. (2001). *Standard Specifications Section 301*. Georgia Department of Transportation, Atlanta, GA.

George, K.P. (2002). *Minimizing Cracking in Cement-Treated Materials for Improved Performance*. Report RD123, Portland Cement Association, Skokie, IL, pp. 44.

George, K.P. (2006). *Soil Stabilization Field Trial*. Report No. FHWA/MS-DOT-RD-05-133, Mississippi Department of Transportation, pp. 68.

Griffin, J.R. and Tingle, J.S. (2009). *In Situ Evaluation of Unsurfaced Portland Cement-Stabilized Soil Airfields*. Report ERDC/GSL TR-09-20, U.S. Army Engineer Research and Development Center, Vicksburg, MS, pp. 47.

Guthrie, W.S., Young, T.B., Blankenagel, B.J., and Cooley, D.A. (2005). "Early-Age Assessment of Cement-Treated Base Material." *Transportation Research Record: Journal of the Transportation Research Board*, 1936, 12-19.

Halsted, G.E., Luhr, D.R., and Adaska, W.S. (2006). *Guide to Cement-Treated Base (CTB)*. PCA. Publication No. EB236, Portland Cement Association, Stokie, IL.

Hansen, P.F. and Pedersen, J. (1977). "Maturity Computer for Controlled Curing and Hardening of Concrete." *Nordisk Betong*, 1, 19-34.

Howard, I.L., Doyle, J.D., White, T.D., Ivy, J., and Booth, O. (2010). *PURWheel Laboratory Wheel Tracker Operator's Manual*. Manual No. CMRC M 10-2 Version 1, Construction Materials Research Center, Mississippi State University, pp. 65.

James, R.S., Cooley, Jr., L.A., and Ahlrich, R.C. (2009). *Chemically Stabilized Soils*. Report No. SPR-1(51), Mississippi Department of Transportation, Jackson, MS.

Kasama, K., Zen, K., Iwataki, K. (2007). "High-strengthening of cement-treated clay by mechanical dehydration," *Soils and Foundations.* Vol. 47, No. 2, pp 171-184.

Kolias, S. and Williams, R.I.T. (1984). "Estimation of the modulus of elasticity of cement stabilized materials," *Geotechnical Testing Journal*, Vol. 7, No. 1, pp. 26-35.

KYTC. (2012). *Standard Specifications for Road and Bridge Construction*. Kentucky Transportation Cabinet, Frankfort, KY.

LaDOTD. (2006). *Standard Specifications for Road and Bridges*. Louisiana Department of Transportation and Development, Baton Rouge, LA.

Ma, W., Sample, D., Martin, R., and Brown, P.W. (1994). "Calorimetric Study of Cement Blends Containing Fly Ash, Silica Fume, and Slag at Elevated Temperatures." *Journal of Cement, Concrete and Aggregates*, 16(2), 93-99.

MDOT. (2004). *Mississippi Standard Specifications for Road and Bridge Construction*. Mississippi Department of Transportation, Jackson, MS.

Mohsen, J.P., Bernard, L.R., and Kessinger, D.T. (2004). "Maturity Method Applied to Highway Construction." *Transportation Research Record: Journal of the Transportation Research Board*, 1900, 79-85.

Morabito, P. (1998). "Methods to Determine the Heat of Hydration of Concrete." In *Prevention of Thermal Cracking in Concrete at Early Ages*. RILEM Report 15. Springenschmid, R. (Ed.), E&FN Spon, London, pp. 1-25.

NCDOT. (2002). *Standard Specifications for Road and Structures*. North Carolina Department of Transportation, Raleigh, NC.

Nurse, R.W. (1949). "Steam Curing of Concrete." *Magazine of Concrete Research*, 1(2), 79-88.

Okamoto, P.A., Bock, B.T., and Nussbaum, P.J. (1991). "Nondestructive Tests for Determining Compressive Strength of Cement-Stabilized Soils." *Transportation Research Record: Journal of the Transportation Research Board*, 1295, 1-8.

Okyay, U.S. and Dias, D. (2010). "Use of lime and cement treated soils as pile supported load transfer platform," *Engineering Geology*, Vol. 114, pp. 34-44.

Ott, R.L. and Longnecker, M. (2010). *An Introduction to Statistical Methods and Data Analysis*, 6th Ed., Brooks/Cole, Belmont, CA.

PCA. (1992). *Soil-Cement Laboratory Handbook*. PCA. Publication No. EB052.07S, Portland Cement Association, Stokie, IL.

PCA. (2001). *Soil-Cement Inspector's Manual*. PCA. Publication No. PA050.03, Portland Cement Association, Stokie, IL.

Peethamparan, S., Olek, J., and Lovell, J. (2008). "Influence of Chemical and Physical Characteristics of Cement Kiln Dusts (CKDs) on Their Hydration Behavior and Potential Suitability for Soil Stabilization." *Cement and Concrete Research*, 38, 803-815.

Reinhold, F. (1955). "Elastic behavior of soil-cement mixtures," *Soil and Soil-Aggregate Stabilization*, Highway Research Board, No. 108, Washington, DC, pp. 128-137.

Samson, L.R. (1986). *A Study of the Precision Limits of Wet/Dry Brushing Durability Test for Cement-Stabilized Materials*. Technical Report RP/26, National Institute of Technology Raipur and Council for Scientific and Industrial Research, South Africa.

Saul, A.G.A. (1951). "Principles Underlying the Steam Curing of Concrete at Atmospheric Pressure." *Magazine of Concrete Research*, 2(6), 127-140.

Scavuzzo, R. (1991). "Determining Cement Content of Soil-Cement by Heat of Neutralization." *Transportation Research Record: Journal of the Transportation Research Board*, 1295, 17-22.

SCDOT. (2007). *Standard Specifications for Highway Construction*. South Carolina Department of Transportation, Columbia, SC.

Schindler, A.K. (2004). "Effect of Temperature on the Hydration of Cementitious Materials." *ACI Materials Journal*, 101(2) 72-81.

Scullion, T., Sebesta, S., Harris, J.P., and Syed, I. (2005). *Evaluating the Performance of Soil-Cement Modified Soil for Pavements: A Laboratory Investigation.* Report RD120, Portland Cement Association, Skokie, Illinois, pp. 142.

Sebesta, S. (2005). "Use of Microcracking to Reduce Shrinkage Cracking in Cement-Treated Bases." *Transportation Research Record: Journal of the Transportation Research Board*, 1936, 3-11.

Sullivan, W.G. (2012). *Investigation of Compaction and Corresponding Thermal Measurement Techniques for Cementitiously Stabilized Soils.* Master's Thesis, Mississippi State University. http://sun.library.msstate.edu/ETD-db/ETD-search/search

Sullivan, W.G., Cost, T., and Howard, I.L. (2012). "Measurement of Cementitiously Stabilized Soil Slurry Thermal Profiles." *Proceedings of GeoCongress 2012: State of the Art and Practice in Geotechnical Engineering* (GSP225). March 25-29, Oakland, CA, pp. 958-967.

TDOT. (2006). *Standard Specifications for Road and Bridge Construction*. Tennessee Department of Transportation, Nashville, TN.

Teng, T.C.P. and Fulton, J.P. (1974). "Field Evaluation Program of Cement-Treated Bases." *Transportation Research Record: Journal of the Transportation Research Board*, 501, 14-27.

Terrel, R.L., Epps, J.A., Barenberg, E.J., Mitchell, J.K., and Thompson, M.R. (1979). *Soil Stabilization in Pavement Structures: A User's Manual Vol. 2: Mixture Design Considerations*. Report No. FHWA-IP 80-2, Federal Highway Administration, Washington, D.C.

Thompson, M.R. (1966). "Shear strength and elastic properties of lime-soil mixtures," *Highway Research Record*, HRB, No. 139, Washington, D.C., pp. 1-14.

Tikalsky, P.J., Tepke, D.G., Camisa, S., and Soltesz, S. (2003). *Maturity Method Demonstration*. Report No. FHWA-OR-DF-04-01, Federal Highway Administration, Washington, D.C.

Toklu, V.C., Etude des mortiers des graves traitees aux liants hydrauliques et aux liants mixtes en rue de la reduction de leur fissuration de retrait, Ministere de l'equipement Laboratoires des Ponts et Chaussees, Rapport de recherché No. 60, Oct. 1976, p 99.

TxDOT. (2004). *Standard Specifications for Construction and Maintenance of Highways, Streets, and Bridges*. Texas Department of Transportation, Austin, TX.

USACE. (1994). *Soil Stabilization of Pavements*. Technical Manual No. TM5-822-14, United States Army Corps of Engineers, Department of the Army, the Navy, and the Air Force, Washington, D.C.

Varner, R.L. (2011). *Variability of Cement-Treated Layers in MDOT Road Projects.* State Study 227, Mississippi Department of Transportation, Jackson, MS.

VDOT. (2007). *Road and Bridge Specifications*. Virginia Department of Transportation, Richmond, VA.

Williams, R.I.T. and Patankar, V.D., (1968). "The effect of cement type, aggregate type and mix water content on the properties of lean concrete mixes," *Roads and Road Construction*, Vol. 46, pp. 542-543.

Wu and Yang (2012). *Evaluation of Current Louisiana Flexible Pavement Structures Using PMS Data and New Mechanistic-Empirical Pavement Design Guide*. LTRC Project No. 07-6P, Louisiana Transportation Research Center, Baton Rouge, LA, pp. 169.

WVDOT. (2002). *Construction Manual*. West Virginia Department of Transportation, Charleston, WV.